

**Band Gap Engineering of Donor-Acceptor
 π -Conjugated Poly(heteroarylene)s and
Poly(heteroaryleneethynylene)s**

Dissertation

Zur Erlangung des akademischen Grades
doctor rerum naturalium (Dr. rer. nat.)

vorgelegt dem Rat der Chemisch-Geowissenschaftlichen Fakultät
der Friedrich-Schiller-Universität Jena

von M.Sc. M.Phil Raja Shahid Ashraf
geboren am 24.01.1976 in Gujrat

Jena, May 2005

Gutachter:

1. Prof. Dr. E. Klemm
2. PD Dr. M. Thelakkat

Tag der öffentlichen Verteidigung: 29-06-2005

Content

1	Introduction.....	1
1.1	π -Conjugated Polymers.....	1
1.2	Band Gap Engineering of π -Conjugated Polymers.....	3
1.3	Donor–Acceptor π -Conjugated Polymers.....	3
2	General Part.....	9
2.1	Mechanism of Sonogashira Cross-Coupling.....	9
2.2	Mechanism of Suzuki Cross-Coupling.....	12
2.3	Basics of Polycondensation.....	15
3	Results and Discussion.....	17
3.1	Monomer Synthesis.....	17
3.1.1	<i>Diethynyl Monomers.....</i>	<i>17</i>
3.1.1.1	<i>2,5-Diethynyl Alkyl Substituted Thiophenes.....</i>	<i>17</i>
3.1.1.2	<i>1,4-Diethynyl-2,5-Dialkoxy Substituted Phenylens.....</i>	<i>18</i>
3.1.2	<i>Dibromo Monomers.....</i>	<i>18</i>
3.1.3	<i>Dioxaborolane Monomers.....</i>	<i>21</i>
3.2	Benzothiadiazole and Thiophene Based Poly(heteroaryleneethynylene)s.....	23
3.2.1	<i>Synthesis and Characterization of the Polymers.....</i>	<i>23</i>
3.2.2	<i>Optical Properties.....</i>	<i>26</i>
3.2.3	<i>Aggregate Formation in Solvent/Nonsolvent Solution.....</i>	<i>28</i>
3.2.4	<i>Electrochemical Studies.....</i>	<i>30</i>
3.2.5	<i>Photovoltaic Studies.....</i>	<i>32</i>
3.3	Quinoxaline and Thiophene Based Poly(heteroaryleneethynylene)s.....	35
3.3.1	<i>Synthesis and Characterization of the Polymers.....</i>	<i>35</i>
3.3.2	<i>Optical Properties.....</i>	<i>39</i>
3.3.3	<i>Aggregate Formation in Solvent/Nonsolvent Solution.....</i>	<i>41</i>
3.3.4	<i>Electrochemical Studies.....</i>	<i>45</i>
3.4	Thienopyrazine Based Low Band Gap Poly(heteroaryleneethynylene)s.....	47
3.4.1	<i>Synthesis and Characterization of the Polymers.....</i>	<i>47</i>
3.4.2	<i>Optical Properties.....</i>	<i>51</i>
3.4.3	<i>Aggregate Formation in Solvent/Nonsolvent Solution.....</i>	<i>53</i>
3.4.4	<i>Electrochemical Studies.....</i>	<i>54</i>

3.5 PE/PPV Hybrid Polymers	56
3.5.1 <i>Synthesis and Characterization of the Polymers</i>	56
3.5.2 <i>Optical Properties</i>	59
3.5.3 <i>Electrochemical Studies</i>	62
3.6 Thienopyrazine and Fluorene Based Poly(heteroarylene)s	64
3.6.1 <i>Synthesis and Characterization</i>	64
3.6.2 <i>Optical Properties</i>	69
3.6.3 <i>Aggregate Formation in Solvent/Nonsolvent Solution</i>	70
3.6.4 <i>Stability of the Polymers</i>	71
3.6.5 <i>Electrochemical Studies</i>	72
3.7 Quinoxaline and Fluorene Based Poly(heteroarylene)s	74
3.7.1 <i>Synthesis and Characterization</i>	74
3.7.2 <i>Optical Properties</i>	77
3.7.3 <i>Aggregate Formation in Solvent/Nonsolvent Solution</i>	79
3.7.4 <i>Electrochemical Studies</i>	80
3.7.5 <i>Photophysical Properties of Binary Blends of the Polymers P-14 and P-19</i>	81
4 Experimental	84
4.1 Instrumentation.....	84
4.2 Synthesis: (Synthesis of Monomer Precursors)	86
4.3 Monomers Synthesis	93
4.4 Synthesis of Polymers	99
5 Zusammenfassung in Thesen	106
6 References	113
7 Appendix	124
7.1 ¹³ C-NMR Spectra	124
7.2 Molecular Formulae	133
7.3 Abbreviations	136
Curriculum Vitae	138
List of Publications	139
Acknowledgement	140
Selbständigkeitserklärung	141

This thesis consists of: 141 Pages
 90 Figures
 24 Tables
 28 Schemes

1 Introduction

1.1 π -Conjugated Polymers

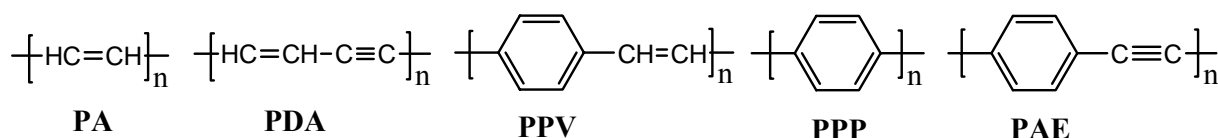
The emergence of conjugated polymers¹ as a new class of electronic materials, has attracted considerable attention, since the study of these systems has generated entirely new scientific concepts as well as potential for new technology. Conjugated polymers are organic semiconductors and as such important materials for applications in electronic and photonic devices. Prime examples are polymeric light-emitting diodes,² plastic lasers,³ and polymer-based photovoltaic cells,⁴ but at least in principle, conjugated polymers⁵ should be able to pertain all of the functions an inorganic semiconductor displays, FETs,⁶ and may lead in the future to "molecular electronics".⁷ The primary advantage of organic polymers over their inorganic counterparts is their ease of processing by dip coating, spin casting, printing,⁸ or use of doctor blade techniques. However, conjugated polymers are likewise important as sensory materials for water, organic vapors, and explosives either by fluorescence quenching or in artificial nose devices, which change their conductivity upon exposure to a suitable analyte.⁹

The goal with organics-based devices is not necessarily to attain or exceed the level of performance of inorganic semiconductor technologies (silicon is still the best at the many things that it does) but to benefit from a unique set of characteristics combining the electrical properties of (semi)conductors with the properties typical of plastics, that is, low cost, versatility of chemical synthesis, ease of processing, and flexibility. Interest in conjugated polymers picked up significantly after the 1976 discovery that they can be made highly electrically conducting following a redox chemical treatment.¹⁰ This discovery led to the 2000 Nobel Prize in Chemistry awarded to Alan Heeger, Alan MacDiarmid, and Hideki Shirakawa. By the mid-eighties, many research teams in both academia and industry were investigating π -conjugated oligomers and polymers for their nonlinear optical properties or their semiconducting properties, paving the way to the emergence of the fields of plastic electronics and photonics.¹

During the past 20 years these conjugated polymers have given rise to an enormous amount of experimental and theoretical work devoted to (i) the analysis of their structure and properties using a whole arsenal of physical techniques, (ii) the development of synthetic methods allowing a better control of their structure and electronic properties, (iii) the synthesis of functional polymers in which the electronic properties are associated with specific properties afforded by

covalently attached prosthetic groups,¹¹⁻¹³ and (iv) the analysis of their multiple technological applications extending from bulk utilizations such as antistatic coatings, energy storage, to highly sophisticated electronic, photonic, and bioelectronic devices.

The class of conjugated polymers which has found the most attention in the past are undoubtedly the poly(*p*-phenylenevinylene)s (**PPVs**) which "made it big" since Friend's 1990 report of organic polymeric LEDs.^{2,14} Other well-established classes of conjugated polymers are the polydiacetylene (**PDA**),¹⁵ polyphenylene (**PPP**),^{16,17} and polyacetylene (**PA**).¹⁸ However, the structurally closest relative to PPV, the poly(phenyleneethynylene)s (**PPEs**)^{19f} or poly(aryleneethynylenes) (**PAEs**); have attracted much less attention in the polymer community, despite their fascinating properties. Recently the groups of Bunz,¹⁹ Jenekhe,²⁰ Müllen,²¹ Swager,²² Weder^{23,24} Yamamoto,²⁵ and our group²⁶ demonstrated that PAEs with their unique property profile are fantastic materials in such different areas as explosive detection,²² molecular wires in bridging nanogaps,^{27,28} and polarizers for LC displays.



1.2 Band Gap Engineering of π -Conjugated Polymers

The existence of a bandgap for a one-dimensional system, which conjugated chains are, was already predicted by Peierls²⁹ in 1956, long before the first synthesis of a polyacetylene was reported by Shirakawa in 1971. Peierls predicted in his theorem the lifting of the bond length degeneracy, leading to significant bond length alternation, which causes the bandgap in one dimensional systems. The individual factors that play an important role in the synthesis of low bandgap polymers are (a) Bond length alternation, (b) aromaticity, (c) conjugation length, (d) substituents effect, and (e) intermolecular interactions.

Different structure elements have been proposed to influence the bandgap of conjugated polymers. For example, two widely used approaches are:

- Push–pull polymers with alternating electron rich and electron poor units (donor–acceptor approach).
- The introduction of a methine group between the rings is a further popular way to decrease the bandgap. By this approach, the double bond character of the bridging bond leads to a more flat structure and hinders angular rotation between the rings. Due to a better theoretical understanding,^{29–32} and much synthetic effort, several new polymers have been proposed with a lower bandgap such as poly-ethylenedioxythiophene,³³ polydithienothiophenes^{34–36} or copolymers.

1.3 Donor–Acceptor π -Conjugated Polymers

A strategy to induce minimum twisted arrangements between consecutive repeating units in conjugated polymers involves construction of A–B type systems where the ‘A’ unit has strong electron-donating and the ‘B’ unit has strong electron-withdrawing moieties. Interaction of the donor–acceptor moieties enhances the double bond character between the repeating units, which stabilizes the low band gap quinonoid-like forms within the polymer backbones. Hence, a conjugated polymer with an alternating sequence of the appropriate donor and acceptor units in the main chain can induce a reduction in its band gap energy.

Recent molecular orbital calculations have shown that the hybridization of the energy levels of the donor and the acceptor moieties result in D–A systems with unusually low HOMO–LUMO separation.³⁷

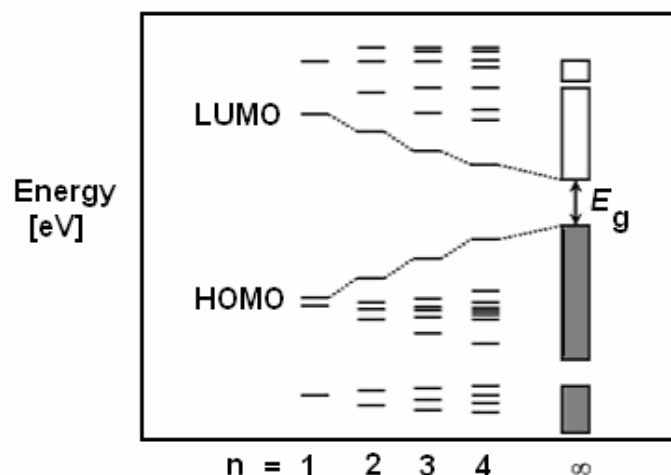


Figure 1.1. Band formation during the polymerization of a conjugated monomer into a π -conjugated polymer. (ref. ³⁸)

If the HOMO levels of the donor and the LUMO levels of the acceptor moiety are close in energy the resulting band structure will show a low energy gap as depicted in Figure 1.2. Further hybridization upon chain extension reduces the band gap as shown in Figure 1.1. During the progress of polymerization, the HOMO and LUMO levels of the repeating unit disperse into the valance and conduction bands.

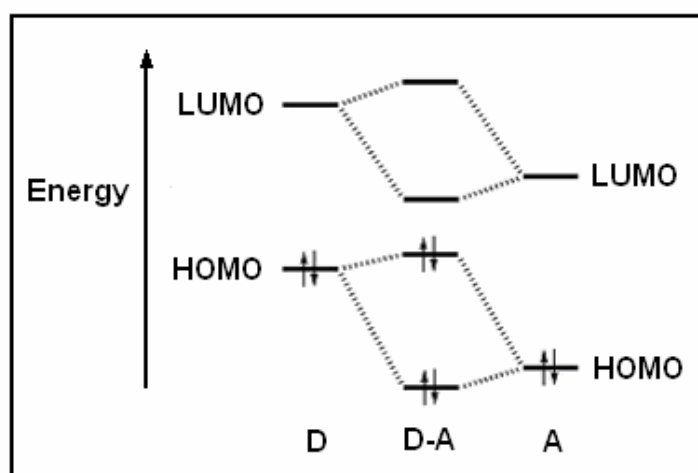
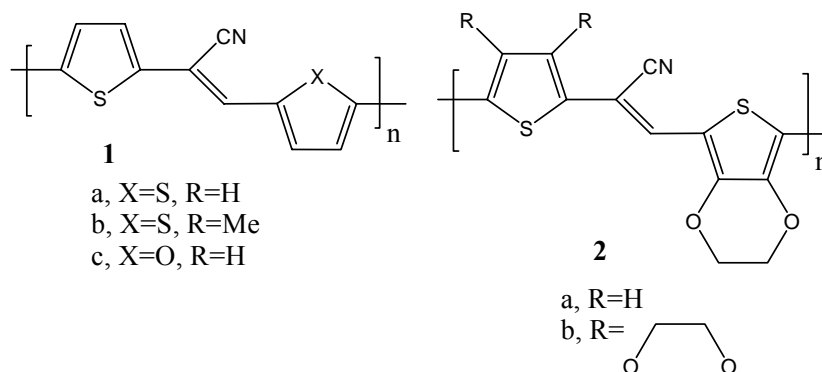


Figure 1.2. Molecular orbital interaction in donor (D) and acceptor (A) moieties leading to a D-A monomer with an unusually low HOMO-LUMO energy separation (ref. ³⁸)

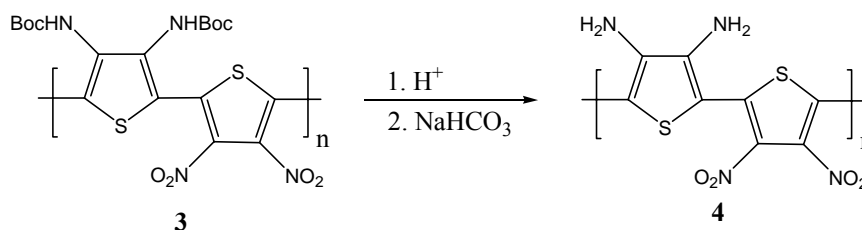
Further reduction in band gap is possible by enhancing the strength of donor and acceptor moieties *via* strong orbital interactions. In donor-acceptor systems, the introduction of electron withdrawing groups reduces E_g by lowering the LUMO levels whereas, the introduction of

electron donating groups reduces E_g by raising the HOMO levels. Therefore, designing of extremely low E_g polymers requires strong donors and acceptors. The synthetic principles for lowering the bandgap of linear π -conjugated polymers have been reviewed by Roncali.³⁰

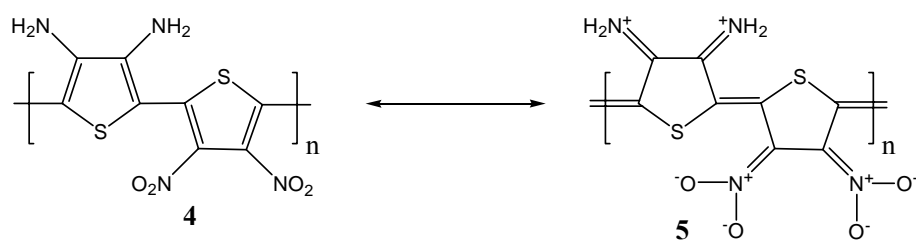
Commonly employed electron-donating moieties are thiophene and pyrrole with various substitution patterns, which often represent the best choice since these are electron rich subunits that allow numerous chemical transformations. The most widely used electron withdrawing groups are cyano and nitro groups. In addition copolymers containing electron withdrawing moieties such as quinoxalines, pyrazines and thiadiazoles, are reported to possess low band gaps. Using combinations of these donor and acceptor groups, a variety of monomers have been synthesized which undergo facile electrochemical or chemical polymerization leading to the formation of a number of low band gap polymers, a few representative examples of which are shown below.³⁸⁻⁴¹



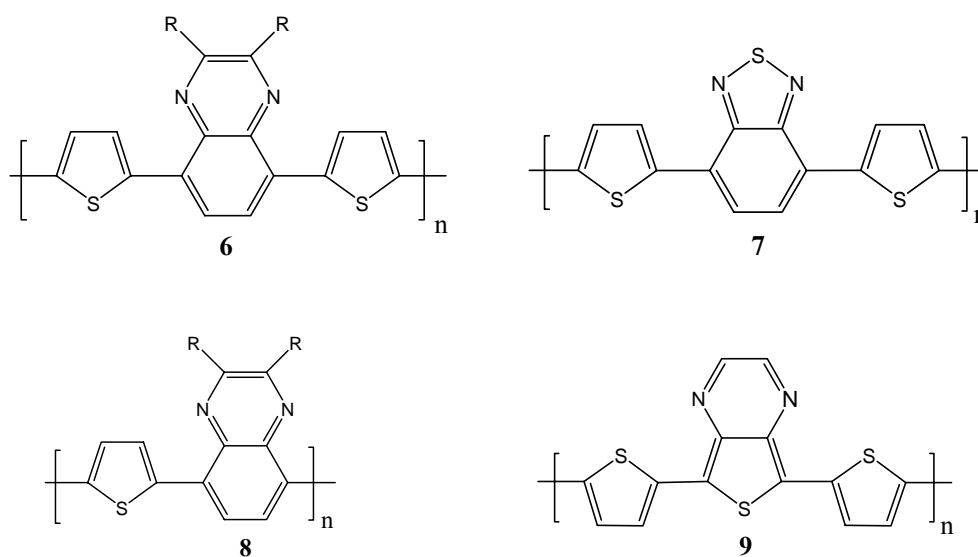
Conjugated polymers containing pyrrole and/or thiophene as electron donating and cyano-substituted aryl unit as electron accepting groups have been prepared by electrochemical oxidation methods.^{40, 41} A polythiophene **4** containing nitro groups as the electron acceptors and amino groups as electron donors is reported by Zhang and Tour (Scheme 1.1).⁴² Solution and solid-state optical band gaps of the polymer **4** are 1.4 and 1.1 eV, respectively. This low E_g observed in the solid state, suggests that the conjugated backbone is rigid due to the contribution of the mesomeric structure **5**, which may presumably be weak in the solution state (Scheme 1.2).

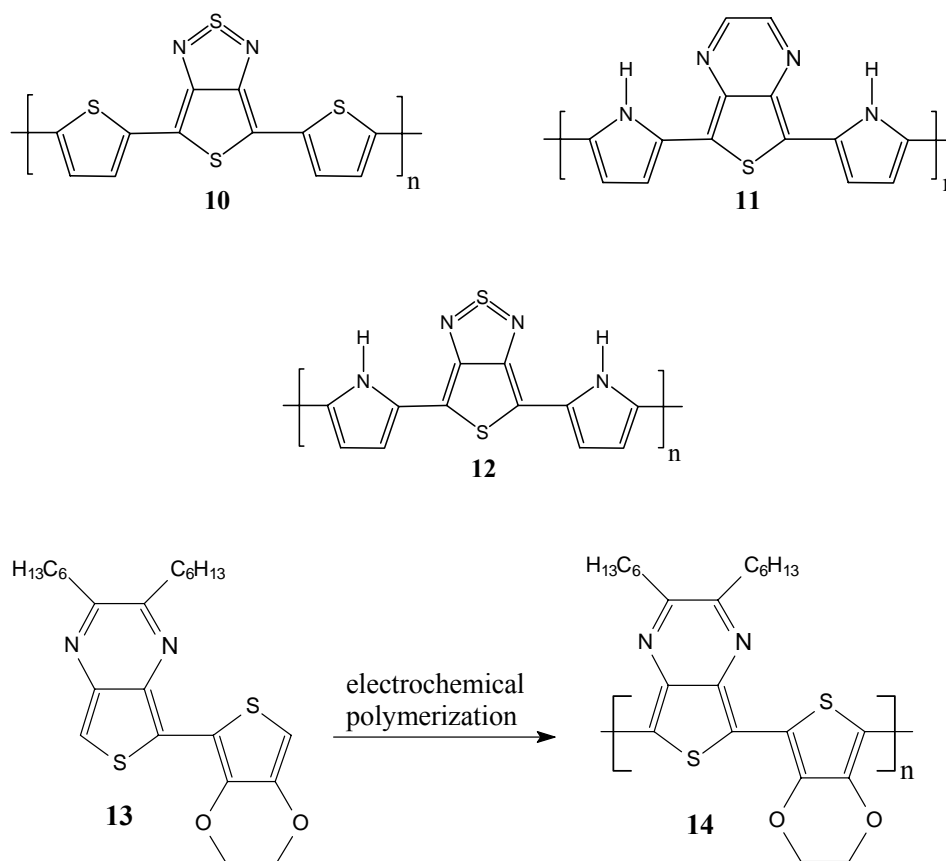


Scheme 1.1.

**Scheme 1.2.**

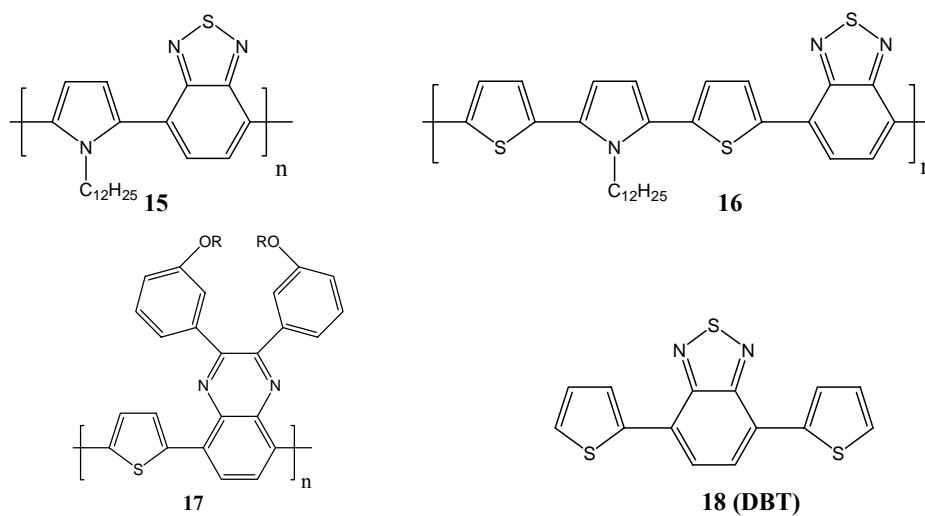
Yamashita and coworkers have reported a variety of low band gap polymers containing pyrazine or thiadiazole acceptor units, which are fused onto phenyl or thiophene rings.⁴³ The polymers in which the electron acceptor moieties are attached to a thiophene are known to have better reduction in band gaps. Since the coupling positions are part of a 5-membered thiophene ring, the electron donating sulfur atom will contribute more to the orbital coefficients. A number of trimeric thiophene derivatives have been synthesized in which the middle thiophene unit is fused with pyrazine or thiadiazole moieties which can subsequently be electropolymerized to the corresponding low band gap polymers **9** and **10**, respectively. The optical absorption and redox properties of **9** can be appreciably controlled by placing appropriate substituents on the pyrazine and thiophene rings. Compared to isothianaphthalene derivatives, the thienothiadiazoole moiety of the polymer **10** has a lower HOMO–LUMO gap. Excellent results were obtained by the electropolymerization of pyrrole-based monomers containing thienothiadiazoole or pyrazine as the acceptor and pyrrole as the donor leading to polymers **11** and **12**, respectively. Electropolymerization of a bithiophene monomer containing alternate pyrazine and dioxoethylene moieties resulted in a donor–acceptor polymer **14** with a reported band gap of 0.36 eV (Scheme 1.3).⁴⁴

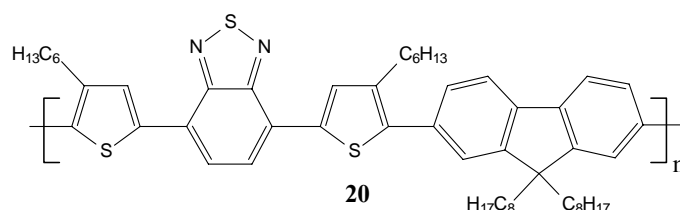
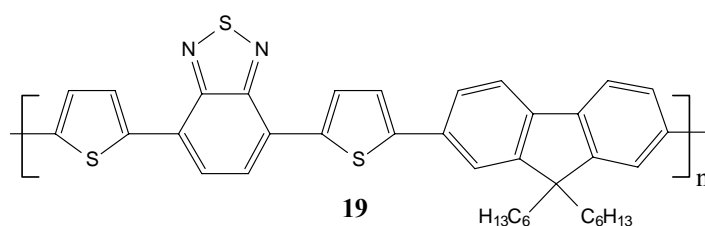




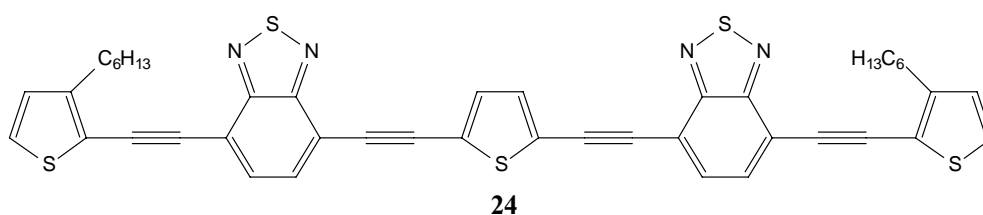
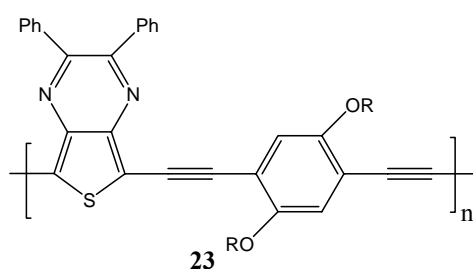
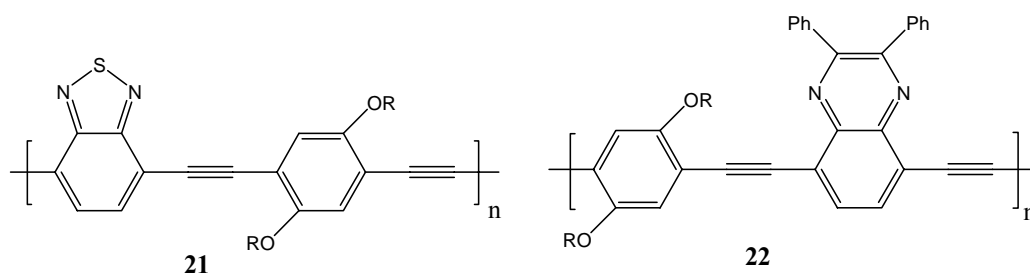
Scheme 1.3.

With in the class of low bandgap alternating D-A polymers, solution-processable materials are scarce and only few examples has been reported. Several processable conjugated polymers consisting of benzothiadiazole/quinoxaline and pyrrole/thiophene are reported in literature.⁴⁵⁻⁴⁷ Recently, many groups have reported alternating polymers of fluorene and 4,7-dithienyl-2,1,3-benzothiadiazole (DBT).⁴⁸⁻⁵³





Donor-acceptor aryl heterocyclic poly(heteroaryleneethynylene)s (PAEs) **21-23** containing benzothiadiazole/quinoxaline/thienopyrazine and 2,5-dialkoxy-*p*-phenylene units has been reported.^{19, 25, 54} These PAEs showed a strong tendency to form a stacked and ordered assembly in the solid state, presumably owing to the presence of the electron-accepting units and electron-donating units to give an intermolecular CT (charge transfer) interaction. Because of the molecular assembly, these polymers showed interesting optical properties. Kitamura et al. has also reported ethyne-linked pentamer **24** of 2,1,3-benzothiadiazole and thiophene.⁵⁵

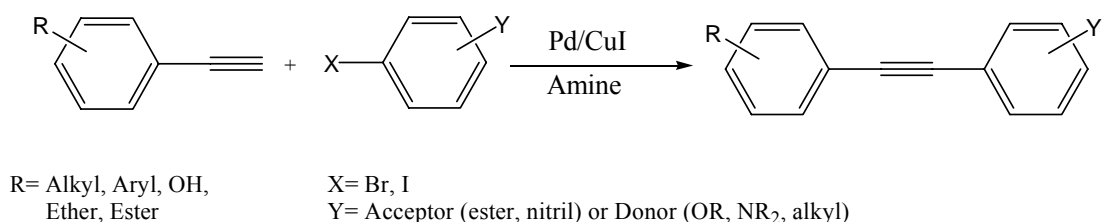


2 General Part

2.1 Mechanism of Sonogashira Cross-Coupling

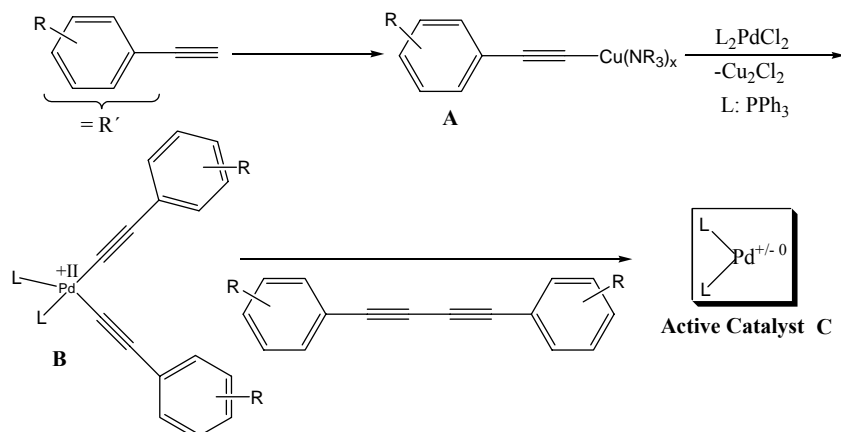
The Pd-catalyzed coupling of terminal alkynes to aromatic bromides or iodides in amine solvents has been known since 1975. It is called the Heck-Cassar-Sonogashira-Hagihara reaction and is probably one of the most frequently used C-C bond forming processes in organic chemistry.⁵⁶⁻⁵⁸ This coupling is powerful to form C-C single bonds between an sp- and an sp²-hybridized carbon center. The generally accepted mechanism of this reaction is depicted in Scheme 1 and will be discussed here with respect to its implications in polymer synthesis. In the first step (Scheme 2.2) two molecules of a cuprated alkyne, **A**, transmetalate the Pd catalyst precursor and form **B**. **B** is not stable under the reaction conditions but reductively eliminates a symmetrical butadiyne and creates the active catalyst **C**. In an oxidative addition the aromatic bromide or iodide forms the intermediate **D**, which after transmetalation with **A** leads to the diorgano-Pd species **E**. This species undergoes reductive elimination to the product and re-forms the active catalyst **C**.

1-Overall Reaction:

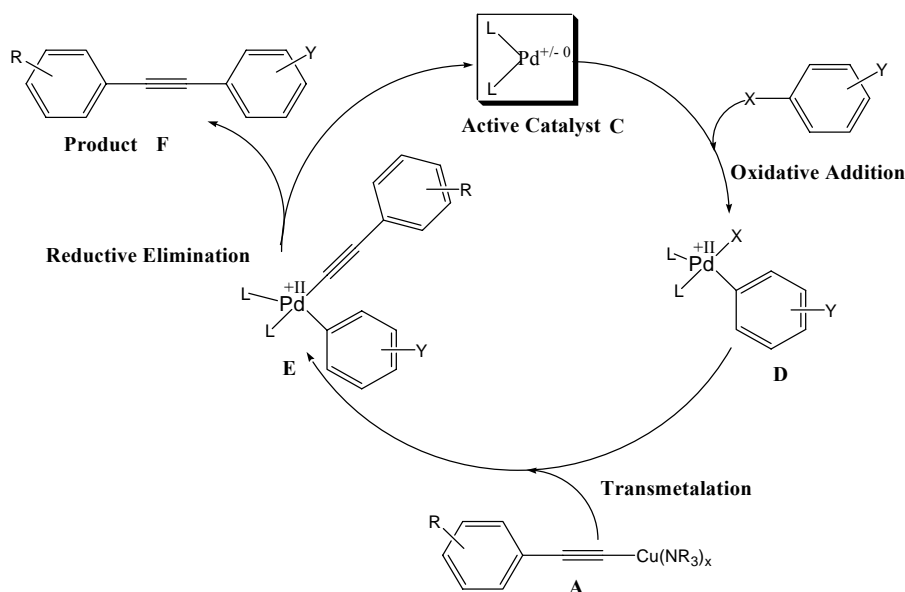


Scheme 2.1.

2- Catalyst Activation:



3- Catalytic Cycle:



Scheme 2.2. Mechanism of Sonogashira Coupling^{19f}

Both bromo- and iodoaromatic compounds work in this reaction. For aryl bromides, coupling have to be conducted at elevated temperatures, at approximately 80 °C. However, the corresponding iodides do react considerably faster, in quantitative yield, at room temperature. As a consequence polymer formation can be conducted under mild conditions when iodides are used, so that problems including cross-linking and formation of defects are minimized. With iodides the oxidative addition, i.e.; the formation of **D** is much more facile than with the corresponding bromides. The reason for that is probably both thermodynamic as well as kinetic in nature. If available, iodoarenes are the preferred substrates for Pd-catalyzed couplings. The active catalyst of type **C** is an electron-rich species, and as a consequence, oxidative addition, is dramatically influenced by the nature of the substituents Y on the aromatic nucleus. The more electron-withdrawing Y is, the faster its oxidative addition to the electron-rich Pd^0 proceeds. Most frequently 0.1-6 mol % $(Ph_3P)_2PdCl_2$ and varying amounts of CuI are used in both "organic" and polymer-forming reactions. The activation step (if using Pd^{2+}) uses up some of the alkyne present in the reaction mixture. It thus leads to an imbalanced stoichiometry and to the formation of 1-10% of the corresponding diyne during the activation step, depending upon the amount of catalyst used. That is no problem when making low-molecular-weight compounds. It necessarily decreases the molecular weight and the degree of polymerization (DP) if not a small excess of diyne is used in the reaction mixture. This will offset the amount of alkyne consumed by the Pd^{2+} precatalyst. However, the disadvantage of the approach is the presence of several

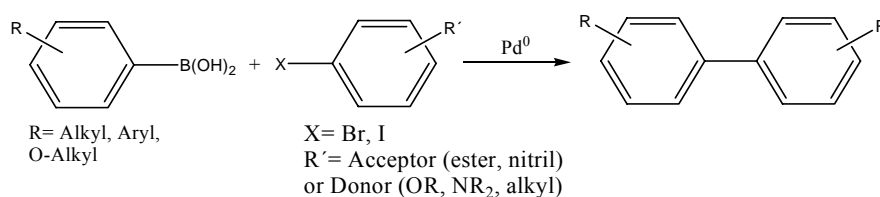
percent of butadiyne defects in the formed PAEs. To achieve butadiyne defect free structures, Pd⁰ as catalyst precursor should be used and trace amounts of oxygen have to be rigorously excluded. If Pd(PPh₃)₄ is employed with aromatic iodides at temperatures around 70 °C in diisopropylamine, this protocol can lead⁵⁹⁻⁶¹ to the formation of high-molecular-weight PPEs. However, even with a Pd⁰ catalyst source, Swager⁶⁰ reports that a small excess of bisalkyne has to be used to obtain high-molecular-weight materials. CuI as co-catalyst seems to be necessary for the conversion of dibromoarenes into the corresponding alkynylated products, but Linstrumelle⁶² demonstrated that if iodoarenes are coupled in the presence of a suitable amine, CuI can be omitted. The presence of CuI however does not seem to harm the progress of the reaction, and insofar it can always be added. Its proposed role is the formation of a copper(I) σ- or π-acetylide to activate the alkyne toward transmetalation.

A good choice of amine to couple aromatic iodides seems to be diisopropylamine, it seems to work particularly efficiently in combination with a Pd⁰ source such as (PPh₃)₄Pd at elevated temperatures. Generally, the yield and purity of the coupling products in the Heck-Cassar-Sonogashira-Hagihara reactions are very dependent upon the careful choice of amine and cosolvent. It was found that piperidine, pyrrolidine, and morpholine often work very well. Particularly piperidine is very powerful for these couplings and seems to outperform triethylamine in the case of the iodides. However, for unclear reasons, piperidine is not ideal for the coupling of aryl bromides to terminal alkynes. For bromides the amine bases, triethylamine and Hünig's base di(isopropyl)ethylamine are better choice.¹⁹ It is generally a good idea to conduct these reactions in concentrated or highly concentrated solutions to ensure fast coupling. However, in concentrated solutions the heat development of the reaction can be quite substantial, and mild cooling may be necessary. Sometimes it is desirable to add a cosolvent to ensure solubility of the formed polymer. Piperidine and triethylamine are not prime solvents for PPEs. THF, ethyl ether, and toluene have been used, but chloroform and dichloromethane should likewise work as additives.

2.2 Mechanism of Suzuki Cross-Coupling

The Pd-catalysed Suzuki–Miyaura (SM) coupling reaction⁶³ is one of the most efficient methods for the construction of C–C bonds. Although several other methods (e.g. Kharash coupling, Negishi coupling, Stille coupling, Himaya coupling, Liebeskind–Srogl coupling and Kumuda coupling) are available for this purpose, the SM cross-coupling reaction which produces biaryls has proven to be the most popular in recent times. The preference for the SM cross-coupling reaction above the other Pd-catalysed cross-coupling reactions is not incidental. The key advantages of the SM coupling are the mild reaction conditions and the commercial availability of the diverse boronic acids that are environmentally safer than the other organometallic reagents.^{64–71} In addition, the handling and removal of boron-containing by-products is easy when compared to other organometallic reagents, especially in a large-scale synthesis.

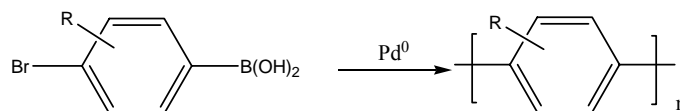
1-Overall Reaction



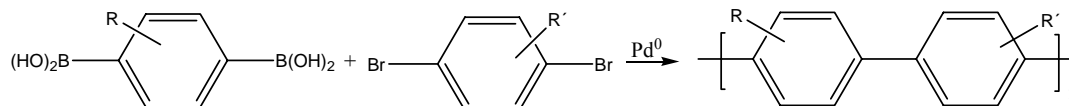
Scheme 2.3.

SM cross-coupling reaction is also used for polycondensation and can proceed in two ways as shown in scheme 2.4. In AB type,⁷² a bifunctional monomer leads to polycondensation, while AA/BB type polycondensation involves two types of monomers with different functionalities, yielding alternative copolymers.^{73, 74}

AB-Polycondensation

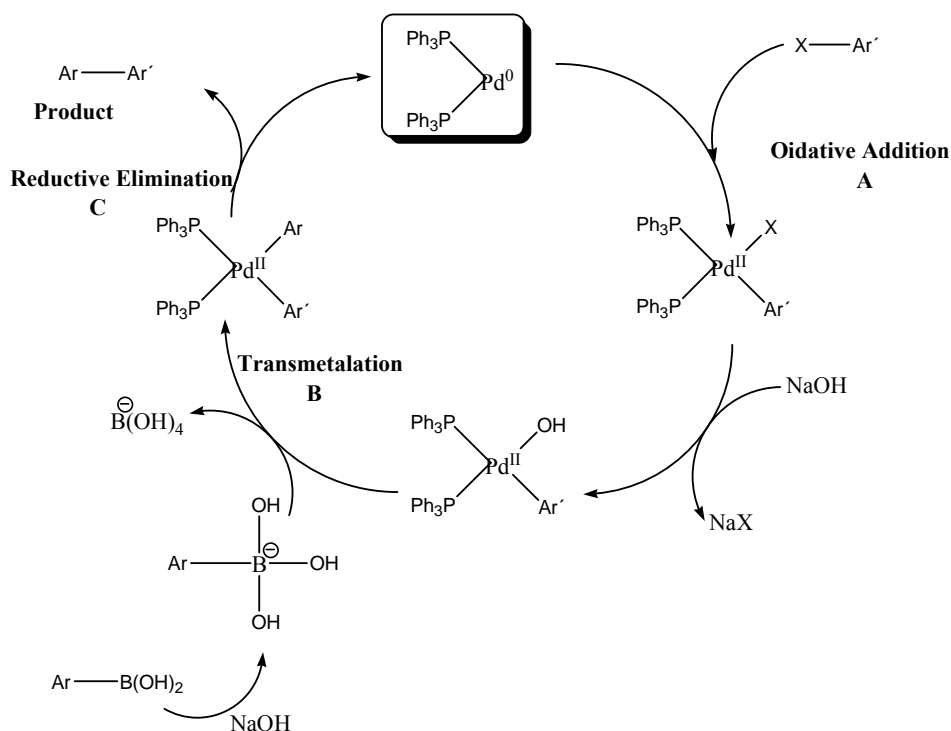


AA/BB-Polycondensation



Scheme 2.4.

2- Catalytic Cycle



Scheme 2.5. Mechanism of Suzuki Coupling

The general catalytic cycle for the cross-coupling of organometallics with organic halides catalysed by transition metals, which involves (a) oxidative addition, (b) transmetalation, (c) reductive elimination sequences, is widely accepted. Although a similar catalytic cycle has also been suggested for the Suzuki reaction,⁷⁵ it differs in that two equivalent bases are required (Scheme 2.5). The coupling reaction of organic boron compounds proceeds only in the presence of bases. This is due to the fact that the organic group on boron is not nucleophilic enough for the transfer from the boron to the palladium in the transmetalation step because of the strong covalent character of the B-C bond in boron compounds. Therefore, it is necessary to increase the carbanion character of organic groups by the formation of an organoborate with a tetravalent boron atom, which utilizes base. Further, it is known that bases substitute for Pd-X to form Pd-OH (or Pd-OR) which has higher activity. Thus, the transmetalation reaction in the Suzuki reaction is favored by the formation of both four-coordinated boron compounds and Pd-OH (or Pd-OR).

Aryl halide and aryl triflate function as electrophiles whose reactivity order is Ar-I > Ar-Br > Ar-OTf >> Ar-Cl. Aryl chlorides are usually not reactive enough, with the exception of those having heteroaromatic rings and electron-withdrawing groups. This is because the oxidative addition of aryl chlorides to palladium complexes is too slow to develop the catalytic cycle. A recent paper showed that the use of nickel catalysts for the cross-coupling reaction with aryl

chlorides obtained favorable results.⁷⁶ Although the most often used catalyst in the Suzuki reaction is $\text{Pd}(\text{PPh}_3)_4$, various palladium catalysts are also employed, such as $\text{Pd}(\text{dppb})\text{Cl}_2$, $\text{PdCl}_2(\text{PPh}_3)_2$, $\text{Pd}(\text{OAc})_2$ and PdCl_2 etc. $\text{PPh}_2(\text{m-C}_6\text{H}_4\text{SO}_3\text{Na})$ is used as phosphine ligand when the reaction is carried out in aqueous solvent. For example, the cross coupling reaction using the water-soluble palladium complex $\text{Pd}[\text{PPh}_2(\text{m-C}_6\text{H}_4\text{SO}_3\text{Na})]_3$ between sodium 4-bromobenzenesulfonate and 4-methylbenzeneboronic acid obtained the corresponding biaryl in good yield,⁷⁷ compared to using $\text{Pd}(\text{PPh}_3)_4$ in a two-phase organic solvent. Bases are always required in the Suzuki reaction as opposed to the coupling reaction using organotin or organozinc reagents. The best results are achieved with the use of a relatively weak base and Na_2CO_3 is a most frequently used. However, the strong bases such as $\text{Ba}(\text{OH})_2$ and K_3PO_4 are efficient in reactions involving steric hindrances.

It is known that the base is involved in the coordination sphere of the palladium and the formation of the $\text{Ar-PdL}_2\text{-OR}$ from $\text{Ar-PdL}_2\text{-X}$ is known to accelerate the transmetalation step. There are some drawbacks with the Pd-mediated SM cross coupling reaction. Only aryl bromides and iodides can be used, as the chlorides only react slowly. Some of the recent results to overcome this problem are addressed by Kotha et al. in a review.⁷⁸ By-products such as self-coupling products, coupling products of phosphine-bound aryls, are often formed. The most frequently used catalyst, $\text{Pd}(\text{PPh}_3)_4$, suffers from this drawback and the phenyl group of the PPh_3 becomes incorporated in the products giving scrambled derivatives. A bulky phosphine ligand $(\text{o-MeOC}_6\text{H}_4)_3\text{P}$ is sufficient to retard this type of side-reactions and deliver high yields of the desired product. Under oxygen-free conditions, homocoupling products can be avoided and, in order to remove the dissolved oxygen, it is desirable to de-gas the solvents by a suitable method.

2.3 Basics of Polycondensation

The classical subdivision of polymers into two main groups was made around 1929 by W. H. Carothers, who proposed that a distinction be made between polymers prepared by the stepwise reaction of monomers (condensation polymers) and those formed by chain reactions (addition polymers).

One basic simplifying assumption proposed by Flory, was that all functional groups can be considered as being equally reactive. This implies that a monomer will react with both monomer or polymer species with equal ease.

Carothers Equation

W. H. Carothers, pioneer of step-growth reactions, proposed a simple equation relating number-average degree of polymerisation \bar{P}_n to a quantity p describing the extent of the reaction for linear polycondensations or polyadditions.

If N_0 is the original number of molecules present in an A-B monomer system and N the number of all molecules remaining after time t , then the total number of the functional groups of either A or B which have reacted is $(N_0 - N)$. At that time t the extent of reactivity p is given by

$$P = (N_0 - N)/N_0 \quad \text{or} \quad N = N_0(1 - p)$$

If we remember that $\bar{P}_n = N_0/N$, a combination of expression gives the Carothers equation,

$$\bar{P}_n = 1/(1 - p) \quad \text{(Eq. 2.1)}$$

The Carothers equation is particularly enlightening when we examine the numerical relation between \bar{P}_n and p ; thus for $p = 95\%$, $\bar{P}_n = 20$ and when $p = 99\%$, then $\bar{P}_n = 100$. Graphically Carothers equation can be represented as mentioned below.

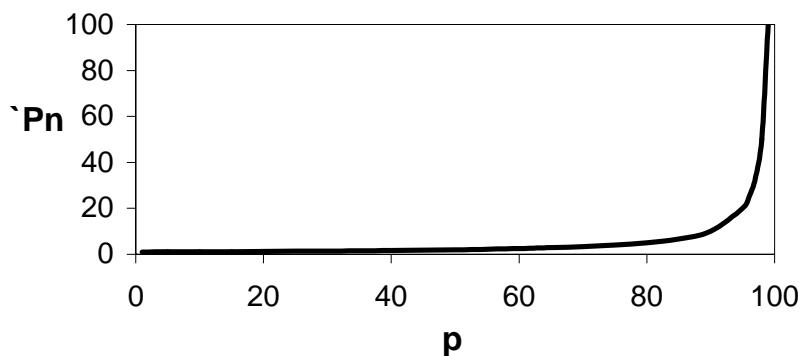


Figure 2.1. Graphical presentation of Carothers equation.

This equation is also valid for an A-A + B-B reaction when one considers that in this case there are initially $2N_0$ molecules. More usefully, a precisely controlled stoichiometry is required and stoichiometric factor r can be added to Carothers equation and extended form can be expressed as

$$\bar{P}_n = (1 + r)/(1 + r - 2rp); \quad r = n_A/n_B \leq 1 \quad \text{(Eq. 2.2)}$$

where r is the ratio of the number of molecules of the reactants.⁷⁹

3 Results and Discussion

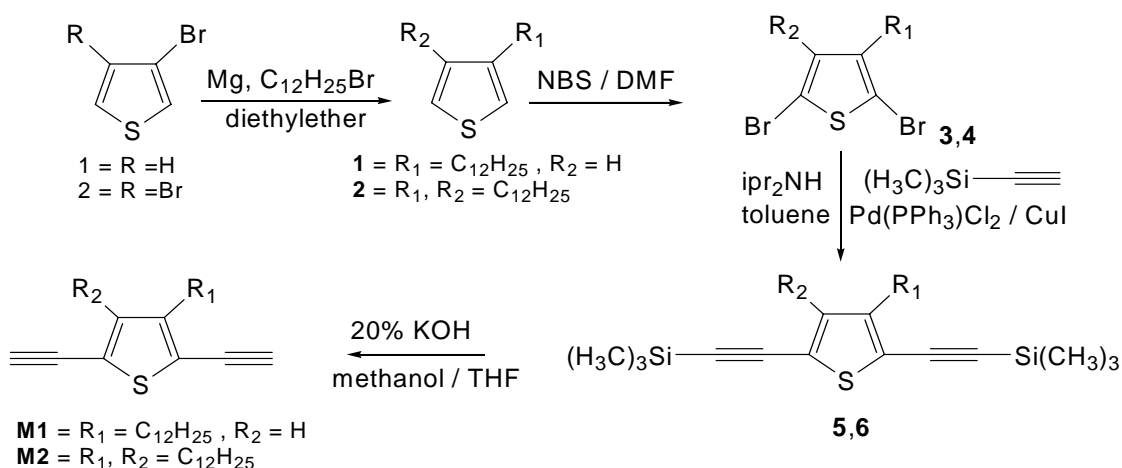
3.1 Monomer Synthesis

3.1.1 Diethynyl Monomers

3.1.1.1 2,5-Diethynyl Alkyl Substituted Thiophenes

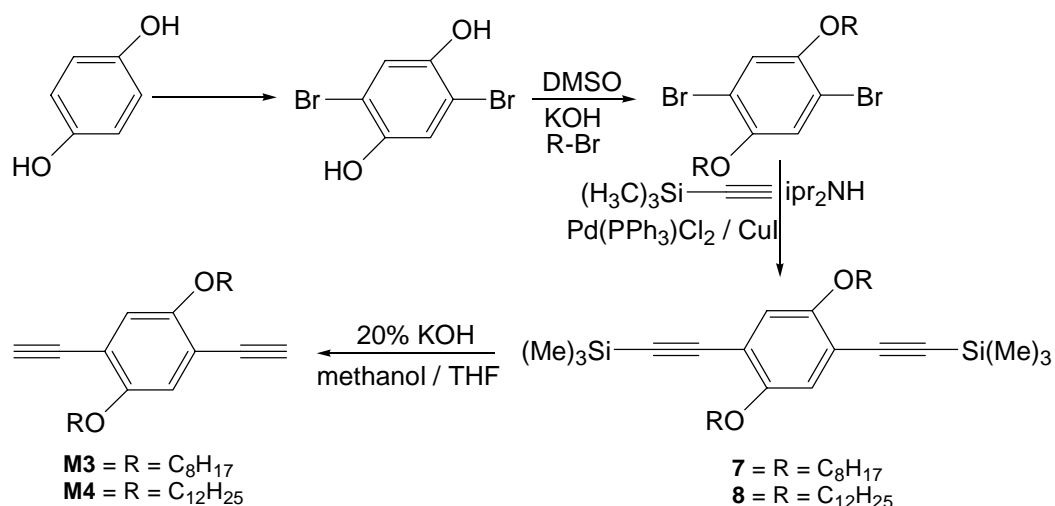
In recent years, a wide variety of the thiophene (Th) derivatives have been synthesized, because of their high susceptibilities to the light and electronic stimulations, in order to develop new functional organic materials such as opto-electronic devices.⁸⁰ The oligomers and polymers of thiophene tend to form aggregates, and in the solid state they display a great diversity of conformation and packing.⁸¹ The nature of the interactions driving the self-assembly of these compounds is not yet well understood. Since the electronegativity of sulfur is very close to that of carbon, there are not hydrogen-bonding interactions of the type as those observed, for example, in polypyrroles as a recurrent motif involving the nitrogen atom.⁸² The analysis of the conformation and packing in single crystals of thiophene oligomers and polymers indicates that both are determined by the interplay of numerous, weak, and directional interactions (S...S, C-H...S, C-H... π , van der Waals and stacking interactions) whose balance varies case by case.⁸³ There are conflicting requirements for the optimisation of charge transport or fluorescence in these compounds, as optimization of charge transport requires crystalline morphologies, high molecular ordering, and close packing of the molecules, which are instead detrimental to fluorescence.

2,5-Diethynyl alkyl substituted thiophenes were prepared by known literature.⁸⁴ Starting from 3-bromothiophene or 3,4-dibromothiophene, respective alkyl substituted thiophenes were prepared by Kumada coupling reaction in high yields. Bromination of these alkyl substituted thiophenes were achieved by NBS in DMF in dark. By Sonogashira cross coupling reaction of bromo derivatives with trimethylsilylacetylene and finally deprotection led to the monomers **M1** and **M2** as reddish yellow liquids respectively in quantitative yield. (Scheme 3.1)

Scheme 3.1. Synthesis of monomers **M1** and **M2**.

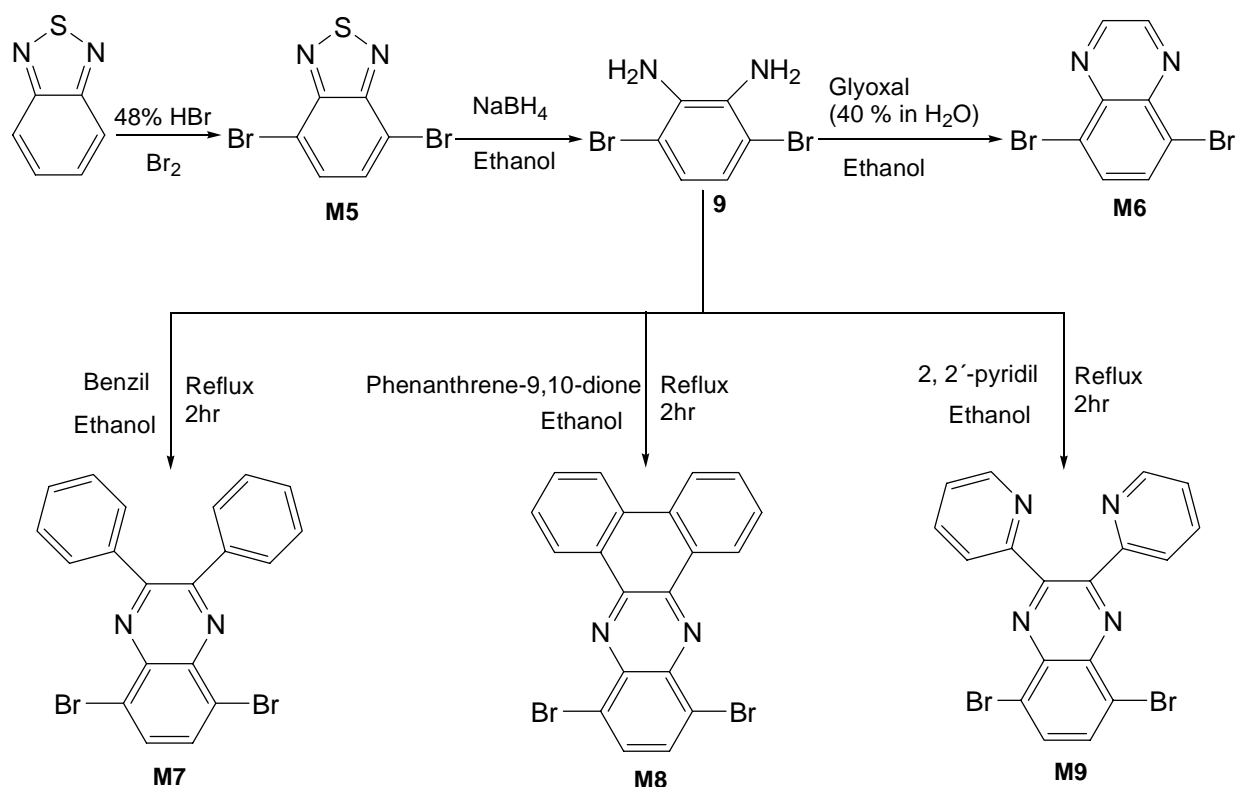
3.1.1.2 1,4-Diethynyl-2,5-Dialkoxy Substituted Phenylenes

Similarly the 1,4-diethynyl-2,5-dialkoxybenzene monomers (**M3** and **M4**) were prepared according to known literature.⁸⁵ (Scheme 3.2)

Scheme 3.2. Synthesis of monomers **M3** and **M4**.

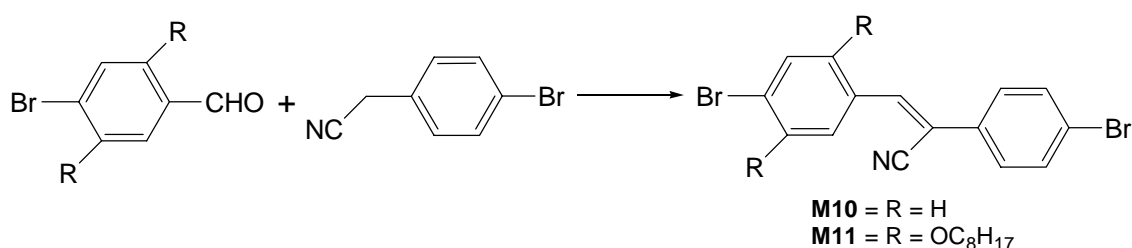
3.1.2 Dibromo Monomers

Starting from 2,1,3-benzothiadiazole, 4,7-dibromo-2,1,3-benzothiadiazole (**M5**) was prepared by bromination of 2,1,3-benzothiadiazole in 48% HBr.⁸⁶ To obtain the quinoxaline derivatives, 4,7-dibromo-2,1,3-benzothiadiazole is reduced by NaBH₄ in absolute ethanol to 2,3-diamino-1,4-dibromobenzene (**9**).⁸⁶ The condensation of the amine with respective diones in absolute ethanol yielded respective quinoxalines (**M6-M9**).^{86c, d} (Scheme 3.3)



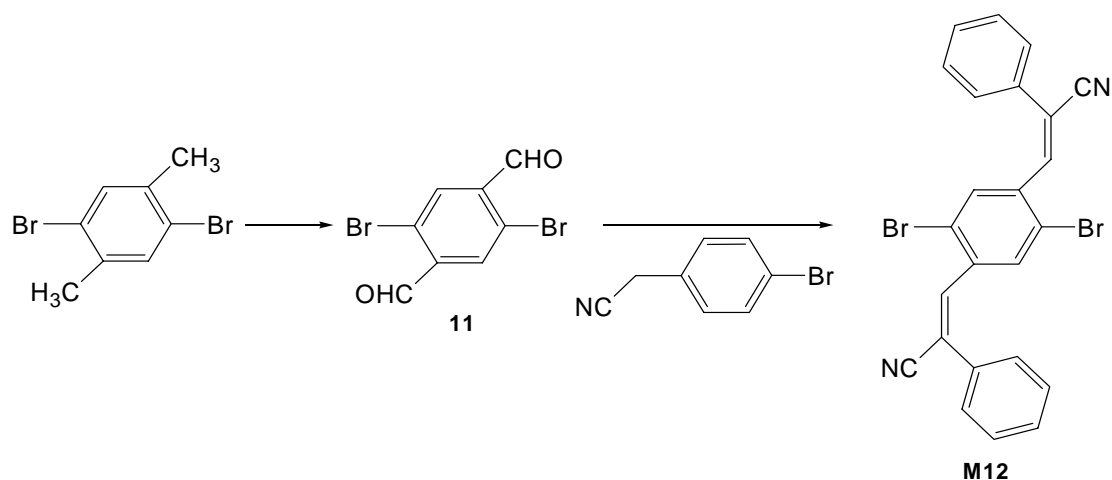
Scheme 3.3. Synthesis of monomers **M5–M9**.

To prepare cyanovinylenes (**M10**, **M11**) p-bromophenylacetonitrile is coupled with 4-bromobenzaldehyde or 4-bromo-2,5-dioctyloxy benzaldehyde (**10**)⁸⁷ by Knoevenagel condensation. **M10** is a white powdered material,⁸⁸ while **M11** is obtained as a bright yellow powder.



Scheme 3.4. Synthesis of monomers **M10** and **M11**.

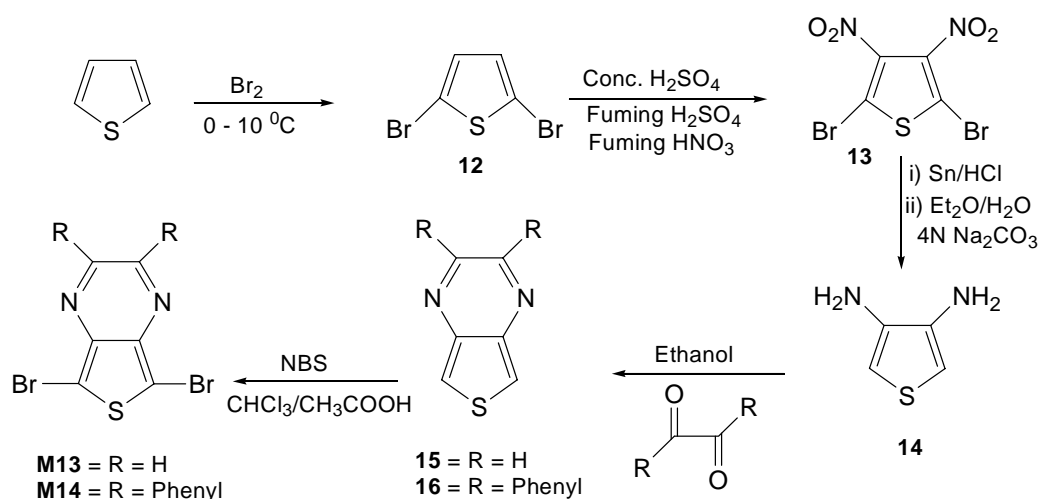
Similarly, 1,4-dibromo-p-xylene was converted to 2,5-dibromobenzene-1,4-carbaldehyde (**11**).⁸⁹ By the Knoevenagel condensation of **11** and phenylacetonitrile in toluene and tert-butanol, a fibrous yellow material (**M12**) in good yield was obtained.



Scheme 3.5. Synthesis of monomer **M12**.

Thieno[3,4-*b*]pyrazine and its 2,3-disubstituted analogues can be readily synthesized from thiophene as shown in Scheme 1.^{54, 90} Compound **13** was readily produced by the nitration of **12** via fuming HNO₃ and H₂SO₄. Without the use of the fuming acids, only the mononitro product was produced. Likewise, an extended 3h reaction time was required, as lesser times resulted in mixtures of mono- and dinitro- products. Treatment of **13** with Sn and HCl, both reduced the NO₂ functionalities and removed the Br protecting groups. As the reduction was carried out under acidic conditions, the isolated precipitate is the diammonium salt of **14**. The isolated 3·2H⁺ salt was purified by diethyl ether and acetonitrile washes.^{90d} To obtain **14**, the salt is taken in diethyl ether and water (1:1) at 0 °C and basify it with 4N Na₂CO₃. The amine is highly hygroscopic and has to be subsequently used in next step.

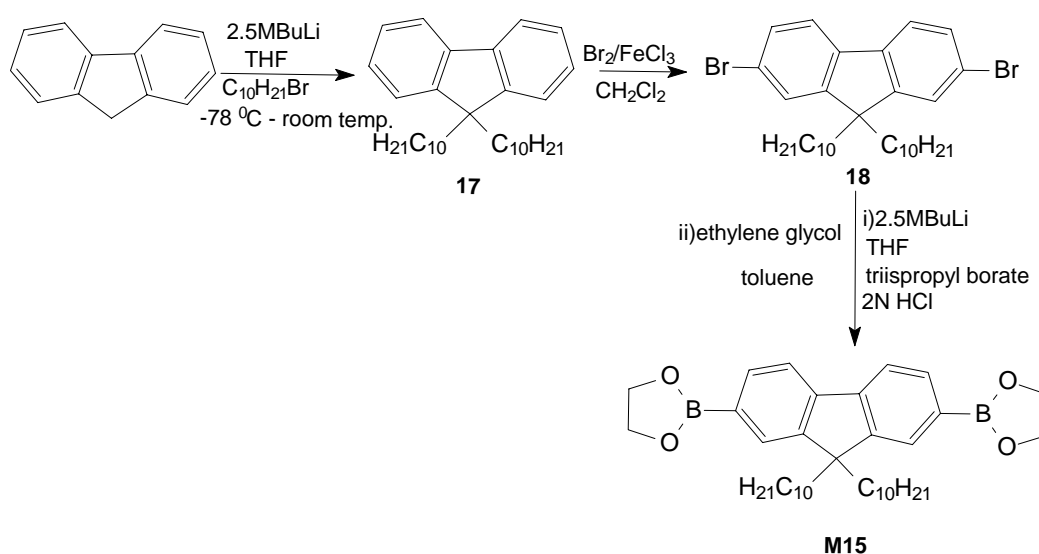
Condensation of **14** with the α -diones readily occurred at room temperature in an ethanol solution for 24h and the thieno[3,4-*b*]pyrazines (**15** and **16**) were recovered in higher yields. Obtained yields are relatively lower when amine is condensed with the α -diones, due to instability of amine. To overcome this problem we have treated the diammonium salt with diones in ethanol and higher yields were obtained. The initially isolated products were all relatively free of impurities, and analytical samples could be prepared by either recrystallization or chromatography. The dibromo derivatives were prepared by bromination of **15** and **16** using NBS in CHCl₃/CH₃COOH (1:1) in dark under argon.



Scheme 3.6. Synthesis of monomers **M13** and **M14**.

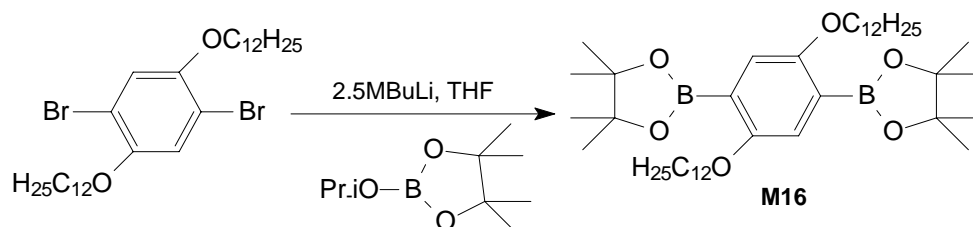
3.1.3 Dioxaborolane Monomers

2,7-Dioxaborolan-9,9-didecylfluorene (**M15**) was synthesized by reported literature.^{67, 72, 91} Starting from commercially available fluorene, 9,9-didecylfluorene (**17**) was prepared, 2.5M butyl lithium (BuLi) in hexanes was added slowly to a THF solution of fluorene at -78°C and 1-bromodecane was added slowly at this temperature. Treatment of **17** with bromine in presence of iron chloride in dichloromethane at 0°C in dark yields 2,7-dibromo-9,9-didecylfluorene (**18**). 9,9-Didecylfluorene-2,7-diboronic acid was obtained in good yield by reaction of **18** with BuLi and then triisopropyl borate was added slowly at -78°C and the reaction mixture was quenched by HCl after 24h. Treatment of obtained diboronic acid with ethylene glycol in toluene in a dean stark apparatus yields 2,7-Dioxaborolan-9,9-didecylfluorene (**M15**).



Scheme 3.7. Synthesis of monomer **M15**.

Almost similar procedure is followed as above mentioned for conversion of 2,7-dibromo-9,9-didecylfluorene (**18**) to 9,9-Didecylfluorene-2,7-diboronic acid, here instead of triisopropyl borate, 2-isopropoxy-4,4,5,5-tetramethyl-[1,3,2]dioxaborolane is used and after 24h room temperature stirring the organic phase is extracted with diethyl ether, washed with brine and dried. The crude product **M16** is recrystallized from ethyl acetate.⁹²



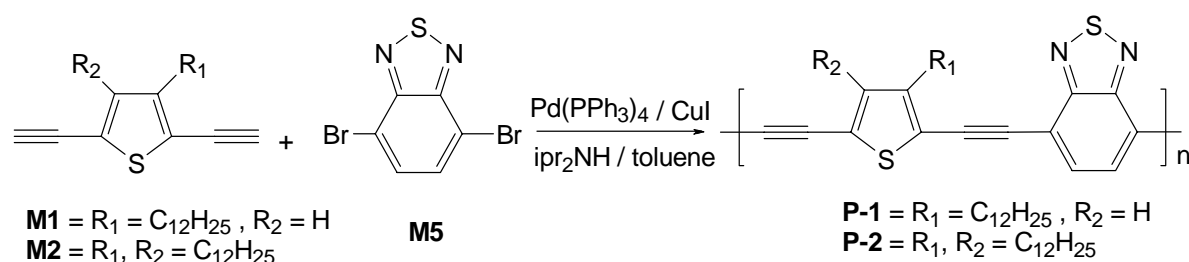
Scheme 3.8. Synthesis of monomer **M16**.

3.2 Benzothiadiazole and Thiophene Based Poly(heteroaryleneethynylene)s

The 2,1,3-benzothiadiazole unit is a typical electron-accepting unit,⁸⁶ and its homopolymer and copolymers have been synthesized; the benzothiadiazole unit^{86,93} is useful to tune electronic states of π -conjugated polymers as in the cases of the copolymers with fluorene, carbazole, and thiophene.⁴⁵⁻⁵³ Kitamura et al.⁵⁵ has reported a pentamer of thiophene and 2,1,3-benzothiadiazole by Sonogashira methodology. Recently several groups have reported 2,1,3-benzothiadiazole and alkoxy phenylene based PAEs.^{19,25,93d} Using the poly(D-A) approach, this requires the use of moderately strong donors and acceptors along the chain.

3.2.1 Synthesis and Characterization of the Polymers

The general synthetic routes towards the polymers are outlined in Scheme 3.9. By employing the Pd catalysed Sonogashira coupling,^{56,58} the polymers (**P-1** and **P-2**) were synthesized from thiophene diacetylenes (**M1** and **M2**) and 4,7-dibromo-2,1,3-benzothiadiazole **M5**.⁸⁶ Yields of the both polymers were higher than 75%. The polymer **P-1** is red, while the **P-2** is violet in colour. **P-1** was not completely soluble in organic solvents like THF, CHCl₃ and toluene etc., only 50 % of the polymer was soluble and used for further studies. So in this case the polycondensation time was shortened up to 8h to get maximum soluble polymer (about 80%). Less solubility is might be due to presence of only one alkyl chain on thiophene moiety, **P-2** is soluble in common organic solvents (THF, CHCl₃ etc.).



Scheme 3.9. Synthesis of Polymers **P-1** and **P-2**.

The chemical structure of the polymers was confirmed by FTIR, ¹H, ¹³C NMR and elemental analysis. In FTIR the strong $\nu(\text{C}\equiv\text{CH})$ peak near 3290 cm⁻¹ of the monomers disappeared on polycondensation, and a new $\nu(\text{C}=\text{C})$ peak appeared at about 2200 cm⁻¹. ¹H NMR data were consistent with the proposed structure of the polymers. Compared with the ¹H NMR peaks of monomers, those of the polymers were broadened and somewhat shifted to a lower magnetic field. The ¹H NMR spectra of **P-1** in CDCl₃ showed two peaks indicating two protons of

benzothiadiazole and one proton of thiophene units at $\delta = 7.80$ and 7.10 ppm respectively. While that of $-\text{CH}_2$ protons adjacent to thiophene ring appeared at $\delta = 2.92$ and other alkyl side chain protons signals were present at $\delta = 1.75$ - 0.90 ppm. Presence of only one signal for thiophene moiety indicates that the polymer is highly regioregular and main combination of monomers is HT (head to tail) type. The ^1H NMR data is comparable with that of reported one for other regioregular thiophene polymers.⁹⁴

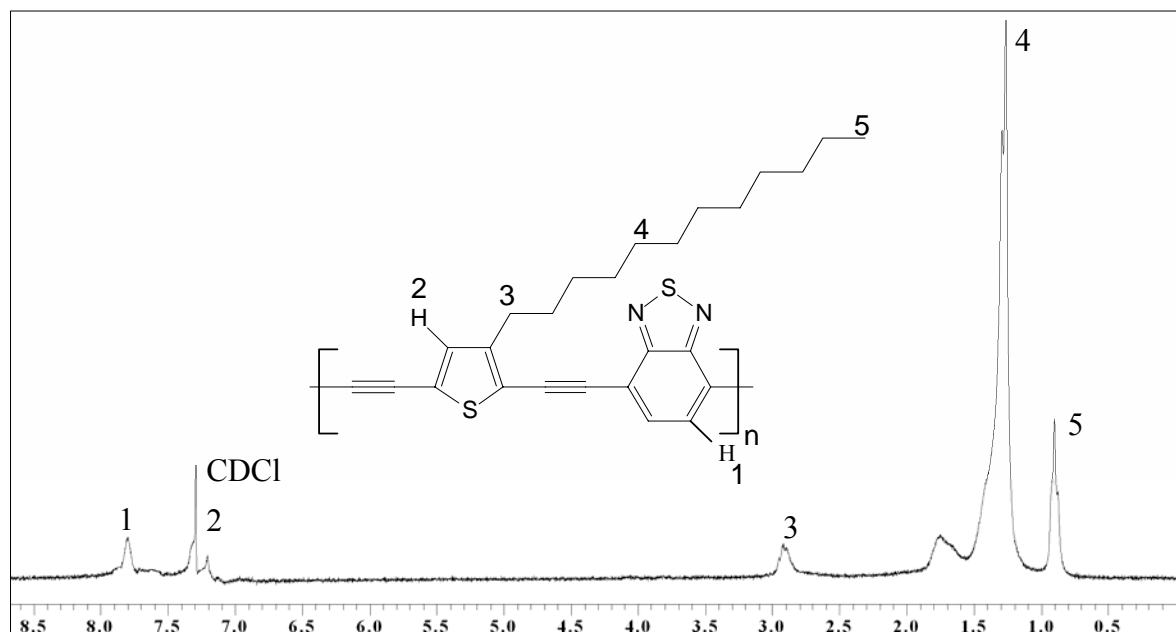


Figure 3.1. ^1H NMR of **P-1**.

Similarly the ^1H NMR spectra of **P-2** in CDCl_3 showed one peak indicating two protons of benzothiadiazole unit at $\delta = 7.70$ ppm. While that of $-\text{CH}_2$ protons adjacent to thiophene ring appeared at $\delta = 2.83$ and other alkyl side chain protons signals were present at $\delta = 1.68$ - 0.83 ppm (Figures 3.1 and 3.2).

The ^{13}C NMR spectra of **P-1** and **P-2** showed the thiophene and benzothiadiazole carbons signals between 155 to 117 ppm. The signals due to the triple bond carbons were present between $\delta = 94.7$ and 91.0 ppm. The alkyl carbons signals appeared upfield between 32.4 and 14 ppm. The peaks due to terminal $-\text{C}\equiv\text{CH}$ in ^1H NMR and ^{13}C NMR spectra were absent. In ^{13}C NMR spectra the signals oxidative coupling reaction of acetylenes to diacetylenes ($-\text{C}\equiv\text{C}-$) between 80 to 70 ppm were absent, indicating no diyne defects in structures.

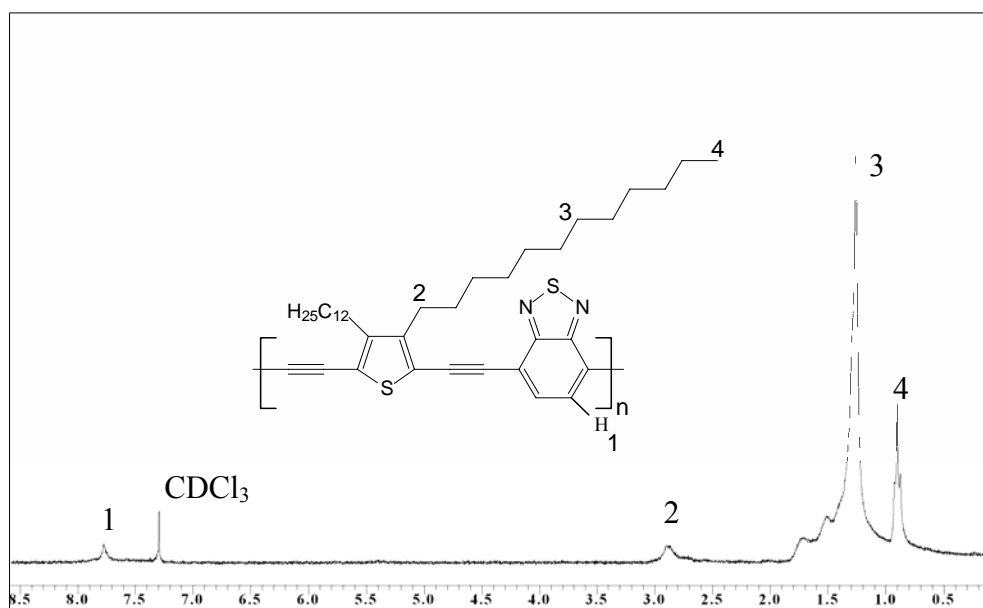


Figure 3.2. ^1H NMR of **P-2**.

The average molecular weights were determined by GPC with polystyrene as standards. The THF served as eluting solvent. The number-average molecular weight \bar{M}_n values were 5900 g/mol (polymer **P-1**) and 16400 g/mol (polymer **P-2**) leading to degree of polymerisation of 14 and 27 respectively. The polydispersity indices (PDI) were found between 2.7 and 5.0 respectively. For further confirmation, \bar{M}_n of **P-2** was also measured by VPO (vapour pressure osmometry), both values by GPC and VPO, are comparable to each other. Data from GPC and VPO are given in Table 3.1.

Table 3.1. GPC and VPO data of polymers **P-1**, **P-2**.

Polymer	\bar{M}_n [g/mol]	\bar{M}_w [g/mol]	M_w/M_n	\bar{P}_n	Yield (%)
P-1	5900 ^a	15900	2.71	14	83
P-2	16400 ^a (16200) ^b	82600	5.04	27	78

^a \bar{M}_n , GPC (polystyrene standards).

^b \bar{M}_n , VPO (vapour pressure osmometry).

Thermogravimetric analysis carried out at a heating rate of 10 K/min under air indicates high thermal stability of polymers **P-1** and **P-2** (Figure 3.3). Thermal decomposition starts around 350 °C, where approximately 5% weight loss was recorded. The polymer **P-1** exhibit comparatively higher thermal stability.

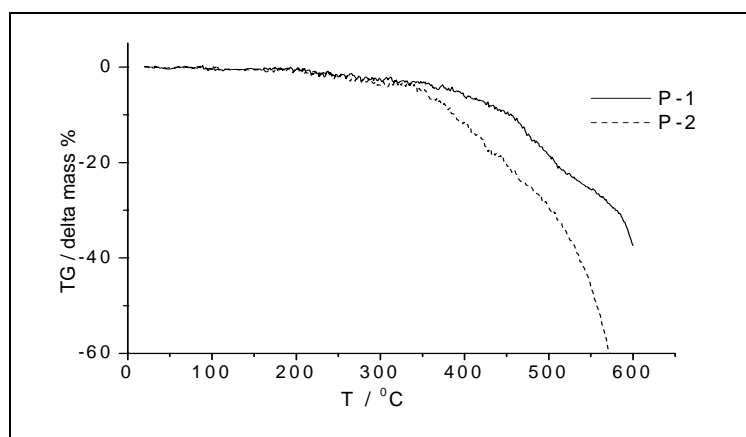


Figure 3.3. TGA of polymers **P-1**, **P-2**.

3.2.2 Optical Properties

The photophysical characteristics of the polymers were investigated by UV-vis absorption and photoluminescence in dilute chloroform solution as well as in solid (films). Results from the absorption and emission spectra are summarized in Table 3.2. Figures 3.4 and 3.5 show the absorption and emission spectra of polymers **P-1** and **P-2**. The absorption maximum of **P-2**, at $\lambda_{\max, \text{abs}} = 540 \text{ nm}$ ($\epsilon = 45800 \text{ L. mol}^{-1} \cdot \text{cm}^{-1}$) is 36 nm red-shifted relative to that of **P-1**, at $\lambda_{\max, \text{abs}} = 504 \text{ nm}$ ($\epsilon = 43900 \text{ L. mol}^{-1} \cdot \text{cm}^{-1}$). The differences in absorption are probably due to more

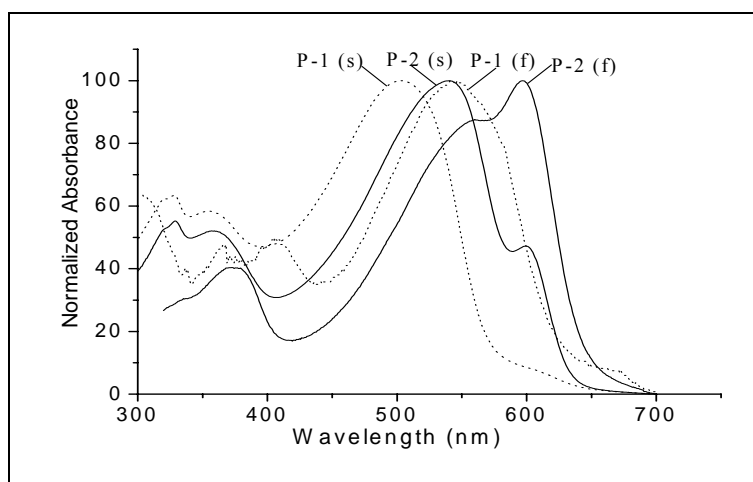


Figure 3.4. Normalized UV-vis spectra of **P-1** and **P-2** in solution (CHCl_3 10^{-7} mol) and in solid state (film from chlorobenzene) (**P-1** in dotted lines) (**P-2** in solid lines) (f = film, s = solution).

planar structure of **P-2** and hence an increase in effective conjugation length. Both **P-1** and **P-2** show a strong red shift of λ_{\max} (approximately 45-60 nm) when spin cast into thin films on quartz substrate from a chlorobenzene solution. **P-1** and **P-2** have their solid-state absorption

bands centered at $\lambda_{\max, \text{abs}} = 547$ nm and 596 nm respectively. This red shift observed when going from solution to a solid film and the appearance of some vibronic structure in the spectra of **P-1** and **P-2** is similar to that observed for poly(3-alkylthiophenes).^{94a,95} This indicates interchain interactions due to stacking of the polymers in the solid state, possibly assisted by planarization and with it an increase of conjugation length.⁹⁶

Stacking of poly(aryleneethynylene)⁹⁷ with a charge transfer structure⁹⁸ was also reported previously, and it caused red shift of the UV-vis absorption band of the polymers. It is important to note that we established that shift of absorption onset of **P-1** and **P-2** is not due to partial oxidation under ambient conditions and that the spectra corresponds to those of pristine materials.

Table 3.2. UV-Vis Data of polymers **P-1** and **P-2** in Dilute CHCl_3 Solution and in Solid State (Thin Films of 100-150 nm Thickness Spin-Casted from Chlorobenzene Solution).

Polymer	UV-vis λ_{\max} , nm				E_g opt. eV ^c	
	CHCl_3 [log ϵ] ^a	$\lambda_{0.1\max}$	film ^b	$\lambda_{0.1\max}$	CHCl_3	film
P-1	504 [4.0]	597	547	638	2.08	1.95
P-2	540, 599 ^{sh} [4.2]	636	596	670	1.95	1.85

^aMolar absorption coefficient. Molarity is based on the repeating unit. ^bSpin coated from chlorobenzene solution. ^c E_g opt. = $hc / \lambda_{0.1\max}$. ^{sh} shoulder.

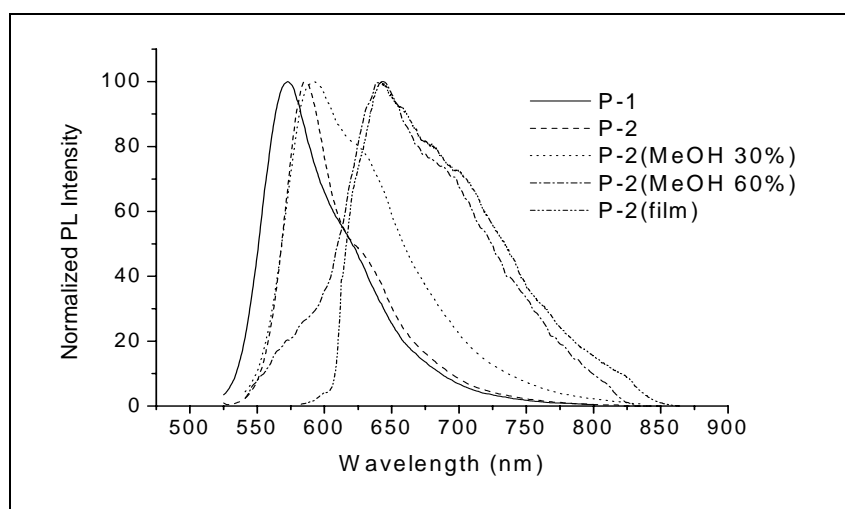
The thin film absorption spectra show that for **P-1** and **P-2** the onset of the absorption is ~638 nm (1.95 eV) and ~670 nm (1.85 eV) respectively. As anticipated, the alternation of electron-rich thiophene and electron-deficient benzothiadiazole units along conjugated backbone results in a low optical band gap. The emission maximum of **P-1** in dilute chloroform solution is at $\lambda_{\max, \text{em}} = 573$ nm, while the emission curve of **P-2**, showing its maximum at $\lambda_{\max, \text{em}} = 585$ nm, are almost identical to each other. The fluorescence quantum yields were found to be around 36 and 41% for **P-1** and **P-2** respectively. The emission maximum of **P-2** in solid film is located at $\lambda_{\max, \text{em}} = 642$ nm leading to Stokes shift of 40 nm, and a lower fluorescence quantum yield of 4% (Figures 3.4 and 3.5).

Table 3.3. Photoluminescence Data of **P-1** and **P-2** in Dilute CHCl_3 Solution ($\sim 10^{-7}$ M) and in Solid State.^a

Polymer	UV-em λ_{em} , nm		Stokes shift, nm		% ϕ_{PL}	
	CHCl_3	film	CHCl_3	film	CHCl_3	film
P-1	573		69		36	
P-2	585	642	45	46	41	4

^bSpin coated from chlorobenzene solution.

We assumed, the reason for the low photoluminescence (PL) efficiency is a π - π stacking of the conjugated backbone cofacial to each other due to the favourable inter-chain π - π interactions, which lead to a self-quenching process of the excitons.⁹⁹⁻¹⁰¹ Triple-bonds in the polymer main chain (like in poly(aryleneethynyls)) lead to stiffness and rigidity of the polymer backbones, which thereby reinforce the inter-chain interactions.¹⁰² Moreover inner heavy-atom effects of bromo end groups can possibly also contribute to the deactivation of the excitons in the solid state.¹⁰³

**Figure 3.5.** Normalized emission spectra of **P-1** and **P-2** in solution ($\text{CHCl}_3 10^{-7}$ mol) and **P-2** in solid state (film from chlorobenzene) and in different concentration of Methanol.

3.2.3 Aggregate Formation in Solvent/Nonsolvent Solution

The absorption and emission spectra of polymers **P-1** and **P-2** in chloroform/methanol mixtures with different volume concentrations of methanol are shown in Figures 3.6 and 3.7, respectively. It should be noted here that in all cases the bulk solution maintains homogeneity. With an increase of methanol concentration, the maximum absorption of the polymer shifts from 540 nm observed in pure chloroform to 594 nm in case of **P-2** and only slight shift was observed in case

of **P-1** from 504 to 515 nm and appearance of a shoulder at higher wavelength. When the methanol concentration reaches 50 vol %, the 594 nm band becomes stronger than the 540 nm band in **P-2**.

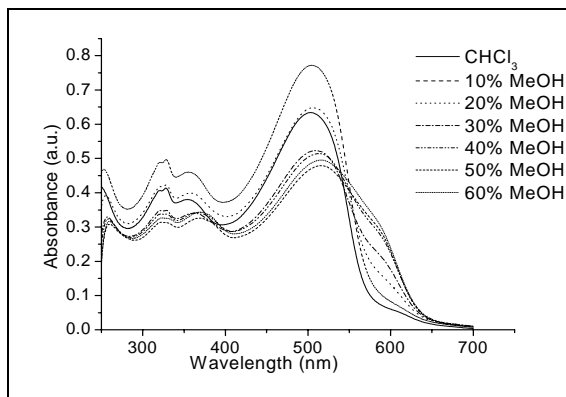


Figure 3.6. UV-vis spectra of **P-1** in CHCl_3 with different concentration of MeOH.

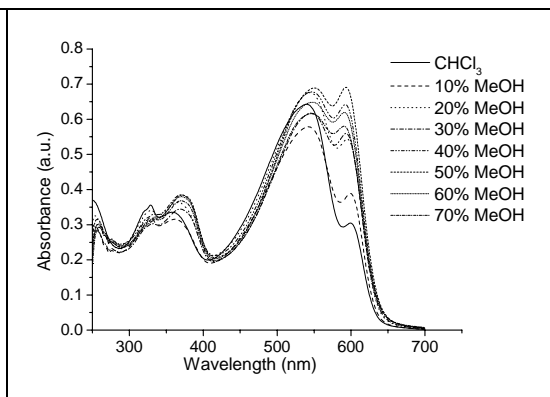


Figure 3.7. UV-vis spectra of **P-2** in CHCl_3 with different concentration of MeOH.

The spectral red shift corresponds to a disorder-to-order transformation of the conjugated polymer chains. Since polymers **P-1** and **P-2** are insoluble in methanol, the addition of methanol to the homogeneous chloroform solution leads to aggregate formation. In the aggregate the polymer possesses a more planarized structure, so the new band at higher wavelength could be related to the degree of chromophore-chromophore interaction in the aggregate. Similar phenomena were found in chloroform/methanol solutions of 2,5-dialkylpoly(*p*-phenyleneethynylene)s,^{19a} poly(fluorenyleneethynylene)s,^{19b} and poly(*p*-phenyleneethynylene) copolymers^{19c} by Bunz et al.

On the addition of methanol, the emission spectra of polymer **P-2** show a similar red shift. In pure chloroform, the emission spectrum of polymer **P-2** displays a peak at 585 nm and a shoulder at 630 nm. On adding methanol to 30 vol %, the emission peak shifts to 592 nm with a weak shoulder at ~640 nm. When the methanol concentration reaches 60 vol %, the emission peak shifts to 643 nm. The ~8 nm red shift in the PL spectrum of the solution with 30 vol % methanol originates from intermolecular excimer formation.^{19c} The new band at 643 nm results from aggregate formation. Moreover there is a decrease in the fluorescence quantum yields with the increase in methanol concentration, with 60 vol% methanol only 1.7% was obtained for **P-2**. This confirms the aggregation, due to which we observe a red shift in fluorescence emission spectra but decrease in fluorescence quantum yields. The fluorescence spectrum taken in methanol overlaid with the solid-state spectrum (Figure 3.5) shows the similarity of both. Thus,

according to our experiments, the red-shifted optical features in absorption/emission spectra must be due to aggregate formation in **P-2**.

3.2.4 Electrochemical Studies

The cyclic and square-wave voltammetry were carried out using thin films of polymers prepared from dichloromethane (5 mg/mL) in acetonitrile at a potential scan rate of 15 mV/s. Ag/AgCl served as the reference electrode; it was calibrated with ferrocene ($E_{\text{ferrocene}}^{1/2} = 0.52$ V vs Ag/AgCl). The supporting electrolyte was tetrabutylammonium hexafluorophosphate (*n*-Bu₄NPF₆) in anhydrous acetonitrile (0.1 M). The onset potentials are the values obtained from the intersection of the two tangents drawn at the rising current and the baseline charging current of the CV curves. Several ways to evaluate HOMO and LUMO energy levels from the onset potentials, $E^{\text{ox/onset}}$ and $E^{\text{red/onset}}$, have been proposed in the literature.¹⁰⁴⁻¹⁰⁸ These were estimated here on the basis of the reference energy level of ferrocene (4.8 eV below the vacuum level)¹⁰⁶ according to the following equation:

$$E^{\text{HOMO/LUMO}} = [-(E_{\text{onset (vs. Ag/AgCl)}} - E_{\text{onset (Fc/Fc+ vs. Ag/AgCl)}})] - 4.8 \text{ eV.}$$

The onset and the peak potentials, the electrochemical band gap energy, and the estimated position of the upper edge of the valence band (HOMO) and of the lower edge of conduction band (LUMO) are listed in Table 3.3. The electrochemical reduction (n-doping) of **P-1** starts at about -0.7 V Ag⁺/Ag and gives two n-doping peaks at -0.87 and -1.23 V vs Ag⁺/Ag, respectively. Similarly for **P-2** reduction starts at about -1.0 V Ag⁺/Ag and gives two n-doping peaks at -1.16 and -1.66 V vs Ag⁺/Ag, respectively (Figure 3.8). Of the two aromatic units (2,1,3-benzothiadiazole and thiophene units), the 2,1,3-benzothiadiazole unit receives the reduction at higher potential [e.g., n-doping peak of poly(thiadiazole) = -1.9 V vs Ag⁺/Ag]⁸⁶ than the thiophene ring [e.g., n-doping peak of poly(thiophene) (PTh) = -0.58-0.61 V vs Ag⁺/Ag].¹⁰⁹ Consequently, peaks are considered to be mainly concerned with the reduction of the 2,1,3-benzothiadiazole unit and the thiophene unit, respectively, although the generated negative charge seems to be delocalized along the polymer chain to some extent. In a range from 0.0 to -2.2 V vs Ag⁺/Ag, the film revealed stable in repeated scanning of CV, giving same CV curves. However, oxidation of the polymers **P-1** and **P-2** was irreversible with peaks at 1.60 V and 1.62 V respectively and accompanied by change in colour from violet to black. Such irreversibility in the electrochemical processes has been reported for several other π -conjugated polymers.^{110a}

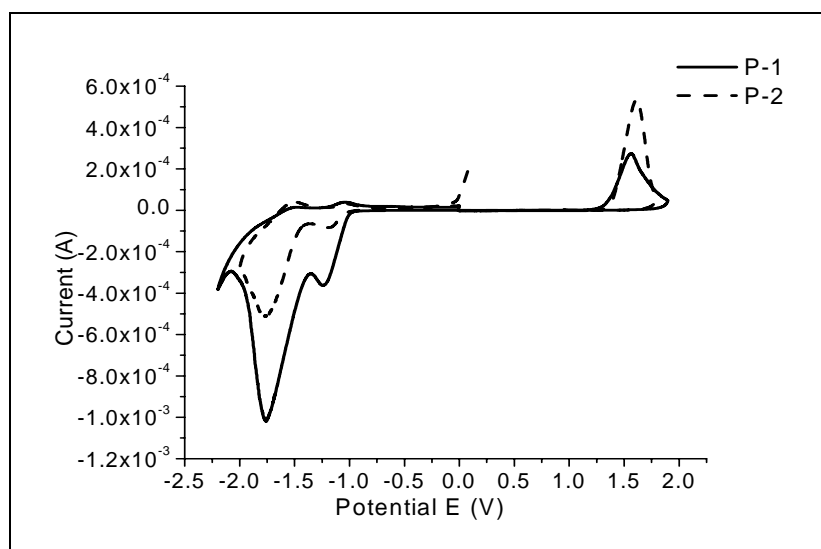


Figure 3.8. Cyclic voltammety-curves of polymers(**P-1** in solid line and **P-2** in dotted line) in 0.1M TBAPF₆/CH₃CN at 25 °C.

The oxidation and reduction values are comparable to that of reported one (1.66, -1.09).⁵⁵ The reduction peak potential at around -1.16 V and -1.23 prove that the reduction processes are limited basically in the arylene ethynylene compounds due to the high electron affinity of the triple bonds.^{110b} The band gap energy directly measured from CV is ($E_{g\text{ ec/onset}}$ 2.03 eV for **P-1** and 2.39 for **P-2**) and the optical band gap energy is ($E_{g\text{ opt/onset}}$ 1.95 eV for **P-1** and 1.85 for

Table 3.4. Electrochemical Potentials and Energy Levels of the Polymers **P-1**, **P-2**.

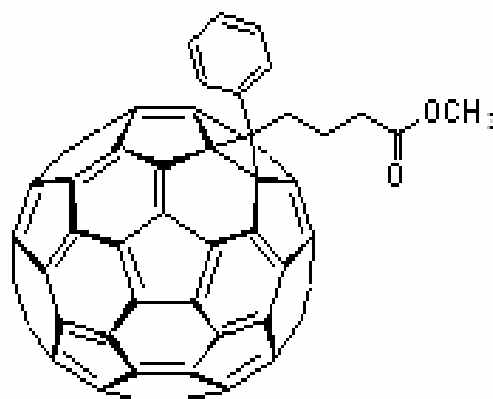
Polymer	Oxidation Potential		Reduction Potential		Energy Levels ^b		Band Gap	
	E_{ox}^{a} (V vs Ag/Ag ⁺)	$E_{\text{onset, Ox}}$	$E_{\text{red}}^{\text{a}}$ (V vs Ag/Ag ⁺)	$E_{\text{onset, Red}}$	HOMO (eV)	LUMO (eV)	Band ^{cc} Gap (eV)	Optical Band Gap (eV)
P-1	1.60	1.34	-0.87	-0.69	-5.62	-3.59	2.03	1.95
			-1.23	-1.00				
P-2	1.62	1.40	-1.16	-1.04	-5.63	-3.24	2.39	1.85
			-1.66	-1.47				

^aReduction and oxidation potential measured by cyclic voltammetry. ^bCalculated from the reduction and oxidation potentials assuming the absolute energy level of ferrocene/ferrocenium to be 4.8 eV below vacuum.

P-2), with the electrochemical band gap being slightly larger. The band gaps are higher than the optically determined ones due to interface barrier for charge injection.^{111,112} Clearly in the case of polymer **P-1** this difference is small due to presence of only one alkyl chain causing less steric hindrance. From the onset potentials, HOMO and LUMO energy levels were estimated. The HOMO for **P-1** and **P-2** were around -5.62 and -5.68 eV, while LUMO around -3.59 and -3.24 eV respectively.

3.2.5 Photovoltaic Studies

It is well-known that solar cells containing a heterojunction between two different polymers, with one acting as the hole acceptor and the other as an electron acceptor, show much better performances than single component devices.¹¹³⁻¹¹⁵ Photogenerated excitons in the polymer layer can be efficiently dissociated into free charge carriers at the interface between the electron-donating and the electron-accepting polymers. This heterojunction can be introduced either by preparing double layer devices or by blending the two polymers, yielding a distributed bulk heterojunction. Solar cells in which the active layer is prepared from a polymer blend have the advantage of a larger interfacial area. To test the applicability of the polymer **P-2** for light energy conversion, photovoltaic cells consisting of a composite film (**P-2:PCBM**, 1:2 wt.%) as the active layer sandwiched between a transparent indium tin oxide (ITO) front electrode covered with a conducting layer of poly(3,4-ethylenedioxythiophene):poly(styrene sulfonic acid) (PEDOT:PSS) and an aluminum back electrode were prepared and studied under inert conditions (preparation of active layer in air, electrode evaporation inside the glove box (Argon)). The requirement of an intimate intermixing of donor and acceptor phases in the bulk heterojunction makes this approach especially sensitive to the nanoscale morphology.^{116,117} It is clear that the control of morphology in dispersed heterojunction devices is a critical point. The degree of phase separation and domain size depend on solvent choice, speed of evaporation, solubility, miscibility of the donor and acceptor etc. Figure 3.9 shows AFM image of the surfaces of **P-2:PCBM** (1-(3-methoxycarbonyl)-propyl-1-phenyl-(6,6)C₆₁) blend films spin-coated using dichlorobenzene as solvent. The image shows the surface morphology, indicating phase separation of the constituents.



1-(3-methoxycarbonyl)-propyl-1-phenyl-(6,6)C₆₁ (**PCBM**)

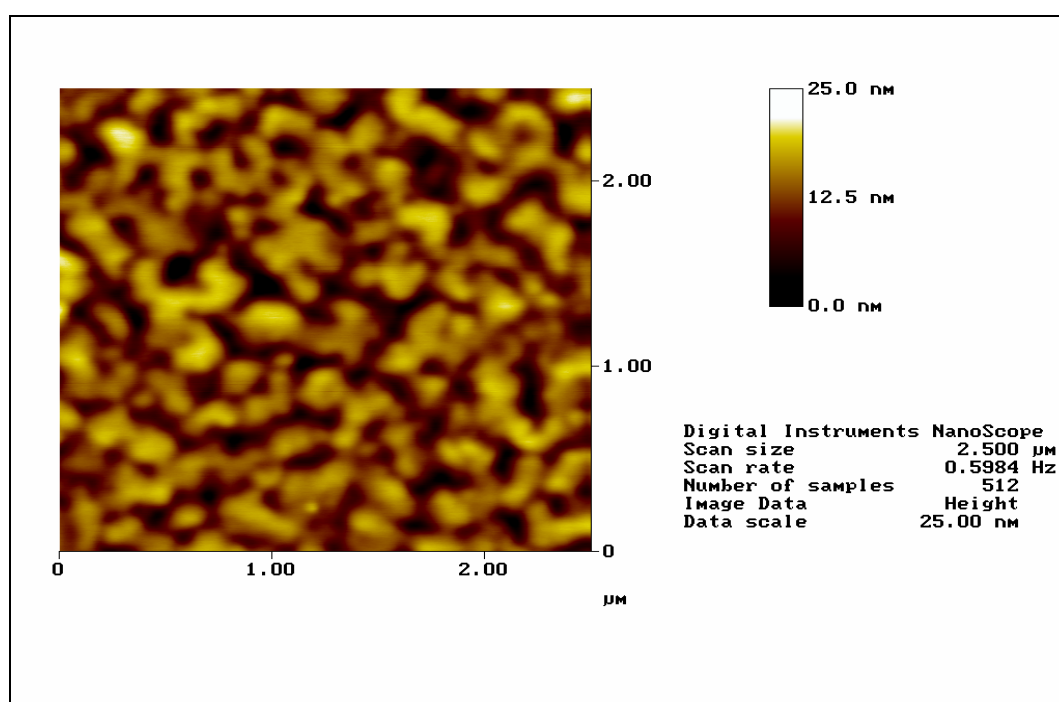


Figure 3.9. AFM image (acquired in the tapping mode) showing the surface morphology of **P-2 : PCBM** (1:2 by wt.) blend film spin-coated from a dichlorobenzene solution.

Under white-light illumination from a solar simulator (AM 1.5) an open circuit voltage of $V_{oc} = 0.50$ V and short circuit current of $I_{sc} = 0.46 \text{ mA/cm}^2$ were obtained. The fill factor (FF), defined as $(I_{max} \times V_{max}) / (I_{sc} \times V_{oc})$, with I_{max} and V_{max} corresponding to the point of maximum output, was $FF = 0.38$. Under these conditions the power conversion efficiency ($IPCE = (P_{out}/P_{in}) \times 100 = (FF \times V_{oc} \times I_{sc}/P_{in}) \times 100$) is about 0.08% (Figure 3.10). The overall low power conversion efficiency can be explained due to presence of bulky side chains steric hindrance. In our case combination with **PCBM** the I/U-curves (Figure 3.11) yield the highest fill factors FF, as well the highest I_{sc} , but the lowest V_{oc} ; the V_{oc} stays below that of P3HT^{117,118} based devices and the I_{sc} is one order of magnitude lower. Also there is a high field dependence of the photocurrent,

pointing to transport limitations. Full optimisation of our devices has not yet been carried out, but is underway. For the combination with **PCBM** some improvements are to be expected and further testing is in progress.

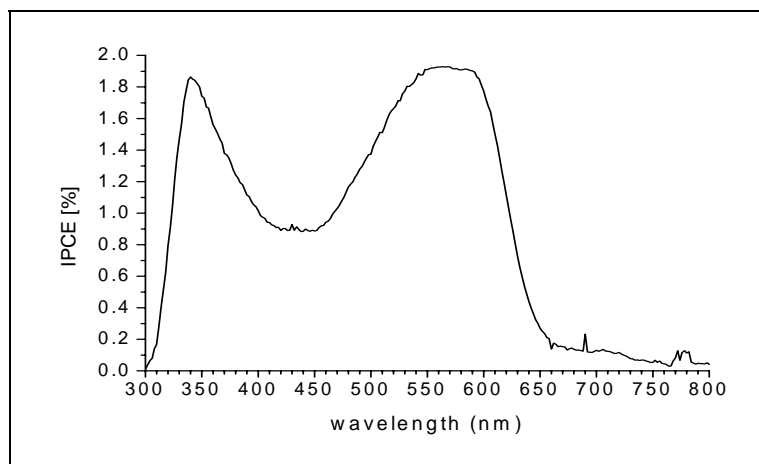


Figure 3.10. IPCE (external quantum efficiency) spectrum of **P2:PCBM** 1:2 solar cells.

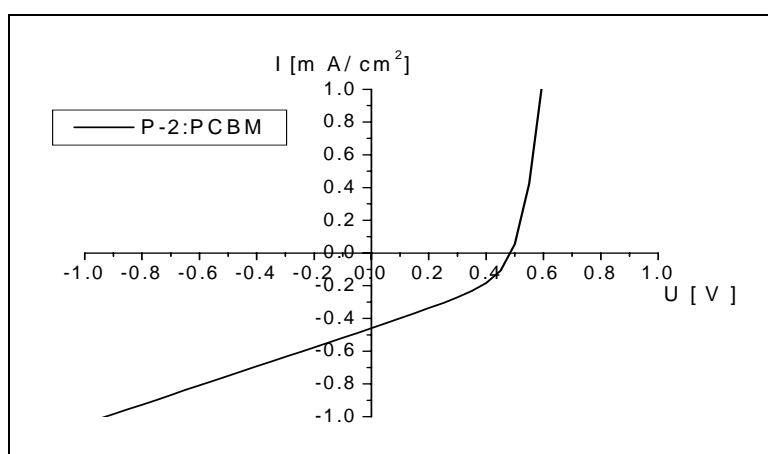
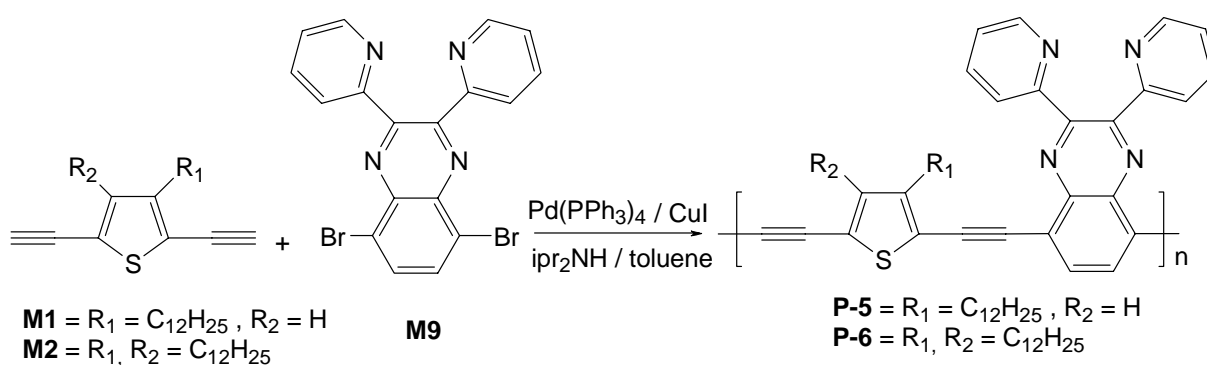


Figure 3.11. **P-2/PCBM** film (from dichlorobenzene and annealing for short time at 145°C).

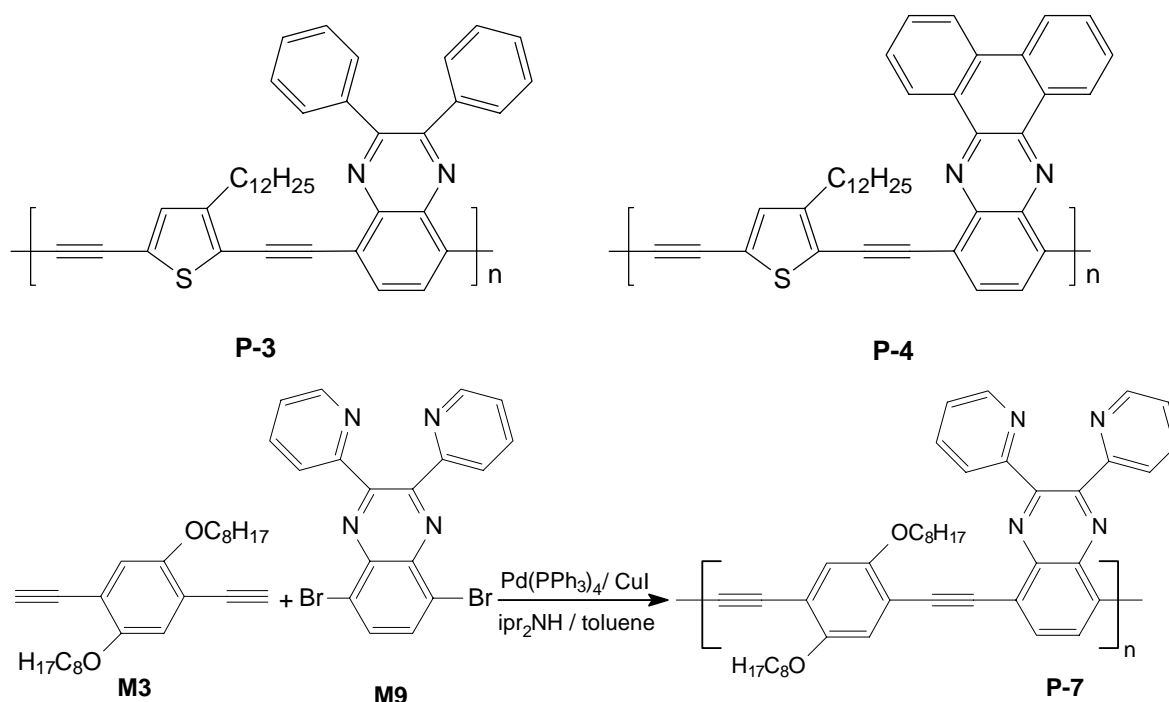
3.3 Quinoxaline and Thiophene Based Poly(heteroaryleneethynylene)s

3.3.1 Synthesis and Characterization of the Polymers

The Synthesis of polymers (**P-3-P-7**) was carried out by employing the Pd catalysed Sonogashira coupling,^{56,58} The polymers were synthesized from thiophene diacetylenes (**M1** and **M2**), phenylene diacetylenes (**M3**) and dibromo-quinoxalines (**M7**, **M8** and **M9**) (Scheme 3.10 and 3.11). Yields of all the polymers were higher than 75%. These polymers are red in colour. **P-3**, **P-5**, **P-6** and **P-7** are soluble in organic solvents (THF, CHCl₃ etc.), while **P-4** is only sparingly soluble, less solubility of **P-4** is due to rigid structure of phenazine ring which makes the polymer chains more planar and rigid.



Scheme 3.10. Synthesis of Polymers **P-5** and **P-6**.



Scheme 3.11. Synthesis of Polymer **P-7**.

The chemical structure of the polymers was confirmed by FTIR, ^1H , ^{13}C NMR and elemental analysis. In FTIR the strong $\nu(\text{C}\equiv\text{CH})$ peak near 3290 cm^{-1} of the monomers disappeared on polycondensation, and a new $\nu(\text{C}\equiv\text{C})$ peak appeared at about $2195\text{-}2210\text{ cm}^{-1}$.

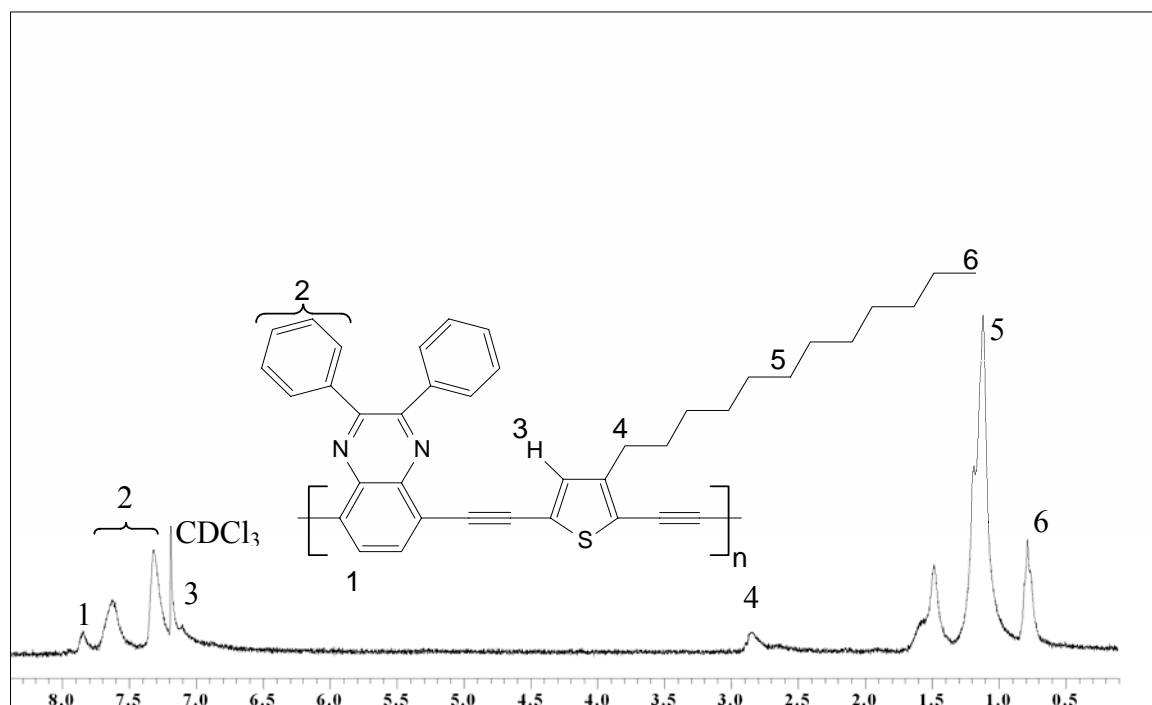


Figure 3.12. ^1H NMR of **P-3**.

^1H NMR data were consistent with the proposed structure of the polymers. Compared with the ^1H NMR peaks of monomers, those of the polymers were broadened and somewhat shifted to a lower magnetic field. The ^1H NMR spectrum of **P-3** in CDCl_3 showed peaks indicating protons of 2,3-diphenyl-2-ylquinoxaline and thiophene units at $\delta = 7.74, 7.63, 7.32$ and 7.18 ppm respectively. While that of $-\text{CH}_2$ protons adjacent to thiophene ring appeared at $\delta = 2.83$ ppm and other alkyl side chain protons signals were present at $\delta = 1.48\text{-}0.79$ ppm (Figure 3.12). The ^1H NMR spectra of **P-5**, **P-6** and **P-7** in CDCl_3 showed peaks indicating protons of 2,3-dipyridine-2-ylquinoxaline units between $\delta = 8.34$ and 7.88 ppm, while protons of alkoxy phenylene and thiophene units appear upfield between 7.26 and 7.22 ppm respectively. While that of $-\text{CH}_2$ protons adjacent to thiophene ring appeared at $\delta = 2.90$ and other alkyl side chain protons signals were present at $\delta = 1.7\text{-}0.87$ ppm. Similarly the $-\text{OCH}_2$ protons of alkoxy phenylene appeared at $\delta = 4.12$ ppm and other alkyl side chain protons signals were present at $\delta = 1.86\text{-}0.86$ ppm (Figure 3.13 and 3.14).

In case of **P-3** and **P-5** there is only one prominent peak for thiophene proton (3-H) indicating the high regioregular polymers. The ^1H NMR data is comparable with that of reported one for other regioregular thiophene polymers.⁹⁴

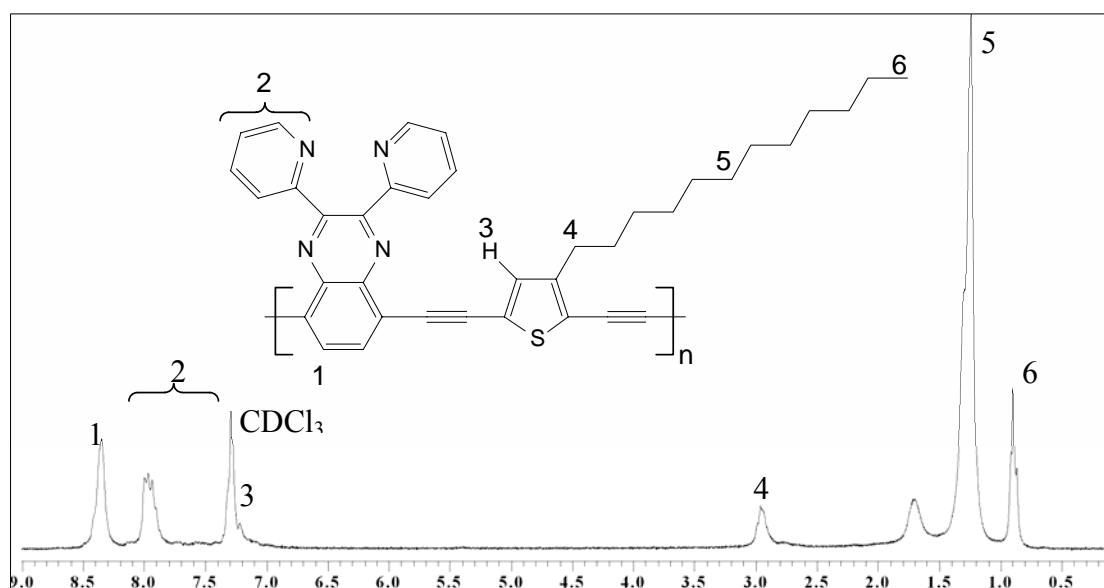


Figure 3.13. ^1H NMR of P-5.

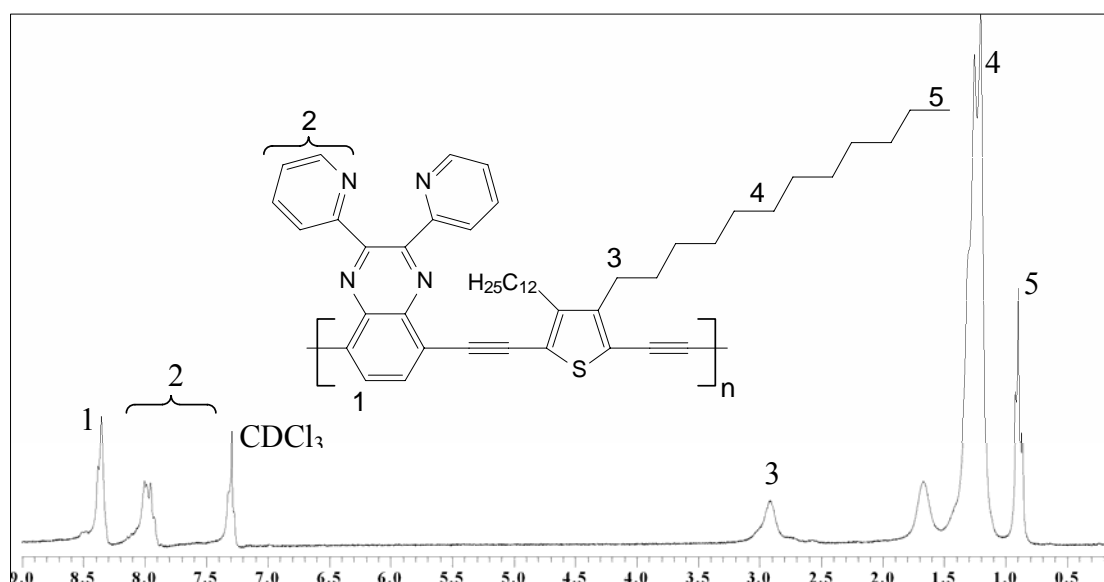


Figure 3.14. ^1H NMR of P-6.

The ^{13}C NMR spectra of polymers (P-3, P-5, P-6 and P-7) showed aromatic carbons signals between 158 and 118 ppm. The signals due to the triple bond carbons were present between $\delta = 94.81$ and 91.50 ppm. The alkoxy carbons signal appeared at 69.96 ppm and alkyl carbons signals appeared upfield between 34 and 14 ppm. The peaks due to terminal $-\text{C}\equiv\text{CH}$ in ^1H NMR and ^{13}C NMR spectra were absent. In ^{13}C NMR spectra the signals due to oxidative coupling reaction of acetylenes to diacetylenes ($-\text{C}\equiv\text{C}-$) between 80 to 70 ppm were absent, indicating no diyne defects in structures. The number-average molecular weight, \bar{M}_n , of the polymers (P-3-P-7) was determined by GPC (polystyrene standards), VPO (vapour pressure osmometry) and bromo end groups (Table 3.5). The \bar{M}_n of the polymers (P-3, P-4, P-5, P-6 and P-7) were

10600, 5200, 7700, 16400 and 7200 with polydispersity indices of 2.18, 3.43, 2.30, 1.70 and 2.34 respectively. \bar{M}_n values of 8300 and 16200 for **P-5** and **P-6** respectively, obtained by VPO in CHCl_3 , are approximately the same as those from GPC (Table 3.5). So we postulate that also in other polymers both values are approximately the same.

Table 3.5. GPC and VPO data of polymers **P-3-P-7**.

Polymer	\bar{M}_n [g/mol]	\bar{M}_w [g/mol]	M_w/M_n	\bar{P}_n	Yield (%)
P-3	10600 ^a	23200	2.18	18	83
P-4	5200 ^a	17900	3.43	9	83
P-5	7700 ^a (8300) ^b	17700	2.30	13	72
P-6	16400 ^a (16200) ^b	27900	1.70	22	80
P-7	7200 ^a	16900	2.34	11	75

^a \bar{M}_n , GPC (polystyrene standards).

^b \bar{M}_n , VPO (vapour pressure osmometry).

The thermal stability of PAE polymers (**P-3-P-7**) was investigated in air. Thermo gravimetric analysis (TGA) of the polymers **P-3**, **P-6** and **P-7** exhibited an apparent degradation at approximately at 350 °C with a weight loss of around 5%. The polymer **P-5** exhibit comparatively higher thermal stability. The thermal decomposition for **P-5** under air starts above 450 °C (Figure 3.15).

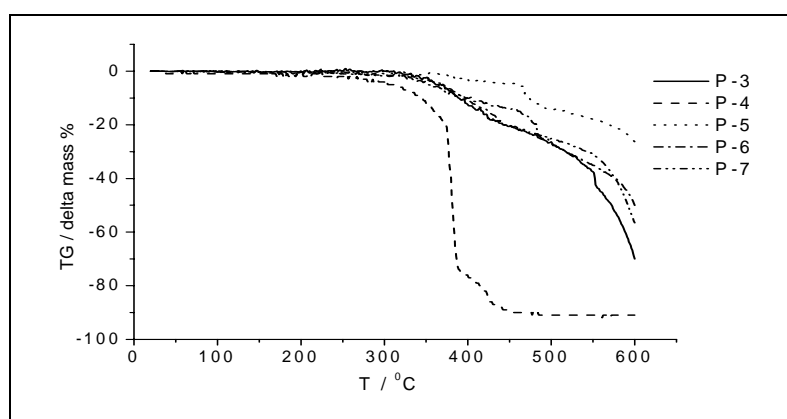


Figure 3.15. TGA of polymers **P-3-P-7**.

3.3.2 Optical Properties

The photophysical characteristics of the new polymers were investigated by UV-vis absorption and photoluminescence in dilute chloroform solution as well as in solid state. Results from the absorption and emission spectra are summarized in Table 3.6 and 3.7. All emission data given here were obtained after exciting at the wavelength of the main absorption band. Figure 3.16 and 3.17 show the absorption and emission spectra of polymers **P-3-P-7**.

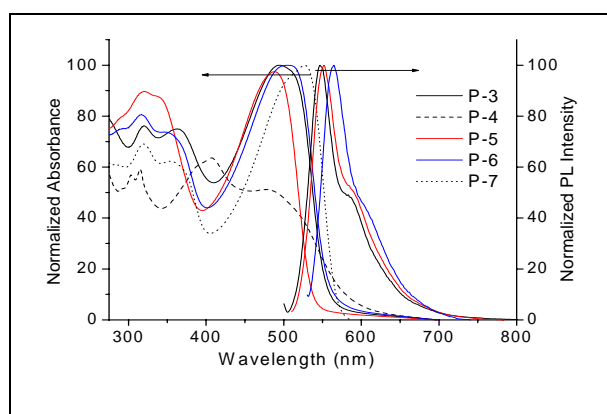


Figure 3.16. Normalized UV-vis spectra of **P-3-P-7** and emission spectra of **P-3**, **P-5** and **P-6** in solution (CHCl_3 10^{-7} mol).

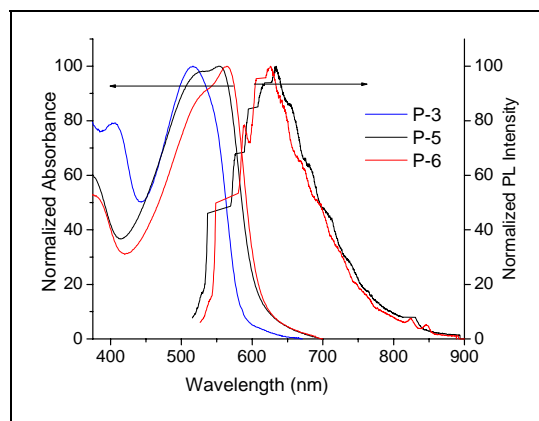
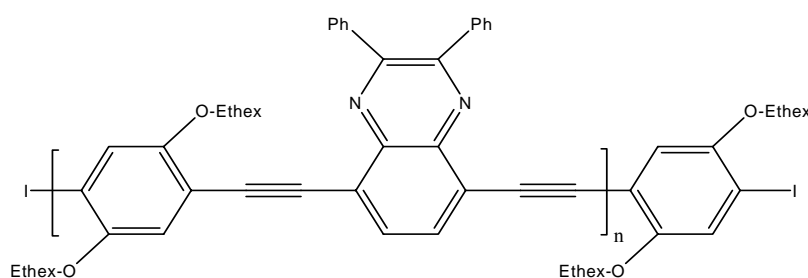


Figure 3.17. Normalized UV-vis spectra of **P-3**, **P-5** and **P-6** and emission spectra of **P-5** and **P-6** in solid state. (film from chlorobenzene)

The absorption maxima of **P-3**, **P-4**, **P-5** and **P-6** are red-shifted relative to that of **P-7** and PAEs reported by Bunz et al.¹⁹



PAEs by Bunz et al.

The difference in absorption is due to the presence of thiophene moiety in the polymers **P-3-P-6** and alkoxy phenylene in case of **P-7**, indicating better donor property of thiophene. The copolymers, **P-3-P-6**, show the lowest energy absorption peak at a longer wavelength than the homopolymers,^{86d} presumably due to an intramolecular charge transfer structure of the copolymers (Table 3.6). The quinoxaline unit is a π -accepting unit whereas the thiophene unit serves as a π -donor. Similar shifts to a longer wavelength has been reported for other quinoxaline copolymers with thiophene¹¹⁹ and has been explained by the intramolecular charge transfer structure.

Table 3.6. Optical data of **P-3-P-7**.

Polymer	UV-vis λ_{\max} , nm				E_g opt. eV ^c	
	CHCl ₃ [log ϵ] ^a	$\lambda_{0.1\max}$	film ^b	$\lambda_{0.1\max}$	CHCl ₃	film
P-3	495 [4.5]	560	545	590	2.21	2.10
P-4	499 [4.2]	608			2.04	
P-5	505 [4.5]	564	554	596	2.20	2.08
P-6	527 [4.5]	571	565	599	2.17	2.07
P-7	488 [4.5]	539			2.30	

^aMolar absorption coefficient. Molarity is based on the repeating unit. ^bSpin coated from chlorobenzene solution. ^c E_g opt. = $hc / \lambda_{0.1\max}$.

The emission maximum of **P-3**, at $\lambda_{\max,em} = 547$ nm, while the emission curves of **P-5** and **P-6** showing maxima at $\lambda_{\max,em} = 552$ and 565 nm, are almost identical to each other. The fluorescence quantum yields were found to be around 30, 36 and 38% for **P-3**, **P-5** and **P-6** respectively. The optical band gap varies from 2.04 to 2.30 eV depending on number and position of alkyl chains and the presence of thiophene or phenylene units. The optical band gap in case of the polymer **P-4** is lowest about 2.04, indicating the planar structure of the polymer due to presence of phenazine ring, which increases conjugation and we observe a broad band in this case.(Table 3.6 and 3.7).

Thin films of **P-3**, **P-5** and **P-6** were spun cast from a chlorobenzene solution on the quartz substrate. **P-3**, **P-5** and **P-6** have their solid-state absorption bands centered at $\lambda_{\max,abs} = 545$ nm, 554 nm and 565 nm respectively. The emission maxima of **P-5** and **P-6** are located at $\lambda_{\max,em} = 634$ nm and 625 nm, leading to large Stokes shift of 80 nm and 60 nm respectively, and a lower fluorescence quantum yield of 2%. We assumed, the reason for the low photoluminescence (PL) efficiency is a π - π stacking of the conjugated backbone cofacial to each other due to the favourable inter-chain π - π interactions, which lead to a self-quenching process of the excitons.⁹⁹⁻
¹⁰¹ Triple-bonds in the polymer main chain (like in poly(aryleneethynyls)) lead to stiffness and rigidity of the polymer backbones, which thereby reinforce the inter-chain interactions.¹⁰²

Moreover inner heavy-atom effects of bromo end groups can possibly also contribute to the deactivation of the excitons in the solid state.¹⁰³ It is also interesting to make a comparison between the photophysical properties of PAEs **P-3**, **P-5** and **P-6** and poly((3-hexylthiophenylene)ethynylene) (P3HTE).⁹⁴ The PL quantum efficiencies of PAEs, however, are about 2 times as high as P3HTE ($\Phi_{\text{PL}} = 0.18$). Clearly alternate replacement of the thiophene rings along the P3HTE chain with quinoxaline unit has a large impact on the nonradiative decay process. The enhancement is even more pronounced in the solid state, as the PAEs film emits more strongly than P3HTE film with a head-to-tail chain sequence⁹⁴ under the identical conditions.

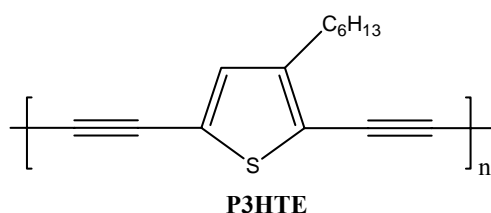


Table 3.7. Photoluminescence Data of **P-3**, **P-5** and **P-6** in Dilute CHCl_3 Solution ($\sim 10^{-7}$ M) and in Solid State.^a

Polymer	UV-em λ_{em} , nm		Stokes shift, nm		% ϕ_{PL}	
	CHCl_3	film	CHCl_3	film	CHCl_3	film
P-3	547		52		30	
P-5	552	634	47	80	36	2
P-6	565	625	38	60	38	2

^bSpin coated from chlorobenzene solution.

3.3.3 Aggregate Formation in Solvent/Nonsolvent Solution

In order to obtain further information on the assumed self assembly of these polymers and aggregation, different solvent/nonsolvent solutions of the **P-5** and **P-6** were investigated. Figure 3.18-3.27 show the changes in UV-vis spectra of **P-5** and **P-6**. UV-vis spectra were measured in chloroform with different concentration of other solvents like acetonitrile, 1-decanol, hexane, methanol and tetrahydrofuran to observe changes due to these solvent mixtures. As we know both **P-5** and **P-6** are not soluble in pure acetonitrile, 1-decanol, hexane and methanol, however up to 80% of these solvents can be added to a dilute chloroform solution of polymers **P-5** and **P-6** without visible precipitation. The extremely fine suspensions formed are stable for hours. Addition of these solvents to the chloroform solution of **P-5** and **P-6** led to a change in the λ_{max} and above 50 % Vol. of these solvents (acetonitrile, 1-decanol, hexane and methanol), a decrease in the intensity of the first band and appearance of a new peak (or shoulder) at higher

wavelength was observed. There was no effect observed when THF was added to chloroform solution of these polymers.

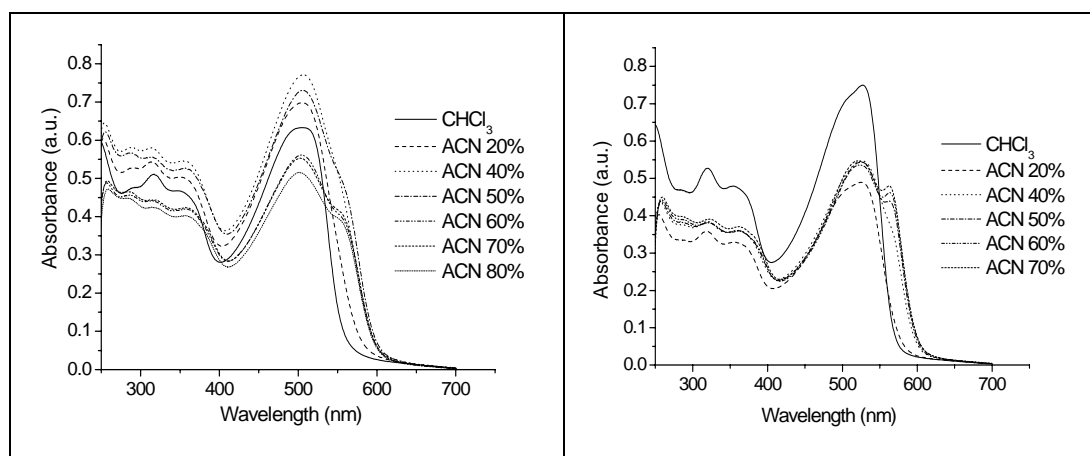


Figure 3.18. UV-vis spectra of **P-5** in CHCl_3 with different concentration of Acetonitrile (A). **Figure 3.19.** UV-vis spectra of **P-6** in CHCl_3 with different concentration of Acetonitrile (A).

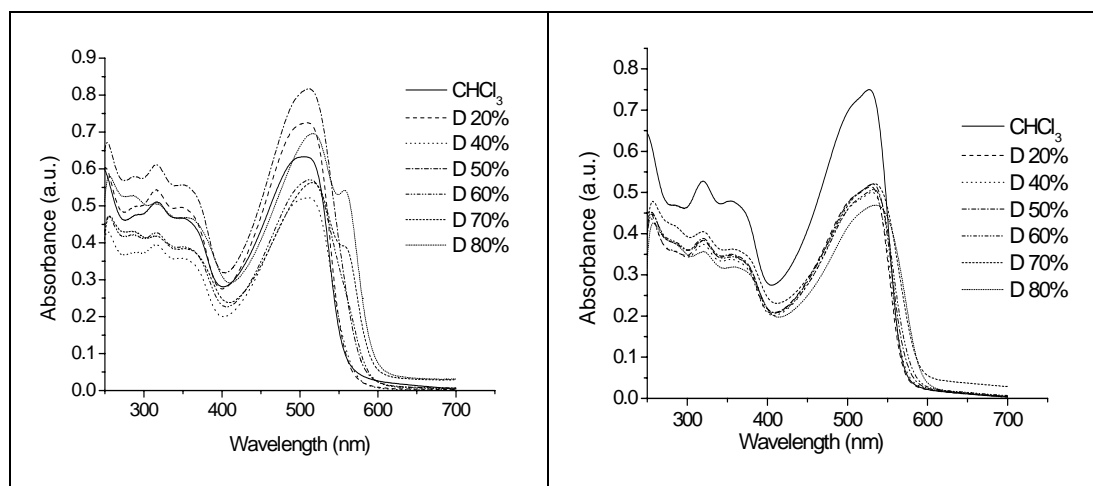


Figure 3.20. UV-vis spectra of **P-5** in CHCl_3 with different concentration of 1-decanol (D). **Figure 3.21.** UV-vis spectra of **P-6** in CHCl_3 with different concentration of 1-decanol (D).

The examination of the absorptive behaviour of **P-5** and **P-6** in chloroform, chloroform/acetonitrile, 1-decanol, hexane, methanol and tetrahydrofuran solutions, corroborates the presence of aggregates in the mixed chloroform/ acetonitrile, 1-decanol, hexane, methanol solvents. It could be that aggregates consisting of many PAE chains form in the solid state, and the electronic communication of the π -systems via tight packing and a π - π -stacking effect leads to the observed bathochromic shift.¹²⁰ Alternatively, the occurrence of the red-shifted feature is a single molecule effect, similarly to that observed by Roughopoot et al.¹²¹ for polythiophenes, in which planarization of the π -system is induced by aggregation.

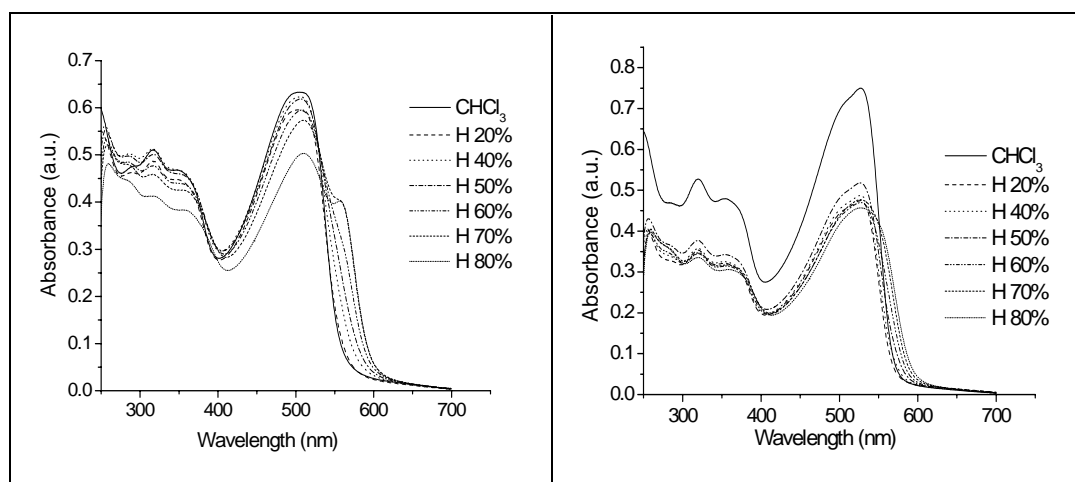


Figure 3.22. UV-vis spectra of P-5 in CHCl₃ with different concentration of Hexane (H).

Figure 3.23. UV-vis spectra of P-6 in CHCl₃ with different concentration of Hexane (H).

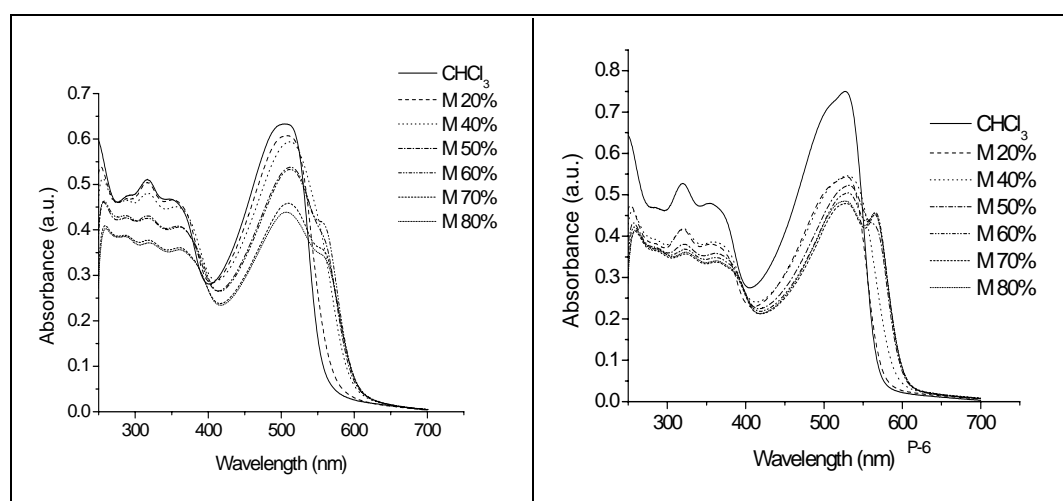


Figure 3.24. UV-vis spectra of P-5 in CHCl₃ with different concentration of methanol (M).

Figure 3.25. UV-vis spectra of P-6 in CHCl₃ with different concentration of methanol (M).

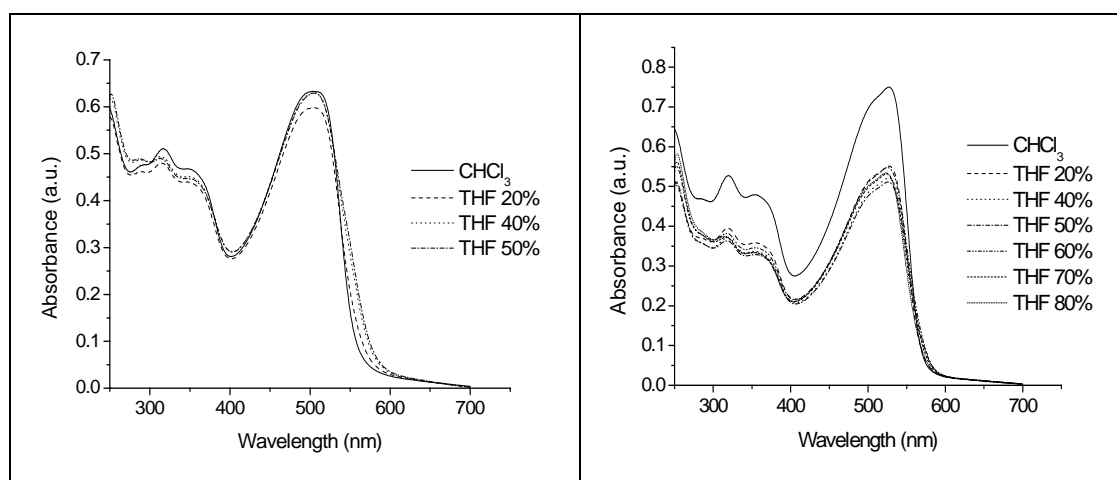


Figure 3.26. UV-vis spectra of P-5 in CHCl₃ with different concentration of THF.

Figure 3.27. UV-vis spectra of P-6 in CHCl₃ with different concentration of THF.

The forced planarization then leads to increased conjugation and thus to a lower band gap. We infer aggregate formation of PAEs **P-5** and **P-6** from the following observations. The absorption changes and red-shifted transitions are observed, once acetonitrile, 1-decanol, hexane and methanol are added to a solution of **P-5** and **P-6**. A very similar spectral feature is observed by Bunz et al¹⁹ during their studies of PAEs. The golden luster and presence of the electron withdrawing quinoxaline units suggests these polymers are electronically different from the PPEs. We observed more changes in UV-vis of **P-5** than **P-6** indicating that the structure of the polymer also play an important role, as in case of **P-6**, two alkyl chains presence on thiophene unit delayed the aggregation formation but can not completely prevent it.

Moreover there is a decrease in the photoluminescence quantum yields of the both polymers with the increase in methanol concentration, with 50 vol % methanol only 11 and 8 % was obtained for **P-5** and **P-6** respectively. While at 70 vol% methanol 5 and 1 % fluorescence quantum yields was obtained for polymers **P-5** and **P-6**. (Figures 3.28 and 3.29). This confirms the aggregation, due to which we observe a red shift in fluorescence emission spectra but decrease in photoluminescence quantum yields. The fluorescence spectra taken in methanol overlaid with the solid-state spectrum shows the similarity of both. Thus, according to our experiments, the red-shifted optical features in absorption/emission spectra must be due to aggregate formation in **P-5** and **P-6**. As suggested from absorption measurements, we believe that the appearance of the fluorescence red-shifted band can be interpreted by the molecular exciton model, assuming J-aggregates formed. Thus, the quenching of the photoluminescence efficiency would arise from J-aggregates formation.¹²²

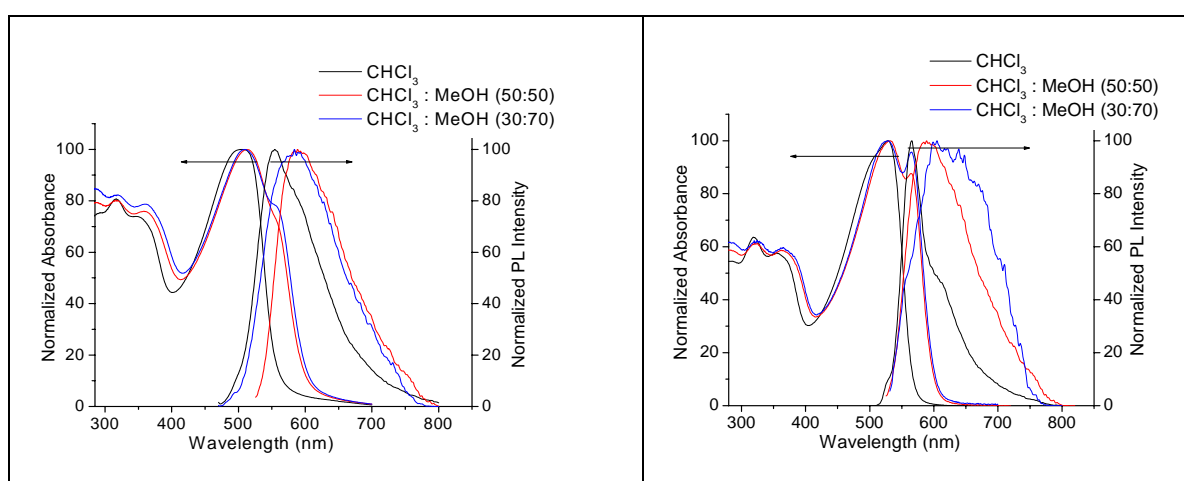


Figure 3.28. Normalized UV-vis and emission spectra of **P-5** in solution (CHCl_3 10^{-7} mol) and different concentration of methanol.

Figure 3.29. Normalized UV-vis and emission spectra of **P-6** in solution (CHCl_3 10^{-7} mol) and different concentration of methanol.

Electrochemical Studies

Thin films of the polymers were spun cast from dichloromethane (5 mg/mL). The CV of polymers was carried out in acetonitrile at a potential scan rate of 15 mV/s. Ag/AgCl served as the reference electrode; it was calibrated with ferrocene ($E_{\text{ferrocene}}^{1/2} = 0.52 \text{ V vs Ag/AgCl}$). The supporting electrolyte was tetrabutylammonium hexafluorophosphate ($n\text{-Bu}_4\text{NPF}_6$) in acetonitrile (0.1 M). Several ways to evaluate HOMO and LUMO energy levels from the onset potentials, $E^{\text{ox/onset}}$ and $E^{\text{red/onset}}$, have been proposed in the literature.¹⁰⁴⁻¹⁰⁸ HOMO and LUMO energy levels were estimated here on the basis of the reference energy level of ferrocene (4.8 eV below the vacuum level)¹⁰⁶ according to the following equation:

$$E^{\text{HOMO/LUMO}} = [-(E_{\text{onset (vs. Ag/AgCl)}} - E_{\text{onset (Fc/Fc+ vs. Ag/AgCl)}})] - 4.8 \text{ eV}.$$

The onset and the peak potentials, the electrochemical band gap energy, and the estimated position of the upper edge of the valence band (HOMO) and of the lower edge of conduction band (LUMO) are listed in Table 3.8. The CV of polymers for oxidation did not provide clear and sharp peaks. Peaks were obtained around 1.48 V, 1.44 V and 1.48 V with estimated onset values around 1.30 V, 1.21 V and 1.28 V for **P-3**, **P-5** and **P-6** respectively. The CV reduction process was reversible. Reduction peaks for **P-3**, **P-5** and **P-6** were around -1.32, -1.32 and -1.28 V (onset values -1.18, -1.16 and -1.14 V) respectively. The quinoxaline units are less electron accepting than the benzothiadiazole unit mentioned by Bunz et al.,¹⁹ but the trend in cyclic voltammogram is mirrored indicating the alkoxy phenylene and quinoxaline based PAEs have higher reduction potential than alkoxy phenylene and benzothiadiazole based PAEs. Similar observation has been found in our case, indicating higher reduction potential (-1.32 V) of thiophene and quinoxaline based PAEs than benzothiadiazole and thiophene based PAEs (-1.23 V). In case of **P-3** and **P-6** a second reduction is observed at -1.84 V and -1.78 V suggesting that the polymer chains can be higher charged. It is reasonable to assume that in the first step only every second repeating unit is charged in **P-3** and **P-6** and that in a second reduction step the remaining quinoxaline modules are reduced. The band gap energy directly measured from CV ($E_{\text{g ec/onset}}$ 2.48 eV for **P-3**, 2.37 eV for **P-5** and 2.42 eV for **P-6**) and the optical band gap energy was ($E_{\text{g opt}}$ 2.10 eV for **P-3**, 2.08 eV for **P-5** and 2.07 eV for **P-6**). The discrepancy (ΔE_{g}) of both values lies within the range of error.

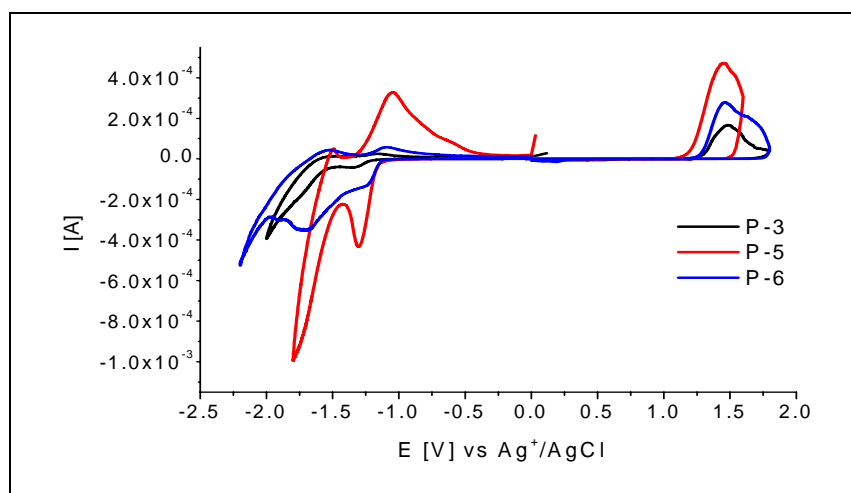


Figure 3.30. Cyclic voltammety-curves of polymers (**P-3**, **P-5** and **P-6**) in 0.1M TBAPF₆/CH₃CN at 25 °C.

From the onset potentials, HOMO and LUMO energy levels were estimated. The HOMO energy levels for **P-3**, **P-5** and **P-6** were around -5.58, -5.49 and -5.56 eV, while LUMO energy levels around -3.10, -3.12 and -3.14 eV respectively.

Table 3.8. Electrochemical Potentials and Energy Levels of the Polymers **P-3**, **P-5** and **P-6**.

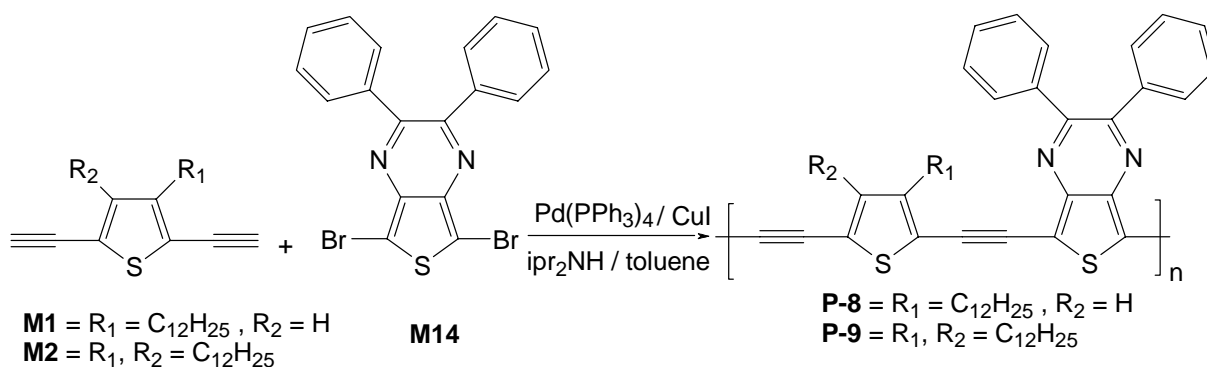
Polymer	Oxidation Potential		Reduction Potential		Energy Levels ^b		Band Gap	
	E _{ox} ^a (V vs Ag/Ag ⁺)	E _{onset, Ox}	E _{red} ^a (V vs Ag/Ag ⁺)	E _{onset, Red}	HOMO (eV)	LUMO (eV)	Band Gap (eV)	Optical Band Gap (eV)
P-3	1.48	1.30	-1.32	-1.18	-5.58	-3.10	2.48	2.10
			-1.78	-1.49				
P-5	1.44	1.21	-1.32	-1.14	-5.49	-3.12	2.37	2.08
P-6	1.48	1.28	-1.28	-1.16	-5.56	-3.14	2.42	2.07
			-1.84	-1.49				

^aReduction and oxidation potential measured by cyclic voltammetry. ^bCalculated from the reduction and oxidation potentials assuming the absolute energy level of ferrocene/ferrocenium to be 4.8 eV below vacuum.

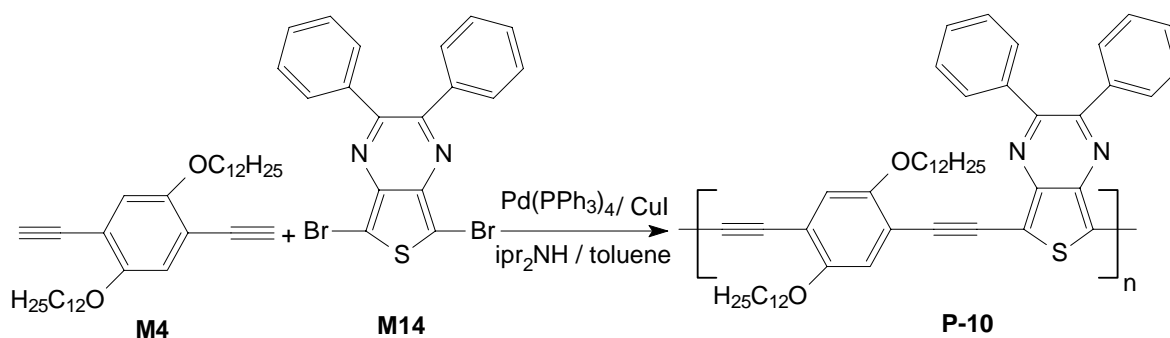
3.4 Thienopyrazine Based Low Band Gap Poly(heteroaryleneethynylene)s

3.4.1 Synthesis and Characterization of the Polymers

The general synthetic routes towards the polymers are outlined in Schemes 3.12 and 3.13. By employing the Pd catalysed Sonogashira coupling,^{56,58} the polymers (**P-8**, **P-9** and **P-10**) were synthesized from thiophene diacetylenes (**M1** and **M2**), phenylene diacetylenes (**M4**) and 5,7-dibromo-2,3-diphenylthieno[3,4-*b*]pyrazine (**M14**). Yields of the three polymers were between 60-90%. The polymers are dark blue in colour, almost similar to that of poly(2,3-dihexylthieno[3,4-*b*]pyrazine),¹²³ which is dark blue. The solubility of **P-8** was not good in organic solvents like THF, CHCl₃ and toluene etc., only 70 % of the polymer was soluble and used for further studies. Presence of one alkyl chain on thiophene moiety accounts for the less solubility of the polymer. The polycondensation time was shortened up to 8h to get maximum soluble polymer (about 80%). **P-9** and **P-10** are soluble in common organic solvents (THF, CHCl₃ etc.). The polymer **P-10** is reported⁵⁴ but in that case phenylene unit has octyloxy chain and in our case its dodecyloxy one. No detailed characterization is reported for this polymer.



Scheme 3.12. Synthesis of Polymers **P-8** and **P-9**.



Scheme 3.13. Synthesis of Polymer **P-10**.

The chemical structure of the polymers was confirmed by FTIR, ^1H , ^{13}C NMR and elemental analysis. The strong $\nu(\text{C}\equiv\text{CH})$ IR absorption near 3290 cm^{-1} of the monomers disappeared on polycondensation, and a new $\nu(\text{C}\equiv\text{C})$ peak appeared at about 2200 cm^{-1} . ^1H NMR data were consistent with the proposed structure of the polymers. Compared with the ^1H NMR peaks of monomers, those of the polymers were broadened and somewhat shifted to a lower magnetic field. The ^1H NMR spectra of **P-8** in CDCl_3 showed peaks indicating protons of phenyl rings of thienopyrazine unit between $\delta = 7.52\text{--}7.33$ and one proton of thiophene units at $\delta = 6.97$ ppm respectively. While that of $-\text{CH}_2$ protons adjacent to thiophene ring appeared at $\delta = 2.84$ and other alkyl side chain protons signals were present at $\delta = 1.70\text{--}0.84$ ppm. Presence of only one main signal for thiophene moiety indicates that the polymer is highly regioregular and main combination of monomers is HT (head to tail) type. Similarly the ^1H NMR spectra of **P-9** in CDCl_3 showed peaks indicating protons of phenyl rings of thienopyrazine between $\delta = 7.37\text{--}7.12$ ppm. While that of $-\text{CH}_2$ protons adjacent to thiophene ring appeared at $\delta = 2.63$ and other alkyl side chain protons signals were present at $\delta = 1.48\text{--}0.64$ ppm. The ^1H NMR spectra of **P-10** in CDCl_3 showed peaks indicating protons of phenyl rings of thienopyrazine between $\delta = 7.56\text{--}7.28$ ppm. The two protons of alkoxy phenylene unit show a peak at $\delta = 7.02$ ppm. While that of $-\text{OCH}_2$ protons adjacent to phenyl ring appeared at $\delta = 4.06$ and other alkyl side chain protons signals were present at $\delta = 2.34\text{--}0.84$ ppm (Figure 3.31, 3.32 and 3.33).

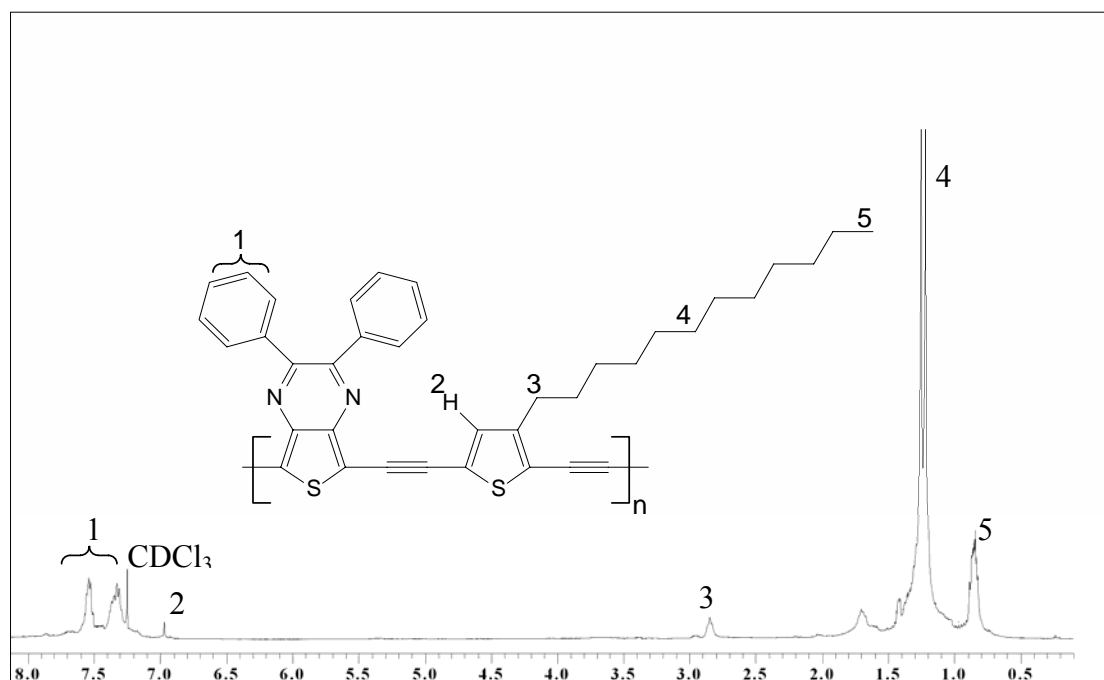


Figure 3.31. ^1H NMR of **P-8**.

The ^{13}C NMR spectra of **P-8** and **P-9** showed the thiophene and thienopyrazine units carbons signals between 155 to 115 ppm. The signals due to the triple bond carbons were present between $\delta = 95$ and 89 ppm. The alkyl carbons signals appeared upfield between 32 and 14 ppm. Similarly the ^{13}C NMR spectra of **P-10** showed the alkoxy phenylene and thienopyrazine units carbons signals between 154 to 114 ppm. The signals due to the triple bond carbons were present at $\delta = 98.31$ and 87.42 ppm. The alkoxy carbons signals appeared at 69.76 ppm and that of alkyl carbons signals appeared upfield between 32 and 14 ppm.

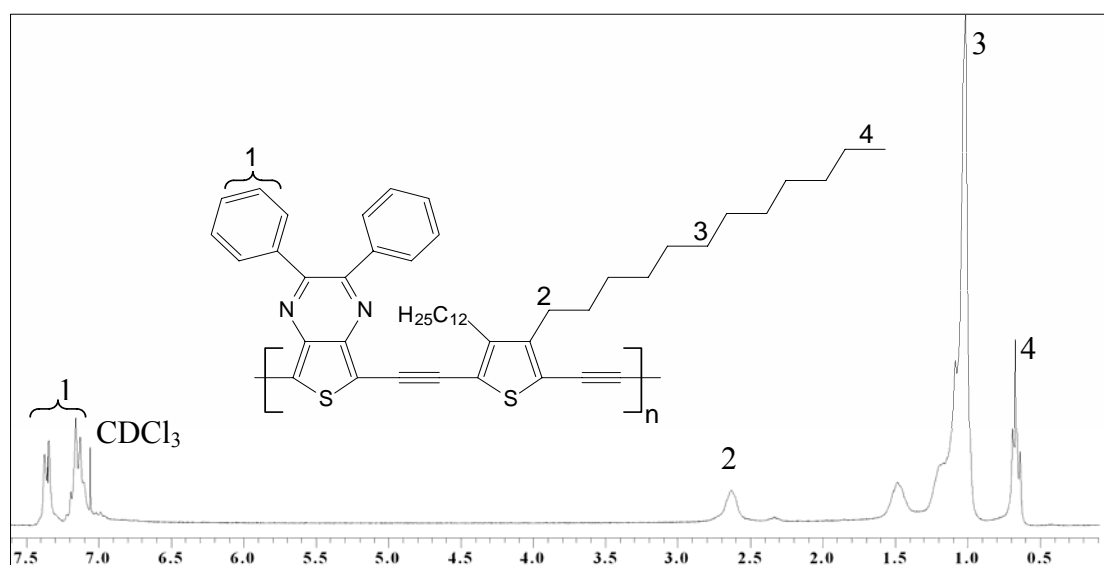


Figure 3.32. ^1H NMR of **P-9**.

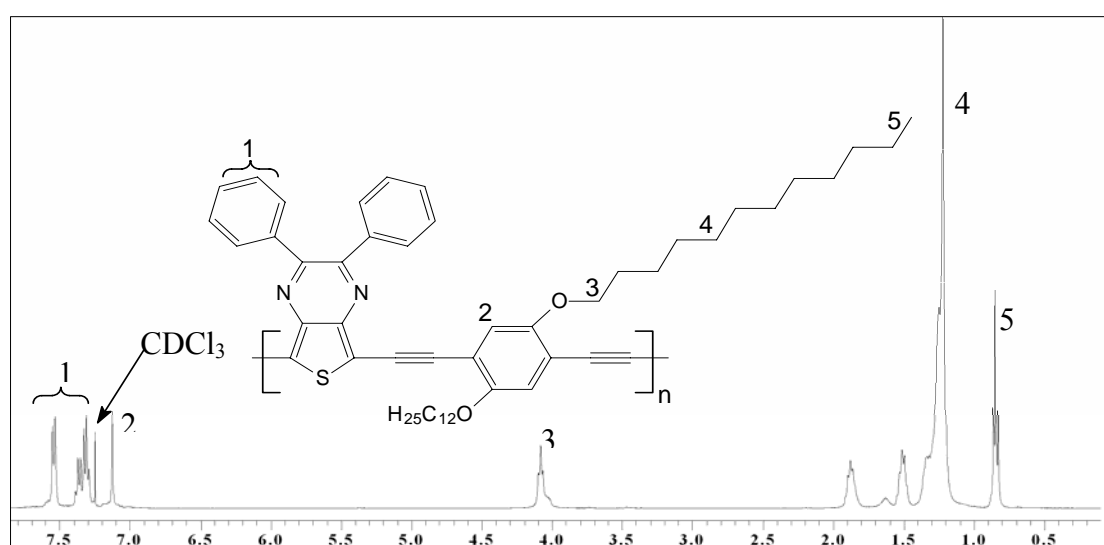


Figure 3.33. ^1H NMR of **P-10**.

The peaks due to terminal $-C\equiv CH$ in 1H NMR and ^{13}C NMR spectra were absent. The ^{13}C NMR spectra showed no signals due to oxidative coupling reaction of acetylenes to diacetylenes ($-C\equiv C-$) between 80 to 70 ppm, indicating no diyne defects in structures. The number-average molecular weight, \bar{M}_n and weight-average molecular weight \bar{M}_w of the polymers (**P-8**, **P-9** and **P-10**) was determined by GPC (polystyrene standards). The \bar{M}_n values obtained by GPC in THF were 10900 g/mol ($\bar{DP} = 19$), 14000 g/mol ($\bar{DP} = 19$) and 5600 g/mol ($\bar{DP} = 7$). The \bar{M}_w values were 34500 g/mol, 22700 g/mol and 27000 g/mol with polydispersity indices of 3.17, 1.62 and 4.81 for **P-8**, **P-9** and **P-10** respectively.

Table 3.9. GPC data of polymers **P-8**, **P-9** and **P-10**.

Polymer	\bar{M}_n [g/mol]	\bar{M}_w [g/mol]	M_w/M_n	\bar{P}_n	Yield (%)
P-8	10900 ^a	34500	3.17	19	62
P-9	14000 ^a	22700	1.62	19	87
P-10	5600 ^a	27000	4.81	7	78

^a \bar{M}_n , GPC (polystyrene standards).

The thermal properties of the copolymers were investigated by thermogravimetric analysis (TGA) and differential scanning calorimetry (DSC) at a heating rate of 10 K/min. The polymers **P-9** and **P-10** are more thermally stable and have 5% weight loss temperatures in air >300 °C (Figure 3.34). There were no phase transition signals detected during repeated heating/cooling DSC cycles for all the polymers. This observation probably results from the stiffness of the polymer's chains.

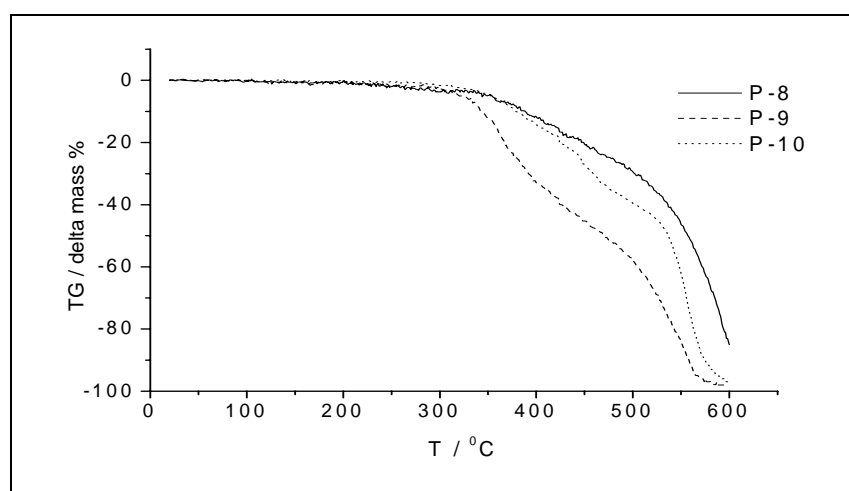


Figure 3.34. TGA of polymers **P-8**, **P-9** and **P-10**.

3.4.2 Optical Properties

The photophysical characteristics of the polymers were investigated by UV-vis absorption and photoluminescence in dilute chloroform solution as well as in solid films. Results from the absorption and emission spectra are summarized in Tables 3.10 and 3.11.

Table 3.10. UV-Vis Data of polymers **P-8-P-10** in Dilute Toluene Solution and in Solid State (Thin Films of 100-150 nm Thickness Spin-Casted from Chlorobenzene Solution).

Polymer	UV-vis λ_{\max} , nm				E_g opt. eV ^c	
	Toluene [log ϵ] ^a	$\lambda_{0.1\max}$	film ^b	$\lambda_{0.1\max}$	Toluene	film
P-8	588 [4.2]	736	646	775	1.68	1.60
P-9	628 [4.4]	740	650	790	1.67	1.57
P-10	605 [4.4]	677	694	790	1.83	1.57

^aMolar absorption coefficient. Molarity is based on the repeating unit. ^bSpin coated from chlorobenzene solution. ^c E_g opt. = $hc / \lambda_{0.1\max}$.

Figures 3.35 and 3.36 show the absorption and emission spectra of polymers **P-8**, **P-9** and **P-10**. The absorption maximum of the three polymers are almost same to each other showing their $\lambda_{\max,abs} \sim 600$ nm. The three polymers show a strong red shift of λ_{\max} (approximately 30-90 nm) when spin cast into thin films on quartz substrate from a chlorobenzene solution.

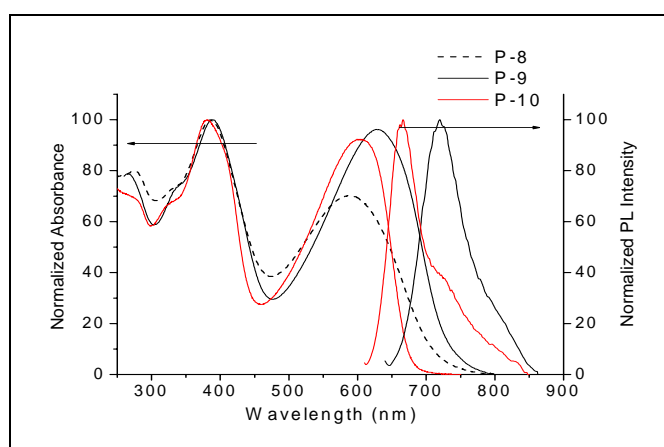


Figure 3.35. Normalized UV-vis spectra of **P-8**, **P-9** and **P-10** and emission spectra of **P-9** and **P-10** in solution (Toluene 10^{-7} mol).

The polymer **P-10** was more red shifted than **P-8** and **P-9** (90 nm). This observed red shift going from solution to a solid film indicates interchain interactions in the solid state, possibly assisted by planarization and an increase of conjugation length.⁹⁶ According to this picture, the phenyl rings would assume more coplanarity and maximization of conjugation with concomitant bathochromic shift only upon transition into the solid state. This explanation is tentative. The thin film absorption spectra show that for **P-8**, **P-9** and **P-10**, the onset of the absorption is ~775 nm (1.60 eV), ~790 nm (1.57 eV) and ~790 nm (1.57 eV) respectively. As anticipated, the alternation of electron-rich thiophene and alkoxy phenylene with that of electron-deficient thienopyrazine units along conjugated backbone results in a low optical bandgap.

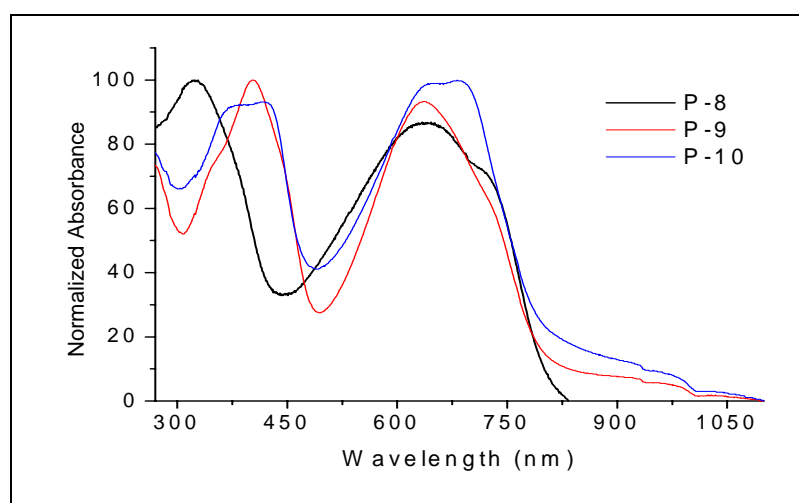


Figure 3.36. Normalized UV-vis spectra of **P-8**, **P-9** and **P-10** in solid state (film from chlorobenzene).

The optical bandgap is higher than poly(thieno[3,4-*b*]pyrazine)¹²³ which was designed on the basis of theoretical calculations predicting a bandgap of 0.80 eV.¹²⁴ Furthermore, reduced steric interaction between adjacent monomer units was also expected. The electronic spectrum of this polymer showed an absorption maximum at 875 nm (in CHCl₃ solution) and at 915 nm for a solution cast film with a bandgap of 0.95 eV. Yamashita et al. have synthesized a series of trimers containing a median thieno[3,4-*b*]pyrazine ring system.⁴³ These compounds can be electropolymerized and the bandgap of these polymers estimated from electrochemical and optical data were in the range of 1.00-1.50 eV.⁴³ The problem of steric interactions in this particular system has been analyzed in more detail by Ferraris et al. who synthesized 2,5-di(2-thienyl)pyridino[*c*]thiophene.¹²⁵ It can be depicted that these materials (**P-8**, **P-9** and **P-10**) behave like those one prepared by Yamashita et al. and the optical band gaps are comparable.

Table 3.11. Photoluminescence Data of **P-9** and **P-10** in Dilute Toluene Solution ($\sim 10^{-7}$ M) and in Solid State.^a

Polymer	UV-em λ_{em} , nm		Stokes shift, nm		% ϕ_{PL}	
	Toluene	film	Toluene	film	Toluene	film
P-9	719		91		02	0
P-10	666	732	61	38	15	0.5

^bSpin coated from chlorobenzene solution.

The emission maximum of **P-9** in dilute chloroform solution is at $\lambda_{max,em} = 719$ nm, while the emission curve of **P-10**, showing its maximum at $\lambda_{max,em} = 666$ nm. The fluorescence quantum yields were found to be around 2 and 15% for **P-9** and **P-10** respectively. The emission maximum of **P-10** in solid film is located at $\lambda_{max,em} = 732$ nm leading to Stokes shift of 38 nm, and a lower fluorescence quantum yield of 0.5%. there was no emission observed for **P-8** and **P-9** in solid state. We assumed, the reason for the low photoluminescence (PL) efficiency is a π - π stacking of the conjugated backbone cofacial to each other due to the favourable inter-chain π - π interactions, which lead to a self-quenching process of the excitons.⁹⁹⁻¹⁰¹ Triple-bonds in the polymer main chain (like in poly(aryleneethynylenes)) lead to stiffness and rigidity of the polymer backbones, which thereby reinforce the inter-chain interactions.¹⁰² Moreover, we assume that thienopyrazine moiety serves as a quenching channel (both radiative and non-radiative) in these polymers.

3.4.3 Aggregate Formation in Solvent/Nonsolvent Solution

The absorption spectra of polymers **P-9** in chloroform/methanol mixture with different volume concentrations of methanol are shown in Figure 3.37. It should be noted here that in all cases the bulk solution maintains homogeneity. With an increase of methanol concentration, there is increase in the intensity of the band and appearance of a shoulder at higher wavelength when the methanol concentration reaches 50 vol % in **P-9**. The spectral red shift corresponds to a disorder-to-order transformation of the conjugated polymer chains.

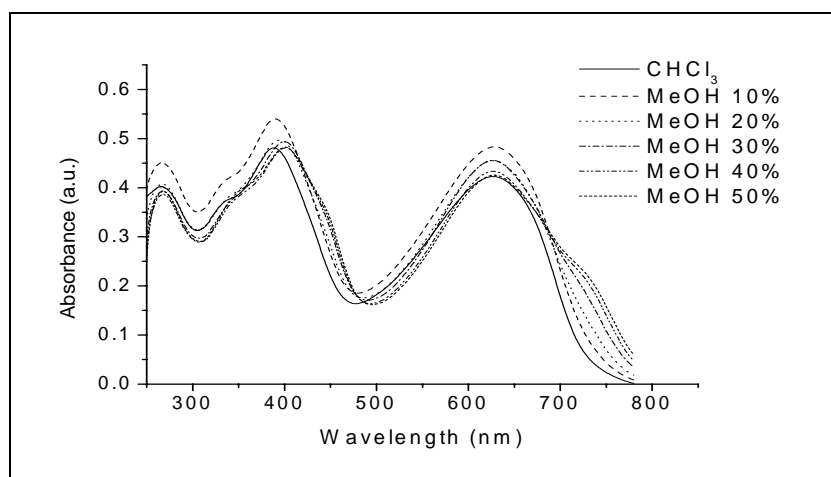


Figure 3.37. UV-vis spectra of **P-9** in CHCl_3 with different concentration of MeOH.

Since polymers **P-9** is insoluble in methanol, the addition of methanol to the homogeneous chloroform solution leads to aggregate formation. In the aggregate the polymer possesses a more planarized structure, hence extension in conjugation length, so the new band at higher wavelength can be assigned to the aggregate. Similar phenomena were found in chloroform/methanol solutions of 2,5-dialkylpoly(*p*-phenyleneethynylene)s,^{19a} poly(fluorenyleneethynylene)s,^{19b} and poly(*p*-phenyleneethynylene) copolymers^{19c} by Bunz et al.

3.4.4 Electrochemical Studies

The electrochemical behavior of the copolymers was investigated by cyclic voltammetry (CV). The CV was carried out using thin films of polymers prepared from dichloromethane (5 mg/mL) in acetonitrile at a potential scan rate of 15 mV/s. Ag/AgCl served as the reference electrode; it was calibrated with ferrocene ($E^{1/2}_{\text{ferrocene}} = 0.52 \text{ V vs Ag/AgCl}$). The supporting electrolyte was tetrabutylammonium hexafluorophosphate ($n\text{-Bu}_4\text{NPF}_6$) in anhydrous acetonitrile (0.1 M). The onset potentials are the values obtained from the intersection of the two tangents drawn at the rising current and the baseline charging current of the CV curves. Several ways to evaluate HOMO and LUMO energy levels from the onset potentials, $E^{\text{ox/onset}}$ and $E^{\text{red/onset}}$, have been proposed in the literature.^{25,28-31} These were estimated here on the basis of the reference energy level of ferrocene (4.8 eV below the vacuum level)²⁹ according to the following equation:

$$E^{\text{HOMO/LUMO}} = [-(E_{\text{onset (vs. Ag/AgCl)}} - E_{\text{onset (Fc/Fc+ vs. Ag/AgCl)}})] - 4.8 \text{ eV.}$$

The onset and the peak potentials, the electrochemical band gap energy, and the estimated position of the upper edge of the valence band (HOMO) and of the lower edge of conduction

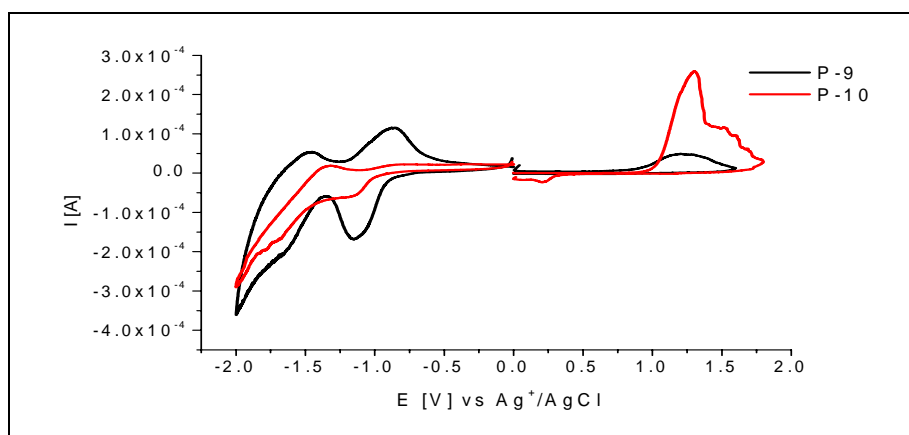


Figure 3.38. Cyclic voltammograms of polymers (**P-9** and **P-10**) in 0.1M TBAPF₆/CH₃CN at 25 °C.

band (LUMO) are listed in Table 3.12. The CV for oxidation show peaks around 1.20 V with estimated onset values around 0.94 V for **P-9**. The oxidation CV traces of the **P-10** show peaks at 1.31 V (onset at 1.01 V). The CV for reduction process was reversible. Reduction peaks for **P-9** and **P-10** were around -1.15 and -1.17 V (onset values -0.92 and -0.98 V), respectively. These moderately negative reduction potentials have been attributed to the electron withdrawing effects of thieno[3,4-*b*]pyrazine moiety.⁴³ The band gap energy directly measured from CV ($E_{g_{ec}/onset}$ 1.86 eV for **P-9** and 1.99 eV for **P-10**) and the optical band gap energy are close to each other. The discrepancy (ΔE_g) of both values lies within the range of error. From the onset potentials, HOMO and LUMO energy levels were estimated. The HOMO for **P-9** and **P-10** were around -5.22 and -5.29 eV, while LUMO around -3.36 and -3.30 eV respectively.

Table 3.12. Electrochemical Potentials and Energy Levels of the **P-9** and **P-10**.

Polymer	Oxidation Potential		Reduction Potential		Energy Levels ^b		Band Gap	
	E_{ox}^a (V vs Ag/Ag ⁺)	$E_{onset, Ox}$	E_{red}^a (V vs Ag/Ag ⁺)	$E_{onset, Red}$	HOMO (eV)	LUMO (eV)	Band Gap ^{ec} (eV)	Optical Band Gap (eV)
P-9	1.20	0.94	-1.15	-0.92	-5.22	-3.36	1.86	1.57
P-10	1.31	1.01	-1.17	-0.98	-5.29	-3.30	1.99	1.57

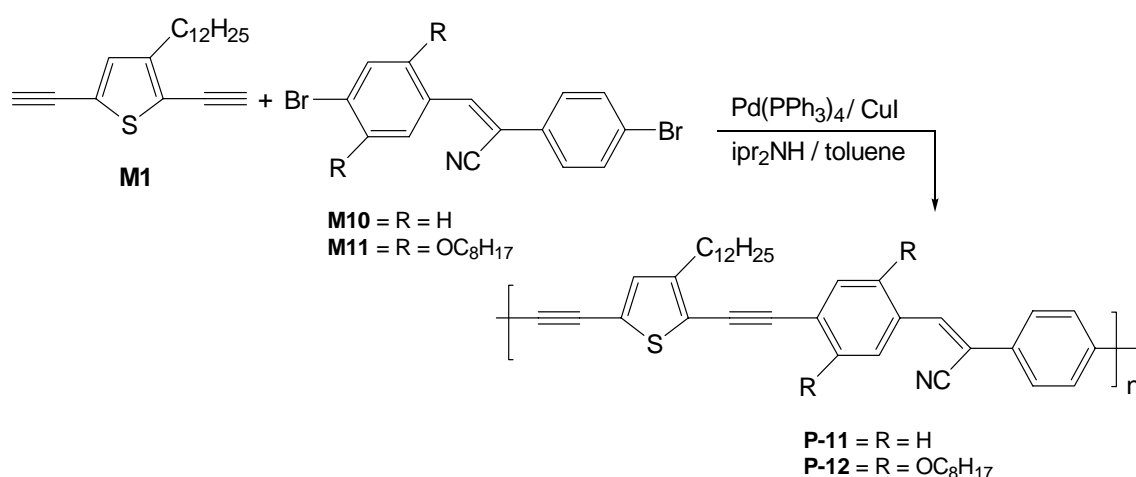
^aReduction and oxidation potential measured by cyclic voltammetry. ^bCalculated from the reduction and oxidation potentials assuming the absolute energy level of ferrocene/ferrocenium to be 4.8 eV below vacuum.

3.5 “Cyanostilbene as Acceptor” PE/PPV Hybrid Polymers

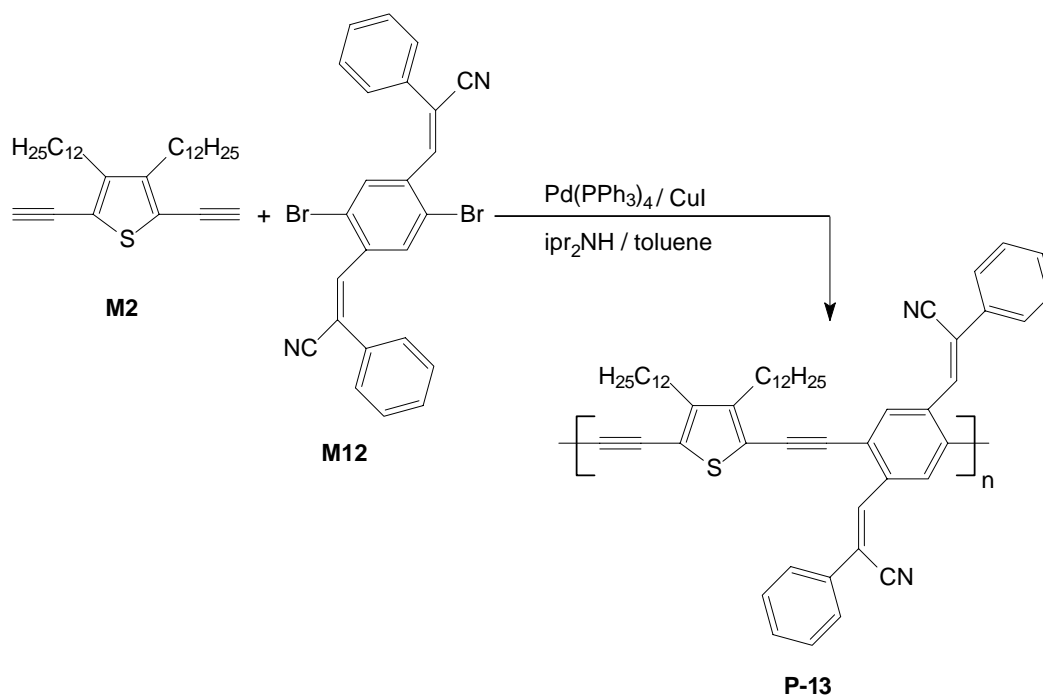
PPV is an adequate hole-transporting material; thus, the modification of this polymer to improve its electron transport properties has been a challenging issue. It was discovered by Bunz et al.¹²⁶ and Klemm et al.¹²⁷ that incorporating electron-withdrawing acetylene ($-C\equiv C-$) bonds into the PPV backbone to obtain hybrid phenylenevinylene/ phenyleneethynylene (PV/PE) materials confers several advantages, especially a high oxidation potential. Materials with similar structures¹²⁸ which can be used in photovoltaic cells and LEDs have been subsequently reported. Pang et al.^{128c} also developed green-emitting PE/PV hybrid polymers with phenyl rings linked alternately at meta and para positions, providing an efficient intramolecular energy transfer across *m*-phenylene. Here in, we have synthesized new PE/PV hybrid polymers bearing cyano group on vinylene position to enhance electron affinity.

3.5.1 Synthesis and Characterization of the Polymers

By employing the Pd catalysed Sonogashira coupling,^{56,58} the polymers (**P-11**, **P-12** and **P-13**) were synthesized from thiophene diacetylenes (**M1** and **M2**), 1,2-bis(4-bromophenyl)-1-cyanovinylene (**M10**), 3-(4-bromo-2,5-dioctyloxyphenyl)-2-(4-bromophenyl)-acrylonitrile (**M11**) and 3-[2,5-dibromo-4-(2-cyano-2-phenylvinyl)-phenyl]-2-phenylacrylonitrile (**M12**). The general synthetic routes towards the polymers are outlined in Schemes 3.14 and 3.15. The yields were between 63-72%. The polymers are red in colour in solid state and the polymer **P-12** show green metallic luster. The polymers are scarcely soluble in organic solvents like THF, $CHCl_3$ and toluene etc., the polymers **P-11** and **P-13** show better solubility than **P-12** in above mentioned solvents and further investigated. Less solubility can be attributed, as well as to the presence of less number of alkyl chains and more rigid structures.



Scheme 3.14. Synthesis of Polymers **P-11** and **P-12**.



Scheme 3.15. Synthesis of Polymer **P-13**.

The chemical structure of the polymers was verified by FTIR, ^1H , ^{13}C NMR and elemental analysis. The strong IR absorption peak $\nu(\text{C}\equiv\text{CH})$ near 3290 cm^{-1} of the monomers disappeared on polycondensation, and a new $\nu(\text{C}\equiv\text{C})$ peak appeared at about 2200 cm^{-1} . ^1H NMR data were consistent with the proposed structure of the polymers. Compared with the ^1H NMR peaks of monomers, those of the polymers were broadened and somewhat shifted to a lower magnetic field. The ^1H NMR spectra of **P-11** in CDCl_3 showed peak indicating vinylic proton at 7.91 ppm, peaks for protons of phenyl rings between $\delta = 7.77\text{--}7.50$ and one proton of thiophene units

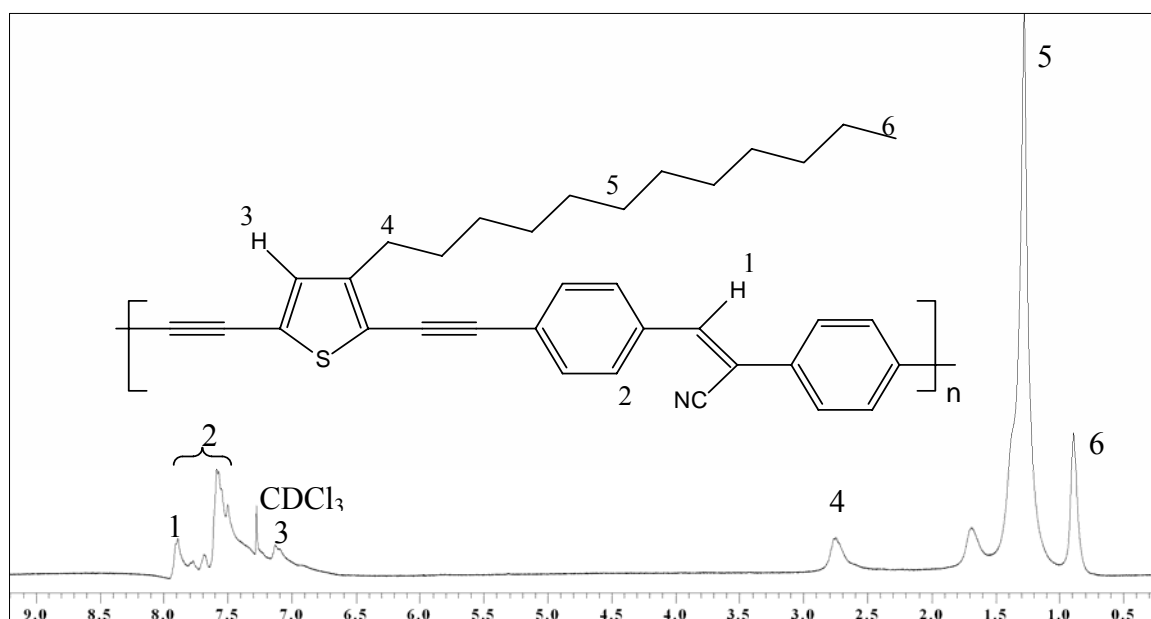


Figure 3.39. ^1H NMR of **P-11**.

at $\delta = 7.13$ ppm respectively. While that of $-\text{CH}_2$ protons adjacent to thiophene ring appeared at $\delta = 2.76$ and other alkyl side chain protons signals were present at $\delta = 1.69$ - 0.89 ppm (Figure 3.39). Similarly the ^1H NMR spectra of **P-13** in CDCl_3 showed peak indicating vinylene protons between 8.52 - 8.30 ppm and peaks indicating protons of phenyl rings between $\delta = 8.09$ - 7.39 ppm. While that of $-\text{CH}_2$ protons adjacent to thiophene ring appeared at $\delta = 2.67$ and other alkyl side chain protons signals were present at $\delta = 1.54$ - 0.86 ppm (Figure 3.40).

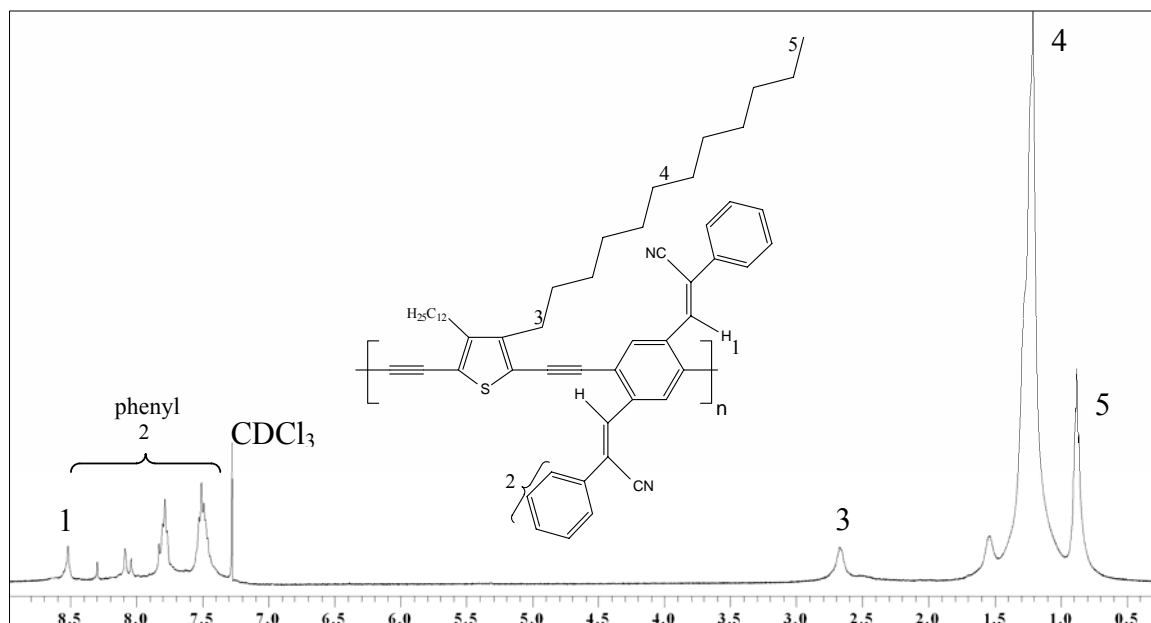


Figure 3.40. ^1H NMR of **P-13**.

The ^{13}C NMR spectra of **P-11** and **P-13** showed the thiophene and phenyl units carbons signals between 142 to 117 ppm. The signals due to the triple bond carbons were present between $\delta = 95$ and 85 ppm. The alkyl carbons signals appeared upfield between 32 and 14 ppm. The peaks due to terminal $-\text{C}\equiv\text{CH}$ in ^1H NMR and ^{13}C NMR spectra were absent. In ^{13}C NMR spectra the carbon signals due to oxidative coupling reaction of acetylenes to diacetylenes ($-\text{C}\equiv\text{C}-$) between 80 to 70 ppm were absent, indicating no diyne defects in structures. The number-average molecular weight, \bar{M}_n and weight-average molecular weight, \bar{M}_w of the soluble portion of the polymers (**P-11**, **P-12** and **P-13**) was determined by GPC (polystyrene standards). The \bar{M}_n values obtained by GPC in THF were 4100 g/mol ($\bar{DP} = 8$), 3200 g/mol ($\bar{DP} = 4$) and 6600 g/mol ($\bar{DP} = 8$), respectively. The \bar{M}_w values were 15000 g/mol, 8200 g/mol and 19000 g/mol with polydispersity indices of 3.63 , 2.54 and 2.88 for **P-11**, **P-12** and **P-13** respectively. The relatively low molecular weights of these polymers may be due to

precipitation in the solvents during the polycondensation, thus preventing further propagation reactions.

Table 3.13. GPC data of polymers **P-11**, **P-12** and **P-13**.

Polymer	\bar{M}_n [g/mol]	\bar{M}_w [g/mol]	M_w/M_n	\bar{P}_n	Yield (%)
P-11	4100 ^a	15000	3.63	8	72
P-12	3200 ^{a,b}	8200	2.54	4	63
P-13	6600 ^a	19100	2.88	8	87

^a \bar{M}_n , GPC (polystyrene standards). ^b Soluble portion.

The thermal properties of these copolymers were investigated by thermogravimetric analysis (TGA) and differential scanning calorimetry (DSC) at a heating rate of 10 K/min. The polymers **P-11** and **P-12** are thermally stable up to 300 °C (Figure 3.41). In the DSC no phase transition signals were detected during repeated heating/cooling DSC cycles for these polymers. This observation probably results from the stiffness of the polymer's chains due to presence of rigid units.

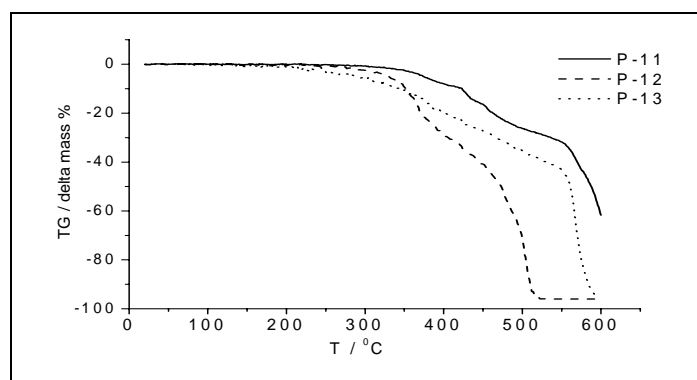


Figure 3.41. TGA of polymers **P-11**, **P-12** and **P-13**.

3.5.2 Optical Properties

The photophysical characteristics of the polymers were investigated by UV-vis absorption and photoluminescence in dilute chloroform solution as well as in solid films. Results from the absorption and emission spectra are summarized in Table 3.14 and 3.15.

Figure 3.42 and 3.43 show the absorption and emission spectra of polymers **P-11**, **P-12** and **P-13**. The absorption maximum of the polymer **P-12** is about 31 nm red shifted than **P-11** due to presence of alkoxy phenylene units. Similarly the absorption maximum of the polymer **P-13** is blue shifted from both **P-11** and **P-12** but also showed a shoulder at higher wavelength.

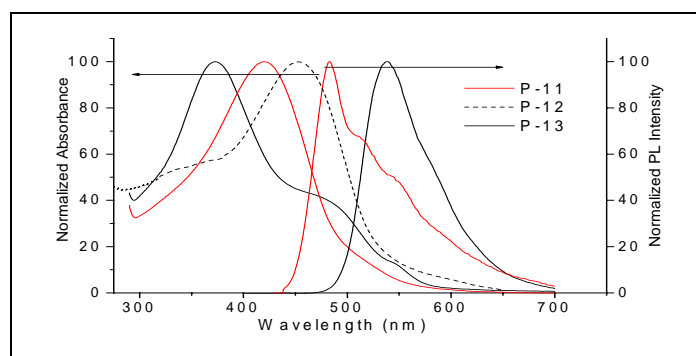


Figure 3.42. Normalized UV-vis spectra of **P-11**, **P-12**, **P-13** and emission spectra of **P-11** and **P-13** in solution (Toluene 10^{-7} mol).

The UV-vis absorption spectrum of **P-13** is almost same as for the **PPE/PPV** hybrid polymer reported by Bunz et al. ($\lambda_{\max} = 354, 417^{\text{sh}}$),^{126b} the absorption maximum is red shifted due to better donor-acceptor relationship between both segments of the polymer **P-13**.

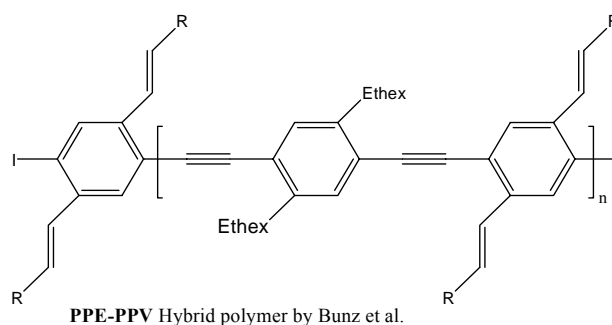


Table 3.14. UV-Vis Data of polymers **P-11-P-13** in Dilute Toluene Solution and in Solid State (Thin Films of 100-150 nm Thickness Spin-Casted from Chlorobenzene Solution).

Polymer	UV-vis λ_{\max} , nm				E_g opt. eV ^c	
	Toluene [log ϵ] ^a	$\lambda_{0.1\max}$	film ^b	$\lambda_{0.1\max}$	Toluene	film
P-11	421 [4.5]	545	434	600	2.27	2.06
P-12	452 [4.4]	552			2.25	
P-13	373, 480 ^{sh} [4.6]	560	380	575	2.21	2.16

^aMolar absorption coefficient. Molarity is based on the repeating unit. ^bSpin coated from chlorobenzene solution. ^c E_g opt. = $hc / \lambda_{0.1\max}$. ^{sh} shoulder.

The two polymers **P-11** and **P-13** show a small red shift of λ_{\max} (approximately 7-13 nm) when spin cast into thin films on quartz substrate from a chlorobenzene solution. The relatively identical absorption spectra of **P-11** and **P-13** in solution and as a solid film indicated that there was little difference in the two states, indicating the planarization of the chains is not very distinct due to presence of bulky cyano groups. The Stokes shifts between the absorption and emission of the polymers **P-11** and **P-13** are relatively large (219 and 213 nm) and showed a lower fluorescence quantum yield of 0.5 and 1 % respectively.

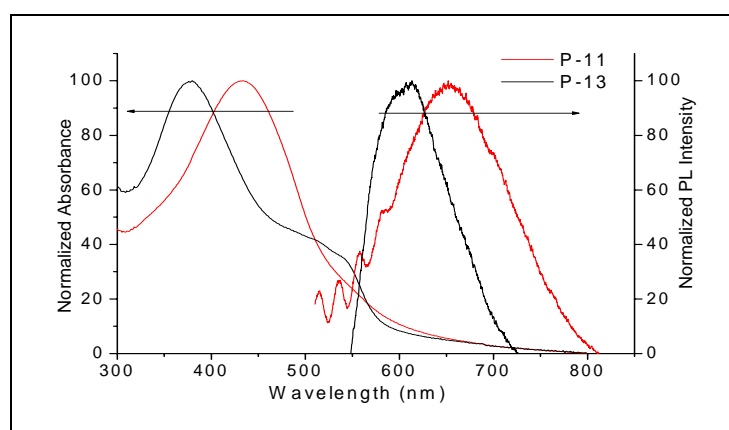


Figure 3.43. Normalized UV-vis and emission spectra of **P-11** and **P-13** in film.

Usually the Stokes shift comes from the two sources: emission either from the excited segments of a conjugated polymer undergoing deformation into more planar conformation along the chain or from the migrated excitons in other segments where ring rotations are not hindered.¹²⁹ The absence of any alkyl chain on phenyl rings adjacent to vinylene units and presence of bulky cyano groups enable strong π - π interchain interaction, leading to the formation of excimers which provide radiationless decay channels for the excited states and hence resulting in very large Stokes shifts and lower fluorescence quantum yields.⁹⁹⁻¹⁰¹

Table 3.15. Photoluminescence Data of **P-11** and **P-13** in Dilute Toluene Solution ($\sim 10^{-7}$ M) and in Solid State.^a

Polymer	UV-em λ_{em} , nm		Stokes shift, nm		% ϕ_{PL}	
	Toluene	film	Toluene	film	Toluene	film
P-11	483	653	62	219	07	0.5
P-13	539	593	166	213	09	1

^aSpin coated from chlorobenzene solution.

3.5.3 Electrochemical Studies

The polymers solution was prepared in dichloromethane (5 mg/mL). The DPP (Differential pulse polarography) of polymers was carried out in dichloromethane at a potential scan rate of 15 mV/s. Ag/AgCl served as the reference electrode; it was calibrated with ferrocene ($E_{\text{ferrocene}}^{1/2} = 0.52 \text{ V vs Ag/AgCl}$). The supporting electrolyte was tetrabutylammonium hexafluorophosphate ($n\text{-Bu}_4\text{NPF}_6$) in acetonitrile (0.1 M). Several ways to evaluate HOMO and LUMO energy levels from the onset potentials, $E^{\text{ox/onset}}$ and $E^{\text{red/onset}}$, have been proposed in the literature.¹⁰⁴⁻¹⁰⁸ HOMO and LUMO energy levels were estimated here on the basis of the reference energy level of ferrocene (4.8 eV below the vacuum level)¹⁰⁶ according to the following equation:

$$E^{\text{HOMO/LUMO}} = [-(E_{\text{onset (vs. Ag/AgCl)}} - E_{\text{onset (Fc/Fc+ vs. Ag/AgCl)}})] - 4.8 \text{ eV}.$$

It was of interest to evaluate the effect of cyano vinylene in **P-11** and how the substituted styryl side chains would modulate the electrochemical behavior of **P-13** due to presence of bulky cyano groups. The onset and the peak potentials, the electrochemical band gap energy, and the estimated position of the upper edge of the valence band (HOMO) and of the lower edge of conduction band (LUMO) are listed in Table 3.16. The samples of the **P-11** and **P-13** are irreversibly oxidized at peak potentials around 0.78 and 1.43 V and second peaks at 1.38 and 1.74 V with estimated onset values around 0.70 and 1.28 V respectively. Interestingly enough, the reduction potential of the polymer **P-13** was around -0.68 V (onset value -0.62 V), while that of **P-11** was around -1.47 V with estimated onset value around -0.99 V. The polymers **P-13** show second and third reduction peaks at -0.91 and -1.08 V suggesting that the polymer chains can be higher charged. Similarly **P-11** show second reduction peak at -1.77 V. It is reasonable to assume that in the first step only every second repeating unit is charged in both **P-11** and **P-13** and that in a second and third reduction steps the remaining side chains modules are reduced. From these data one can obtain two series of band gaps that correspond either to the *onset* of oxidation and reduction (small values) or to the peak to peak distances (larger values). Janietz et al.¹¹² suggest that the difference in the onset of reduction and oxidation is a good measure for the band gap given an ideal sample (monodisperse, defect free). Our material are polydisperse and amorphous and have multiple degrees of rotational freedom with respect to both the main and side chains. We estimated the optical band gaps of **P-11** and **P-13** as the edge of absorption spectrum. Both the oxidation and the reduction potentials are affected by the attachment of the styryl side chain and also due to cyano group to the PAE main chain (Figure 3.44). The effect of the styryl side chains and cyano group is two fold: they act as electronwithdrawing substituents

for the PPE main chain and thus decrease the reduction potential of the new polymer as compared to dialkyl-PPEs. On the other hand, the nature of the distyrylbenzene core largely determines the oxidation potential of the polymer **P-13**, suggesting that its HOMO has a significant electron density on the styryl sidearms. Whether the two crossed systems are

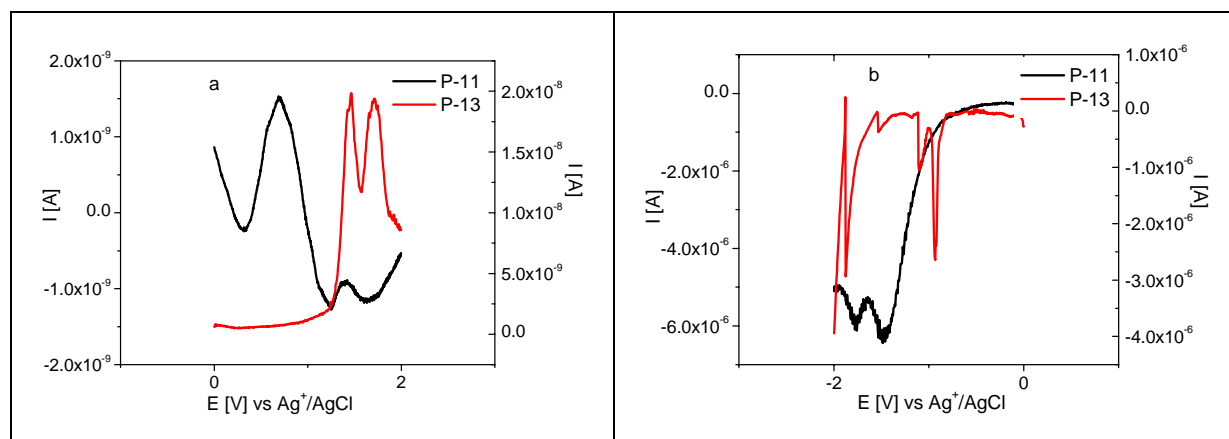


Figure 3.44. Differential pulse polarographic-curves of polymers **P-11** and **P-13** in CH_2Cl_2 at 25 $^\circ\text{C}$ (a : oxidation curves; and b : reduction curves).

electronically coupled or only topologically cross-conjugated is difficult to say, but attachment of styryl side chains and presence of cyano groups significantly modulates the electronic properties of the polymers **P-11** and **P-13**.¹³⁰ The HOMO and LUMO energy levels clearly indicate that **P-13** has better electron affinity than **P-11**. It is also evident from this data that cyano group in side chains show more prominent effect than in main chain.

Table 3.16. Electrochemical Potentials and Energy Levels of the Polymers **P-11** and **P-13**.

Polymer	Oxidation Potential		Reduction Potential		Energy Levels ^b		Band Gap	
	E_{ox}^{a} (V vs Ag/Ag ⁺)	$E_{\text{onset, Ox}}$	$E_{\text{red}}^{\text{a}}$ (V vs Ag/Ag ⁺)	$E_{\text{onset, Red}}$	HOMO (eV)	LUMO (eV)	Band Gap (eV)	Optical Band Gap (eV)
P-11	0.78	0.70	-1.47	-0.99	-4.98	-3.29	1.69	2.06
	1.38		-1.77					
P-13	1.43	1.28	-0.68	-0.62	-5.56	-3.66	1.90	2.16
	1.74		-0.91					
			-1.08					

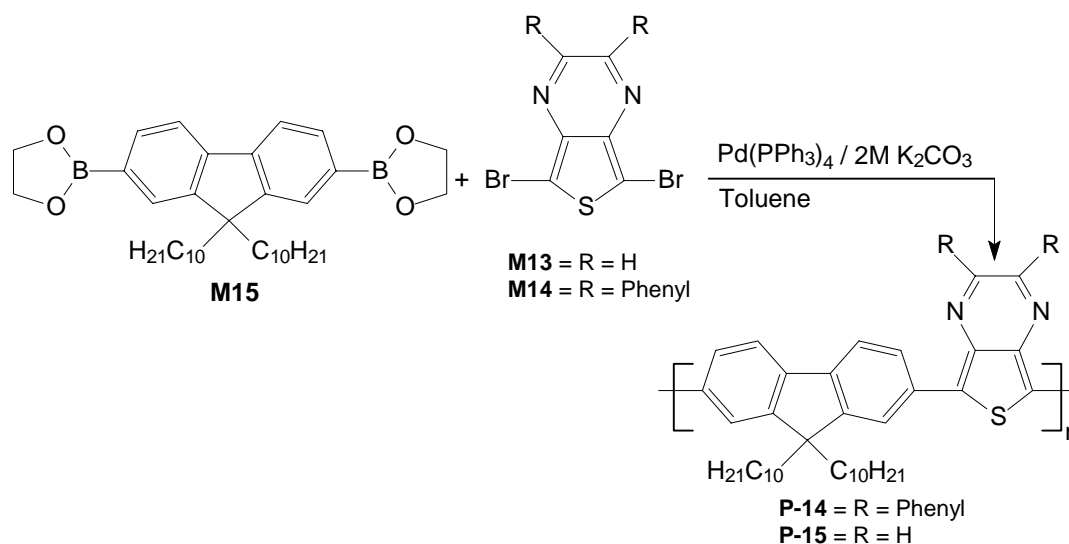
^aReduction and oxidation potential measured by differential pulse polarography. ^bCalculated from the reduction and oxidation potentials assuming the absolute energy level of ferrocene/ferrocenium to be 4.8 eV below vacuum.

3.6 Thienopyrazine and Fluorene Based Poly(heteroarylene)s

Polyfluorenes are promising new materials for light emitting diodes because of their thermal and chemical stability and exceptionally high fluorescence quantum yields (0.6–0.8) in thin solid films.¹³¹ Normally, polyfluorene homopolymers have large bandgaps and emit blue light. The emission color of polyfluorenes can be tuned over the entire visible region by incorporating narrow band-gap comonomers into the polyfluorene backbone.^{132,133} The most widely used narrow band-gap comonomers are a variety of aromatic heterocycles such as thiophene,^{134–147} ethylenedioxythiophene^{134–139} and benzothiadiazole.^{145–149} Here in, first time copolymers of fluorene and thieno[3,4-*b*]pyrazine has been synthesized.

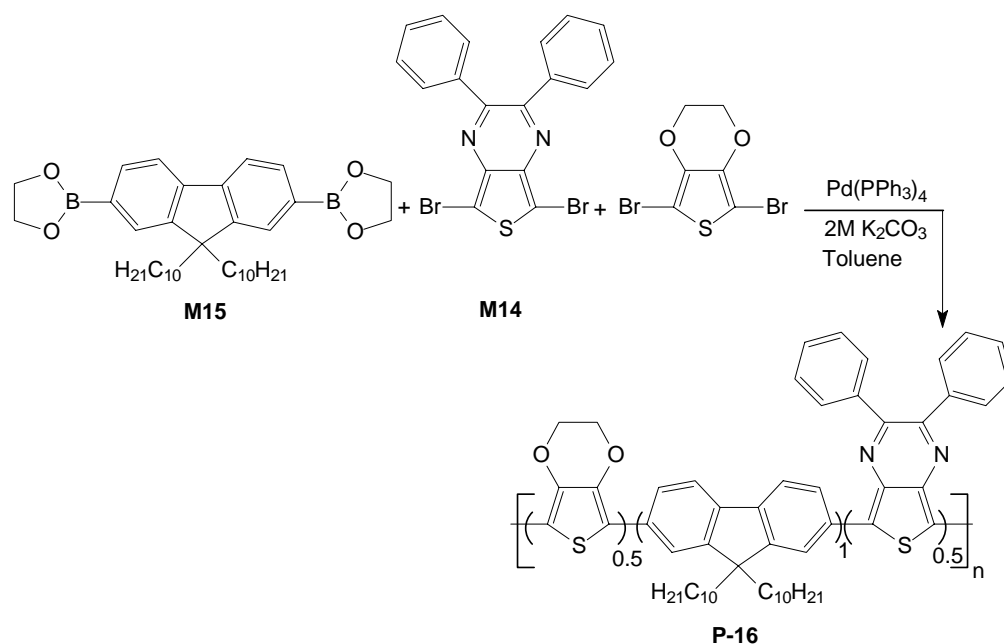
3.6.1 Synthesis and Characterization

The basic strategy employed for the synthesis of the polymers (**P-14**, **P-15**, **P-16** and **P-17**) is based on the Suzuki reaction,⁶⁷ which was carried out in a mixture of toluene and potassium carbonate (2M) containing 1mol % Pd(PPh₃)₄ under vigorous stirring at 85-90 °C for 60-70h. The synthetic routes to all the four polymers are illustrated in scheme 3.16, 3.17 and 3.18.

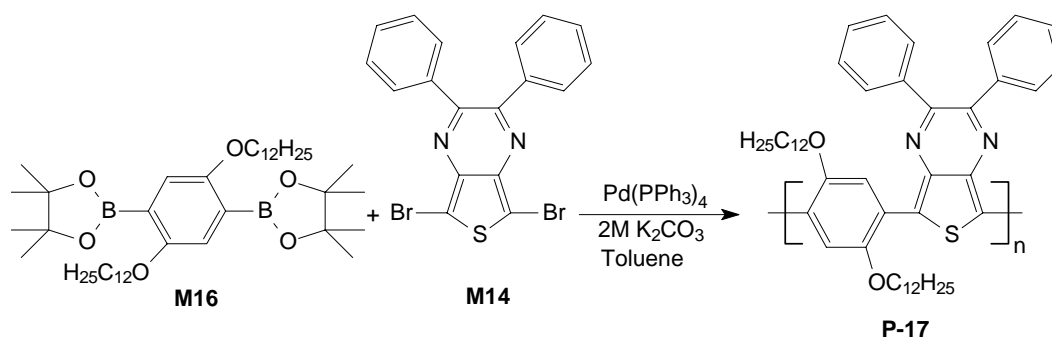


Scheme 3.16. Synthesis of Polymers **P-14** and **P-15** .

The polymers were obtained with satisfactory yields. After purification and drying, **P-14**, **P-15**, **P-16** and **P-17** were obtained as blue solids. All these polymers readily dissolve in common organic solvents, such as chloroform, THF, toluene and chlorobenzene.



Scheme 3.17. Synthesis of Polymer **P-16**.



Scheme 3.18. Synthesis of Polymer **P-17**.

The number-average molecular weights, \bar{M}_n , of the polymers (**P-14**, **P-15**, **P-16** and **P-17**) were determined by GPC (polystyrene standards) were 13100, 5700, 4700, and 1740 with polydispersity indices of 4.02, 1.70, 1.75 and 1.06 respectively (see Table 3.17). From GPC it is clearly indicative, **P-22** at best is an oligomer.

Table 3.17. GPC data of polymers **P-14-P-17**.

Polymer	\bar{M}_n [g/mol]	\bar{M}_w [g/mol]	M_w/M_n	\bar{P}_n	Yield (%)
P-14	13100 ^a	52800	4.02	18	82
P-15	5700 ^a	9700	1.70	10	87
P-16	4700 ^a	8300	1.75	7	87
P-17	1740 ^a	1850	1.06	2	61

^a \bar{M}_n , GPC (polystyrene standards).

The chemical structures of the polymers were verified by ^1H NMR, ^{13}C NMR, FTIR and elemental analyses. Figure 3.45 displays the ^1H NMR spectrum of the polymer **P-14**. There are five peaks in the aromatic region for **P-14**. The three peaks in the lower field at 8.5, 8.3 and 7.86 ppm are attributed to the different kinds of protons on the fluorene ring. The other peaks between 7.67 and 7.37 ppm belong to the protons of the phenyl rings of the thienopyrazine unit.

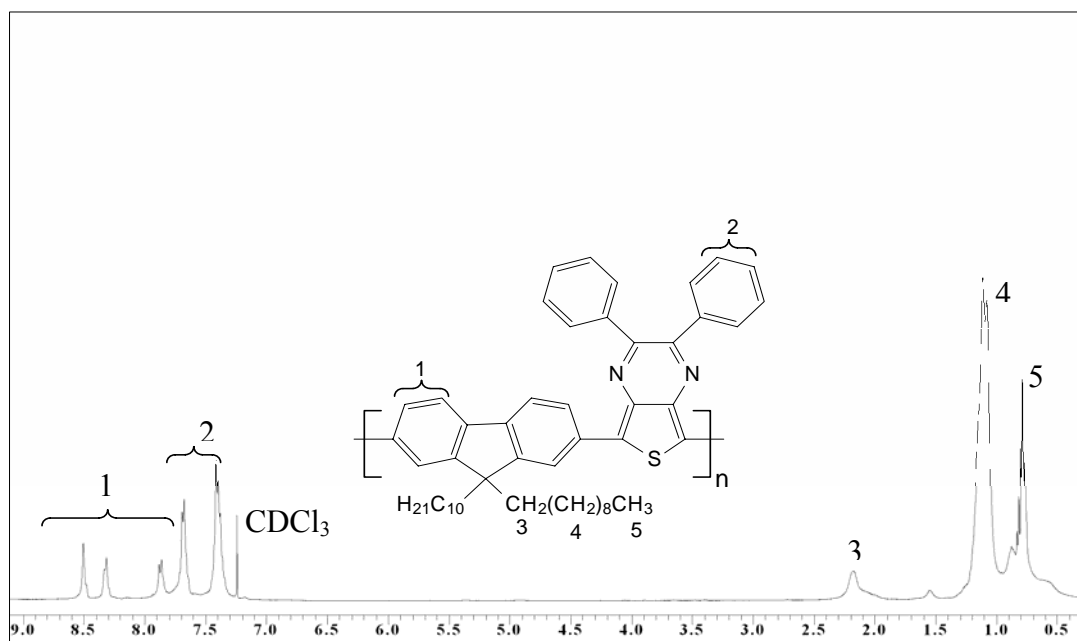


Figure 3.45. ^1H NMR of **P-14**.

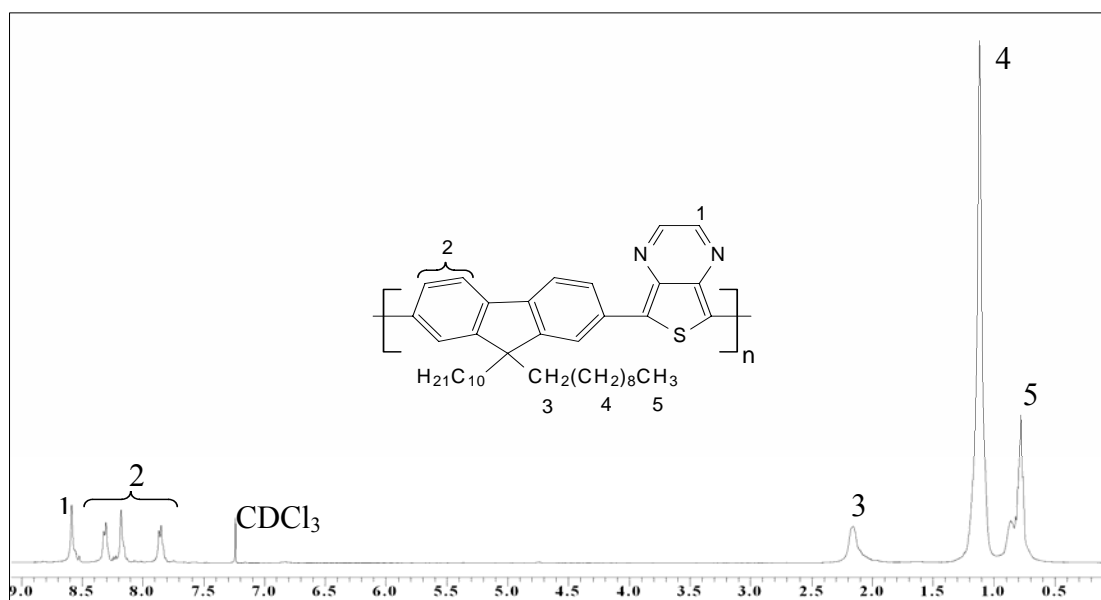


Figure 3.46. ^1H NMR of **P-15**.

Similarly the aromatic region of **P-16** is quite similar to that of **P-14**. The three peaks in the lower field at 8.49, 8.30 and 7.85 ppm are attributed to the protons of the fluorene ring and the other peaks between 7.66 and 7.38 ppm belongs to the protons of the phenyl ring of thienopyrazine unit (Figure 3.47).

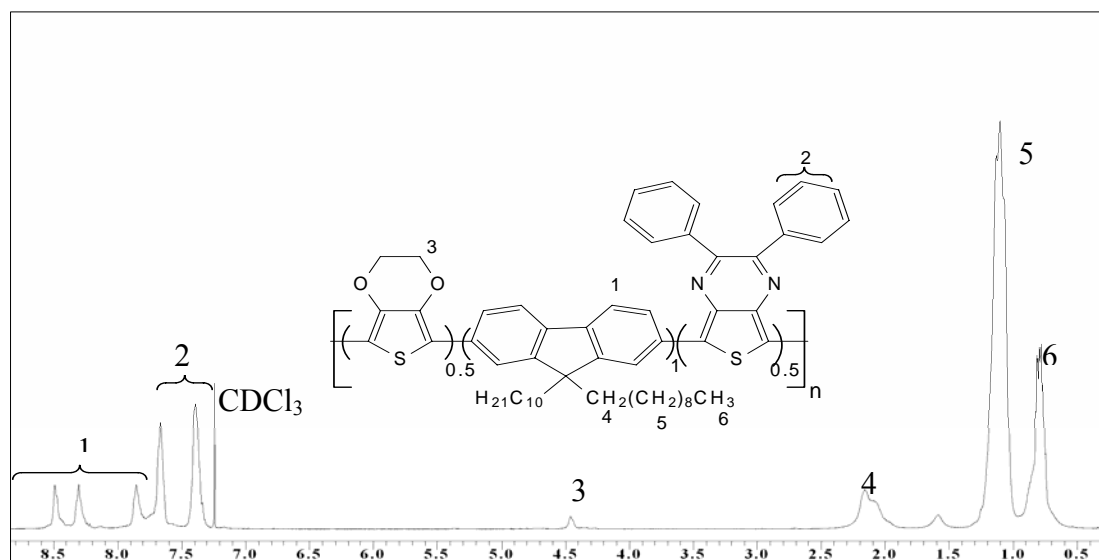


Figure 3.47. ^1H NMR of **P-16**.

The aromatic region of **P-15** is similar to that of **P-14** and **P-16** with all peaks slightly shifted to lower field. There is one peak around 8.58 ppm for the protons of the thienopyrazine and the other peaks between 8.32–7.85 ppm belongs to the protons on the fluorene ring. In case of **P-16** the $-\text{OCH}_2$ protons of the EDOT ring appeared around 4.45 ppm. The $-\text{CH}_2$ protons adjacent to the fluorene ring appeared around 2.18 to 2.10 ppm in the three polymers. Similarly signals for the other alkyl protons appeared upfield between 1.23–0.76 ppm (Figure 3.46).

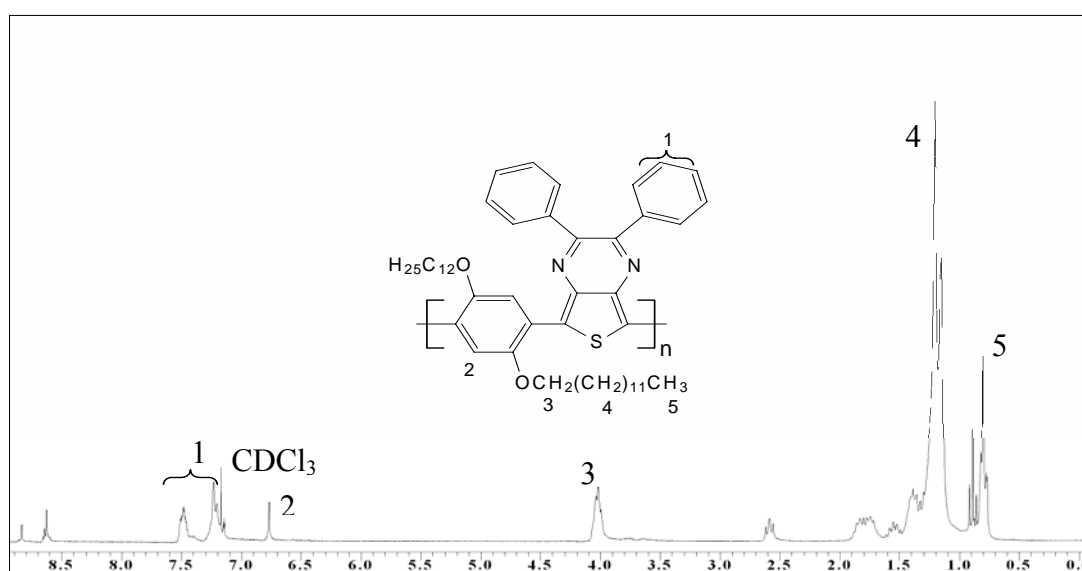


Figure 3.48. ^1H NMR of **P-17**

Similarly the ^1H NMR spectrum of **P-17** in CDCl_3 showed peaks indicating protons of phenyl rings of thienopyrazine unit and alkoxy phenylene unit at $\delta = 7.51$, 7.32 and 6.77 ppm respectively, $-\text{OCH}_2$ protons appeared at $\delta = 4.03$ ppm and other alkyl side chain protons signals were present at $\delta = 1.83$ - 0.77 ppm (Figure 3.48). **P-17** was given the same reaction conditions as others but apparently due to high steric hindrance caused by alkoxy chains, only dimer was obtained.

The ^{13}C NMR spectra of **P-14**, **P-15**, **P-16** and **P-17** display peaks in aromatic region between 153.22 - 114.02 ppm. In case of **P-17** the alkoxy carbons signal appeared at 69.89 and 68.52 ppm and alkyl carbons signals of all the polymers appeared upfield between 55 - 14 ppm. FTIR studies reveal that these polymers give characteristic peaks.

We investigated the thermal properties of these copolymers by thermogravimetric analysis (TGA) and differential scanning calorimetry (DSC) at a rate of 10 K/minute. All the polymers are thermally stable and have 5% weight loss temperatures in air >315 $^\circ\text{C}$ (Figure 3.49). We did not detect any possible phase transition signals during repeated heating/cooling DSC cycles for **P-14**. This observation probably results from the stiffness of the polymer's chains. In the case of **P-15** and **P-16**, we observed distinct glass transition temperatures at 82 and 88 $^\circ\text{C}$, which are higher than that of poly(9,9-dioctylfluorene) (POF; T_g) ca. 75 $^\circ\text{C}$).¹⁵⁰ The increased value of T_g can be attributed to the presence of the rigid thienopyrazine unit, which enhances the molecular rigidity of the polymers and restrict their segmental mobility. It is important that PLEDs be constructed from materials having a relatively high value of T_g to avoid the problems associated with the formation of aggregates and excimers upon exposure to heat.¹⁵¹ In case of **P-17** we observed a melt point at 43.9 $^\circ\text{C}$, indicating its a low molecular weight.

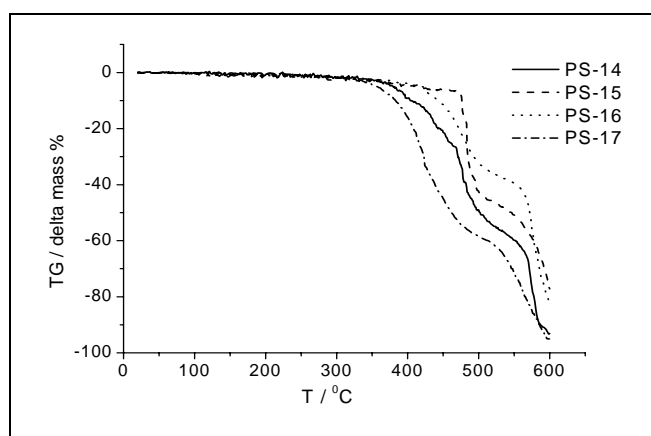


Figure 3.49. TGA of polymers **P-14-P-17**.

3.6.2 Optical Properties

The spectroscopic properties of the polymers/oligomers **P-14–P-17** were measured both in solution (chloroform and toluene) and in thin films (spin coated from chlorobenzene solutions). The UV-vis absorption and photoluminescence (PL) spectra of the polymers/oligomers **P-14–P-17** in toluene (ca : 1×10^{-5} M) are shown in Figure 3.50 and 3.51. The polymer **P-14** exhibited the absorption maximum at 628 nm ($\epsilon = 43000$ L. mol⁻¹. cm⁻¹). Its PL spectrum peaked at 693 nm. In comparison with **P-15**, **P-14** had shown obvious spectral red shift both in absorption ($\Delta = 55$ nm) and in emission ($\Delta = 33$ nm). This obvious spectral difference could be understood in terms of presence of phenyl rings on the thienopyrazine moiety, which increased the conjugation system, and hence leading to the spectral red shift. Similarly **P-16** exhibited the UV-vis absorption maximum at 584 nm ($\epsilon = 41000$ L. mol⁻¹. cm⁻¹) and PL spectrum at 679 nm.

Table 3.18. UV-Vis Data of **P-14–P-17** in Dilute Toluene Solution and in Solid State (Thin Films of 100-150 nm Thickness Spin-Casted from Chlorobenzene Solution).

Polymer	UV-vis λ_{\max} , nm				E_g opt. eV ^c	
	Toluene [log ϵ] ^a	$\lambda_{0.1\max}$	film ^b	$\lambda_{0.1\max}$	Toluene	film
P-14	378, 628 [4.5, 4.3]	680	629	705	1.82	1.76
P-15	378, 573 [4.3, 4.3]	668	590	695	1.86	1.78
P-16	368, 584 [4.4, 4.1]	670	595	673	1.85	1.84
P-17	345, 534 [4.1, 3.5]	620			2.00	

^aMolar absorption coefficient. Molarity is based on the repeating unit. ^bSpin coated from chlorobenzene solution. ^c E_g opt. = $hc / \lambda_{0.1\max}$.

The absorption and PL spectra of **P-20** are also red shifted than **P-15** but blue shifted than **P-14**. The insertion of EDOT unit brought only small spectral changes in **P-16** with respect to **P-14** and **P-15**. The absorption spectra of these polymers consist of two peaks both in solution and in solid states. The absorption peak appeared at ca. 380 nm is consistent with those reported for poly(9,9'-dihexylfluorene) homopolymer (388 nm).¹⁵² The **P-17** exhibited the UV-vis absorption maximum at 534 nm ($\epsilon = 35000$ L. mol⁻¹. cm⁻¹) and PL spectrum at 641 nm. Small absorption coefficient is also indicative of low molecular weight oligomer. The absorption

maxima of the polymers (**P-14**, **P-15** and **P-16**) are red shifted than reported copolymer of 9,9-dioctylfluorene (DOF) and 4,7-di-2-thienyl-2,1,3-benzothiadiazole (DBT) (525 nm).⁵³ This indicate a better donor-acceptor relationship between fluorene and thienopyrazine moieties. Results from the absorption and emission spectra are summarized in Table 3.18 and 3.19. All emission data given here were obtained after exciting at the wavelength of the main absorption band.

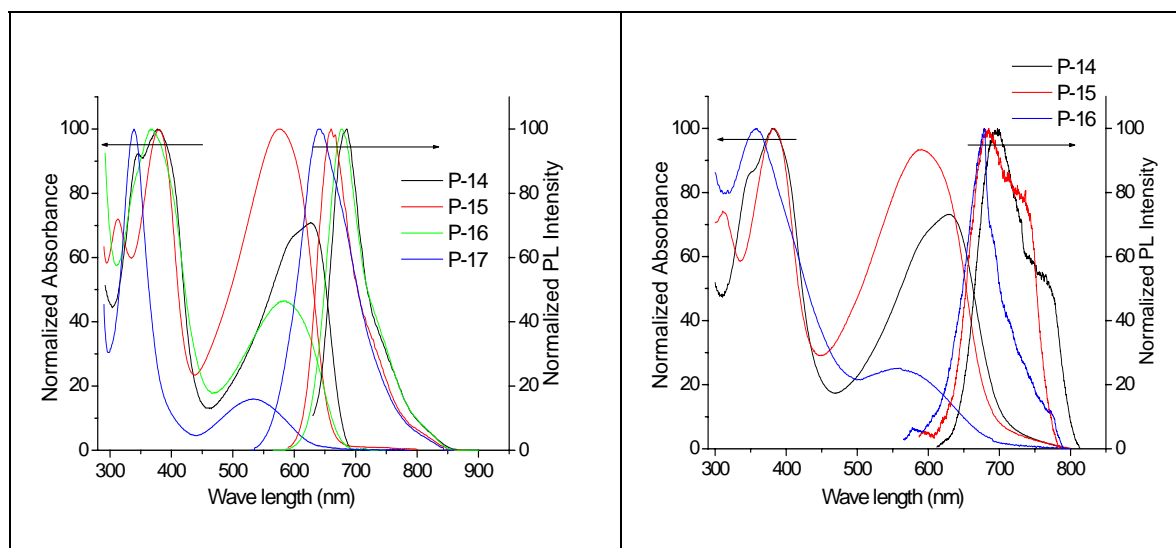


Figure 3.50. Normalized UV-vis and emission spectra of **P-14 – P-17** in solution (toluene 10^{-7} mol).

Figure 3.51. Normalized UV-vis and emission spectra of **P-14, P-15** and **P-16** in solid state (film from chlorobenzene)

Table 3.19. Photoluminescence Data of **P-14–P-17** in Dilute Toluene Solution ($\sim 10^{-7}$ M) and in solid state.^a

Polymer	UV-em λ_{em} , nm		Stokes shift, nm		% ϕ_{PL}	
	Toluene	film	Toluene	film	Toluene	film
P-14	693	697	65	68	28	2
P-15	660	685	87	95	21	1
P-16	679	677	95	82	20	1
P-17	641		107		21	

^bSpin coated from chlorobenzene solution.

3.6.3 Aggregate Formation in Solvent/Nonsolvent Solution

The absorption spectra of polymers **P-14** in chloroform/methanol and toluene/methanol mixture with different volume concentrations of methanol are shown in Figures 3.52 and 3.53. It should

be noted here that in all cases the bulk solution maintains homogeneity. In case of toluene/methanol solution, with an increase of methanol concentration, there is increase in the intensity of the band observed. The spectral red shift corresponds to a disorder-to-order transformation of the conjugated polymer chains. In case of chloroform/methanol there is a decrease in intensity observed mainly due to instability of the polymer in chloroform solution.

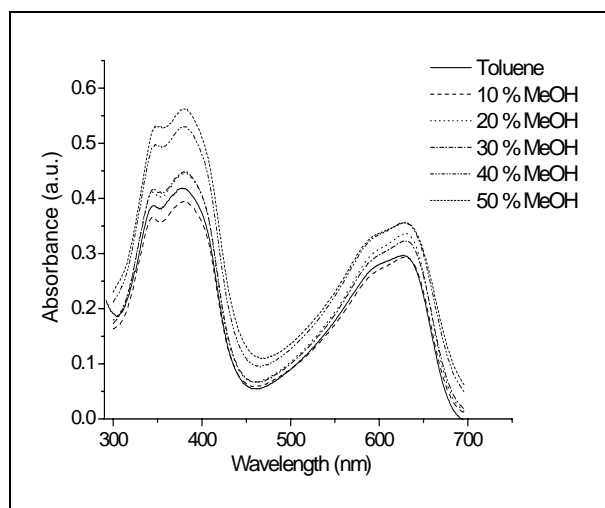


Figure 3.52. UV-vis spectra of P-14 in toluene with different concentration of MeOH.

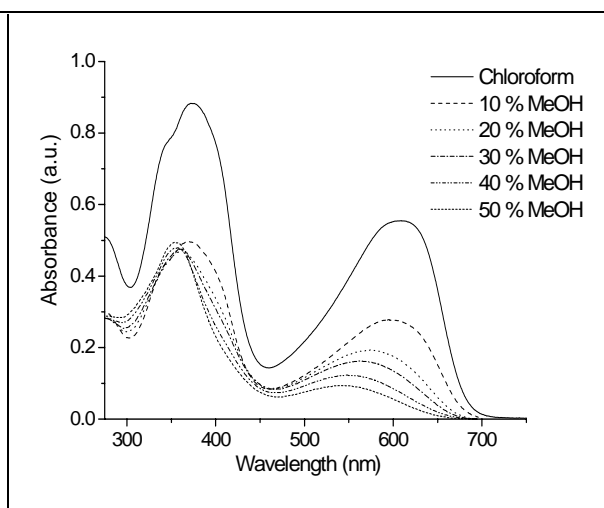


Figure 3.53. UV-vis spectra of P-14 in CHCl₃ with different concentration of MeOH.

3.6.4 Stability of the Polymers

The UV-vis absorption in solution and of thin films of the polymers **P-14**, **P-15** and **P-16** decreased rapidly when exposed to light and air. For example, when **P-14** was exposed to ordinary domestic lighting, it lost most of its color in 4h in chloroform solution (Figure 3.54). Thicker films are more stable, and the polymers are much more stable when stored in the dark. No change in absorbance has been seen for films stored dark for several months. When the concentration of nitrogen in air is increased, by repeatedly evacuating to 0.4 mbar and refilling with N₂(g), the degradation is considerably reduced. This change is more prominent in case of chloroform than toluene, indicating their better stability in toluene solution (Figure 3.55), indicating more charge separation in polar solvents like chloroform and enhancement in oxidation process. FT-IR spectra of relatively thick films of **P-14** exposed to light and air for 24h show formation of carbonyl peaks at 1655 cm⁻¹(Figure 3.56). This suggests a reaction with oxygen and ketone presence in the α -carbon position of the alkyl side chains or susceptibility to oxidation at the C-9 position of the 9,9'-didecylfluorene units and formation of keto defects.¹⁵³ We think it likely that above mentioned reasons and the side chains are oxidized in the

degradation process. Possible explanations for the low stability of the polymers are the labile hydrogens of the side chains^{154,155} or the extended conjugation caused by the fused ring.¹⁵⁶

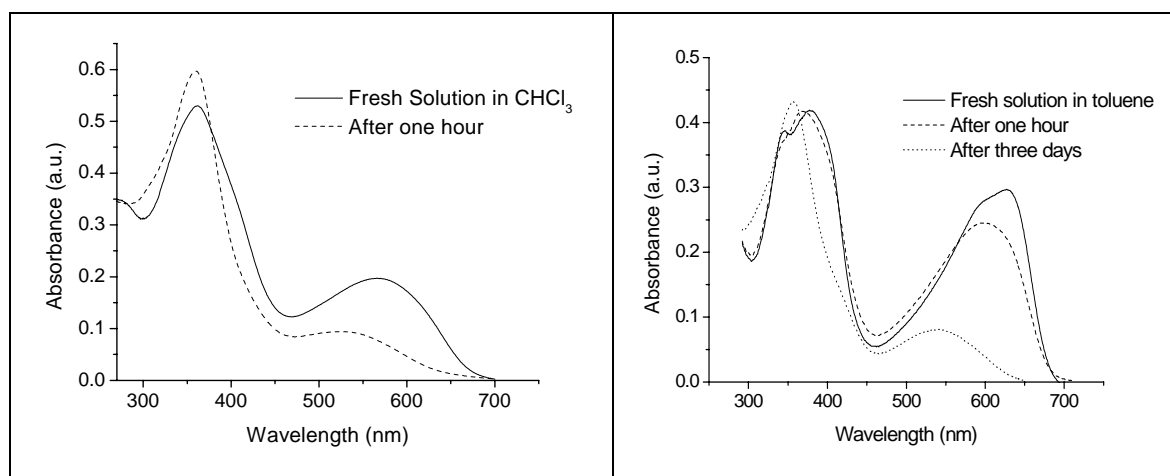


Figure 3.54. UV-vis spectra of **P-14** in CHCl₃. **Figure 3.55.** UV-vis spectra of **P-14** in toluene.

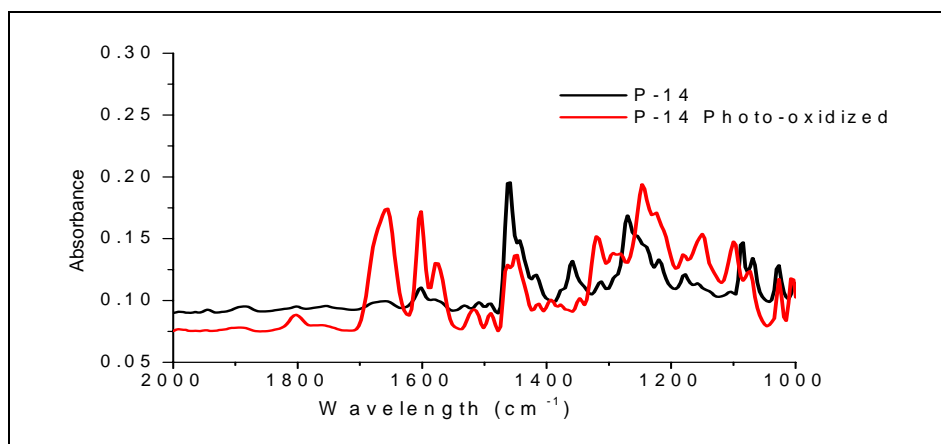


Figure 3.56. Enlarged FT-IR spectra of **P-14** before and after photo-oxidation. The spectra have been offset for clarity.

3.6.5 Electrochemical Studies

The electrochemical properties of the copolymers were investigated by cyclic voltammetry (CV) in order to gauge their electronic properties. All the electrochemical data for the polymers (**P-14**, **P-15** and **P-16**) obtained from the films are listed in Table 3.20. As shown by the cyclic voltammograms in Figure 3.57, the polymers showed reversibility in n-doping processes and irreversibility for their p-doping processes. The electrochemical reduction (or n-doping) of **P-14** starts at about -1.08 V Ag⁺/Ag and gives n-doping peak at -1.39 V vs Ag⁺/Ag, respectively. In a

range from 0.0 to -2.2 V vs Ag^+/Ag , the film revealed stable in repeated scanning of CV, giving same CV curves. Similarly the reduction of **P-15** and **P-16** starts at about -1.17 and -1.06 V Ag^+/Ag and gives n-doping peaks at -1.37 and -1.26 V Ag^+/Ag , respectively. However, oxidation of the polymers **P-14**, **P-15** and **P-16** was irreversible with peaks at 1.44, 1.46 and 1.59 V, respectively. Such irreversibility in the electrochemical processes has been reported for several other π -conjugated polymers.^{110a} These moderately negative reduction potentials have been attributed to the electron withdrawing effects of thieno[3,4-*b*]pyrazine moiety.⁴³ Since the oxidation potential for polyfluorene homopolymer was observed typically at 1.4 V,¹¹² the oxidation wave can be assigned to the oxidation process for the fluorene segments in the copolymers. HOMO and LUMO levels are listed in Table 3.20.

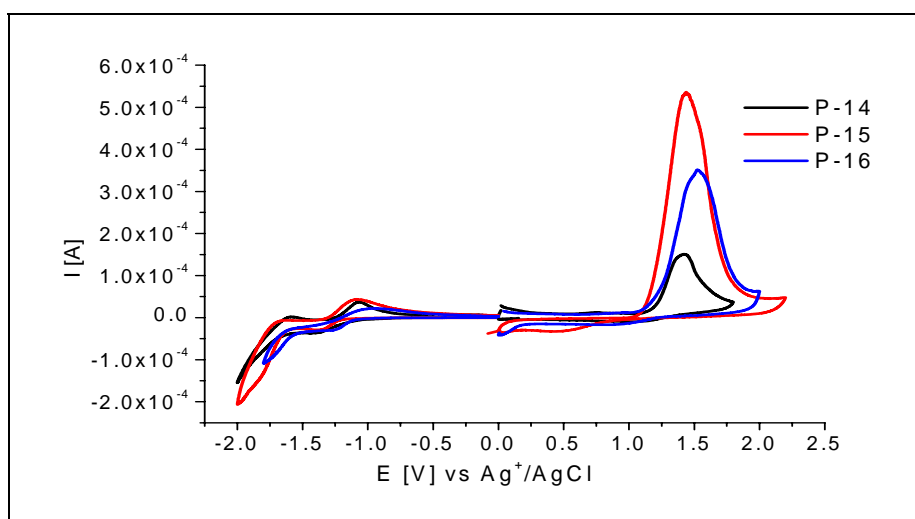


Figure 3.57. Cyclic voltammetry-curves of polymers (**P-14**, **P-15** and **P-16**) in 0.1M TBAPF₆/CH₃CN at 25 °C.

Table 3.20. Electrochemical Potentials and Energy Levels of the Polymers **P-14**, **P-15** and **P-16**.

Polymer	Oxidation Potential		Reduction Potential		Energy Levels ^b		Band Gap	
	E_{ox}^{a} (V vs Ag/Ag^+)	$E_{\text{onset, Ox}}$	$E_{\text{red}}^{\text{a}}$ (V vs Ag/Ag^+)	$E_{\text{onset, Red}}$	HOMO (eV)	LUMO (eV)	Band Gap (eV)	Optical Band Gap (eV)
P-14	1.44	1.21	-1.39	-1.08	-5.49	-3.20	2.29	1.76
P-15	1.46	1.18	-1.37	-1.17	-5.46	-3.11	2.35	1.78
P-16	1.59	1.21	-1.26	-1.06	-5.49	-3.22	2.27	1.84

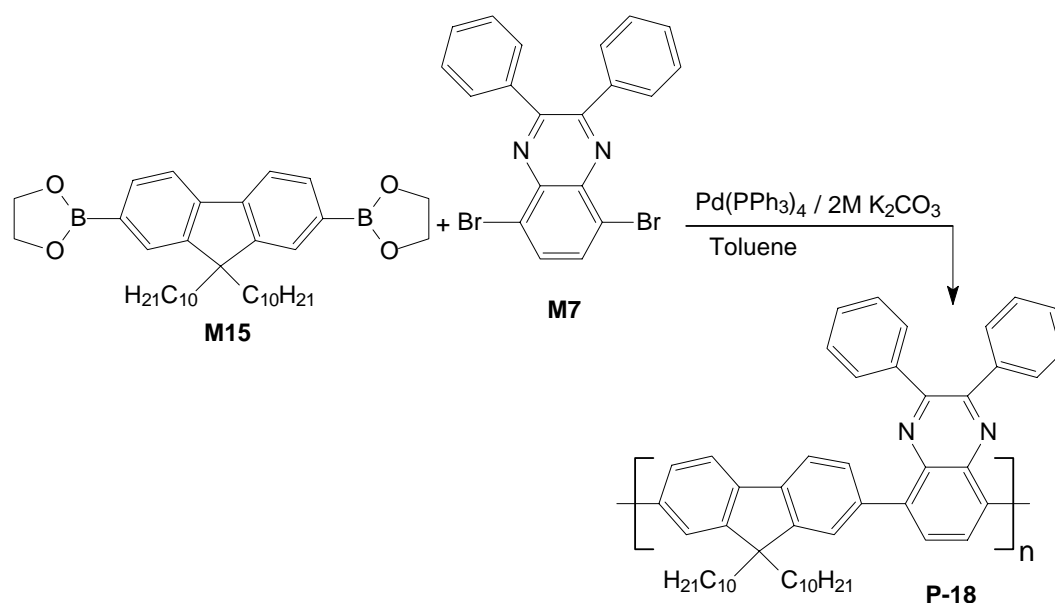
^aReduction and oxidation potential measured by cyclic voltammetry. ^bCalculated from the reduction and oxidation potentials assuming the absolute energy level of ferrocene/ferrocenium to be 4.8 eV below vacuum.

3.7 Quinoxaline and Fluorene Based Poly(heteroarylene)s

Due to their high PL quantum yields, polyfluorenes have been copolymerised with a host of other comonomers, both p-type and n-type, to tune the emission colour or enhance the charge-injection and -transport properties in the predominantly p-type poly(9,9'-dioctylfluorene) (PFO) backbone.¹⁵⁷⁻¹⁶⁰ Our motivation was to synthesize polyfluorenes with improved electron-injection and transport characteristics by copolymerising an electron-deficient (n-type) building block. We point out that such an approach to improving the electron transport ability of polyfluorenes has also been employed previously by using n-type building blocks such as benzothiadiazole,⁴⁵⁻⁵³ oxadiazole,^{159a} quinoline,^{159b} pyridine,^{159c} and quinoxaline,^{159b,160} either in the main chain or as pendants to polyfluorenes backbone. We choose quinoxaline as the n-type building block since it is known to have high electron affinity and good thermal stability and has been successfully incorporated in polymers for use as electron-transport materials in multilayer OLEDs.^{161,162} The only alternating copolymers of fluorene and quinoxaline reported has been used as pendent group or by different attachment,^{159b,160,161} not as mentioned by us in main chain.

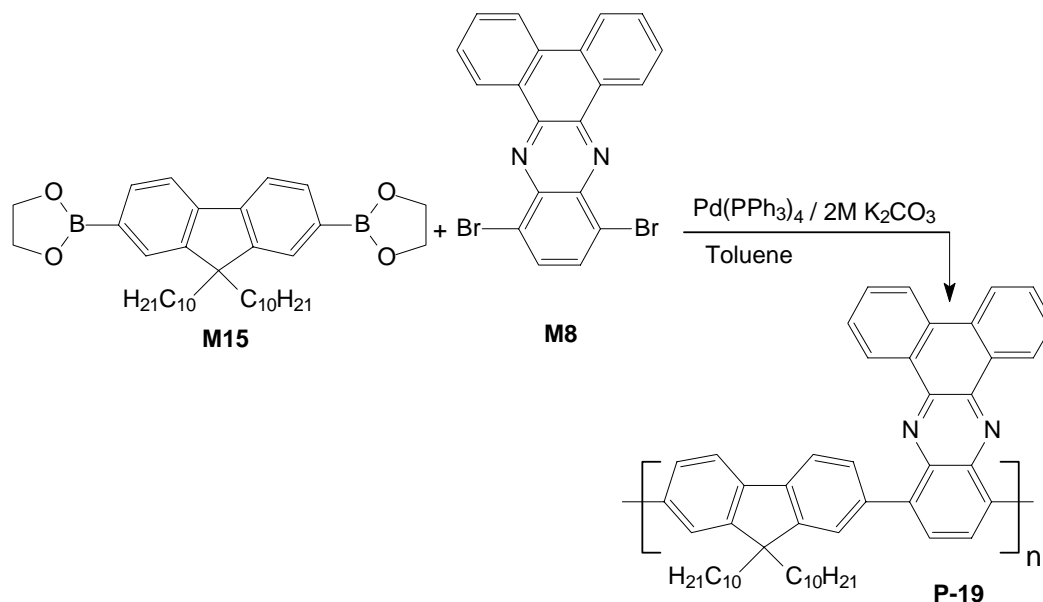
3.7.1 Synthesis and characterization

The basic strategy employed for the synthesis of the polymers **P-18** and **P-19** is based on the Suzuki reaction,¹⁸ which was carried out in a mixture of toluene and potassium carbonate (2M) containing 1mol % Pd(PPh₃)₄ under vigorous stirring at 85-90 °C for 60-70h. The synthetic routes for the both polymers are illustrated in scheme 3.19 and 3.20.



Scheme 3.19. Synthesis of Polymers **P-18** .

The polymers were obtained with satisfactory yields. After purification and drying, **P-18** and **P-19** were obtained as yellow solids. Both the polymers readily dissolve in common organic solvents, such as chloroform, THF, toluene and chlorobenzene.



Scheme 3.20. Synthesis of Polymer **P-19**.

The number-average molecular weights, \bar{M}_n , of the polymers (**P-18** and **P-19**) determined by GPC (polystyrene standards) were 4400 and 8800 with polydispersity indices of 1.60 and 2.0 respectively (see Table 3.21).

Table 3.21. GPC data of polymers **P-18** & **P-19**.

Polymer	\bar{M}_n [g/mol]	\bar{M}_w [g/mol]	M_w/M_n	\bar{P}_n	Yield (%)
P-18	4400 ^a	7000	1.60	6	61
P-19	8800 ^a	17600	2.0	12	65

^a \bar{M}_n , GPC (polystyrene standards).

The chemical structures of the polymers were verified by ^1H NMR, ^{13}C NMR, FTIR and elemental analyses. Figure 3.58 displays the ^1H NMR spectrum of the polymer **P-18**. There are three peaks in the aromatic region for **P-18**. The peaks in the lower field at 7.96-7.89 ppm are attributed to the different kinds of protons on the fluorene ring. The other peaks between 7.59 and 7.26 ppm belong to the protons of the phenyl rings of the quinoxaline unit. The aromatic region of **P-19** is almost similar to that of **P-18** with all peaks slightly shifted to lower field. There is peaks around 9.02 ppm for the protons of the phenyl rings of phenazine and the other

peaks between 8.00-7.56 ppm belongs to the protons of the phenyl rings of phenazine and the fluorene ring (Figure 3.59).

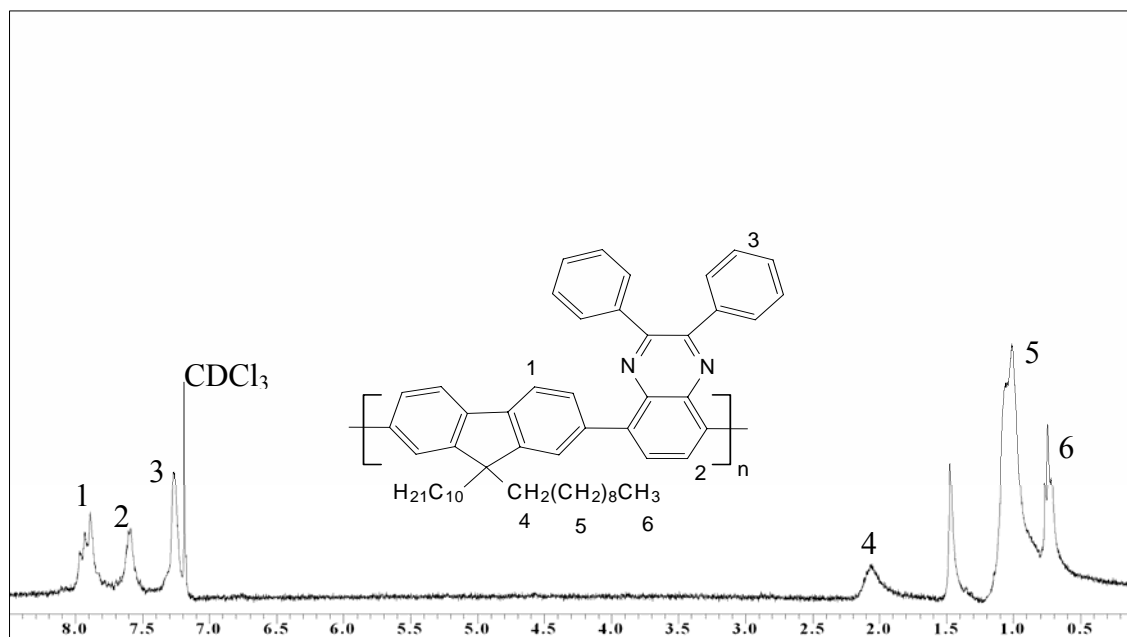


Figure 3.58. ^1H NMR of P-18.

The $-\text{CH}_2$ protons adjacent to the fluorene ring appeared around 2.16 to 2.07 ppm in both the polymers. Similarly signals for the other alkyl protons appeared upfield between 1.47-0.68 ppm.

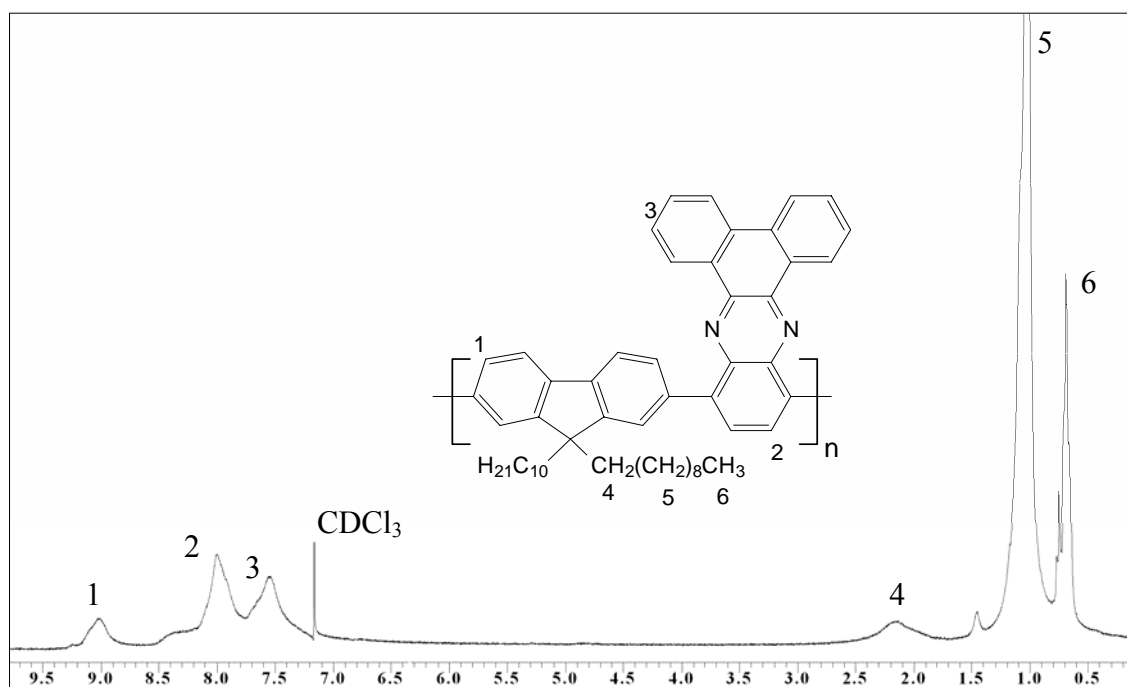


Figure 3.59. ^1H NMR of P-19.

The ^{13}C NMR spectra **P-18** and **P-19** display peaks in aromatic region between 151.33-119.39 ppm. The alkyl carbons signals of both the polymers appeared upfield between 56-14 ppm. FTIR studies reveal that these polymers give characteristic peaks.

The thermal properties of these copolymers were investigated by thermogravimetric analysis (TGA) and differential scanning calorimetry (DSC) at a heating rate of 10 K/min. All the polymers are thermally stable and have 5% weight loss temperatures in air >350 °C (Figure 3.60). We did not detect any possible phase transition signals during repeated heating/cooling DSC cycles for **P-18** and **P-19**. This observation probably results from the stiffness of the polymer's chains due to presence of rigid quinoxaline units. The polymer **P-19** show better thermal stability than **P-18**, due to presence of more rigid phenazine moiety.

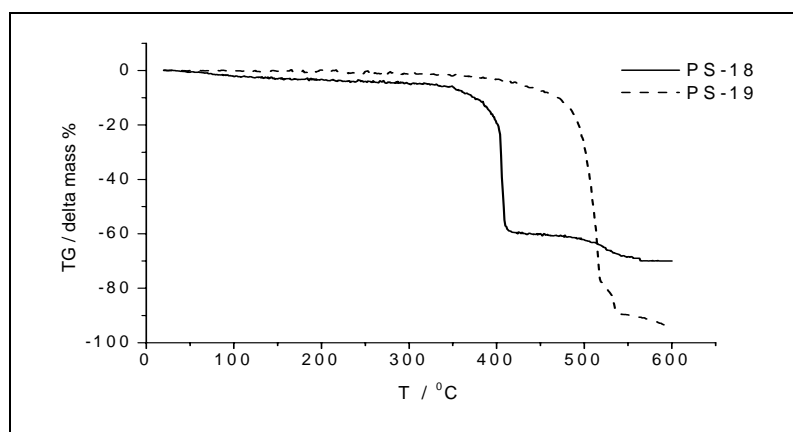


Figure 3.60. TGA of polymers **P-18**, **P-19**.

3.7.2 Optical Properties:

The spectroscopic properties of the polymers **P-18** and **P-19** were measured both in solution (chloroform and toluene) and in thin films (spin coated from chlorobenzene solutions). The UV-vis absorption and photoluminescence (PL) spectra of the polymers **P-18** and **P-19** in toluene (ca : 1×10^{-5} M) are shown in Figure 3.61 and 3.62. The polymer **P-18** exhibited the absorption maximum at 419 nm ($\epsilon = 40000$ L. mol $^{-1}$. cm $^{-1}$). Its PL spectrum peaked at 492 nm. In comparison with **P-18**, **P-19** had shown obvious spectral red shift both in absorption ($\Delta = 31$ nm) and in emission ($\Delta = 32$ nm). This obvious spectral difference could be understood in terms of planar phenazine moiety, which increased the effective conjugation length, and hence leading to the spectral red shift.

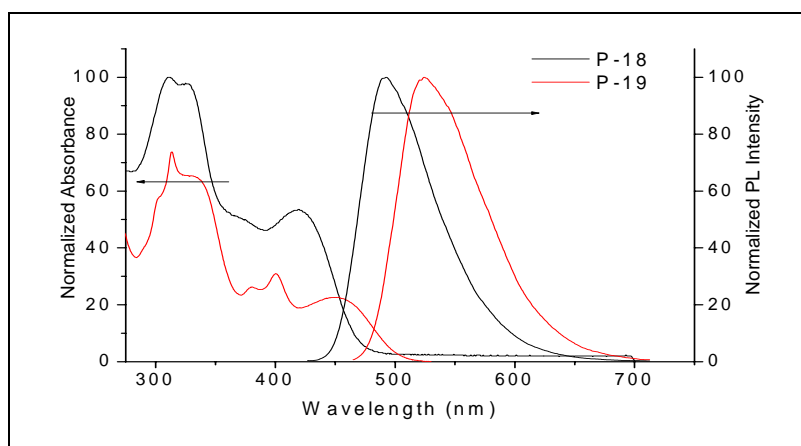


Figure 3.61. Normalized UV-vis and emission spectra of **P-18** and **P-19** in solution (toluene 10^{-7} mol).

Table 3.22. UV-Vis Data of polymers **P-18** and **P-19** in Dilute Toluene Solution and in Solid State (Thin Films of 100-150 nm Thickness Spin-Casted from Chlorobenzene Solution).

Polymer	UV-vis λ_{\max} , nm				E_g opt. eV ^c	
	Toluene [log ϵ] ^a	$\lambda_{0.1\max}$	film ^b	$\lambda_{0.1\max}$	Toluene	film
P-18	419 [4.0]	475	426	485	2.61	2.56
P-19	450 [4.2]	504	461	523	2.46	2.37

^aMolar absorption coefficient. Molarity is based on the repeating unit. ^bSpin coated from chlorobenzene solution. ^c E_g opt. = $hc/\lambda_{0.1\max}$. ^{sh} shoulder.

The fluorescence quantum yields in toluene solution were found to be around 32 and 53% for **P-18** and **P-19** respectively. The emission maximum of **P-18** and **P-19** in solid film is located at $\lambda_{\max,em} = 504$ and 545 nm leading to Stokes shift of 78 and 84 nm, and a lower fluorescence quantum yield of 5 and 4 %, respectively. We assumed, the reason for the low photoluminescence (PL) efficiency is a π - π stacking of the conjugated backbone cofacial to each other due to the favourable inter-chain π - π interactions, which lead to a self-quenching process of the excitons.⁹⁹⁻¹⁰¹

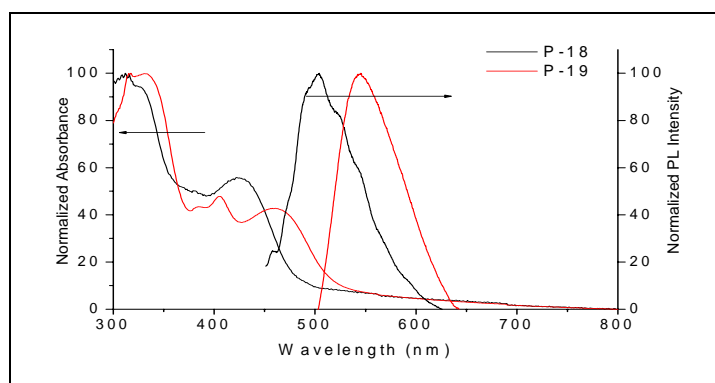


Figure 3.62. Normalized UV-vis and emission spectra of **P-18** and **P-19** in solid state (film from chlorobenzene).

Table 3.23. Photoluminescence Data of **P-18** and **P-19** in Dilute Toluene Solution ($\sim 10^{-7}$ M) and in solid state.^a

Polymer	UV-em λ_{em} , nm		Stokes shift, nm		% ϕ_{PL}	
	Toluene	film	Toluene	film	Toluene	film
P-18	492	504	73	78	32	5
P-19	524	545	74	84	53	4

^bSpin coated from chlorobenzene solution.

3.7.3 Aggregate Formation in Solvent/Nonsolvent Solution

The absorption spectra of polymer **P-19** in chloroform/methanol mixture with different volume concentrations of methanol are shown in Figures 3.63. It should be noted here that in all cases the bulk solution maintains homogeneity. With an increase of methanol concentration, there is increase in the intensity of the band. The slight spectral red shift corresponds to a disorder-to-order transformation of the conjugated polymer chains.

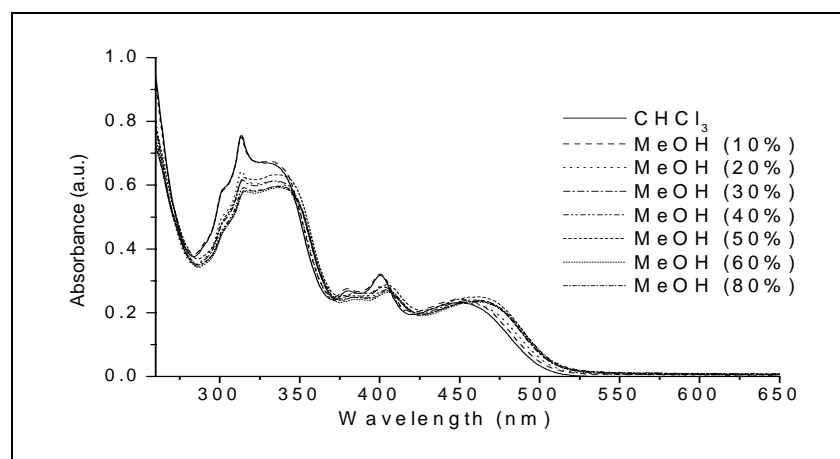


Figure 3.63. UV-vis spectra of **P-19** in CHCl_3 with different concentration of MeOH .

Since polymers **P-19** is insoluble in methanol, the addition of methanol to the homogeneous chloroform solution leads to aggregate formation. In the aggregate the polymer possesses a more extended conjugated structure, so the increase in the intensity and shifting of band at higher wavelength can be assigned to the aggregate.

3.7.4 Electrochemical Studies

The electrochemical behaviour of the copolymer **P-19** was investigated by cyclic voltammetry (CV). The CV was carried out using thin films of polymer prepared from dichloromethane (5 mg/mL) in acetonitrile at a potential scan rate of 15 mV/s. Ag/AgCl served as the reference electrode; it was calibrated with ferrocene ($E_{\text{ferrocene}}^{1/2} = 0.52 \text{ V vs Ag/AgCl}$). The supporting electrolyte was tetrabutylammonium hexafluorophosphate ($n\text{-Bu}_4\text{NPF}_6$) in anhydrous acetonitrile (0.1 M). As shown by the cyclic voltammograms in Figure 3.64, the polymer **P-19** showed reversibility in n-doping processes and irreversibility for its p-doping processes. The electrochemical reduction (or n-doping) of **P-19** starts at about $-0.79 \text{ V Ag}^+/\text{Ag}$ and gives two n-doping peaks at -1.16 and $-1.42 \text{ V vs Ag}^+/\text{Ag}$, respectively. In a range from 0.0 to $-2.2 \text{ V vs Ag}^+/\text{Ag}$, the film revealed stable in repeated scanning of CV, giving same CV curves. However, oxidation of the polymer **P-19** was irreversible with peak at 1.76 V . Such irreversibility in the electrochemical processes has been reported for several other π -conjugated polymers.¹¹⁰

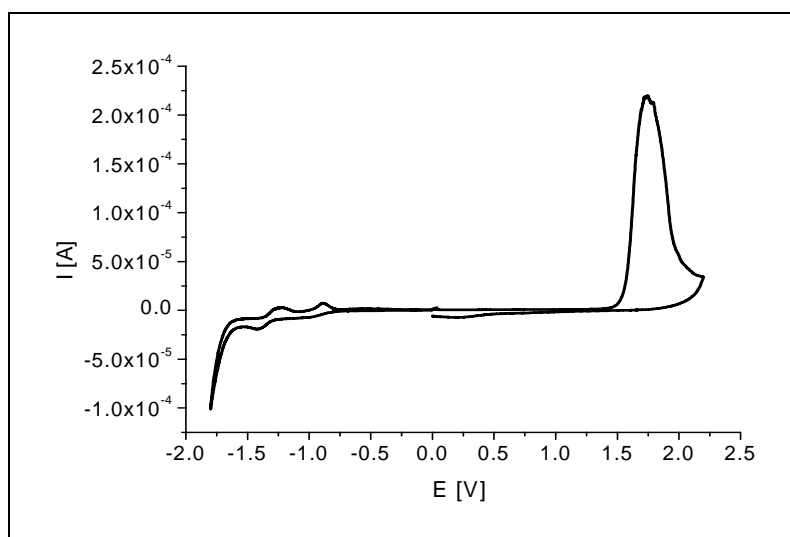


Figure 3.64. Cyclic voltammetry-curves of polymer **P-19** in 0.1M TBAPF₆/CH₃CN at 25 °C.

The band gap energy directly measured from CV is ($E_{g \text{ ec/onset}} 2.24 \text{ eV}$) and the optical band gap energy is ($E_{g \text{ opt/onset}} 2.37 \text{ eV}$), with the electrochemical band gap being slightly lower. The discrepancy (ΔE_g) of both values lies within the range of error. From the onset potentials,

HOMO and LUMO energy levels were estimated. The HOMO for **P-19** was around -5.82 eV, while LUMO around -3.58 eV. These data are comparable to those of poly(quinoxaline-5,8-diyl) ($I_p = 5.7-5.9$ eV, $E_g = 2.3-2.6$ eV, and $E_A = 3.1-3.3$)^{86d} and poly(2,7-(9,9-di-*n*-octylfluorene)-*alt*-benzothiadiazole) (F8BT) ($I_p = 5.8-5.9$ eV, $E_g = 2.6$ eV, and $E_A = 3.2-3.3$).¹⁵¹ These values indicate high electron affinity of the polymer **P-19** making it suitable candidate for electron-injection and transport.

Table 3.24. Electrochemical Potentials and Energy Levels of the Polymer **P-19**

Polymer	Oxidation Potential		Reduction Potential		Energy Levels ^b		Band Gap	
	E_{ox}^a (V vs Ag/Ag ⁺)	$E_{onset, Ox}$	E_{red}^a (V vs Ag/Ag ⁺)	$E_{onset, Red}$	HOMO (eV)	LUMO (eV)	Band Gap (eV)	Optical Band Gap (eV)
P-19	1.76	1.54	-0.99	-0.79	-5.82	-3.58	2.24	2.37
			-1.42	-1.16				

^aReduction and oxidation potential measured by cyclic voltametry. ^bCalculated from the reduction and oxidation potentials assuming the absolute energy level of ferrocene/ferrocenium to be 4.8 eV below vacuum.

3.7.5 Photophysical Properties of Binary Blends of the Polymers P-14 and P-19

Blends of donor and acceptor conjugated polymers with favorable electronic structures (HOMO/LUMO levels) represent one option to achieve balanced charge injection and transport in polymer light-emitting diodes and solar cells. However, for photoinduced charge transfer and quenching of electroluminescence in such bipolar blends of conjugated polymers, the blend components should be such that their electronic structures disfavor to the excitation energy transfer and favor electron transfer. Because the **P-19** has n-type (electron accepting) properties, we selected the polymer **P-14** blend component. In this chapter, we report the photophysics of binary blends of **P-19** as the electron transport (n-type) component and **P-14** as a hole transport (p-type) component. The molecular structures and the HOMO/LUMO energy level diagram of these polymer blend components are given in Figure 3.68.

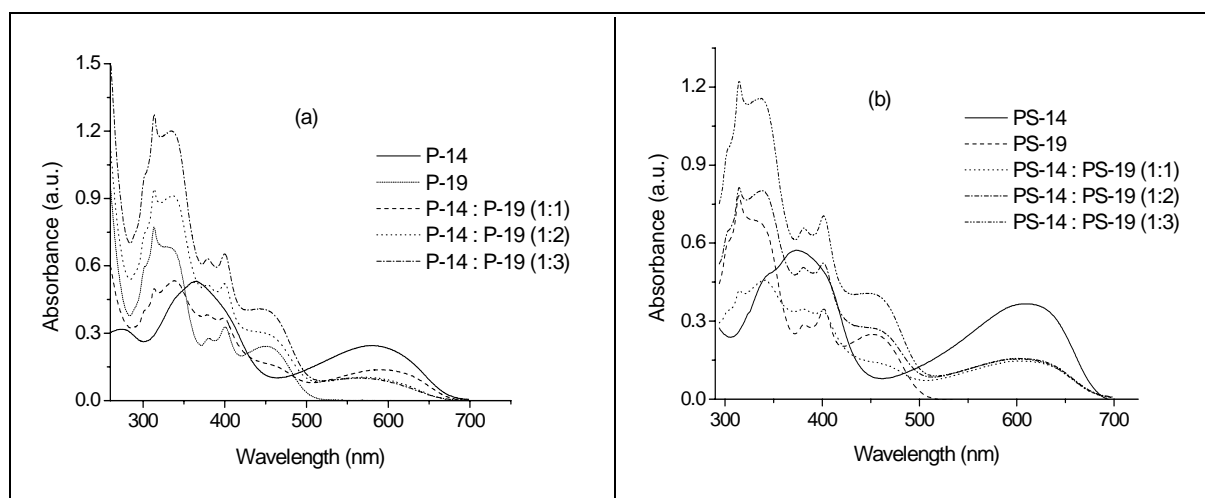


Figure 3.65. UV-vis spectra of blends of **P-14** and **P-19** in chloroform (a) and toluene (b) in different molar concentrations.

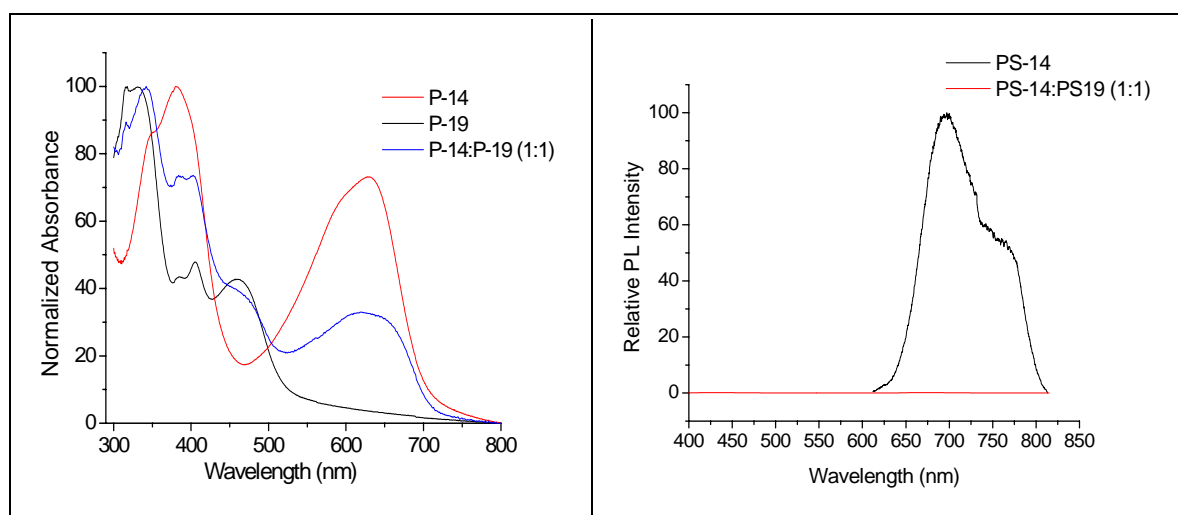


Figure 3.66. Normalized UV-vis spectra of **P-14** and **P-19** and a blend (1:1) in solid state (film from chlorobenzene).

Figure 3.67. Normalized Photoluminescence spectra of **P-14** and a **P-14/P-19** blend (1:1) in solid state (film from chlorobenzene).

Figures 3.65 and 3.66 show the optical absorption spectra of **P-14**, **P-19** and **P-14/P-19** blends in chloroform and toluene solution and films deposited from a chlorobenzene solution. There is no apparent charge transfer observed in binary blends.

Figure 3.68 b show the energy band diagram of **P-14** and **P-19** derived from the cyclic voltammographic data. The polymer **P-14** here show distinctively higher energy level of its HOMO in comparison to **P-19**. Figure 3.66 b clearly displays the difference of 0.38 eV between the LUMOs of **P-14** and **P-19**, which should allow an effective charge transfer. Photoluminescence measurements were used to investigate the photoinduced charge generation and charge transfer in blend of **P-14** and **P-19**. Photoexcited excitons can undergo several

consecutive processes: recombination with in the polymer (donor) or at the donor-acceptor interface, energy transfer between the materials followed by radiative or non-radiative recombination or charge transfer (exciton splitting) at the donor-acceptor interface. With in the scope of investigated system **P-14/P-19**, one can consider the charge transfer as the preferred process due to intensive photoluminescence of the polymer **P-14** and its quenching in the presence of **P-19**. The measurements of photoluminescence were performed on a thin polymer (donor) film and compared with the photoluminescence of the blend film of donor and acceptor. The effective quenching of photoluminescence of the polymer **P-14** in the presence of **P-19** indicates an effective charge transfer from **P-14** to the acceptor **P-19** (Figure 3.67).

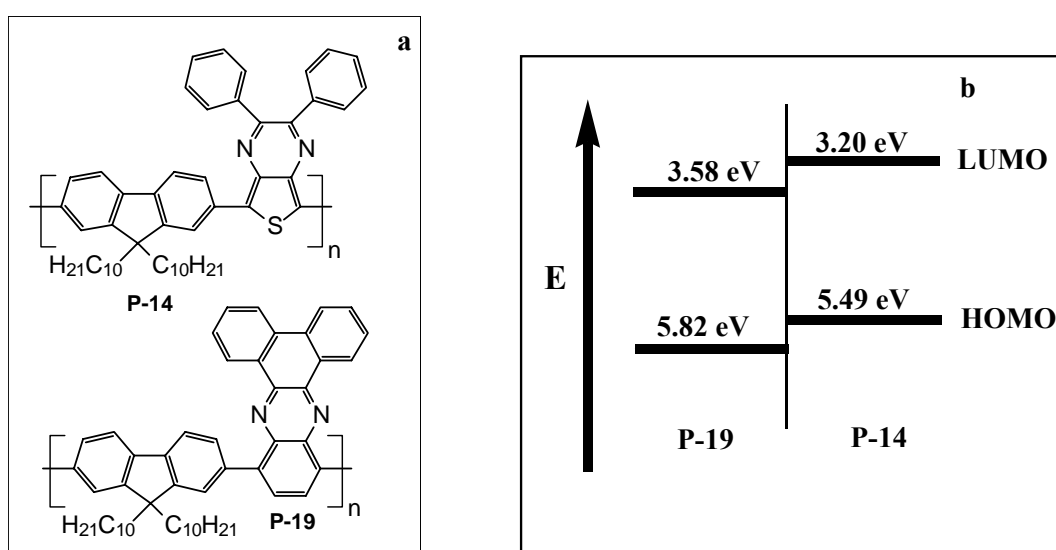


Figure 3.68. (a) Chemical structures and (b) HOMO/LUMO energy level diagram of polymers **P-14** and **P-19**.

4 Experimental

4.1 Instrumentation

Melting Point. Melting points were obtained by a melting point apparatus *Melting Point B-540 of Büchi*.

NMR Spectroscopy. ^1H NMR and ^{13}C NMR spectra were recorded using a Bruker DRX 400 and a Bruker AC 250. The ^1H NMR was checked by using 250 MHz and 400 MHz while ^{13}C NMR by using 62 MHz and 400 MHz. The deuterated solvents used were CDCl_3 , Acetone- D_6 and $\text{DMSO-}^{\text{D}}_6$. Chemical shifts (δ values) are given in parts per million with tetramethylsilane as an internal standard.

Elemental Analysis. The C-H-N-S was measured on a CHNS-932 Automat Leco. While the Bromine was measured by potentiometric titration.

FT-IR. Infrared spectroscopy was recorded on a Nicolet Impact 400.

Thermogravimetric Analysis (TGA). A homemade apparatus served for the thermogravimetric measurements.

Vapour Pressure Osmometry (VPO). The measurements were performed in chloroform in an Knauer Osmometer.

Gel Permeation Chromatography (GPC). The GPC measurements were performed on a set of Knauer using THF as eluent and polystyrene as a standard.

UV/Vis-Spectroscopy. The absorption spectra were recorded in dilute chloroform solution (10^{-5} - 10^{-6} M) on a Perkin-Elmer UV/vis-NIR spectrometer Lambda 19.

Luminescence Spectroscopy. Quantum-corrected emission spectra were measured in dilute chloroform solution (10^{-6} M) with an LS 50 luminescence spectrometer (Perkin-Elmer). Photoluminescence quantum yields were calculated according to Demas and Crosby¹⁶² against quinine sulfate in 0.1 N sulfuric acid as a standard ($\phi_{\text{fl}} = 55\%$). The solid-state absorption and emission were measured with a Hitachi F-4500. The films were cast from chlorobenzene. The quantum yield in the solid state was determined against a $\text{CF}_3\text{P-PPV}$ (poly{1,4-phenylene-[1-(4-trifluoromethylphenyl)ethenylene]-2,5-dimethoxy-1,4-phenylene-[2-(4-trifluoromethylphenyl)ethenylene]}) copolymer reference that has been measured by integrating sphere as 0.43.

Cyclic Voltammetry. For study on electrochemical behavior, a polymer thin film was prepared on a platinum wire as a working electrode, using a platinum wire as the counter electrode and Ag/Ag⁺ as the reference electrode in a solution of tetrabutylammonium hexafluorophosphate (0.1 M) in acetonitrile. The reference electrode potential vs normal hydrogen electrode (NHE) is 0.2223 V.¹⁶³ The cyclic voltammogram was recorded on a computer-controlled EG&G potentiostat/galvanostat model 283. The lowest unoccupied molecular orbital (LUMO) and the highest occupied molecular orbital (HOMO) energy levels of the polymers were converted from the onset reduction and oxidation potentials, respectively, with the assumption that the energy level of ferrocene/ferrocenium (Fc) is 4.8 eV below vacuum.¹⁰⁶

Differential Scanning Calorimetry (DSC). The glass transition temperature *T_g* was measured by DSC. For the measurements an instrument *Perkin-Elmer-DSC 2C*.

Materials. All starting materials were purchased from commercial suppliers (Fluka, Merck, and Aldrich). Toluene, tetrahydrofuran and diethyl ether were dried and distilled over sodium and benzophenone. Diisopropylamine was dried over KOH and distilled. If not otherwise specified, the solvents were degassed by sparkling with argon or nitrogen 1h prior to use.

4.2 Synthesis: (Synthesis of Monomer Precursors)

1,4-Dialkoxy-2,5-dibromobenzene⁸⁷ was prepared from 1,4-dibromohydroquinone.¹⁶⁴

3-Dodecylthiophene (1).⁸⁴ 1-Bromododecane (24.92 g, 23.965 mL, 100 mmol) was slowly added dropwise to a suspension of magnesium turnings (2.431 g, 100 mmol) in diethyl ether (10 mL), and the reaction mixture was heated to reflux for 2h. The Grignard solution was transferred to the dropping funnel of a second apparatus via canola and was added dropwise, through a frit, to an ice-cooled solution of 3-bromothiophene (13.587 g, 7.89 mL, 83.3 mmol) and Ni(dppp)Cl₂ (0.045 g, 8.33 mmol) in diethyl ether (57 mL). The mixture was refluxed for 20h, cooled to room temperature, and hydrolysed with 1M HCl. The ether phase was separated, neutralized, washed with water, dried over sodium sulphate, and evaporated. The residue was fractionated under reduced pressure (b.p. 112⁰C/10⁻² mmHg). 3-Dodecylthiophene (21 g, 83 %) was obtained as liquid. ¹H NMR (250 MHz, CDCl₃): δ = 7.34 (dd, J = 7.5 Hz, 2H), 6.97 (s, 1H), 2.78 (2H, t, J = 6.5 Hz, -CH₂-), 1.78-0.75 (-(CH₂)₁₀CH₃). ¹³C NMR (62 MHz, CDCl₃): δ = 143.64, 128.69, 125.45, 119.16, 32.47, 32.21, 31.10, 30.81, 30.23, 30.16, 30.03, 29.91, 23.50, 22.95, , 22.80, 14.89, 14.63, 14.34.

3,4-Didodecylthiophene (2).⁸⁴ Same procedure was followed as mentioned above for 1.1-Bromododecane (12.96 g, 52 mmol), 3,4-dibromothiophene (5.50 g, 22.7 mmol), Ni (dppp)Cl₂ (0.125 g, 0.23 mmol). The orange brown solution was heated at reflux for 18h and then poured onto an excess of water. The organic layer was collected and dried, the solvent was eliminated by using a rotary evaporator, and 3,4-didodecylthiophene was then purified by flash chromatography on silica gel using hexane as eluent. Yield: 6.5 g (68%). ¹H NMR (250 MHz, CDCl₃): δ = 6.95 (s, 2H), 2.50 (2H, t, ³J = 6.5 Hz, -CH₂-), 1.60-1.18 (-(CH₂)₁₀), 0.90 (t, J = 6.6 Hz, 3H). ¹³C NMR (62 MHz, CDCl₃): δ = 142.51, 120.27, 33.10, 32.70, 32.01, 30.09, 30.05, 29.71, 23.11, 14.53.

2,5-Dibromo-3-dodecylthiophene (3).⁸⁴ In the absence of light, a solution of NBS (7.12 g, 40 mmol) in DMF (40 mL) was slowly and dropwise added to a solution of 3-dodecylthiophene (5.05 g, 20 mol) in DMF (40 mL), and the mixture was stirred at 40 ⁰C for 3h, poured onto ice, and extracted several times with diethyl ether. The organic phases were combined, washed with water, and dried over sodium sulfate. Evaporation of the solvent and distillation under reduced pressure yielded 2,5-dibromo-3-dodecylthiophene (5.7 g, 70%) as a yellowish liquid (b.p. 150-160 ⁰C/10⁻³ mmHg). ¹H NMR (250 MHz, CDCl₃): δ = 6.80 (s, 1H), 2.50 (2H, t, ³J = 6.5 Hz, -

CH₂-), 1.62-1.18 (-(CH₂)₁₀), 0.90 (t, J = 6.6 Hz, 3H). ¹³C NMR (62 MHz, CDCl₃): δ = 143.35, 131.32, 110.77, 108.38, 32.78, 32.10, 31.10, 30.13, 30.03, 29.81, 23.50, 22.95, , 22.80, 14.89, 14.60.

2,5-Dibromo-3,4-didodecylthiophene (4).⁸⁴ Same procedure was followed as mentioned above for **3**. 3,4-Didodecylthiophene (5 g, 11.88 mmol), NBS (5.29 g, 29.7 mmol). 2,5-Dibromo-3,4-didodecylthiophene was purified by column chromatography using hexane as eluent. Yield: 4.5 g (65%). ¹H NMR (250 MHz, CDCl₃): δ = 2.50 (2H, t, ³J = 6.5 Hz, -CH₂-), 1.56-1.16 (-(CH₂)₁₀), 0.88 (t, J = 6.6 Hz, 3H). ¹³C NMR (62 MHz, CDCl₃): δ = 141.86, 108.19, 31.91, 30.81, 30.05, 29.71, 29.51, 29.36, 28.47, 22.70, 14.12.

2,5-Bis(trimethylsilylethynyl)-3-dodecylthiophene (5). To a degassed solution of diisopropylamine (40 ml) and toluene (70 ml) were added 2,5-dibromo-3-dodecylthiophene (6 g, 14.6 mmol), trimethylsilylacetylene (4.3 g, 43.8 mmol), bis(triphenylphosphine)-palladium(II)chloride([Pd(PPh₃)₂]Cl₂) (420 mg, 0.6 mmol) and copper(I)iodide(CuI) (114 mg, 0.6 mmol). The reaction mixture was stirred at 60 °C for 6h under inert gas atmosphere (argon). After cooling, the ammonium bromide precipitates were filtered off. The solvent was removed under reduced pressure, and the residue was chromatographed over a silica gel column with n-hexane as eluent to obtain 2,5-bis(trimethylsilylethynyl)-3-dodecylthiophene as light yellow liquid. Yield: 4.9g(75%). ¹H NMR (250 MHz, CDCl₃): δ = 7.09 (-C_{aryl}-H), 2.41 (2H, t, ³J = 6.5 Hz, -CH₂-), 1.63-0.67 (-(CH₂)₁₀CH₃), 0.12 (-Si(CH₃)₃)₂. ¹³C NMR (62 MHz, CDCl₃): δ = 148.52 (C_{aryl}-H), 133.58 (C_{aryl}-CH₂-), 122.84, 119.4 (C_{aryl}-C≡), 101.89, 99.50, 88.09, 86.04 (-C≡C-)₂, 32.03, 31.94, 31.70, 29.53, 29.45, 29.39, 29.36, 29.30, 26.19, 22.80, 14.23 (CH₃(CH₂)₁₁-), 0.09 (-Si(CH₃)₃)₂.

2,5-Bis(trimethylsilylethynyl)-3,4-didodecylthiophene (6). Same procedure was followed as mentioned above for **5**. 2,5-Dibromo-3,4-didodecylthiophene (**5**) (3.7 g, 6.4 mmol), trimethylsilylacetylene (1.9 g, 19 mmol), bis(triphenylphosphin)-palladium(II)chloride([Pd(PPh₃)₂]Cl₂) (370 mg, 0.53 mmol) and copper(I)iodide (CuI) (100 mg, 0.53 mmol). The product was chromatographed over a silica gel column with n-hexane as eluent, 2,5-bis(trimethylsilylethynyl)-3,4-didodecylthiophene as light yellow liquid was obtained. Yield: 3.3 g (84%). ¹H NMR (250 MHz, CDCl₃): δ = 2.41 (4H, m, -CH₂-), 1.33-0.72 (-(CH₂)₁₀CH₃), 0.12 (-Si(CH₃)₃)₂. ¹³C NMR (62 MHz, CDCl₃): δ = 147.62 (C_{aryl}-CH₂-)₂, 119.12

(C_{aryl}-C≡)₂, 104.04, 96.07 (-C≡C-)₂, 32.04, 31.71, 30.07, 29.71, 29.53, 29.48, 29.34, 29.17, 28.93, 28.62, 22.81, 14.22 (CH₃(CH₂)₁₁-)₂, 0.45 (-Si(CH₃)₃)₂.

1,4-Dioctyloxy-2,5-bis(trimethylsilylethynyl)benzene (7).⁸⁵ 6.03 g (12.3 mmol) of 1,4-Dioctyloxy-2,5-dibromobenzene,¹⁵⁹ 420 mg (0.6 mmol) Pd(PPh₃)₂Cl₂ and 115 mg (0.6 mmol) CuI were dissolved in 150 mL dried diisopropylamine. 2.66 g (27.1 mmol) trimethylsilylacetylene was added over a period of 10 min to the vigorously stirred solution. The reaction mixture was then stirred at reflux for 3.5h. After cooling, toluene (100 ml) was added and the white ammonium bromide precipitates were filtered off. The solvent was removed on a rotary evaporator; the remaining brown solid was dissolved in toluene and passed through a 4 cm plug of silica gel. The evaporation of the solvent led to a light brown oil which crystallized upon standing. Recrystallization (twice) from ethanol/chloroform (v/v : 5/3) yielded 4.9 g of white needles. ¹H NMR (250 MHz, CDCl₃): δ = 6.86 (s, 2H, aryl-H), 3.94 (t, 4H, -OCH₂-), 1.80-1.26 (m, 24H), 0.86 (t, 6H), 0.23 (s, 18H, Si(CH₃)₃). ¹³C NMR (62 MHz, CDCl₃): δ = 153.99, 117.78, 113.29, 101.09, 99.86, (-C≡C-), 69.47 (-OCH₂-), 31.84, 29.35, 26.02, 22.65, 14.06 (CH₃), 0.05 (Si(CH₃)₃).

C₃₂H₅₄Si₂O₂ Calculated: C, 72.94; H, 10.33
(526.92) Found: C, 72.84; H 10.42.

1,4-Didodecyloxy-2,5-bis(trimethylsilylethynyl)benzene (8).⁸⁵ Same procedure was followed as mentioned above for **7**. Yield: 76%; ¹H NMR (250 MHz, CDCl₃): δ = 6.87 (s, 2H, aryl-H), 3.91 (t, 4H, -OCH₂-), 1.78-1.23 (m, 40H), 0.86 (t, 6H), 0.23 (s, 18H, Si(CH₃)₃). ¹³C NMR (62 MHz, CDCl₃): δ = 154.05, 117.28, 114.19, 101.09, 100.25, (-C≡C-), 69.50 (-OCH₂-), 31.92, 29.44, 29.35, 26.02, 22.68, 14.10 (CH₃), 0.042 (Si(CH₃)₃).

C₄₀H₇₀Si₂O₂ Calculated: C, 75.17; H, 11.04
(639.17) Found: C, 74.90; H 10.95.

2,3-Diamino-1,4-dibromobenzene (9).^{86c} To a suspension of 4,7-Dibromo-2,1,3-benzothiadiazole (5.0 g, 17 mmol) in absolute ethanol (170 mL), NaBH₄ (11.4 g, 300 mmol) was added portionwise at 0 °C. The mixture was stirred for 20h at room temperature. After evaporation in vacuum H₂O (100 mL) was added, and the mixture was extracted with Et₂O. The organic phase was washed with brine and dried (Na₂SO₄). Evaporation in vacuum gave 2,3-Diamino-1,4-dibromobenzene (**9**) as white solid. Yield: 3.9 g (87%). M.p. 94 ± 95 °C. ¹H NMR

(250 MHz, CDCl₃): δ = 3.89 (br. s, 4 H); 6.84 (s, 2H). ¹³C NMR (62 MHz, CDCl₃): δ = 109.74; 123.33; 133.83.

1-Bromo-4-formyl-2,5-dioctyloxybenzene (10).⁸⁷ To a solution of 1,4-dibromo-2,5-dioctyloxybenzene¹⁵⁹ (4.9 g, 10 mmol) in diethyl ether (150 mL), cooled at 10 °C and kept under argon, was added a solution of butyllithium (2.7 M in heptane, 3.75 mL, 10 mmol). After 15 min, DMF (0.96 mL, 12.5 mmol) was added to the mixture, while the temperature was allowed to rise to 15 °C. The clear solution was kept between 10 and 15 °C and was stirred for 1.5h. A 10% aqueous HCl solution (50 mL) was subsequently added to the mixture, and the phases were separated. The organic phase was washed with a NaHCO₃ solution and dried over CaCl₂. Diethyl ether was then distilled off, and the residue was recrystallized from methanol. Thus 2.7 g (61%) of light yellow crystals was obtained. Mp: 62-63 °C. ¹H NMR (250 MHz, CDCl₃): δ = 10.39 (s, 1H, CHO), 7.35 and 7.05 (m, 2 H, aryl-H), 4.0-3.80 (-OCH₂-), 1.79-0.81 (m, 30 H). ¹³C NMR (62 MHz, CDCl₃): δ = 189.33 (-CHO), 156.15, 150.24, 124.65, 121.34, 118.84, 111.01, 70.22, 69.85, 32.16, 32.14, 29.62, 29.58, 29.44, 29.39, 26.37, 26.31, 23.02, 14.46, 14.45.

C₂₃H₃₇BrO₃ Calculated: C, 62.57; H, 8.44; Br, 18.09.
(441.46) Found: C, 62.68; H, 8.55; Br, 18.40.

2,5-Dibromobenzene-1,4-dicarbaldehyde (11).⁸⁹ Sulfuric acid (70 mL) was added dropwise into a suspension containing 20 g of 2,5-dibromo-*p*-xylene, 100 mL of acetic acid, and 200 mL of acetic anhydride at 0 °C. CrO₃ was added to the mixture in portions. The resulting mixture was stirred vigorously at this temperature for another 5h until the reaction was completed. The greenish slurry was poured into ice water and filtered. The white solid was washed with water and cold methanol. The diacetate was then hydrolyzed by refluxing with a mixture of 100 mL of water, 100 mL of ethyl alcohol, and 10 mL of sulfuric acid for 12h. After cooling, the pale yellow product was separated by filtration. The crude product was purified by recrystallization from chloroform. Yield: 11.1 g (50%). ¹H NMR (250 MHz, CDCl₃): δ = 10.34 (s, 2H), 8.16 (s, 2H). ¹³C NMR (62 MHz, CDCl₃): δ = 190.2, 137.7, 135.4, 125.9.

C₈H₄Br₂O₂ Calculated: C, 32.91; H, 1.38; Br, 54.74.
(291.93) Found: C, 32.63; H, 1.4; Br, 54.60.

2,5-Dibromothiophene (12).⁹⁰ A solution of Br₂ (80.0 g, 0.50 mol) in 48 % aqueous HBr (75 mL) was added over 15 min to a vigorously stirred mixture of thiophene (21.0 g, 0.25 mol), 48 % aqueous HBr (75 mL) and Et₂O (50 mL) at -10 °C. The layers were then separated and

the aqueous layer was extracted with CH_2Cl_2 (4×25 mL). The combined organic phases were washed with H_2O (100 mL), dried (Na_2SO_4), and concentrated at reduced pressure. The remaining liquid was distilled at reduced pressure to give 2,5-dibromothiophene. Yield: 53 g (88 %). B.p. $76 - 80$ °C/ 10 Torr.

2,5-Dibromo-3,4-dinitrothiophene (13).⁹⁰ Concentrated sulfuric acid (130 mL), fuming sulfuric acid (200 mL), and fuming nitric acid (110 mL) were combined in a flask and cooled with an ice bath. 2,5-Dibromothiophene (35 mL, 75.3 g, 311 mmol) was added dropwise to maintain a temperature of 20-30 °C. The mixture was allowed to react for a total of 3 hours and then poured over 900 g of ice. Upon melting of ice, the solid residue was recovered by vacuum filtration and recrystallized via hot methanol to give yellow product. Yield: 48.6 g (47%). M.p. $135.0-137.0$ °C (lit.² $134-135$ °C). ^{13}C NMR (62 MHz, CDCl_3): $\delta = 113.7, 159.7$.

3, 4-Diaminothiophene (14).⁹⁰ To a stirred mixture of 2,5-dibromo-3,4-dinitrothiophene (10 g, 30 mmol) and conc. HCl (205 mL) was added Sn (21.25 g) portionwise and temperature kept below 30 °C. After complete addition, the reaction mixture is stirred for 4h (till complete consumption of Sn) and then kept in refrigerator overnight. The solid was filtered and washed many times first with diethyl ether and acetonitrile to remove impurities and dried in vacuum (5.4 g).

To the suspension of salt in Et_2O (55 mL) and H_2O (55 mL) at 5 °C was added 4N Na_2CO_3 solution to basify the solution. The organic layer was separated, aqueous layer was repeatedly extracted with ether. The combined organic layers were washed with water, dried (Na_2SO_4) and concentrated at reduced pressure. The concentrated liquid was put in refrigerator and after few hours 3, 4-diaminothiophene was obtained as white precipitate. Yield: 1.4 g (43%). M. p. 96 °C.

Thieno[3,4-*b*]pyrazine (15).⁹⁰ Compound **14** (0.210 g, 1.84 mmol) was added to 5% Na_2CO_3 (10 mL). Glyoxal (0.118 g, 2.03 mmol) was then added as an aqueous solution prepared by diluting 0.295 g of a 40% glyoxal solution to 5 mL with water. This mixture was stirred at room temperature for one hour and then extracted repeatedly with ether. The combined ether fractions were washed with water, dried with anhydrous Na_2SO_4 , and concentrated by rotary evaporation without heating to give a light brown oil. Analytical samples were prepared by dissolving the oil in a minimal amount of CH_2Cl_2 and purified by chromatography using ether as the eluting solvent to give 0.19 g of a light tan solid (76%). M.p. $47.3-48.1$ °C (lit.⁹⁰ 46.5 °C); ^1H NMR

(250 MHz, CDCl₃): δ = 8.46 (s, 2H), 8.01 (s, 2H). ¹³C NMR (62 MHz, CDCl₃): δ = 144.4, 142.8, 118.4.

C₆H₄N₂S Calculated: C, 52.92; H, 2.96; N, 20.57.
(136.18) Found: C, 53.03; H, 3.28; N, 20.13.

2,3-Diphenylthieno[3,4-*b*]pyrazine (16).⁹⁰ Compound **14** (0.60 g, 5.26 mmol) and Benzil (1.15 g, 5.46 mmol) were combined in 250 mL ethanol to yield a red orange solution which was stirred overnight in dark and then concentrated by rotary evaporation without heating to give a solid residue. The residue was washed repeatedly with petroleum ether, the combined petroleum ether washes were dried with anhydrous Na₂SO₄, and then concentrated by rotary evaporation to give a light tan product. The product was purified further by chromatography (solvent, dichloromethane) to give light yellow-tan needles. Yield: 0.7 g (46%). M.p. 169.1-171.0 °C. ¹H NMR (250 MHz, CDCl₃): δ = 7.30-7.45 (m), 8.05 (s), ¹³C NMR (62 MHz, CDCl₃): δ = 116.54, 127.13, 127.82, 128.60, 138.12, 140.59, 152.33.

C₁₈H₁₂N₂S Calculated: C, 74.97; H, 4.19; N, 9.71.
(288.37) Found: C, 74.54; H, 4.36; N, 9.65.

9,9-Didecylfluorene (17).^{91b} A 2.5 M *n*-butyllithium solution (160 mmol, in hexane) was added dropwise to a solution of fluorene (13.3 g, 80 mmol) in 150 mL of anhydrous THF at -78 °C. The mixture was stirred at -78 °C for 45 min, and then 1-bromodecane (38.9 g, 176 mmol) was added dropwise followed by further stirring at -78 °C for 1h. The solution was then allowed to warm slowly to room temperature and stirred for another 1h. Then 100 mL aqueous NH₄Cl solution (10%, w/w) was added with stirring. The organic layer was separated and washed twice with 100 mL aliquots of water before being dried over anhydrous MgSO₄. The solvent was then removed under reduced pressure followed by the removal of excess of 1-bromodecane by distillation under vacuum. The product was directly used without further purification. ¹H NMR (250 MHz, CDCl₃): δ = 7.68 (d, *J*) 6.8 Hz, 2H), 7.30 (m, 6H), 1.94 (m, 4H), 0.96-1.24 (m, 28H), 0.81 (t, *J*) 7.2 Hz, 6H), 0.60 (m, 4H).

C₃₃H₅₀ Calculated: C, 88.72; H, 11.28.
(446.76) Found: C, 88.56; H, 11.08.

2,7-Dibromo-9,9-didecylfluorene (18).^{91c} Bromine (23.61 g, 148 mmol) in CH₂Cl₂ (100 mL) was slowly added with stirring at room temperature to a CH₂Cl₂ (200 mL) solution of the above product (**17**) (30 g, 67 mmol) containing 0.2 g of FeCl₃. This is an exothermic reaction, and any

rapid addition of the bromine should be avoided. The solution was stirred at room temperature for 20 h in the dark, and 300 mL of aqueous NaHSO₃ (15%) was added. Vigorous stirring was applied until the red color disappeared (<30 min). The organic layer was separated, washed with water and dried over anhydrous MgSO₄. The solvent was removed under reduced pressure and the product was purified by recrystallization from hexane three times to yield a white crystalline product. The overall yield of these two reactions was 85.4%. Mp: 51.0-53.7 °C. ¹H NMR (250 MHz, CDCl₃): δ = 7.51 (dd, *J* 7.6 Hz, 1.0 Hz, 2H), 7.44 (dd, *J* 7.6 Hz, 1.6 Hz, 2H), 7.43 (s, 2H), 1.90 (m, 4H), 0.98-1.24, (m, 28H), 0.82 (t, *J* 7.2 Hz, 6H), 0.57 (m, 4H).

C₃₃H₄₈Br₂ Calculated: C, 65.56; H, 8.00; Br, 26.43.

(604.55) Found: C, 65.18; H, 8.07; Br, 26.24.

4.3 Monomers Synthesis

2,5-Diethynyl-3-dodecylthiophene (M1). Methanol (70 mL) and aqueous KOH (5 mL, 20%) were added at room temperature to a stirred solution of 2,5-bis(trimethylsilylethynyl)-3-dodecylthiophene (3.5 g, 7.9 mmol) in 140 mL of THF. The reaction mixture was then stirred 3h at room temperature. The solvent was removed on a rotator evaporator, and the residue was chromatographed on a silica gel column with n-haxane as eluent. Thus, a reddish yellow liquid was obtained. Yield: 1.7 g (71%). ^1H NMR (250 MHz, CDCl_3): δ = 7.12 (1H, s, $\text{C}_{\text{aryl}}\text{-H}$), 3.3 (1H, s, $\text{-C}\equiv\text{C-H}$), 3.16 (1H, s, $\text{-C}\equiv\text{C-H}$), 2.53 (2H, t, $^3J = 6.5$ Hz, $\text{-(CH}_2\text{)-}$), 1.78-1.12 (20H, m, $\text{-(CH}_2\text{)}_{10}\text{-}$), 0.84 (3H, t, $^3J = 7.5$ Hz, -CH_3). ^{13}C NMR (62 MHz, CDCl_3): δ = 148.65 ($\text{C}_{\text{aryl}}\text{-CH}_2\text{-}$), 133.72 ($\text{C}_{\text{aryl}}\text{-H}$), 121.99, 118.84 ($\text{C}_{\text{aryl}}\text{-C}\equiv$)₂, 83.88, 83.08, 76.47, 75.97 (-CC-)₂, 34.65, 34.50, 34.50, 31.57, 30.18, 29.65, 29.58, 29.50, 29.04, 26.27, 22.64, 14.10 ($\text{CH}_3(\text{CH}_2)_{11}\text{-}$).

C₂₀H₂₈S Calculated: C, 79.94; H, 9.39; S, 10.67.
(300.51) Found: C, 79.39; H, 9.27; S, 10.53.

2,5-Diethynyl-3,4-didodecylthiophene (M2). Same procedure was followed as above mentioned for **M1**. Yield: 1.1 g (64%). ^1H NMR (250 MHz, CDCl_3): δ = 3.10 (2H, s, $\text{-C}\equiv\text{C-H}$), 2.53 (4H, t, $^3J = 6.5$ Hz, $\text{-(CH}_2\text{)-}$), 1.78-1.12 (40H, m, $\text{-(CH}_2\text{)}_{10}\text{-}$), 0.84 (6H, t, $^3J = 7.5$ Hz, -CH_3). ^{13}C NMR (62 MHz, CDCl_3): δ = 147.65 ($\text{C}_{\text{aryl}}\text{-CH}_2\text{-}$), 121.99 ($\text{C}_{\text{aryl}}\text{-C}\equiv$)₂, 83.08, 75.78 ($\text{-C}\equiv\text{C-}$)₂, 34.65, 34.50, 31.91, 31.57, 30.18, 29.65, 29.50, 29.04, 28.90, 22.64, 14.14 ($\text{CH}_3(\text{CH}_2)_{11}\text{-}$)₂.

C₃₂H₅₂S Calculated: C, 81.98; H, 11.18; S, 6.84.
(468.83) Found: C, 81.74; H, 11.08; S, 6.70.

1,4-Diethynyl-2,5-dioctyloxybenzene (M3).⁸⁵ Methanol (93 mL) and aqueous KOH (6.5 mL, 20%) were added at room temperature to a stirred solution of **7** (5.5 g, 10.44 mmol) in THF (185 ml). After stirring for 2h, the solvent was evaporated and a yellow solid was obtained. Recrystallization from hexane with charcoal yielded pale yellow crystals (4.65 g).

Yield: 90% ^1H NMR (250 MHz, CDCl_3): δ = 6.67 (s, 2H, aryl-H), 4.01 (t, 4H, $\text{-OCH}_2\text{-}$), 3.32 (s, 2H, $\text{-C}\equiv\text{C-H}$), 1.80-1.12 (m, 24H,), 0.84 (t, 6H). ^{13}C NMR (62 MHz, CDCl_3): δ = 152.89, 118.78, 113.29, 83.46, 78.79, ($\text{-C}\equiv\text{C-H}$), 69.68 ($\text{-OCH}_2\text{-}$), 31.78, 29.27, 29.20, 29.12, 25.89, 22.64, 14.08 (CH_3).

C₂₆H₃₈O₂ Calculated: C, 81.62; H, 10.01.
(382.59) Found: C, 81.44; H, 9.84.

1,4-Diethynyl-2,5-didodecyloxybenzene (M4).⁸⁵ Same procedure was followed as above mentioned. Yield: 90% ¹H NMR (250 MHz, CDCl₃): δ = 6.93 (s, 2H, aryl-H), 3.94 (t, 4H, -OCH₂-), 3.30 (s, 2H, -C \equiv C-H), 1.80-1.26 (m, 40H), 0.86 (t, 6H). ¹³C NMR (62 MHz, CDCl₃): δ = 153.99, 117.78, 113.29, 82.36, 79.78, (-C \equiv C-H), 69.68 (-OCH₂-), 31.78, 29.27, 29.20, 29.12, 25.89, 22.64, 14.08 (CH₃).

C₃₄H₅₄O₂ Calculated: C, 82.53; H, 11.00.
(494.80) Found: C, 82.34; H, 10.91.

4,7-Dibromo-2,1,3-benzothiadiazole (M5).⁸⁶ A mixture of 2,1,3-benzothiadiazole (20.0 g, 147 mmol) in aq. HBr (48%, 60 mL) was heated to reflux with stirring, while Br₂ (22.6 mL, 440 mmol) was added slowly within 1h. Towards the end of the addition, the mixture became a suspension. To facilitate stirring, aq. HBr (48%, 40 mL) was added, and the mixture was heated to reflux for 2h after completion of the Br₂ addition. The mixture was filtered while hot, cooled, filtered again, and washed well with H₂O. The compound was dried and recrystallized from methanol to give 4,7-dibromo-2,1,3-benzothiadiazole as white needles. Yield: 38.0 g (88%). M.p. 188 \pm 189 ^oC. ¹H NMR (250 MHz, CDCl₃): δ = 7.71 (s, 2H). ¹³C NMR (62 MHz, CDCl₃): δ = 113.95; 132.42; 153.06.

C₆H₂Br₂N₂S Calculated: C, 24.51; H, 0.69; N, 9.53; S, 10.91; Br, 54.36.
(293.97) Found: C, 24.73; H, 0.71; N, 9.35; S, 10.71; Br, 54.18.

5,8-Dibromoquinoxaline (M6).^{86c,d} An aq. soln. of glyoxal (40%, 0.825 g, 5.6 mmol) was added dropwise to **7** (1.5 g, 5.6 mmol) in ethanol (38 ml). The mixture was heated to reflux for 3h, cooled, and the pale-yellow precipitate was separated by filtration. Recrystallization (acetone) gave 5,8-dibromoquinoxaline as pale-yellow needles. Yield: 0.65 g (40%). M.p. 227^oC. ¹H NMR (250 MHz, CDCl₃): δ = 8.01 (s, 2 H); 9.02 (s, 2H). ¹³C NMR (62 MHz, CDCl₃): δ = 123.98; 133.73; 141.57; 146.04.

C₈H₄Br₂N₂ Calculated: C, 33.37; H, 1.40; N, 9.73; Br, 55.50.
(287.94) Found: C, 33.64; H, 1.25; N, 9.53; Br, 55.33.

5,8-Dibromo-2,3-diphenylquinoxaline (M7).^{86c,d} A soln. of **7** (1.0 g, 3.8 mmol) and benzil (0.80 g, 3.8 mmol) in ethanol (40 mL) and few drops of glacial acetic acid was heated to reflux for 1h, then cooled to 0 ^oC. The formed precipitate was isolated by filtration and washed with ethanol to afford 5,8-dibromo-2,3-diphenylquinoxaline as white solid. Yield: 1.16 g (70%). M.p. 221 \pm 222 ^oC. ¹H NMR (250 MHz, CDCl₃): δ = 7.3 \pm 7.5 (m, 6 H); 7.6 \pm 7.7 (m, 4H); 7.92 (s,

2H). ^{13}C NMR (62 MHz, CDCl_3): $\delta = 123.73; 128.36; 129.57; 130.24; 133.10; 137.95; 139.35; 154.14$.

$\text{C}_{20}\text{H}_{12}\text{Br}_2\text{N}_2$ Calculated: C, 54.58; H, 2.75; N, 6.36; Br, 36.31.

(440.14) Found: C, 54.59; H, 2.89; N, 6.53; Br, 36.38.

10,13-Dibromodibenzo[a,c]phenazine (M8).^{86c} A soln. of **7** (1.03g, 3.9 mmol) and phenanthrene-9,10-dione (0.81 g, 3.9 mmol) in 42 mL ethanol/ acetic acid (20:1) was heated to reflux for 2h, then cooled to 0 $^{\circ}\text{C}$. The precipitate formed was isolated by filtration and washed with ethanol to afford 10,13-dibromodibenzo[a,c]phenazine as yellow solid. Yield: 1.37 g (80%). M.p. 316 ± 317 $^{\circ}\text{C}$. ^1H NMR (250 MHz, CDCl_3): $\delta = 7.79$ (dt, J-7.8, 1.5, 2 H); 7.85 (dt, J-7.8, 1.5, 2 H); 8.04 (s, 2H); 8.57 (dd, J-7.8, 1.5, 2 H); 9.48 (dd, J-7.8, 1.5, 2 H). ^{13}C NMR (62 MHz, CDCl_3): $\delta = 123.10; 124.23; 127.29; 128.39; 129.57; 131.30; 132.68; 132.92; 143.53$.

$\text{C}_{20}\text{H}_{10}\text{Br}_2\text{N}_2$ Calculated: C, 54.83; H, 2.30; N, 6.39; Br, 36.48.

(438.12) Found: C, 54.98; H, 2.46; N, 6.64; Br, 36.36.

5,8-Dibromo-2,3-dipyridylquinoxaline (M9).^{86d} A soln. of **7** (1.0 g, 3.8 mmol) and 2,2'-pyridil (0.806 g, 3.8 mmol) in ethanol (25 mL) was heated to reflux for 3h, then cooled to 0 $^{\circ}\text{C}$. The formed precipitate was isolated by filtration and washed with ethanol to afford 5,8-dibromo-2,3-dipyridylquinoxaline as yellow solid. Yield: 1.16 g (70%). M.p. 251°C . ^1H NMR (250 MHz, CDCl_3): $\delta = 7.27$ (dd, J-4.5, 8.3, 2H); 7.87 (d(br), J-8.0, 2H); 7.97 (s, 2H), 8.29 (m, 4H). ^{13}C NMR (62 MHz, CDCl_3): $\delta = 123.73; 128.36; 129.57; 130.24; 133.10; 137.95; 139.35; 148.16; 153.37, 156.54$.

$\text{C}_{18}\text{H}_{10}\text{Br}_2\text{N}_4$ Calculated: C, 48.90; H, 2.28, N, 12.67; Br, 36.15.

(442.11) Found: C, 48.75; H, 2.23; N, 12.56; Br, 36.21.

1,2-Bis(4-bromophenyl)-1-cyanovinylene (M10).⁸⁸ 4-Bromophenylacetonitrile (1.96 g, 10 mmol) and 4-bromobenzaldehyde (1.85 g, 10 mmol) were dissolved in ethanol (50 mL). To the mixture was added dropwise a solution of NaOH (50 mg) in ethanol (30 mL) under a nitrogen atmosphere. The reaction mixture was stirred at room temperature for 1h. The product was obtained as a precipitate, filtered, and washed with water to give a white powder. Yield: 3.30 g (91%). ^1H NMR (250 MHz, CDCl_3): $\delta = \delta 7.77$ (d, 2H), 7.62-7.52 (m, 6H), 7.45 (s, 1H). ^{13}C NMR (62 MHz, CDCl_3): $\delta = 140.9, 132.8, 132.2, 130.5, 127.3, 125.1, 123.6, 117.2, 111.0$.

$\text{C}_{15}\text{H}_9\text{Br}_2\text{N}$ Calculated: C, 49.63; H, 2.50; N, 3.86; Br, 44.02.

(363.05) Found: C, 49.64; H, 2.54; N, 3.80; Br, 43.91.

3-(4-Bromo-2,5-dioctyloxyphenyl)-2-(4-bromophenyl)-acrylonitrile (M11).⁸⁸ Same procedure was followed as above mentioned for **M10**. 4-Bromophenylacetonitrile (1.96 g, 10 mmol), 4-bromo-2,5-dioctyloxy benzaldehyde (**10**) (4.41 g, 10 mmol). The product obtained as a bright yellow powder. Yield: 4.0 g (65%). ¹H NMR (250 MHz, CDCl₃): δ = 7.83 (s, 1H), 7.53-7.48 (m, 4H), 7.19 (s, 1H), 7.07 (s, 1H), 4.01(t, 2H), 3.91(t, 2H), 1.73-1.21(m, 24H), 0.81(t, 6H). ¹³C NMR (62 MHz, CDCl₃): δ = 150.64, 149.58, 138.25, 132.70, 132.19, 130.65, 127.42, 124.45, 121.34, 120.05, 110.1, 69.8, 67.51, 31.78, 29.21, 29.09, 26.08, 22.64, 14.08.

C₃₁H₄₁Br₂NO₂ Calculated: C, 60.11; H, 6.67; N, 2.26; Br, 25.80.
(619.48) Found: C, 60.01; H, 6.70; N, 2.18; Br, 25.91.

3-[2,5-Dibromo-4-(2-cyano-2-phenylvinyl)-phenyl]-2-phenylacrylonitrile (M12). 2,5-Dibromobenzene-1,4-dicarbaldehyde (**8**) (1.46 g, 5 mmol) and phenylacetonitrile (1.17 g, 10 mmol) were given to a solution of 35 mL toluene and 6 mL of tert-butanol under argon. The temperature was raised to 70°C while stirring, and potassium tert-butoxide (14 mg, 0.12 mmol) dissolved in 5 mL tert-butanol was added to the mixture. It was heated for 3h, whereby the mixture became yellowish in colour. After cooling at room temperature 2 drops of acetic acid were added, poured in methanol and precipitates washed with methanol and water, dried under vacuum. A fibrous yellow material was obtained. Yield: 1.3 g (53 %). ¹H NMR (250 MHz, CDCl₃): δ = 8.39 (s, 2H), 7.79 (s, 2H), 7.75-7.4 (m, 10H). ¹³C NMR (62 MHz, CDCl₃): δ = 150.1, 143.2, 138.32, 136.58, 133.28, 130.28, 129.32, 126.44, 124.08, 116.57.

C₂₄H₁₄Br₂N₂ Calculated: C, 58.81; H, 2.88; N, 5.71; Br, 32.60.
(490.20) Found: C, 59.01; H, 2.77; N, 5.53; Br, 32.37.

5,7-Dibromo-thieno[3,4-*b*]pyrazine (M13).⁵⁴ To Compound **15** (0.476 g, 3.5 mmol) in chloroform/ acetic acid (1:1) 40mL was added NBS (1.37 g, 7.7 mmol) in dark and stirred overnight under argon. The reaction mixture was diluted with equal amount of water, the chloroform layer was separated and washed once with KOH solution and once with water, dried over MgSO₄. The organic layer was concentrated by rotary evaporation without heating to give a solid residue. The product was further purified by chromatography (solvent, dichloromethane) to give greenish yellow solid. Yield: 0.7 g (68%). ¹H NMR (250 MHz, CDCl₃): δ = 8.70 (s, 2H). ¹³C NMR (62 MHz, CDCl₃): δ = 154.4, 152.8, 108.4.

C₆H₂Br₂N₂S Calculated: C, 24.51; H, 0.69; N, 9.53; Br, 54.36.
(293.97) Found: C, 24.30; H, 0.60; N, 9.24; Br, 54.20.

5,7-Dibromo-2,3-diphenylthieno[3,4-*b*]pyrazine (M14).⁵⁴ Same procedure was followed as mentioned above for **M13**. Compound **16** (1.0 g, 3.5 mmol), NBS (1.37 g, 7.7 mmol). Yield: 1.0 g (64%). M.p. 169.1-171.0 °C. ¹H NMR (250 MHz, CDCl₃): δ = 7.44-7.32 (m). ¹³C NMR (62 MHz, CDCl₃): δ = 154.63, 139.29, 138.23, 130.25, 129.86, 129.37, 128.49.

C₁₈H₁₀Br₂N₂S Calculated: C, 48.46; H, 2.26; N, 6.28; Br, 35.82.
(446.16) Found: C, 48.36; H, 2.08; N, 6.24; Br, 35.60.

Synthesis of 2,7-Dioxaborolan-9,9-didecylfluorene (M15).^{72,91} A 2.5M solution of *n*-butyllithium (42 mL, 105 mmol) was added to an argon-purged solution of **18** (30.23 g, 50 mmol) in anhydrous diethyl ether (300 mL) at -78 °C using a syringe. The solution was then allowed to slowly warm to room temperature, and stirred for a further 1h before it was cooled again to -78 °C. Triisopropyl borate (39.5 g, 210 mmol) was added with a syringe. The resulting mixture was once again allowed to warm to room temperature and was stirred for an additional 20h (vigorous stirring was required during this step to avoid gel formation). Then 2N HCl (200 mL) was added to the stirred solution while maintaining the solution at room temperature for 1h. The organic layer was separated and the water layer was extracted with 200 mL of diethyl ether. The combined ether layers were washed twice with 200 mL of water. The solvent was then removed under reduced pressure. The crude product was purified by Soxhlet extraction with hexane to give a white powder.

The crude diboronic acid was suspended in 50 mL of toluene and 30 mmol (1.86 g) of ethylene glycol, and the mixture was stirred and refluxed under a Dean-Stark apparatus for 2-3h. The reaction mixture was cooled and the solvent was removed. The residue was recrystallized from toluene-hexane mixture to provide the diboronate as a white powder in 65% overall yield.

¹H NMR (250 MHz, CDCl₃): δ = 7.86 (6H, m,), 4.53 (8H, s), 2.00 (8H, t, ³J = 6.5 Hz, -OCH₂-), 1.25-1.02 (32H, m), 0.87 (6H, t, ³J = 7.5 Hz, -CH₃). ¹³C NMR (62 MHz, CDCl₃): δ = 150.57, 144.04, 133.63, 129.07, 119.69, 66.07, 55.07, 40.29, 31.87, 30.03, 29.59, 29.51, 29.29, 29.26, 23.74, 22.66, 14.11.

C₃₇H₅₆B₂O₄ Calculated: C, 75.78; H, 9.62.
(586.47) Found: C, 76.02; H, 9.54.

Synthesis of 1,4-Bis[4,4,5,5-tetramethyl-(1,3,2)-dioxaborolan-2-yl]-2,5-didodecyloxyphenylene (M16).⁹² In a three-neck flask is dissolved 3.0 g (4.96 mmol) of 2,5-dibromo-1,4-didodecyloxyphenylene in 40 mL of dry THF. Then, 4.8 mL of *n*-butyllithium (2.5 M in hexanes) is slowly added via a syringe at -78 °C. The mixture is allowed to reach RT for

1h. Then it is cooled again to $-78\text{ }^{\circ}\text{C}$, and 2.05 g (11 mmol) of 2-isopropoxy-4,4,5,5-tetramethyl-[1,3,2]dioxaborolane dissolved in 15 mL of THF is dropwise added via a 50 mL funnel. The mixture is let to reach RT and stirred for 24h. The organic phase is extracted with diethyl ether, washed twice with brine, and dried over magnesium sulfate. The solvent is distilled off, and the crude product is dissolved again in 25 mL of THF. Reprecipitation with *n*-hexanes gives 2.2 g of compound **M16**, that is recrystallized in ethyl acetate. Yield: 57%. ^1H NMR (250 MHz, CDCl_3): δ = 7.38 (s, 2H, Ar-H), 4.02 (t, 4H) $-\text{OCH}_2-$, 1.95-1.05 (m, 64H), 0.79 (s, 6H). ^{13}C NMR (62 MHz, CDCl_3): δ = 158.57, 151.04, 150.53, 137.10, 119.02, 113.03, 69.87, 33.58, 32.33, 30.98, 30.04, 29.76, 26.61, 26.45, 25.26, 23.09, 14.50, 14.38.

C₄₂H₇₆B₂O₂
(698.68)

Calculated: C, 72.20; H, 10.96
Found: C, 71.94, H, 10.81

4.4 Synthesis of Polymers

General Procedure for Polycondensation (Sonogashira Coupling). To a 250 mL flask, charged with the dibromo monomer (**M5-M12**) (1.066 mmol), diethynyl monomer (**M1-M4**) (1.066 mmol), Pd(PPh₃)₄ (74 mg, 0.064 mmol), and CuI (13 mg, 0.064 mmol), were added diisopropylamine (40 mL) and toluene (60 mL) under argon. The mixture was stirred for 0.5h at room temperature and then heated at 65 °C for 30-40h. After being cooled to room temperature, resulting solution was poured into methanol (500 mL). The precipitate was separated by filtration and washed with methanol, soxhlet extraction was made for 24h in methanol and dried under vacuum.

Poly[3-dodecylthiophen-2,5-diylethynylene-(benzo[1,2,5]thiadiazole-4,7-diyl)ethynylene]

(P-1). 4,7-Dibromo-2,1,3-benzothiadiazole **M5** 313 mg (1.066 mmol), 2,5-diethynyl-3-dodecylthiophene **M1** 320 mg (1.066 mmol). Yield: 0.383 g (83 %) red polymer. ¹H NMR (250 MHz, CDCl₃): δ = 7.80 (s, 2H), 7.10 (s, 1H of thiophene), 2.92 (m, 2H), 1.75-0.90 (m, 23H). ¹³C NMR (62 MHz, CDCl₃): δ = 154.90, 147.52, 142.24, 134.85, 132.40, 128.07, 124.39, 121.43, 94.20, 92.60, (-C≡C-), 32.31, 30.60, 30.06, 29.74, 29.51, 22.70, 14.15. **GPC** (Polystyrene standards): \bar{M}_w = 15900 g/mol, \bar{M}_n = 5900; PDI = 2.71; \bar{P}_n = 14. **UV-Vis** (Chloroform): λ_{\max}/nm ($\epsilon/(1 \cdot \text{mol}^{-1} \cdot \text{cm}^{-1})$) 328 (41900), 354 (41600), 504 (43900).

(C₂₆H₂₈N₂S₂)_n Calculated: C, 72.18; H, 6.52; N, 6.47; S, 14.82.

(432.65)_n Found: C, 69.82; H, 6.94; N, 5.46; S, 12.78; Br, 3.85.

Poly[3,4-didodecylthiophen-2,5-diylethynylene-(benzo[1,2,5]thiadiazole-4,7-

diyl)ethynylene] (P-2). 4,7-Dibromo-2,1,3-benzothiadiazole **M5** 313 mg (1.066 mmol), 2,5-diethynyl-3,4-didodecylthiophene **M2** 500 mg (1.066 mmol). Yield: 0.5 g (78 %) violet polymer. ¹H NMR (400 MHz, CDCl₃): δ = 7.70 (s, 2H), 2.83 (m, 4H), 1.68-0.83 (m, 46H). ¹³C NMR (400 MHz, CDCl₃): δ = 154.64, 149.22, 132.39, 128.04, 121.29, 93.47, 91.86, (-C≡C-), 32.34, 30.73, 30.14, 29.90, 29.79, 29.29, 25.79, 23.11, 14.53. **GPC** (Polystyrene standards): \bar{M}_w = 82600 g/mol, \bar{M}_n = 16400; PDI = 5.04; \bar{P}_n = 27. **UV-Vis** (Chloroform): λ_{\max}/nm ($\epsilon/(1 \cdot \text{mol}^{-1} \cdot \text{cm}^{-1})$) 249 (43500) 329 (43300), 357 (43000), 540 (45800) 599 (42600).

(C₃₈H₅₂N₂S₂)_n Calculated: C, 75.95; H, 8.72; N, 4.66; S, 10.67.

(600.976)_n Found: C, 73.95; H, 8.60; N, 4.25; S, 9.95; Br, 3.61.

Poly[3-dodecylthiophene-2,5-diylethynylene-(2,3-diphenyl-2-ylquinoxaline-5,8-diyl)ethynylene] (P-3). 5,8-Dibromo-2,3-diphenylquinoxaline **M7** 469 mg (1.066 mmol), 2,5-diethynyl-3-dodecylthiophene **M1** 320 mg (1.066 mmol). Yield: 0.51 g (83 %) red polymer. $^1\text{H NMR}$ (250 MHz, CDCl_3): $\delta = 7.86$ (s, 2H), 7.63 (m, 4H) 7.32 (m, 6H), 7.09 (s, 1H of thiophene), 2.83 (m, 2H), 1.48-0.79 (m, 23H). $^{13}\text{C NMR}$ (62 MHz, CDCl_3): $\delta = 154.14, 138.95, 134.16, 130.28, 129.50, 128.20, 123.35, 117.57, 94.47, 92.86, (-\text{C}\equiv\text{C}-), 32.34, 31.92, 30.14, 29.66, 29.29, 22.69, 14.14$. **GPC** (Polystyrene standards): $\bar{M}_w = 23200$ g/mol, $\bar{M}_n = 10600$; $\text{PDI} = 2.18$; $\bar{P}_n = 18$. **UV-Vis** (Chloroform): $\lambda_{\text{max}}/\text{nm}$ ($\epsilon/(1 \cdot \text{mol}^{-1} \cdot \text{cm}^{-1})$) 320 (43800), 363 (43700), 495 (45000).

$(\text{C}_{40}\text{H}_{38}\text{N}_2\text{S})_n$ Calculated: C, 83.00; H, 6.62; N, 4.84; S, 5.54.
(578.82) $_n$ Found: C, 82.46; H, 6.87; N, 4.45; S, 5.40; Br, 1.85.

Poly[3-dodecylthiophene-2,5-diylethynylene-(dibenzo[a,c]phenazine-10,13-diyl)ethynylene] (P-4). 10,13-Dibromodibenzo[a,c]phenazine **M8** 467 mg (1.066 mmol), 2,5-diethynyl-3-dodecylthiophene **M1** 320 mg (1.066 mmol). Yield: 0.51 g (83 %) red polymer. **GPC** (Polystyrene standards): $\bar{M}_w = 17900$ g/mol, $\bar{M}_n = 5200$; $\text{PDI} = 3.43$; $\bar{P}_n = 9$. **UV-Vis** (Chloroform): $\lambda_{\text{max}}/\text{nm}$ ($\epsilon/(1 \cdot \text{mol}^{-1} \cdot \text{cm}^{-1})$) 251 (46500) 315 (44000), 388 (43000), 499 (42000).

$(\text{C}_{40}\text{H}_{36}\text{N}_2\text{S})_n$ Calculated: C, 83.29; H, 6.29; N, 4.86; S, 5.56.
(576.805) $_n$ Found: C, 81.69; H, 6.65; N, 4.45; S, 5.22; Br, 3.10.

Poly[3-dodecylthiophene-2,5-diylethynylene-(2,3-dipyridine-2-ylquinoxaline-5,8-diyl)ethynylene] (P-5). 5,8-Dibromo-2,3-dipyridylquinoxaline **M9** 471 mg (1.066 mmol), 2,5-diethynyl-3-dodecylthiophene **M1** 320 mg (1.066 mmol). Yield: 0.45 g (72%) red polymer. $^1\text{H NMR}$ (250 MHz, CDCl_3): $\delta = 8.34$ (s, 2H), 7.98-7.90 (m, 6H), 7.27-7.20 (m, 2H of pyridine, 1H of thiophene), 2.90 (m, 2H), 1.66-0.84 (m, 23H). $^{13}\text{C NMR}$ (62 MHz, CDCl_3): $\delta = 157.90, 153.30, 149.51, 148.52, 141.24, 136.99, 134.09, 133.67, 130.80, 124.77, 123.60, 121.43, 94.72, 92.48, (-\text{C}\equiv\text{C}-), 32.31, 30.60, 30.06, 29.74, 29.51, 23.07, 14.50$. **GPC** (polystyrene standards): $\bar{M}_w = 17700$ g/mol, $\bar{M}_n = 7700$; $\text{PDI} = 2.31$; $\bar{P}_n = 13$. **UV-Vis** (Chloroform): $\lambda_{\text{max}}/\text{nm}$ ($\epsilon/(1 \cdot \text{mol}^{-1} \cdot \text{cm}^{-1})$) 317 (43900), 346 (43700), 506 (44900).

$(\text{C}_{38}\text{H}_{36}\text{N}_4\text{S})_n$ Calculated: C, 78.58; H, 6.25; N, 9.65; S, 5.52.
(580.796) $_n$ Found: C, 77.95; H, 6.44; N, 9.19; S, 5.32; Br, 1.36.

Poly[3,4-didodecylthiophene-2,5-diylethynylene-(2,3-dipyridine-2-ylquinoxaline-5,8-diyl)ethynylene] (P-6). 5,8-Dibromo-2,3-dipyridylquinoxaline **M9** 471 mg (1.066 mmol), 2,5-

diethynyl-3,4-didodecylthiophene **M2** 500 mg (1.066 mmol). Yield: 0.64 g (80%) red polymer. $^1\text{H NMR}$ (250 MHz, CDCl_3): $\delta = 8.35$ (s, 2H), 7.98-7.95 (m, 6H), 7.29-7.27 (m, 2H), 2.91 (m, 4H), 1.66-0.84 (m, 46H). $^{13}\text{C NMR}$ (62 MHz, CDCl_3): $\delta = 157.47, 152.87, 148.08, 140.90, 136.68, 132.73, 124.51, 123.12, 120.48, 94.12, 91.75, (-\text{C}\equiv\text{C}-), 31.93, 30.26, 29.68, 29.37, 28.75, 22.70, 14.14$. **GPC** (Polystyrene standards): $\bar{M}_w = 27900$ g/mol, $\bar{M}_n = 16400$; PDI = 1.70; $\bar{P}_n = 22$. **UV-Vis** (Chloroform): $\lambda_{\text{max}}/\text{nm}$ ($\epsilon/(1\cdot\text{mol}^{-1}\cdot\text{cm}^{-1})$) 247 (45000) 319 (44000), 354 (43700), 527 (45600).

$(\text{C}_{50}\text{H}_{60}\text{N}_4\text{S})_n$ Calculated: C, 80.17; H, 8.07; N, 7.48; S, 4.28.

$(749.12)_n$ Found: C, 79.62; H, 8.21; N, 7.20; S, 4.03; Br, 1.36.

Poly[1,4-dioctyloxyphenylene-2,5-diylethynylene-(2,3-dipyridine-2-ylquinoxaline-5,8-diyl)ethynylene] (P-7). 5,8-Dibromo-2,3-dipyridylquinoxaline **M9** 471 mg (1.066 mmol), 2,5-diethynyl-1,4-dioctyloxyphenylene **M3** 408 mg (1.066 mmol). Yield: 0.53 g (75%) red polymer. $^1\text{H NMR}$ (250 MHz, CDCl_3): $\delta = 8.34$ (s, 2H), 8.10-7.88 (m, 6H), 7.22 (s, 2H), 4.12 (t, 4H), 1.86-0.86 (m, 30H). $^{13}\text{C NMR}$ (62 MHz, CDCl_3): $\delta = 157.58, 153.88, 152.65, 148.11, 141.03, 136.51, 133.44, 124.42, 123.93, 123.03, 118.02, 114.83, 94.81, 92.30, (-\text{C}\equiv\text{C}-), 69.96, 31.78, 29.30, 26.02, 22.63, 14.06$. **GPC** (Polystyrene standards): $\bar{M}_w = 16900$ g/mol, $\bar{M}_n = 7200$; PDI = 2.34; $\bar{P}_n = 11$. **UV-Vis** (Chloroform): $\lambda_{\text{max}}/\text{nm}$ ($\epsilon/(1\cdot\text{mol}^{-1}\cdot\text{cm}^{-1})$) 320 (44700), 488 (45100).

$(\text{C}_{44}\text{H}_{46}\text{N}_4\text{O}_2)_n$ Calculated: C, 79.73; H, 6.99; N, 8.45.

$(662.87)_n$ Found: C, 79.37; H, 7.14; N, 7.98; Br, 1.51.

Poly[3-dodecylthiophene-2,5-diylethynylene-(2,3-diphenylthieno[3,4-*b*]pyrazine-5,7-diyl)ethynylene] (P-8). 5,7-Dibromo-2,3-diphenylthieno[3,4-*b*]pyrazine **M14** 476 mg (1.066 mmol), 2,5-diethynyl-3-dodecylthiophene **M1** 320 mg (1.066 mmol). Yield: 0.39 g (63%) blue polymer. $^1\text{H NMR}$ (400 MHz, CDCl_3): $\delta = 7.56-7.30$ (m, 10H), 6.97(s, 1H of thiophene), 2.84 (m, 2H), 1.70-0.84 (m, 23H). $^{13}\text{C NMR}$ (400 MHz, CDCl_3): $\delta = 154.46, 154.15, 149.38, 148.96, 143.17, 138.64, 130.06, 129.06, 128.14, 127.01, 118.04, 114.22, 93.19, 89.12, (-\text{C}\equiv\text{C}-), 31.91, 30.30, 30.16, 29.70, 29.48, 29.40, 29.34, 22.67, 14.11$. **GPC** (Polystyrene standards): $\bar{M}_w = 34500$ g/mol, $\bar{M}_n = 10900$; PDI = 3.17; $\bar{P}_n = 19$. **UV-Vis** (Chloroform): $\lambda_{\text{max}}/\text{nm}$ ($\epsilon/(1\cdot\text{mol}^{-1}\cdot\text{cm}^{-1})$) 275 (42600), 385 (43500), 588 (42000).

$(\text{C}_{38}\text{H}_{36}\text{N}_2\text{S}_2)_n$ Calculated: C, 78.04; H, 6.20; N, 4.79; S, 10.97.

$(584.85)_n$ Found: C, 77.68; H, 7.03; N, 4.45; S, 10.29; Br, 1.67.

Poly[3,4-didodecylthiophene-2,5-diylethynylene-(2,3-diphenylthieno[3,4-*b*]pyrazine-5,7-diyl)ethynylene] (P-9). 5,7-Dibromo-2,3-diphenylthieno[3,4-*b*]pyrazine **M14** 476 mg (1.066 mmol), 2,5-diethynyl-3,4-didodecylthiophene **M2** 500 mg (1.066 mmol). Yield: 0.7 g (87%) blue polymer. $^1\text{H NMR}$ (250 MHz, CDCl_3): $\delta = 7.37\text{--}7.06$ (m, 10H), 2.63 (m, 4H), 1.48-0.64 (m, 46H). $^{13}\text{C NMR}$ (62 MHz, CDCl_3): $\delta = 154.05, 148.32, 142.86, 138.74, 130.06, 129.20, 128.04, 120.11, 115.50, 95.24, 89.19, (-\text{C}\equiv\text{C}-), 31.92, 30.24, 29.68, 29.37, 28.82, 22.69, 14.13$. **GPC** (Polystyrene standards): $\bar{M}_w = 22700$ g/mol, $\bar{M}_n = 14000$; PDI = 1.62; $\bar{P}_n = 19$. **UV-Vis** (Chloroform): $\lambda_{\text{max}}/\text{nm}$ ($\epsilon/(1 \cdot \text{mol}^{-1} \cdot \text{cm}^{-1})$) 265 (43800), 388 (44600), 628 (44000).

$(\text{C}_{50}\text{H}_{60}\text{N}_2\text{S}_2)_n$ Calculated: C, 79.74; H, 8.03; N, 3.72; S, 8.51.
(753.17) $_n$ Found: C, 79.32; H, 8.21; N, 3.58; S, 8.20; Br, 1.78.

Poly[1,4-didodecyloxyphenylene-2,5-diylethynylene-(2,3-diphenylthieno[3,4-*b*]pyrazine-5,7-diyl)ethynylene] (P-10). 5,7-Dibromo-2,3-diphenylthieno[3,4-*b*]pyrazine **M14** 476 mg (1.066 mmol), 2,5-diethynyl-1,4-didodecyloxyphenylene **M4** 527 mg (1.066 mmol). Yield: 0.65 g (78%) blue polymer. $^1\text{H NMR}$ (400 MHz, CDCl_3): $\delta = 7.57\text{--}7.50$ (m, 8H), 7.4-7.3 (m, 2H), 7.02 (s, 2H), 4.06 (t, 4H)- OCH_2 -, 2.34-1.21 (m, 40H), 0.84 (t, 6H). $^{13}\text{C NMR}$ (400 MHz, CDCl_3): $\delta = 154.00, 153.78, 142.59, 138.78, 130.02, 129.03, 127.92, 116.58, 116.18, 114.15, 98.31, 87.42, (-\text{C}\equiv\text{C}-), 69.76, 31.83, 29.57, 29.27, 29.23, 29.15, 25.91, 22.60, 14.03$. **GPC** (Polystyrene standards): $\bar{M}_w = 27000$ g/mol, $\bar{M}_n = 5600$; PDI = 4.81; $\bar{P}_n = 7$. **UV-Vis** (Chloroform): $\lambda_{\text{max}}/\text{nm}$ ($\epsilon/(1 \cdot \text{mol}^{-1} \cdot \text{cm}^{-1})$) 380 (44200), 605 (44000).

$(\text{C}_{52}\text{H}_{62}\text{N}_2\text{O}_2\text{S}_2)_n$ Calculated: C, 80.16; H, 8.02; N, 3.60; S, 4.12.
(779.14) $_n$ Found: C, 79.80; H, 8.40; N, 3.39; S, 3.72; Br, 1.01.

Poly[3-dodecylthiophene-2,5-diylethynylene-(1,2-Bis(*p*-phenyl)-1-cyanovinylene-4,4'-diyl)ethynylene] (P-11). 1,2-Bis(4-bromophenyl)-1-cyanovinylene **M10** 387 mg (1.066 mmol), 2,5-diethynyl-3-dodecylthiophene **M1** 320 mg (1.066 mmol). Yield: 0.385 g (72%) red polymer. $^1\text{H NMR}$ (400 MHz, CDCl_3): $\delta = 7.91$ (s, 1H), 7.77-7.50 (m, 8H), 7.13 (s, 1H of thiophene), 2.76 (m, 2H), 1.69-0.89 (m, 23H). $^{13}\text{C NMR}$ (400 MHz, CDCl_3): $\delta = 141.25, 133.31, 132.31, 131.75, 130.73, 129.35, 127.49, 125.94, 117.46, 89.19, 87.12, (-\text{C}\equiv\text{C}-), 31.91, 30.11, 29.70, 29.36, 22.69, 14.11$. **GPC** (Polystyrene standards): $\bar{M}_w = 15000$ g/mol, $\bar{M}_n = 4100$; PDI = 3.63; $\bar{P}_n = 8$. **UV-Vis** (Chloroform): $\lambda_{\text{max}}/\text{nm}$ ($\epsilon/(1 \cdot \text{mol}^{-1} \cdot \text{cm}^{-1})$) 421 (45200).

$(\text{C}_{35}\text{H}_{35}\text{NS})_n$ Calculated: C, 83.79; H, 7.03; N, 2.79; S, 6.39.
(501.74) $_n$ Found: C, 83.12; H, 7.41; N, 2.35; S, 6.15; Br, 2.02.

Poly[3-dodecylthiophene-2,5-diylethynylene3-(2,5-dioctyloxyphenyl)-2-(*p*-phenyl)-acrylonitrile-4,4'-diyl)ethynylene] (P-12). 3-(4-Bromo-2,5-dioctyloxyphenyl)-2-(4-bromophenyl)-acrylonitrile **M11** 660 mg (1.066 mmol), 2,5-diethynyl-3-dodecylthiophene **M1** 320 mg (1.066 mmol). Yield: 0.51 g (63%) red polymer. **GPC** (Polystyrene standards): $\bar{M}_w = 8200$ g/mol, $\bar{M}_n = 3200$; PDI = 2.54; $\bar{P}_n = 4$. **UV-Vis** (Chloroform): λ_{\max}/nm ($\epsilon/(1 \cdot \text{mol}^{-1} \cdot \text{cm}^{-1})$) 255 (43000), 452 (44000).

(C₅₁H₆₇NO₂S)_n Calculated: C, 80.80; H, 8.91; N, 1.85; S, 4.23.

(758.16)_n Found: C, 80.24; H, 9.05; N, 1.67; S, 4.10; Br, 1.12.

Poly[3,4-didodecylthiophene-2,5-diylethynylene-(2-cyano-2-phenylvinyl)-phenyl]-2-phenylacrylonitrile-2,5-diyl)ethynylene] (P-13). 3-[2,5-Dibromo-4-(2-cyano-2-phenylvinyl)-phenyl]-2-phenylacrylonitrile **M12** 523 mg (1.066 mmol), 2,5-diethynyl-3,4-didodecylthiophene **M2** 500 mg (1.066 mmol). Yield: 0.5 g (59%) red polymer. **¹H NMR** (400 MHz, CDCl₃): $\delta = 8.62$ -8.52 (s, 2H), 8.30-8.04 (m, 4H), 7.83-7.39 (m, 8H), 2.67 (m, 2H), 1.54-0.86 (m, 23H). **¹³C NMR** (400 MHz, CDCl₃): $\delta = 138.66$, 137.73, 135.82, 133.86, 131.09, 130.14, 129.29, 126.31, 117.06, 93.66, 91.72, (-C≡C-), 31.92, 30.17, 29.69, 29.65, 29.36, 28.86, 22.68, 14.10. **GPC** (Polystyrene standards): $\bar{M}_w = 19100$ g/mol, $\bar{M}_n = 6600$; PDI = 2.88; $\bar{P}_n = 8$. **UV-Vis** (Chloroform): λ_{\max}/nm ($\epsilon/(1 \cdot \text{mol}^{-1} \cdot \text{cm}^{-1})$) 265 (43800), 373 (45900), 480 (43000).

(C₅₀H₆₀N₂S₂)_n Calculated: C, 84.37; H, 8.09; N, 3.51; S, 4.02.

(797.20)_n Found: C, 83.82; H, 8.27; N, 3.12; S, 3.71; Br, 2.08.

General Procedure for Polymerization (Suzuki Coupling). Under an argon atmosphere, dibromo monomers (**M7**, **M9**, **M13**, **M14**) (1 mmol) and dioxaborolane monomer (**M15**, **M16**) (1 mmol) were mixed together with 1.0-1.5% (0.015 mmol) of Pd(PPh₃)₄ in a small flask. Degassed aqueous solution of potassium carbonate 12 mL (2.0 M) and toluene 36 mL (1:3, volume ratio) were added to the flask. The mixture was stirred vigorously at 80-90 °C for 72h under an argon atmosphere. The resulting solution was added dropwise into stirring methanol to precipitate the polymer. The fibrous solid was collected by filtration and washed with methanol and water. The material was washed continuously with methanol and acetone for 2 days in a Soxhlet extractor to remove the oligomers and catalyst residues. The product was dried under reduced pressure overnight.

Copoly(2,3-diphenylthieno[3,4-*b*]pyrazine-*alt*-9,9-didecylfluorene) (P-14). 5,7-Dibromo-2,3-diphenylthieno[3,4-*b*]pyrazine **M14** 446 mg (1 mmol), 2,7-dioxaborolan-9,9-

didecylfluorene **M15** 586 mg (1 mmol). Yield: 0.6 g (82%) blue polymer. $^1\text{H NMR}$ (400 MHz, CDCl_3): $\delta = 8.50\text{-}7.86$ (m, 6H), $7.67\text{-}7.37$ (m, 10H), $2.18\text{-}0.76$ (m, 42H). $^{13}\text{C NMR}$ (400 MHz, CDCl_3): $\delta = 152.20, 151.85, 140.53, 139.54, 138.93, 132.53, 131.95, 129.95, 128.89, 128.09, 126.90, 122.50, 120.31, 55.47, 40.64, 31.84, 30.19, 29.62, 29.51, 29.28, 23.98, 22.61, 14.06$. **GPC** (Polystyrene standards): $\bar{M}_w = 52800$ g/mol, $\bar{M}_n = 13100$; PDI = 4.02; $\bar{P}_n = 18$. **UV-Vis** (Toluene): $\lambda_{\text{max}}/\text{nm}$ ($\epsilon/(1 \cdot \text{mol}^{-1} \cdot \text{cm}^{-1})$) 346 (44000), 377 (44700), 628 (43000).

$(\text{C}_{51}\text{H}_{58}\text{N}_2\text{S})_n$ Calculated: C, 83.79; H, 8.00; N, 3.83; S, 4.39.
(731.10)_n Found: C, 83.12; H, 8.15; N, 3.55; S, 4.04; Br, 0.88.

Copoly(thieno[3,4-*b*]pyrazine-*alt*-9,9-didecylfluorene) (P-15). 5,7-Dibromo-thieno[3,4-*b*]pyrazine **M13** 294 mg (1 mmol), 2,7-dioxaborolan-9,9-didecylfluorene **M15** 586 mg (1 mmol). Yield: 0.5 g (87%) blue polymer. $^1\text{H NMR}$ (250 MHz, CDCl_3): $\delta = 8.58$ (s, 2H), $8.32\text{-}7.85$ (m, 6H), 2.18 (m, 4H), $1.12\text{-}0.76$ (m, 38H). $^{13}\text{C NMR}$ (62 MHz, CDCl_3): $\delta = 151.98, 144.07, 140.63, 140.44, 132.76, 132.17, 127.26, 122.45, 120.36, 55.55, 40.34, 31.84, 30.06, 29.56, 29.26, 23.93, 22.61, 14.05$. **GPC** (Polystyrene standards): $\bar{M}_w = 9700$ g/mol, $\bar{M}_n = 5700$; PDI = 1.70; $\bar{P}_n = 10$. **UV-Vis** (Toluene): $\lambda_{\text{max}}/\text{nm}$ ($\epsilon/(1 \cdot \text{mol}^{-1} \cdot \text{cm}^{-1})$) 378 (43300), 573 (43100).

$(\text{C}_{39}\text{H}_{50}\text{N}_2\text{S})_n$ Calculated: C, 80.92; H, 8.71; N, 4.84; S, 5.54.
(578.90)_n Found: C, 80.18; H, 9.06; N, 4.44; S, 4.98; Br, 1.21.

Copoly(2,3-diphenylthieno[3,4-*b*]pyrazine-*alt*-9,9-didecylfluorene-*alt*-3,4-ethylenedioxythiophene) (P-16). 5,7-Dibromo-2,3-diphenylthieno[3,4-*b*]pyrazine **M14** 223 mg (0.5 mmol), 2,7-dioxaborolan-9,9-didecylfluorene **M15** 586 mg (1 mmol) and 2,5-dibromo-3,4-ethylenedioxythiophene¹⁶⁵ **DBEDOT** 150 mg (0.5 mmol). Yield: 0.52 g (87%) blue polymer. $^1\text{H NMR}$ (250 MHz, CDCl_3): $\delta = 8.49\text{-}7.85$ (m, 6H), $7.66\text{-}7.38$ (m, 10H), 4.45 and 4.35 (s, 4H), 2.16 (m, 4H), $1.58\text{-}0.76$ (m, 38H). $^{13}\text{C NMR}$ (62 MHz, CDCl_3): $\delta = 152.22, 151.90, 140.52, 139.53, 138.92, 132.54, 131.95, 129.94, 128.87, 128.07, 126.91, 126.82, 122.45, 120.29, 55.46, 40.66, 40.49, 31.84, 30.21, 30.12, 29.61, 29.50, 29.27, 23.96, 23.86, 22.62, 14.06$. **GPC** (Polystyrene standards): $\bar{M}_w = 8300$ g/mol, $\bar{M}_n = 4700$; PDI = 1.75; $\bar{P}_n = 7$. **UV-Vis** (Toluene): $\lambda_{\text{max}}/\text{nm}$ ($\epsilon/(1 \cdot \text{mol}^{-1} \cdot \text{cm}^{-1})$) 368 (44000), 584 (41000).

$(\text{C}_{39}\text{H}_{52}\text{O}_2\text{S})_{0.5n}$ (584.91)_{0.5n} , $(\text{C}_{51}\text{H}_{58}\text{N}_2\text{S})_{0.5n}$ (731.10)_{0.5n}
Calculated: C, 82.14; H, 8.42; N, 2.13; S, 4.87.
Found: C, 80.98; H, 8.08; N, 2.10; S, 4.17; Br, 1.13.

Oligo(2,3-diphenylthieno[3,4-*b*]pyrazine-*alt*-2,5-didodecyloxyphenylene) (P-17). 5,7-Dibromo-2,3-diphenylthieno[3,4-*b*]pyrazine **M14** 446 mg (1 mmol), 1,4-bis[4,4,5,5-tetramethyl-(1,3,2)-dioxaborolan-2-yl]-2,5-didodecyloxyphenylene **M16** 699 mg (1 mmol). Yield: 0.46 g (61%) blue oligomer. $^1\text{H NMR}$ (250 MHz, CDCl_3): $\delta = 7.51\text{--}7.32$ (m, 10H), 6.77 (s, 2H) 4.03 (t, 4H), 1.83-0.74 (m, 46H). $^{13}\text{C NMR}$ (62 MHz, CDCl_3): $\delta = 153.22, 151.12, 149.71, 149.07, 139.82, 138.26, 131.96, 131.57, 129.90, 128.38, 127.84, 127.42, 123.01, 121.03, 117.64, 115.76, 114.02, 69.89, 68.52, 32.27, 31.91, 30.28, 29.64, 29.35, 26.20, 22.67, 14.08$. **GPC** (Polystyrene standards): $\bar{M}_w = 1850$ g/mol, $\bar{M}_n = 1740$; PDI = 1.06; $\bar{P}_n = 2.5$. **UV-Vis** (Chloroform): $\lambda_{\text{max}}/\text{nm}$ ($\epsilon/(1 \cdot \text{mol}^{-1} \cdot \text{cm}^{-1})$) 344 (41400), 534 (35000).

$(\text{C}_{48}\text{H}_{62}\text{N}_2\text{O}_2\text{S})_n$ Calculated: C, 78.86; H, 8.55; N, 3.83; S, 4.39.
(731.10)_n Found: C, 76.42; H, 9.52; N, 2.19; S, 2.42; Br, 4.21.

Copoly[2,3-diphenylquinoxaline-*alt*-9,9-didecylfluorene) (P-18). 5,8-Dibromo-2,3-diphenylquinoxaline **M7** 440 mg (1 mmol), 2,7-dioxaborolan-9,9-didecylfluorene **M15** 586 mg (1 mmol). Yield: 0.44 g (61%) yellow polymer. $^1\text{H NMR}$ (250 MHz, CDCl_3): $\delta = 7.37\text{--}7.06$ (m, 10H), 2.63 (m, 4H), 1.48-0.64 (m, 46H). $^{13}\text{C NMR}$ (62 MHz, CDCl_3): $\delta = 154.05, 148.32, 142.86, 138.74, 130.06, 129.20, 128.04, 120.11, 115.50, 95.24, 89.19, 31.92, 30.24, 29.68, 29.37, 28.82, 22.69, 14.13$. **GPC** (Polystyrene standards): $\bar{M}_w = 7000$ g/mol, $\bar{M}_n = 4400$; PDI = 1.60; $\bar{P}_n = 6$. **UV-Vis** (Chloroform): $\lambda_{\text{max}}/\text{nm}$ ($\epsilon/(1 \cdot \text{mol}^{-1} \cdot \text{cm}^{-1})$) 311 (43300), 325 (43000), 419 (40000).

$(\text{C}_{53}\text{H}_{60}\text{N}_2)_n$ Calculated: C, 87.80; H, 8.34; N, 3.86.
(725.07)_n Found: C, 87.32; H, 8.47; N, 3.52; Br, 1.52.

Copoly(dibenzo[a,c]phenazine-*alt*-9,9-didecylfluorene) (P-19). 10,13-Dibromodibenzo[a,c]phenazine **M9** 442 mg (1 mmol), 2,7-dioxaborolan-9,9-didecylfluorene **M15** 586 mg (1 mmol). Yield: 0.47 g (65%) yellow polymer. $^1\text{H NMR}$ (250 MHz, CDCl_3): $\delta = 7.37\text{--}7.06$ (m, 10H), 2.63 (m, 4H), 1.48-0.64 (m, 46H). $^{13}\text{C NMR}$ (62 MHz, CDCl_3): $\delta = 154.05, 148.32, 142.86, 138.74, 130.06, 129.20, 128.04, 120.11, 115.50, 95.24, 89.19, 31.92, 30.24, 29.68, 29.37, 28.82, 22.69, 14.13$. **GPC** (Polystyrene standards): $\bar{M}_w = 17600$ g/mol, $\bar{M}_n = 8800$; PDI = 2.0; $\bar{P}_n = 12$. **UV-Vis** (Chloroform): $\lambda_{\text{max}}/\text{nm}$ ($\epsilon/(1 \cdot \text{mol}^{-1} \cdot \text{cm}^{-1})$) 255 (48000), 313 (42000), 380 (42000), 400 (43000), 450 (42000).

$(\text{C}_{53}\text{H}_{58}\text{N}_2)_n$ Calculated: C, 88.04; H, 8.09; N, 3.87.
(723.06)_n Found: C, 87.62; H, 8.31; N, 3.54; Br, 1.13.

5 Zusammenfassung in Thesen

π -Konjugierte Polymere besitzen aufgrund ihrer elektronischen Struktur eine einzigartige Kombination von Eigenschaften: die elektronischen und optischen Eigenschaften von Metallen und Halbleitern in Kombination mit den vorteilhaften Verarbeitungsmöglichkeiten und mechanischen Eigenschaften von Polymeren. In den vergangenen 10 bis 20 Jahren sind effektive Synthesen zur Herstellung dieser halbleitenden Polymere hoher Reinheit erarbeitet worden und so sind konjugierte Polymere jetzt verfügbar für die Verwendung in "plastic electronic" devices. Das schließt Dioden, photovoltaische Zellen, Sensoren, lichtemittierende Dioden, Laser, Feldeffekt Transistoren und polymerintegrierte Schaltungen ein.

Für ihren Einsatz in photo-optischen Anwendungen z.B. Solarzellen oder OLEDs sind vom chemischen Gesichtspunkt betrachtet u.a. folgende Aspekte wesentlich: Oxidations- und Reduktionspotential, Absorptionsspektren, Filmbildung aus Lösung, thermische Stabilität und darüber hinaus hohe h^+/e^- Ladungsträgerbeweglichkeiten. Für die Herstellung optisch transparenter Filme sind hohe Molekulargewichte erforderlich.

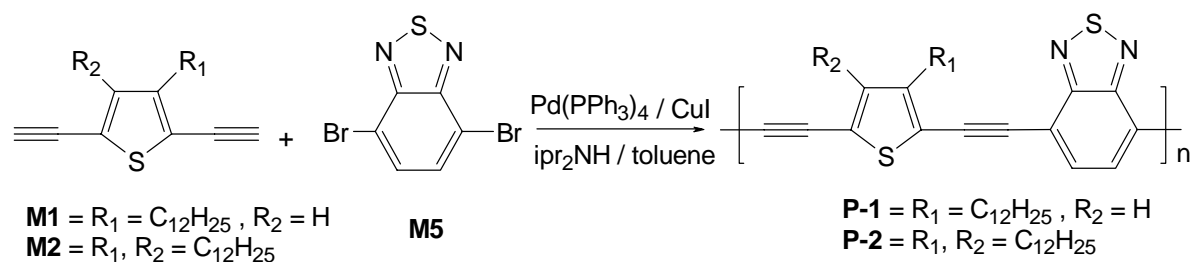
Die Entwicklung neuer Polyheteroarylene und Polyheteroarylenethinylene für Polymersolarzellen zielte darauf ab, lösliche Polymere mit relativ niedriger Bandgap-Energie ($<2,0$ eV) und langwelliger Lichtabsorption (> 550 nm) zu synthetisieren, die oxidationsstabil sind. Es sollten Zusammenhänge zwischen diesen Eigenschaften und der Primärstruktur der Polymere studiert werden.

Derartige Polymere können mittels Übergangsmetall-katalysierten C-C-Kopplungsmethoden synthetisiert werden. Im Rahmen dieser Arbeit ist das Donor/Akzeptor Konzept zur Verifizierung der genannten Eigenschaften angewendet worden. Als Donor-Komponente wurde im wesentlichen Thiophen (substituiert) verwendet und als Akzeptoren N-Heterocyclen.

I. Polyheteroarylenethinylene mit Thiophen als Donator und nachfolgenden Heterocyclen als Akzeptor

2,1,3-Benzothiadiazol als Akzeptor

Die 2,1,3-Benzothiadiazol-enthaltenden Polymere P -1 und P -2 sind in Ausbeuten von etwa 80 % nach Sonogashira erhältlich, P_n beträgt 14 (P-1) bzw. 27 (P-2).

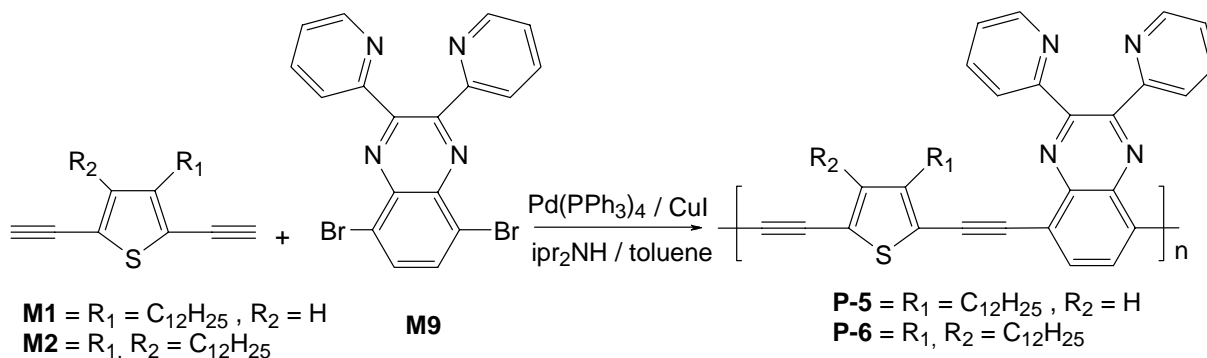


Schema 5.1. Synthesis of Polymers **P-1** and **P-2**.

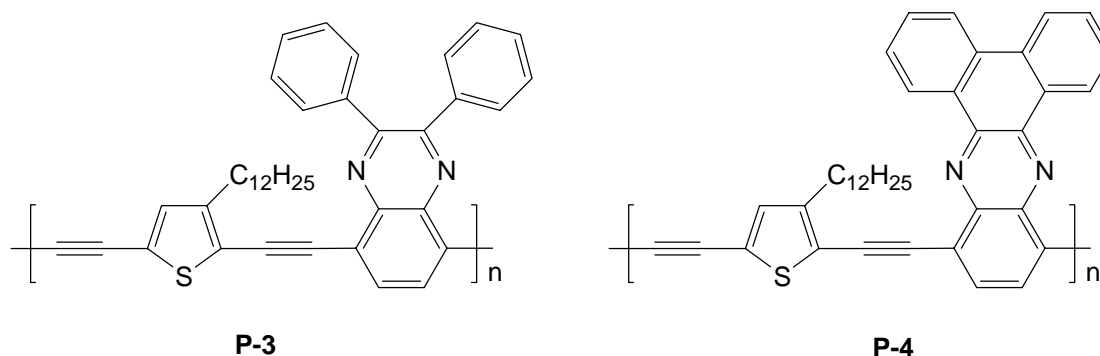
Das Polymer P-2 mit 3,5-Dialkyl-substituierter Thiophenstruktur absorbiert sowohl in Lösung als auch im Festkörper deutlich langwelliger (540, 599 nm) als P-1 mit nur einem Alkylsubstituenten (504 nm). Die Polymere zeigen in $\text{CHCl}_3/\text{MeOH}$ Aggregation (rot Verschiebung von λ_{max}). Beide Polymere besitzen zwei reversible Reduktionspeak Potentiale (P-1: $E_{\text{red}} = -0,87, -1,23 \text{ V vs Ag/Ag}^+$, P-2: $E_{\text{red}} = -1,04, -1,47 \text{ V vs Ag/Ag}^+$). Die Oxidation ist irreversibel. $E_{\text{g}}^{\text{opt}}$ 2,0 eV (Lsg.) 1,85 eV (Film) P-2.

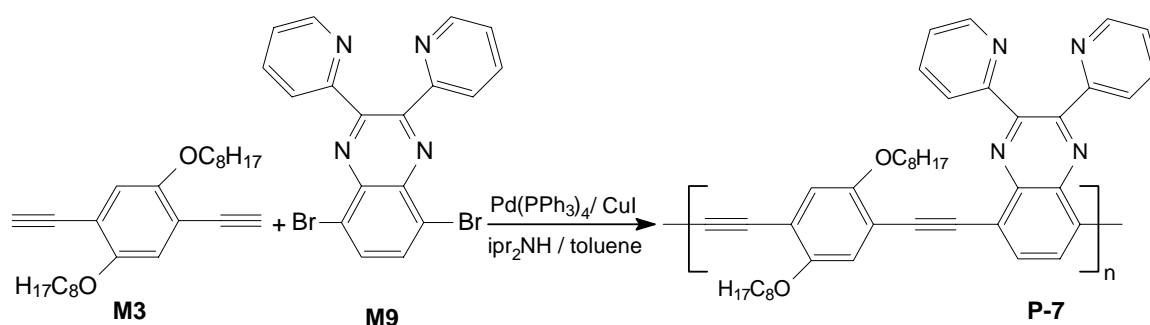
Chinoxalin (Phenazin) als Akzeptor

Alternierende Chinoxalin- (Phenazin) Thiophen enthaltende Akzeptor-Donator Copolymere P-3, P-5 und P-6 (P-4) lassen sich entsprechend nachfolgender Gleichungen in etwa 75 %igen Ausbeuten erhalten.



Schema 5.2. Synthesis of Polymers **P-5** and **P-6**.





Schema 5.3. Synthesis of Polymer **P-7**.

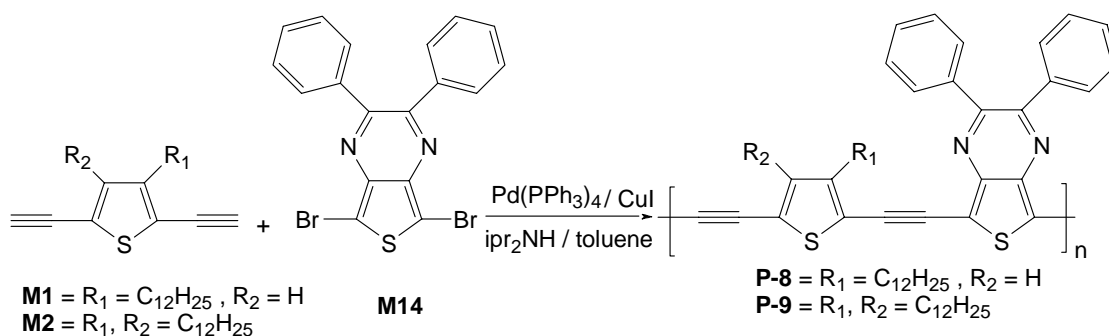
Die tiefroten Polymere sind in den gebräuchlichen organischen Lösungsmitteln löslich, ihre Struktur ist durch NMR und Elementaranalyse gesichert. Die zahlenmittleren Molmassen betragen für P-5 7700 g/mol ($P_n = 13$) und 16400 g/mol ($P_n = 22$) für P-6. Die mittels GPC- und VPO-bestimmten Werte zeigen weitgehende Übereinstimmung. In den optischen Eigenschaften (λ_{\max} , E_g^{opt}) unterscheidet sich das Polymer P-5 nicht wesentlich von dem des Polymer P-1. Dagegen absorbiert P-6 deutlich kürzerwellig als P-2 (Benzothiadiazol als Akzeptor). Wird die Planarität des Akzeptorheterocyclus erhöht, wie in P-4 mit Phenazin, so sind die optischen Eigenschaften nahezu identisch mit denen von P-1, mit Benzothiadiazol-Akzeptor.

Sämtliche Polymere diesen Typs aggregieren, wenn zur Polymerlösung Methanol hinzugefügt wird.

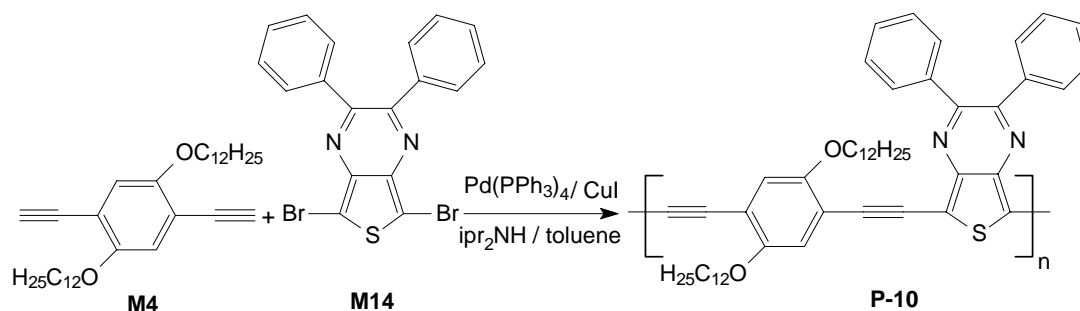
Die elektrochemische Oxidation und Reduktion in Acetonitril gegen Ag/AgCl ergab ein Oxidationspotential ($E_{\text{ox}} = 1,4$ V für P-3, P-5, P-6) und ein Reduktionspotential ($E_{\text{red}} = -1,3$ V), wobei die Reduktion reversibel ist. P-3 und P-6 zeigen noch ein zweites Reduktionspotential bei $-1,84$ und $-1,78$ V, was bedeuten kann, dass zuerst nur jede zweite Chinoxalin-Einheit reduziert wird und dann im nachfolgenden Schritt die übrigen Chinoxalin-Einheiten.

Thieno[3.4-b]pyrazine als Akzeptor

Copolymere diesen Typs konnten gleichfalls unter Sonogashira Bedingungen in 70-80%iger Ausbeute synthetisiert werden



Schema 5.4. Synthesis of Polymers **P-8** and **P-9**.



Schema 5.5. Synthesis of Polymer **P-10**.

Die Copolymere P-8 und P-9 ($\bar{M}_n = 10900$ g/mol entsprechen $P_n = 19$ und $\bar{M}_n = 14000$ g/mol entsprechend $P_n = 19$) sind tiefblau, löslich und filmbildend; die Copolymere P-8 und P-9 sind bisher noch nicht in der Literatur beschrieben.

Die optischen Eigenschaften sind in nachfolgender Übersicht angegeben.

Table 5.1. UV-Vis Data of polymers **P-8-P-10** in Dilute Toluene Solution and in Solid State (Thin Films of 100-150 nm Thickness Spin-Casted from Chlorobenzene Solution).

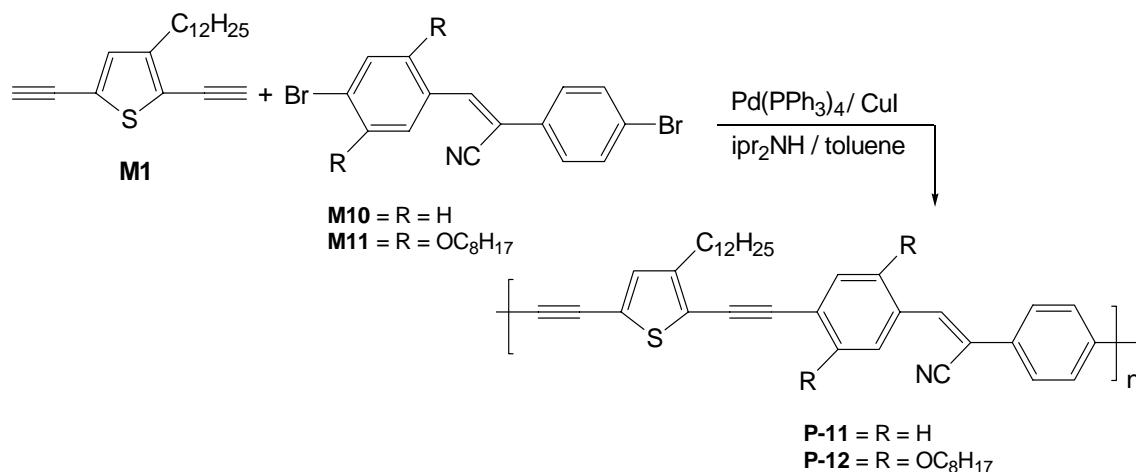
Polymer	UV-vis λ_{max} , nm				E_g opt. eV ^c	
	Toluene [log ϵ] ^a	$\lambda_{0.1\text{max}}$	film ^b	$\lambda_{0.1\text{max}}$	Toluene	film
P-8	588 [4.2]	736	646	775	1.68	1.60
P-9	628 [4.4]	740	650	790	1.67	1.57
P-10	605 [4.4]	677	694	790	1.83	1.57

^aMolar absorption coefficient. Molarity is based on the repeating unit. ^bSpin coated from chlorobenzene solution. ^c E_g opt. = $hc / \lambda_{0.1\text{max}}$.

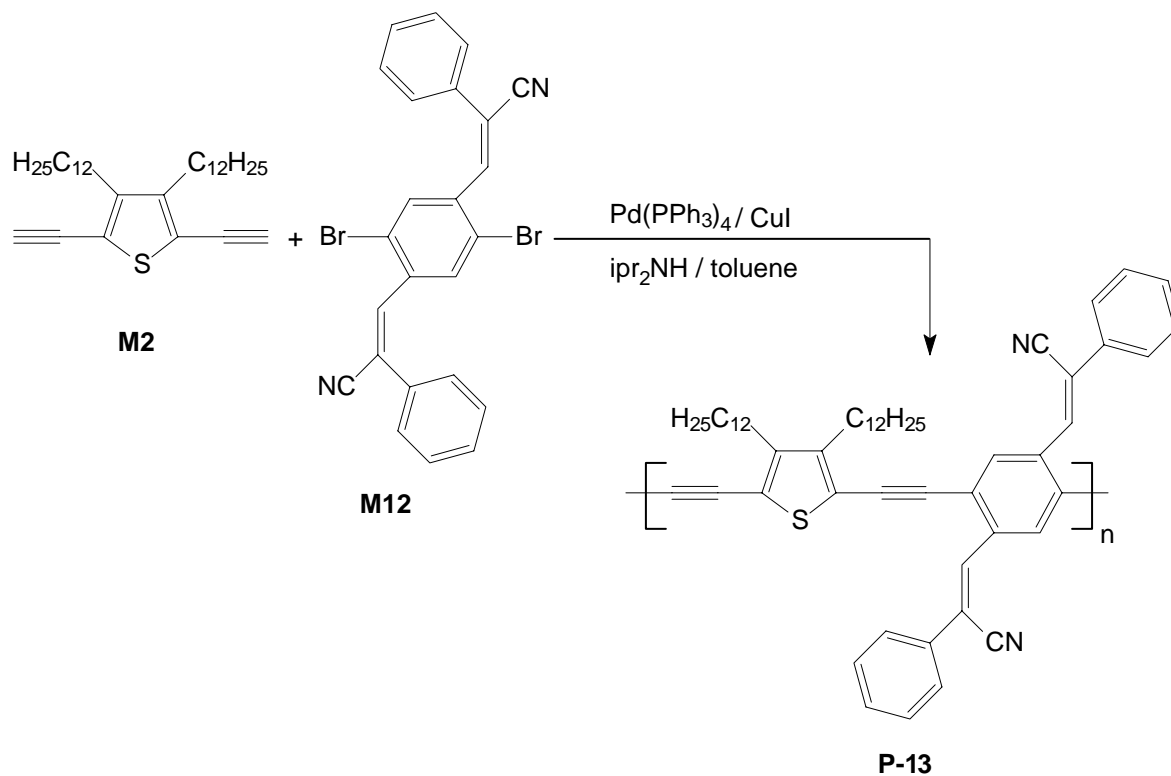
Wie bereits für die vorhergehenden Copolymere beschrieben, tritt auch bei den Thieno[3,4-*b*]pyrazin enthaltenden Copolymeren Assoziation aus Lösung auf (Zugabe von Methanol zur Polymerlösung in Chloroform).

Die Bandgap-Energie, elektrochemisch bestimmt, beträgt 1.86 eV (P-9) und 1.99 eV (P-10); E_g^{opt} beträgt für beide Polymere 1.57 eV.

Cyanostilben als Akzeptor



Schema 5.6. Synthesis of Polymers **P-11** and **P-12**.



Schema 5.7. Synthesis of Polymer **P-13**.

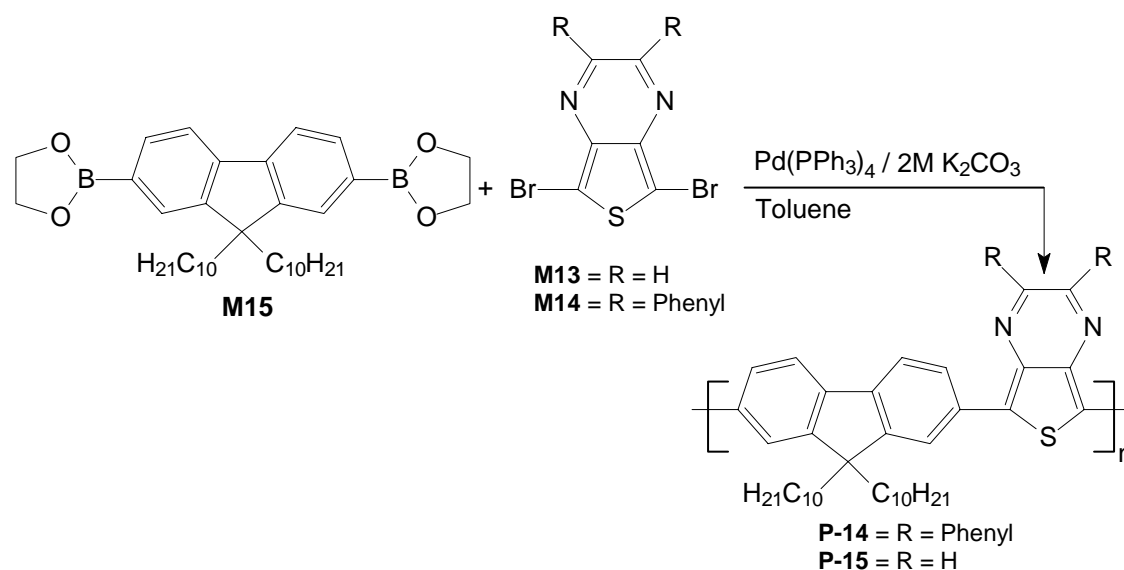
(Polymer P-12 trägt zwei *n*-Octyloxy-Gruppen im Phenylenring)

Im Unterschied zu den bisher genannten D/A-Copolymeren sind die Absorptionsmaxima in Lösung und im Festkörper (Film) praktisch identisch. Sie zeigen einen vergleichsweise großen Stokes-Shift (220 nm). Die Molmassen sind niedrig (4100 g/Mol, 6600 g/Mol für P-11 und P-13, entsprechend $P_n = 8$).

Die Polymere unterscheiden sich in den optischen und elektronischen Eigenschaften deutlich. P-11 absorbiert langwelliger (421 nm) als P-13 (373 nm), die Bandgap-Energie für P-11 beträgt 1.69 eV, für P-13 ist sie 1.90 eV. Das legt den Schluss nahe, dass der elektronische Einfluss der Akzeptorgruppe in der Hauptkette größer ist, als in der Seitengruppe.

II. Polyheteroarylen Copolymere

Polyfluoren und seine Copolymere sind umfassend aus der Literatur bekannt. Sie werden insbesondere wegen ihrer hohen Fluoreszenzquantenausbeute in Lösung und im Festkörper untersucht. Als Comonomere in Suzuki-Kopplungen wurden insbesondere Thiophen, Ethylendioxythiophen und Benzothiadiazol verwendet. Copolymere mit Thieno[3,4,b]pyrazin sind bisher noch nicht bekannt. Sie lassen sich entsprechend nachfolgender Gleichung in 82-87%iger Ausbeute synthetisieren.



Schema 5.8. Synthesis of Polymers **P-14** and **P-15** .

Phenylsubstitution im Thienopyrazin (P-14) führt zu einer Rot-Verschiebung der langwelligen Absorption ($\lambda_{\text{max}} = 628$ nm für P-14, 573 nm für P-15) in Lösung und im Festkörper (Film).

λ_{max} in Lösung und im Film sind praktisch identisch. $E_{\text{g}}^{\text{opt}} = 1.82$ eV (P-14) und 1.86 eV (P-15) in Lösung und im Film beträgt sie 1.76 bzw. 1.78 eV.

Das statistische Copolymer mit EDOT (P-16) zeigt im Vergleich zum alt.-Copolymer P-14 ein kürzerwelliges Absorptionsmaximum (584 nm) und einen höheren Wert für E_g^{opt} (1,85 eV gegenüber 1.82 eV).

Die Polymere P-14, P-15 und P-16 werden in Lösung und im Film photochemisch, besonders in Anwesenheit von Sauerstoff irreversibel oxidiert. Dabei ist im FT-IR Spektrum ein Carbonyl-Peak bei 1655 cm^{-1} nachweisbar. Das unterscheidet die Polymere sehr deutlich von den entsprechenden Heteroarylenethynylenen, die unter diesen Bedingungen stabil sind.

Die Chinoxalin bzw. Phenazin/Dialkylfluoren Copolymere sind in etwa 60proz. Ausbeute herstellbar. Sie zeigen das zu erwartende Eigenschaftsprofil: thermische Stabilität, Assoziation aus Lösung, reversible elektrochemische Reduktion.

Aus einer 1;1 Lösung der Polymere P-14 und P-19 lassen sich Filme (Blends) herstellen. Photolumineszenz-Messungen zeigen einen photoinduzierten Charge-Transfer; es tritt Lumineszenz-Löschung von P-14 auf.

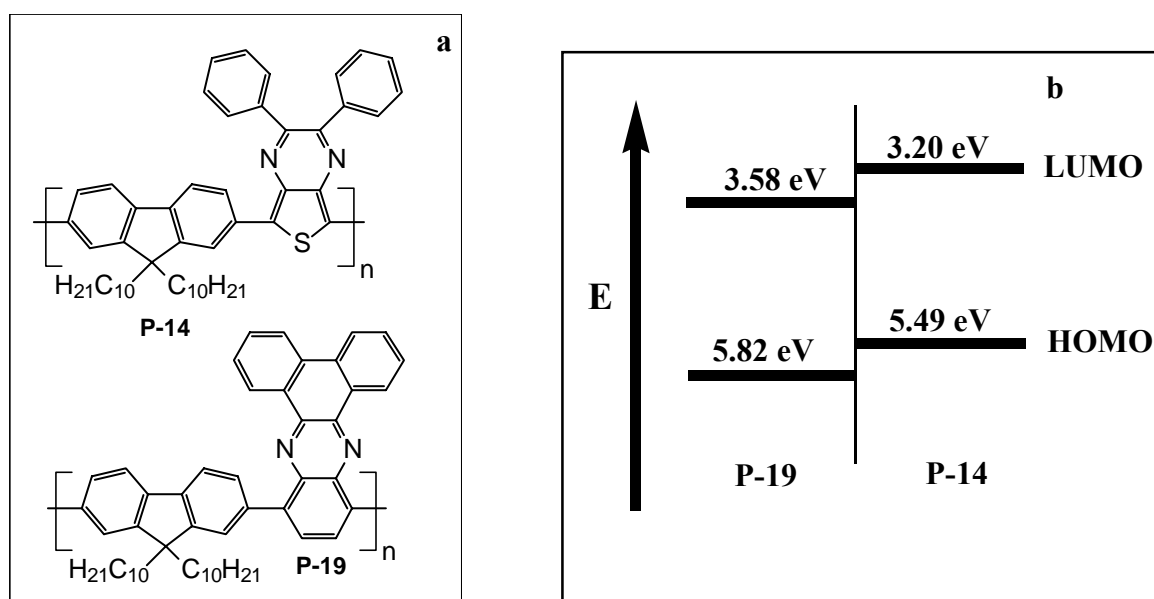


Figure 5.1. (a) Chemical structures and (b) HOMO/LUMO energy level diagram of polymers P-14 and P-19.

6 References

- (1) Skotheim, T. A.; Elsenbaumer, R. L.; Reynolds, J.; Eds. *Handbook of Conducting Polymers*, 2nd ed.; Marcel Dekker: New York, **1998**.
- (2) Kraft, A.; Grimsdale, A. C.; Holmes, A. B. *Angew. Chem.* **1998**, *37*, 402.
- (3) Hide, F.; Diaz-Garcia, M. A.; Schwartz, B. J.; Heeger, A. J. *Acc. Chem. Res.* **1997**, *30*, 430.
- (4) Yu, G.; Gao, J.; Hummelen, J. C.; Wudl, F.; Heeger, A. J. *Science* **1995**, *270*, 1789.
- (5) (a) Jenekhe, S. A.; Osaheni, J. A. *Science* **1994**, *265*, 765. (b) Brédas, J. L.; Beljonne, D.; Coropceanu, V.; Cornil, J. *Chem. Rev.* **2004**, *104*, 4971.
- (6) Ball, P. *Made to Measure: New Materials for the 21st Century*; Princeton University Press: Princeton, NJ, **1997**.
- (7) (a) Seminario, J. M.; Zacarias, A. G.; Tour, J. M. *J. Am. Chem. Soc.* **1999**, *121*, 411. (b) Tour, J. M.; Kozaki, M.; Seminario, J. M. *J. Am. Chem. Soc.* **1998**, *120*, 8486.
- (8) Chang, S. C.; Liu, J.; Bharathan, J.; Yang, Y.; Onohara, J.; Kido, J. *Adv. Mater.* **1997**, *11*, 734.
- (9) Sensors Special Issue. *Acc. Chem. Res.* **1998**, *31* (5).
- (10) Chiang, C. K.; Park, Y. W.; Heeger, A. J.; Shirakawa, H.; Louis, E. J.; MacDiarmid, A. G. *Phys. Rev. Lett.* **1977**, *39*, 1098.
- (11) Roncali, J. *Chem. Rev.* **1992**, *92*, 711.
- (12) Mertz, A. *Topics in Current Chemistry*; Springer-Verlag: Berlin, **1990**, *152*, 49.
- (13) Deronzier, A.; Moutet, J. C. *Acc. Chem. Res.* **1989**, *22*, 249.
- (14) Burroughes, J. H.; Bradley, D. D. C.; Brown, A. R.; Marks, R. N.; Mackay, K.; Friend, R. H.; Burns, P. L.; Holmes, A. *Nature* **1990**, *347*, 539.
- (15) (a) Enkelmann, V. *Adv. Polym. Sci.* **1984**, *63*, 91. (b) Wegner, G. *Z. Naturforsch.* **1969**, *24B*, 824.
- (16) Scherf, U. *Top. Curr. Chem.* **1999**, *201*, 163.
- (17) (a) Schlüter, A. D.; Wegner, G. *Acta Polym.* **1993**, *44*, 59. (b) Schlüter, A. D. *Adv. Mater.* **1991**, *3*, 282.
- (18) (a) Gorman, C. B.; Ginsburg, E. J.; Grubbs, R. H. *J. Am. Chem. Soc.* **1993**, *115*, 1397. (b) Sailor, M. J.; Ginsburg, E. J.; Gorman, C. B.; Kumar, A.; Grubbs, R. H.; Lewis, N. S. *Science* **1990**, *249*, 1146.

- (19) (a) Halkyard, C. E.; Rampey, M. E.; Kloppenburg, L.; Studer-Martinez, S. L.; Bunz, U. H. F. *Macromolecules* **1998**, *31*, 8655. (b) Pschirer, N. G.; Bunz, U. H. F. *Macromolecules* **2000**, *33*, 3961. (c) Pschirer, N. G.; Miteva, T.; Evans, U.; Roberts, R. S.; Marshall, A. R.; Neher, D.; Myrick, M. L.; Bunz, U. H. F. *Chem. Mater.* **2001**, *13*, 2691. (d) Bangcuayo, C. G.; Evans, U.; Myrick, M. L.; Bunz, U. H. F. *Macromolecules* **2001**, *34*, 7592. (e) Bangcuayo, C. G.; Rampey-Vaughn, M. E.; Quan, L. T.; Angel, S. M.; Smith, M. D.; Bunz, U. H. F. *Macromolecules* **2002**, *35*, 1563. (f) Bunz, U.H.F. *Chem. Rev.* **2000**, *100*, 1605.
- (20) (a) Jegou, G.; Jenekhe, S. A. *Macromolecules* **2001**, *34*, 7926.
- (21) Mangel, T.; Eberhardt, A.; Scherf, U.; Bunz, U. H. F.; Müllen, K. *Macromol. Rapid Commun.* **1995**, *16*, 571.
- (22) Yang, J. S.; Swager, T. M. *J. Am. Chem. Soc.* **1998**, *120*, 11864.
- (23) Weder, C.; Sarwa, C.; Montali, A.; Bastiaansen, G.; Smith, P. *Science* **1998**, *279*, 835.
- (24) Montali, A.; Bastiaansen, G.; Smith, P.; Weder, C. *Nature* **1998**, *392*, 261.
- (25) (a) Yamamoto, T.; Kokubo, H.; Morikita, T. *J. Polym. Sci., Part B: Polym. Phys.* **2001**, *39*, 1713. (c) Morikita, T.; Yamaguchi, I.; Yamamoto, T. *Adv. Mater.* **2001**, *13*, 1862.
- (26) Al-Higari, M.; Birckner, E.; Heise, B.; Klemm, E. *J Polym. Sci., A: Polym. Chem.* **1999**, *37*, 4442.
- (27) Bumm, L. A.; Arnold, J. J.; Cygan, M. T.; Dunbar, T. D.; Burgin, T. P.; Jones, L.; Allara, D. L.; Tour, J. M.; Weiss, P. S. *Science* **1996**, *271*, 1705.
- (28) (a) Samori, P.; Francke, V.; Müllen, K.; Rabe, J. P. *Chem. Eur. J.* **1999**, *5*, 2312. (b) Samori, P.; Sikharulidze, I.; Francke, V.; Müllen, K.; Rabe, J. P. *Nanotechnology* **1999**, *10*, 77. (c) Samori, P.; Francke, V.; Müllen, K.; Rabe, J. P. *Thin Solid Films* **1998**, *336*, 13. (d) Samori, P.; Francke, V.; Mangel, T.; Müllen, K.; Rabe, J. P. *Opt. Mater.* **1998**, *9*, 390. (e) Müllen, K.; Rabe, J. P. *Ann. N.Y. Acad. Sci.* **1998**, *852*, 205.
- (29) Peierls, R. E. *Quantum Theory of Solids*, Oxford University Press, London, **1955**.
- (30) Roncali, J. *Chem. Rev.* **1997**, *97*, 173.
- (31) Bredas, J. L. *Adv. Mater.* **1995**, *7*, 263.
- (32) Dkhissi, A.; Louwet, F.; Groenendaal, L.; Beljonne, B.; Lazzaroni, R.; Bredas, J. L. *Chem. Phys. Lett.* **2002**, *359*, 466.
- (33) Groenendaal, L.; Jonas, B. F.; Freitag, D.; Pielartzik, H.; Reynolds, J. R. *Adv. Mater.* **2000**, *12*, 481.

- (34) Aribizzani, C.; Castellani, M.; Cerroni, C. G.; Mastagostino, M. *J. Electroanal. Chem.* **1997**, *423*, 23.
- (35) Castellani, M.; Lazzaroni, R.; Bredas, J. L.; Luzzati, S. *Synth. Met.* **1999**, *101*, 175.
- (36) Cravino, A.; Neugebauer, H.; Luzzati, S.; Castellani, M.; Petr, A.; Dunsch, L.; Sariciftci, N. S. *J. Phys. Chem. B* **2002**, *106*, 3583.
- (37) Brocks, G.; Tol, A. *J. Phys. Chem.* **1996**, *100*, 1838.
- (38) Ajayaghosh, A. *Chem. Soc. Rev.* **2003**, *32*, 181.
- (39) Ho, H. A.; Brisset, H.; Frère, P.; and Roncali, J.; *Chem. Commun.* **1995**, 2309.
- (40) Zotti, G.; Zecchin, S.; Schiavon, G.; Berlin, A.; Pagani, G.; Borgonovo, M.; Lazzaroni, R. *Chem. Mater.* **1997**, *9*, 2876.
- (41) Lin, S.-C.; Chen, J.-A.; Liu, M.-H.; Su, Y. O.; Leung, M.-K. *J. Org. Chem.* **1998**, *63*, 5059.
- (42) Zhang, Q. T.; Tour, J. M. *J. Am. Chem. Soc.* **1998**, *120*, 5355.
- (43) (a) Kitamura, C.; Tanaka, S.; Yamashita, Y. *J. Chem. Soc., Chem. Commun.* **1994**, 1585. (b) Kitamura, C.; Tanaka, S.; Yamashita, Y. *Chem. Mater.* **1996**, *8*, 570.
- (44) Akoudad, S.; Roncali, J. *Chem. Commun.* **1998**, 2081.
- (45) Dhanabalan, A.; van Dongen, J. L. J.; van Duren, J. K. J.; Janssen, H. M.; van Hal, P. A.; Janssen, R. A. J. *Macromolecules* **2001**, *34*, 2495.
- (46) Dhanabalan, A.; van Duren, J. K. J.; van Hal, P. A.; van Dongen, J. L. J.; Janssen, R. A. J. *Adv. Funct. Mater.* **2001**, *11*, 255.
- (47) Yamamoto, T.; Lee, B. -L.; Kokubo, H.; Kishida, H.; Hirota, K.; Wakabayashi, T.; Okamoto, H. *Macromol. Rapid. Commun.* **2003**, *24*, 440.
- (48) Woo, E. P.; Inbasekaran, M.; Shiang, W.; Roof, G. R. WO **1997**, 9905184.
- (49) Yang, J.; Jiang, C. Y.; Zhang, Y.; Yang, R. Q.; Yang, W.; Hou, Q.; Cao, Y. *Macromolecules* **2004**, *37*, 1211.
- (50) Huang, J.; Xu, Y. S.; Hou, Q.; Yang, W.; Yuan, M.; Cao, Y. *Macromol. Rapid Commun.* **2002**, *23*, 709.
- (51) Huang, J.; Niu, Y. H.; Yang, W.; Mo, Y. Q.; Yuan, M.; Cao, Y. *Macromolecules* **2002**, *35*, 6080.
- (52) Hou, Q.; Xu, Y. S.; Yang, W.; Yuan, M.; Peng, J. B.; Cao, Y. *J. Mater. Chem.* **2002**, *12*, 2887.
- (53) Hou, Q.; Zhou, Q.; Zhang, Y.; Yang, W.; Yang, R.; Cao, Y. *Macromolecules* **2004**, *37*, 6299.

- (54) Younus, M.; Kohler, A.; Cron, S.; Chawdhury, N.; Al-Mandhary, M. R. A.; Khan, M. S.; Lewis, J.; Long, N. J.; Friend, R. H.; Raithby, P. R. *Angew. Chem. Int. Ed.* **1998**, *37*, 3036.
- (55) Kitamura, C.; Saito, K.; Nakagawa, M.; Ouchi, M.; Yoneda, A.; Yamashita, Y. *Tetrahedron Lett* **2002**, *43*, 3373.
- (56) Dieck, H. A.; Heck, R. F. *J. Organomet. Chem.* **1975**, *93*, 259.
- (57) Cassar, I. *J. Organomet. Chem.* **1975**, *93*, 253.
- (58) Sonogashira, K.; Tohda, Y.; Hagihara, N. *Tetrahedron Lett.* **1975**, *16*, 4467.
- (59) Ofer, D.; Swager, T. M.; Wrighton, M. S. *Chem. Mater.* **1995**, *7*, 418.
- (60) Zhou, Q.; Swager, T. M. *J. Am. Chem. Soc.* **1995**, *117*, 12593.
- (61) Steiger, D.; Smith, P.; Weder, C. *Macromol. Rapid Commun.* **1997**, *18*, 643.
- (62) Alami, M.; Ferri, F.; Linstrumelle, G. *Tetrahedron Lett.* **1993**, *34*, 6403.
- (63) Miyaura, N.; Yanagi, T.; Suzuki, A. *Synth. Commun.* **1981**, *11*, 513.
- (64) (a) Suzuki, A. *Pure Appl. Chem.* **1985**, *57*, 1749. (b) Suzuki, A. *Pure Appl. Chem.* **1991**, *63*, 419.
- (65) Martin, A. R.; Yang, Y. *Acta Chem. Scand.* **1993**, *47*, 221.
- (66) Suzuki, A. *Pure Appl. Chem.* **1994**, *66*, 213.
- (67) Miyaura, N.; Suzuki, A. *Chem. Rev.* **1995**, *95*, 2457.
- (68) Stanforth, S. P. *Tetrahedron* **1998**, *54*, 263.
- (69) Miyaura, N. *Advances in Metal-organic Chemistry*; Libeskind, L. S., Ed.; Jai: London, **1998**; Vol. 6, pp 187–243.
- (70) Suzuki, A. *J. Organomet. Chem.* **1999**, *576*, 147.
- (71) Suzuki, A. *In Organoboranes for Syntheses*. ACS Symposium Series 783; Ramachandran, P. V.; Brown, H. C., Eds.; American Chemical Society: Washington, DC, **2001**; pp 80–93.
- (72) Rehahn, M.; Schlüter, A. D.; Wegner, G.; Feast, W. J. *Polymer* **1989**, *30*, 1054.
- (73) Rehahn, M.; Schlüter, A. D.; Wegner, G. *Macromol. Chem.* **1990**, *191*, 1991.
- (74) Remmers, M.; Schulze, M.; Wegner, G. *Macromol. Rapid Commun.* **1996**, *17*, 239.
- (75) Miyaura, N.; Yamada, K.; Suginome, H.; Suzuki, A. *J. Am. Chem. Soc.* **1985**, *107*, 972.
- (76) Saito, S.; Sakai, M.; Miyaura, N. *Tetrahedron Lett.* **1996**, *37*, 2993.
- (77) Casalnuovo, A. L.; Calabrese, J. C.; *J. Am. Chem. Soc.* **1990**, *112*, 4324.
- (78) Kotha, S.; Lahiri, K.; Kashinath, D. *Tetrahedron* **2002**, *58*, 9633.

- (79) Cowie, J. M. G. *Polymers: Chemistry and Physics of Modern Materials*, International Textbook Company Ltd., London, **1973**.
- (80) (a) Yu, D.; Gharavi, A.; Yu, L. *J. Am. Chem. Soc.* **1995**, *117*, 11680. (b) Wu, R.; Schumm, J. S.; Pearson, D. L.; Tour, J. M. *J. Org. Chem.* **1996**, *61*, 6906. (c) Greenwald, Y.; Cohen, G.; Poplawski, J.; Ehrenfreund, E.; Speiser, S.; Davidov, D. *J. Am. Chem. Soc.* **1996**, *118*, 2980. (d) Barbarella, G.; Zambianchi, M.; Bongini, A.; Antolini, L. *J. Org. Chem.* **1996**, *61*, 4708. (e) Elandaloussi, E. H.; Frere, P.; Richomme, P.; Orduna, J.; Garin, J.; Roncali, J. *J. Am. Chem. Soc.* **1997**, *119*, 10774. (f) Fajari, Ll.; Brillas, E.; Aleman, C.; Julia, L. *J. Org. Chem.* **1998**, *63*, 5324. (g) Horne, J. C.; Blanchard, G. J. *J. Am. Chem. Soc.* **1998**, *120*, 6336. (h) Mohanakrishnan, A. K.; Lakshmikantham, M. V.; McDougal, C.; Cava, M. P.; Baldwin, J. W.; Metzger, R. M. *J. Org. Chem.* **1998**, *63*, 3105. (i) Jestin, I.; Frere, P.; Mercier, N.; Levillain, E.; Stievenard, D.; Roncali, J. *J. Am. Chem. Soc.* **1998**, *120*, 8150. (j) Huang, S.; Tour, J. M. *J. Org. Chem.* **1999**, *64*, 8898. (k) Breitung, E. M.; Shu, C.-F.; McMahon, R. J. *J. Am. Chem. Soc.* **2000**, *122*, 1154.
- (81) (a) Antolini, L.; Horowitz, G.; Kouki, F.; Garnier, F. *Adv. Mater.* **1998**, *10*, 382. (b) Siegrist, T.; Kloc, C.; Laudise, R. A.; Katz, H. E.; Haddon, R. C. *Adv. Mater.* **1998**, *10*, 379. (c) Horowitz, G.; Bachet, B.; Yassar, A.; Lang, P.; Demanze, F.; Fave, J. L.; Garnier, F. *Chem. Mater.* **1995**, *7*, 1337. (d) Siegrist, T.; Fleming, R. M.; Haddon, R. C.; Laudise, R. A.; Lovinger, A. J.; Katz, H. E.; Bridenbaugh, P.; Davis, D. D. *J. Mater. Res.* **1995**, *10*, 2170. (e) Antolini, L.; Tedesco, E.; Barbarella, G.; Favaretto, L.; Sotgiu, G.; Zambianchi, M.; Casarini, D.; Gigli, G.; Cingolani, R. *J. Am. Chem. Soc.* **2000**, *122*, 9006.
- (82) Sessler, J. L.; Berthon-Gelloz, G.; Gale, P. A.; Camiolo, S.; Anslyn, E. V.; Anzenbacher, P., Jr.; Furuta, H.; Kirkovits, G. J.; Lynch, V. M.; Maeda, H.; Morosini, P.; Scherer, M.; Shriver, J.; Zimmerman, R. S. *Polyhedron* **2003**, *22*, 2063.
- (83) Marseglia, E. A.; Grepioni, F.; Tedesco, E.; Braga, D. *Mol. Cryst. Liq. Cryst.* **2000**, *348*, 137.
- (84) (a) Baeuerle, P.; Pfau, F.; Schlupp, H.; Wuerthner, F.; Gaudl, K. U.; Balparda Caro, M.; Fischer, P. *J. Chem. Soc. Perkin Trans. 2: Physical Organic Chemistry (1972-1999)* **1993**, 489. (b) Andreani, F.; Salatelli, E.; Lanzi, M. *Polymer* **1996**, *37*, 661. (c) Liu, B.; Yu, W.; Lai, Y.; Huang, W. *Macromolecules* **2000**, *33*, 8945. (d) Berlin, A.; Zotti, G.; Zecchin, S.; Schiavon, G.; Cocchi, M.; Virgili, D.; Sabatini, C. *J. Mater. Chem.* **2003**, *13*, 27-33.

- (85) Egbe, D. A. M.; Klemm, E. *Macromol. Chem. Phys.* **1998**, *199*, 2683.
- (86) (a) Pilgram, K.; Zupan, M.; Skiles, R. *J. Heterocycl. Chem.* **1970**, *7*, 629. (b) Kanbara, T.; Yamamoto, T. *Chem. Lett.* **1993**, 419. (c) Edelman, M. J.; Raimundo, J.-M.; Utesch, N. F.; Diederich, F. *Helv. Chem. Acta* **2002**, *85*, 2195. (d) Yamamoto, T.; Sugiyama, K.; Kushida, T.; Inoue, T.; Kanbara, T. *J. Am. Chem. Soc.* **1996**, *118*, 3930.
- (87) (a) Giesa, R.; Schulz, R. C. *Makromol. Chem.* **1990**, *191*, 857. (b) Egbe, D. A. M.; Roll, C. P.; Birckner, E.; Grummt, U.-W.; Stockmann, R.; Klemm, E. *Macromolecules* **2002**, *35*, 3825.
- (88) Zhan, X.; Liu, Y.; Wu, X.; Wang, S.; Zhu, D. *Macromolecules* **2002**, *35*, 2529.
- (89) (a) Peng, Z.; Galvin, M. *Acta Polym.* **1998**, *49*, 244. (b) Xia, C.; and Advincula, R. C. *Macromolecules* **2001**, *34*, 6922.
- (90) (a) Keegstra, M. A.; Brandsma, L. *Synthesis* **1988**, *11*, 890. (b) Mozingo, R.; Harris, S. A.; Wolf, D. E.; Hoffhine, C. E.; Easton, N. R.; Folkers, K. *J. Am. Chem. Soc.* **1945**, *67*, 2902. (c) Outurquin, F.; Paulmier, C. *Bull. Soc. Chim. Fr., II* **1983**, 159. (d) Don, D. K.; Kari, A. M.; Tessa, R. C.; Melanie, R. F.; Daniel, J. S.; Seth, C.R. *J. Org. Chem.* **2002**, *67*, 9073.
- (91) (a) Vahlenkamp, T.; Wegner, G. *Macromol. Chem. Phys.* **1994**, *195*, 1933. (b) Ranger, M.; Rondeau, D.; Leclerc, M. *Macromolecules* **1997**, *30*, 7686. (c) Ding, J.; Day, M.; Robertson, G.; Roovers, J. *Macromolecules* **2002**, *35*, 3474.
- (92) Aubert, P.-H.; Knipper, M.; Groenendaal, L.; Lutsen, L.; Manca, J.; Vanderzande, D. *Macromolecules* **2004**, *37*, 4087.
- (93) (a) Karikomi, M.; Kitamura, C.; Tanaka, S.; Yamashita, Y. *J. Am. Chem. Soc.* **1995**, *117*, 6791. (b) Arias, A. C.; Mackenzie, J. D.; Stevenson, R.; Halls, J. J. M.; Woo, E. P.; Richards, D.; Friend, R. H. *Macromolecules* **2001**, *34*, 6005. (c) Jayakannan, M.; Vanhal, P. A.; Janssen, A. *J. Polym. Sci., Part A: Polym. Chem.* **2002**, *40*, 251. (d) Lu, S. L.; Yang, M. J.; Luo, J.; Cao, Y.; Bai, F. L. *Synth. Met.* **2004**, *146*, 175.
- (94) (a) Chen, T. A.; Wu, X.; Rieke, R. D. *J. Am. Chem. Soc.* **1995**, *117*, 233. (b) Li, J.; Pang, Y. *Macromolecules* **1997**, *30*, 7487. (c) Li, J.; Pang, Y. *Macromolecules* **1998**, *31*, 5740.
- (95) McCullough, R. D.; Lowe, R. D.; Jayaraman, M.; Anderson, D. L. *J. Org. Chem.* **1993**, *58*, 904.
- (96) Apperloo, J. J.; Janssen, R. A. J.; Malenfant, P. R. L.; Frechet, J. M. J. *Macromolecules* **2000**, *33*, 7038.

- (97) (a) Wautelet, P.; Moroni, M.; Oswald, L.; Le Moigne, J.; Pham, T. A.; Bigot, J. Y. *Macromolecules* **1996**, *29*, 446.
- (98) Yamamoto, T.; Kimura, T.; Shiraishi, K. *Macromolecules* **1999**, *32*, 8886.
- (99) McBranch, D. W.; Sinclair, M. B. “*The Nature of The Photoexcitations in Conjugated Polymers*”, Sariciftci, N. S. Ed., World Scientific Publishing, Singapore **1997**, Chapter 20, p. 608.
- (100) Rothberg, L. J.; Yan, M.; Papadimitrakopoulos, F.; Galvin, M. E.; Kwock, E. W.; Miller, T. M. *Synth. Met* **1996**, *80*, 41.
- (101) Peng, Z. *Polym. News* **2000**, *25*, 185.
- (102) Klessinger, M.; Michl, J. “*Lichtabsorption und Photochemie Organischer Moleküle*”, VCH, Weinheim **1990**, p. 215.
- (103) Swanson, L. S.; Lu, F.; Shinar, J.; Ding, Y. W.; Barton, T. J. *SPIE* **1993**, *1910*, 101.
- (104) Mühlbacher, D. Diploma thesis, Linz, Austria, **2002**.
- (105) (a) Bredas, J. L.; Silbey, R.; Boudreau, D. S.; Chance, R. R. *J. Am. Chem. Soc.* **1983**, *105*, 6555. (b) deLeeuw, D. M.; Simenon, M. M. J.; Brown, A. B.; Einerhand, R. E. F. *Synth. Met.* **1997**, *87*, 53.
- (106) Pommerehne, J.; Vestweber, H.; Guss, W.; Mahrt, R. F.; Bassler, H.; Porsch, M.; Daub, J. *Adv. Mater.* **1995**, *7*, 551.
- (107) Gerischer, H., Tobias, C. W., Eds. *Advances in Electrochemistry and Electrochemical Engineering*; John Wiley: New York, **1977**; Vol. *10*, p 213.
- (108) (a) Gomer, R. J.; Tryson, G. *J. Chem. Phys.* **1977**, *66*, 4413. (b) Kötz, R.; Neff, H.; Müller, K. *J. Electroanal. Chem.* **1986**, *215*, 331.
- (109) Yamamoto, T.; Morita, A.; Miyazaki, Y.; Maruyama, T.; Wakayama, H.; Zhou, Z. H.; Nakamura, Y.; Kanbara, T.; Sasaki, S.; Kubota, K. *Macromolecules* **1992**, *25*, 1214.
- (110) (a) Shiraishi, K.; Yamamoto, T. *Synth. Met.* **2002**, *130*, 139. (b) Yamamoto, T. *Bull. Chem. Soc. Jpn.* **1999**, *72*, 621.
- (111) Chen, Z.-K.; Huang, W.; Wang, L.-H.; Kang, E.-T.; Chen, B. J.; Lee, C. S.; Lee, S. T. *Macromolecules* **2000**, *33*, 9015.
- (112) Janietz, S.; Bradley, D. D. C.; Grell, M.; Giebeler, C.; Inbasekaran, M.; Woo, E. P. *Appl. Phys. Lett.* **1998**, *73*, 2453.
- (113) Brabec, C. J.; Sariciftci, N. S.; Hummelen, J. C. *Adv. Funct. Mater.* **2001**, *11*, 15.
- (114) Yu, G.; Gao, J.; Hummelen, J. C.; Wudl, F.; Heeger, A. J. *Science* **1995**, *270*, 1789.

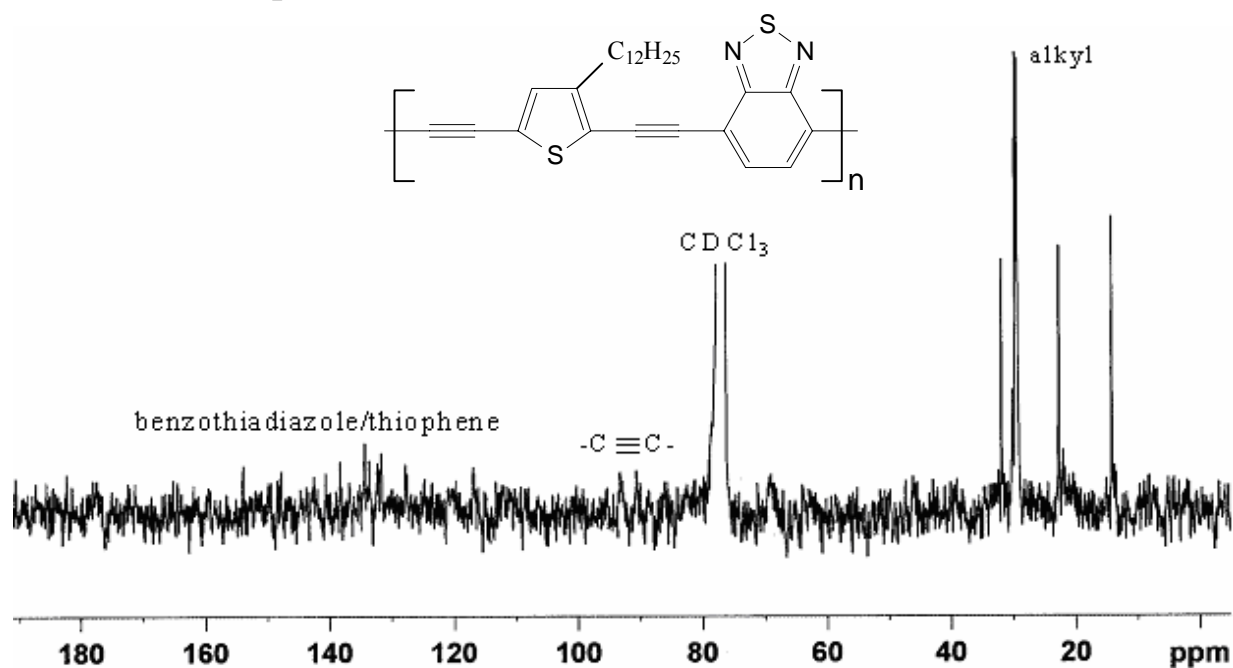
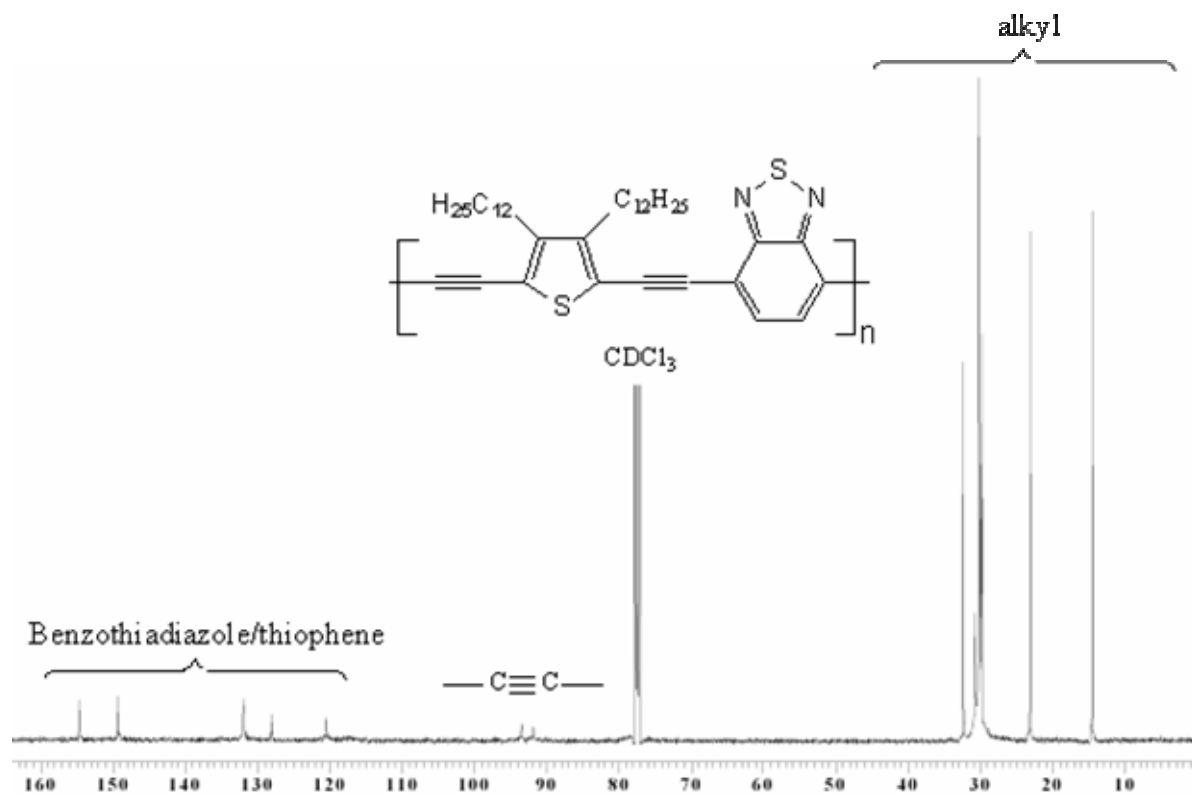
- (115) Halls, J. J. M.; Walsh, C. A.; Greenham, N. C.; Marseglia, E. A.; Friend, R. H.; Moratti, S. C.; Holmes, A. B. *Nature (London)* **1995**, *376*, 498.
- (116) Chen, L. C.; Godovsky, D.; Inganäs, O.; Hummelen, J. C.; Janssen, R. A. J.; Andersson, M. R. *Adv. Mater.* **2000**, *12*, 1367.
- (117) Roman, L. S.; Andersson, M. R.; Yohannes, T.; Inganäs, O. *Adv. Mater.* **1997**, *9*, 1164.
- (118) Chirvase, D.; Chiguvare, Z.; Knipper, M.; Parisi, J.; Dyakonov, V.; Hummelen, J. C. *J. Appl. Phys.* **2003**, *93*, 3376.
- (119) Yamamoto T, Zhou Z-H, Kanbara T, Shimura M, Kizu K, Maruyama T, Nakamura Y, Fukuda T, Lee B-L, Ooba N, Tomaru S, Kurihara T, Kaino T, Sasaki S. *J. Am. Chem. Soc.* **1996**, *118*, 10389.
- (120) (a) Conwell, E. *Trends Polym. Sci.* **1997**, *5*, 218. (b) Hunter, C. A. *Angew. Chem.* **1993**, *32*, 1584. (c) Hunter, C. A. *Chem. Soc. Rev.* **1994**, *23*, 101.
- (121) Rughooputh, S. D. D. V.; Hotta, S.; Heeger, A. J.; Wudl, F. *J. Polym. Sci., Part B: Polym. Phys.* **1987**, *25*, 1071.
- (122) (a) Bouchard, J.; Belletête, M.; Durocher, G.; Leclerc, M. *Macromolecules* **2003**, *36*, 4624. (b) Belletête, M.; Bouchard, J.; Leclerc, M.; Durocher, G. *Macromolecules* **2005**, *38*, 880.
- (123) Pomerantz, M.; Chaloner-Gill, B.; Harding, L. O.; Tseng, J. J.; Pomerantz, W. J. *J. Chem. Soc., Chem. Commun.* **1992**, 1672.
- (124) (a) Nayak, K.; Marynick, D. S. *Macromolecules* **1990**, *23*, 2237. (b) Kastner, J.; Kuzmany, H.; Vegh, D.; Landl, M.; Cuff, L.; Kertesz, M. *Macromolecules* **1995**, *28*, 2922.
- (125) Ferraris, J. P.; Bravo, A.; Kim, W.; Hrnčir, D. C. *J. Chem. Soc., Chem. Commun.* **1994**, 991.
- (126) (a) Brizius, G.; Pschirer, N. G.; Steffen, W.; Stitzer, K.; zur Loye, H.-C.; Bunz, U. H. F. *J. Am. Chem. Soc.* **2000**, *122*, 12435. (b) Wilson, J. N.; Windscheif, P. M.; Evans, U.; Myrick, M. L.; Bunz, U. H. F. *Macromolecules* **2002**, *35*, 8681. (c) Wilson, J. N.; Josowicz, M.; Wang, Y.; Bunz, U. H. F. *Chem. Commun.* **2003**, 2962.
- (127) (a) Egbe, D. A. M.; Tillmann, H.; Birckner, E.; Klemm, E. *Macromol. Chem. Phys.* **2001**, *202*, 2712. (b) Egbe, D. A. M.; Birckner, E.; Klemm, E. *J. Polym. Sci., Polym. Chem.* **2002**, *40*, 2670. (c) Egbe, D. A. M.; Roll, C. P.; Klemm, E. *Des. Monomers Polym.* **2002**, *5*, 245. (d) Egbe, D. A. M.; Bader, C.; Nowotny, J.; Günther, W.; Klemm, E. *Macromolecules* **2003**, *36*, 5459. (e) Egbe, D. A. M.; Bader, C.; Klemm,

- E.; Ding, L.; Karasz, F. E.; Grummt, U.-W.; Birckner, E. *Macromolecules* **2003**, *36*, 9303.
- (128) (a) Ramos, A. M.; Rispens, M. T.; van Duren, J. K. J.; Hummelen, J. C.; Janssen, R. A. J. *J. Am. Chem. Soc.* **2001**, *123*, 6714. (b) Schenning, A. P. H. J.; Tsipis, A. C.; Meskers, S. C. J.; Beljonne, D.; Meijer, E. W.; Bre'das, J. L. *Chem. Mater.* **2002**, *14*, 1362. (c) Chu, Q.; Pang, Y.; Ding, L.; Karasz, F. E. *Macromolecules* **2003**, *36*, 3848.
- (129) (a) Hernandez, V.; Castiglioni, C.; DelZoppo, M.; Zerbi, G. *Phys. Rev. B* **1994**, *50*, 9815. (b) *Conjugated Polymers: The Novel Science and Technology of Highly Conducting and Nonlinear Optically Active Materials*; Bredas, J. L., Silbey, R., Eds.; Kluwer: Dordrecht, The Netherlands, 1991. (c) Bredas, J. L.; Cornil, J.; Heeger, A. J. *Adv. Mater.* **1996**, *8*, 447.
- (130) Egbe, D. A. M.; Kietzke, T.; Carbonnier, B.; Mühlbacher, D.; Hörhold, H.-H.; Neher, D.; Pakula, T. *Macromolecules* **2004**, *37*, 8863.
- (131) Klärner, G.; Lee, J.-I.; Davey, M. H.; Miller, R. D. *Adv. Mater.* **1999**, *11*, 115.
- (132) Klärner, G.; Miller, R. D. *Macromolecules* **1998**, *31*, 2007.
- (133) Bernius, M. T.; Inbasekaran, M.; Brien, J. O.; Wu, W. *Adv. Mater.* **2000**, *13*, 1737.
- (134) Larmat, F.; Reynolds, J. R.; Reinhardt, B. A.; Brott, L. L.; Clarson, S. J. *J. Polym. Sci., Part A: Polym. Chem.* **1997**, *35*, 3627.
- (135) Tsuie, B.; Reddinger, J. L.; Stozing, G. A.; Soloduchko, J.; Katritzky, A. R.; Reynolds, J. R. *J. Mater. Chem.* **1999**, *9*, 2189.
- (136) Donat-Bouillud, A.; Le'vesque, I.; Tao, Y.; D'Iorio, M. *Chem. Mater.* **2000**, *12*, 1931.
- (137) Blondin, P.; Bouchard, J.; Beaupre', S.; Belle'te, M.; Durocher, G.; Leclerc, M. *Macromolecules* **2000**, *33*, 5874.
- (138) Le'vesque, I.; Donat-Bouillud, A.; Tao, Y.; D'Iorio, M.; Beaupre', S.; Blondin, P.; Ranger, M.; Bouchard, J.; Leclerc, M. *Synth. Met.* **2001**, *122*, 79.
- (139) Leclerc, M. *J. Polym. Sci., Part A: Polym. Chem.* **2001**, *39*, 2867.
- (140) Ranger, M.; Leclerc, M. *Can. J. Chem.* **1998**, *76*, 1571.
- (141) Liu, B.; Yu, W.-L.; Lai, Y.-H.; Huang, W. *Macromolecules* **2000**, *33*, 8945.
- (142) Liu, B.; Yu, W.-L.; Pei, J.; Lai, Y.-H.; Huang, W.; Niu, Y.-H.; Cao, Y. *Mater. Sci. Eng. B* **2001**, *85*, 232.
- (143) Charas, A.; Barbagallo, N.; Morgado, J.; Alca'cer, L. *Synth. Met.* **2001**, *122*, 23.
- (144) Zhan, X. W.; Liu, Y. Q.; Zhu, D. B.; Jiang, X. Z.; Jen, A. K.-Y. *Synth. Met.* **2001**, *124*, 323.

- (145) Bernius, M.; Inbasekaran, M.; Woo, E.; Wu, W. S.; Wujkowski, L. *J. Mater. Sci.: Mater. Electron.* **2000**, *11*, 111.
- (146) Inbasekaran, M.; Wu, W. S.; Woo, E. P. *US Pat.* **1998**, 5777070.
- (147) Whitehead, K. S.; Grell, M.; Bradley, D. D. C.; Inbasekaran, M.; Woo, E. P. *Synth. Met.* **2000**, *111*, 181.
- (148) Millard, I. S. *Synth. Met.* **2000**, *111*, 119.
- (149) Inbasekaran, M.; Woo, E. P.; Wu, W. S.; Bernius, M. T. *PCT application* **2000**, W0046321A1.
- (150) Redecker, M.; Bradley, D. D. C.; Inbasekaran, M.; Wu, W. W.; Woo, E. P. *Adv. Mater.* **1999**, *11*, 241.
- (151) Campbell, A. J.; Bradley, D. D. C.; Antoniadis, H. *Appl. Phys. Lett.* **2001**, *79*, 2133.
- (152) Kreyenschmidt, M.; Klaerner, G.; Fuhrer, T.; Ashenurst, J.; Karg, S.; Chen, W. D.; Lee, V. Y.; Scott, J. C.; Miller, R. D. *Macromolecules* **1998**, *31*, 1099-1103.
- (153) (a) Lupton, J. M.; Craig, M. R.; Meijer, E. W. *Appl. Phys. Lett.* **2002**, *80*, 4489. (b) Kulkarni, A. P.; Kong, X.; Jenekhe, S. A. *J. Phys. Chem. B* **2004**, *108*, 8689.
- (154) Ljungqvist, N.; Hjertberg, T. *Macromolecules* **1996**, *28*, 5993.
- (155) Johansson, D. M.; Srdanov, G.; Yu, G.; Theander, M.; Inganas, O.; Andersson, M. R. *Macromolecules* **2000**, *33*, 2525.
- (156) Scurlock, R. D.; Wang, B.; Ogilby, P. R.; Sheats, J. R.; Clough, R. L. *J. Am. Chem. Soc.* **1995**, *117*, 10194.
- (157) (a) Donat-Bouillud, A.; Levesque, I.; Tao, Y.; D'Iorio, M.; Beaupre, S.; Blondin, P.; Ranger, M.; Bouchard, J.; Leclerc, M. *Chem. Mater.* **2000**, *12*, 1931. (b) Hou, Q.; Zhou, Q.; Zhang, Y.; Yang, W.; Yang, R.; Cao, Y. *Macromolecules* **2004**, *37*, 6299. (c) Kong X.; Kulkarni A. P.; Jenekhe, S. A. *Macromolecules* **2003**, *36*, 8992.
- (158) Liu, B.; Yu, W.-L.; Lai, Y.-H.; Huang, W. *Chem. Mater.* **2001**, *13*, 1984.
- (159) (a) Wu, F.-I.; Reddy, S.; Shu, C.-F.; Liu, M. S.; Jen, A. K.-Y. *Chem. Mater.* **2003**, *15*, 269. (b) Zhan, X.; Liu, Y.; Wu, X.; Wang, S.; Zhu, D. *Macromolecules* **2002**, *35*, 2529. (c) Yang, W.; Huang, J.; Liu, C.; Niu, Y.; Hou, Q.; Yang, R.; Cao, Y. *Polymer* **2004**, *45*, 865.
- (160) (a) Sun, Q.; Zhan, X.; Yang, C.; Liu, Y.; Li, Y.; Zhu, D. *Thin Solid Films* **2003**, *440*, 247. (b) Jung, S. H.; Suh, D. H.; Cho, H. N. *Polym. Bull.* **2003**, *50*, 251.
- (161) (a) Fukuda, T.; Kanbara, T.; Yamamoto, T.; Ishikawa, K.; Takezoe, H.; Fukuda, A. *Appl. Phys. Lett.* **1996**, *68*, 2346. (b) O'Brien, D.; Weaver, M. S.; Lidzey, D. G.;

- Bradley, D. D. C. *Appl. Phys. Lett.* **1996**, *69*, 881. (c) Cui, Y.; Zhang, X.; Jenekhe, S. *A. Macromolecules* **1999**, *32*, 3824.
- (162) Crosby, J. N.; Crosby, G. A. *J. Phys. Chem.* **1971**, *75*, 991.
- (163) Milazzo, G.; Caroli, S. *Tables of Standard Electrode Potentials*; Wiley-Interscience: New York, **1977**.
- (164) Saraw, E. *Liebigs Ann. Chem.* **1881**, *209*, 108.
- (165) Zhu, Y.; Wolf, M. O. *J. Am. Chem. Soc.* **2000**, *122*, 10121.

7 Appendix

7.1 ^{13}C -NMR-SpectraFigure 7.1. ^{13}C -NMR of P-1.Figure 7.2. ^{13}C -NMR of P-2.

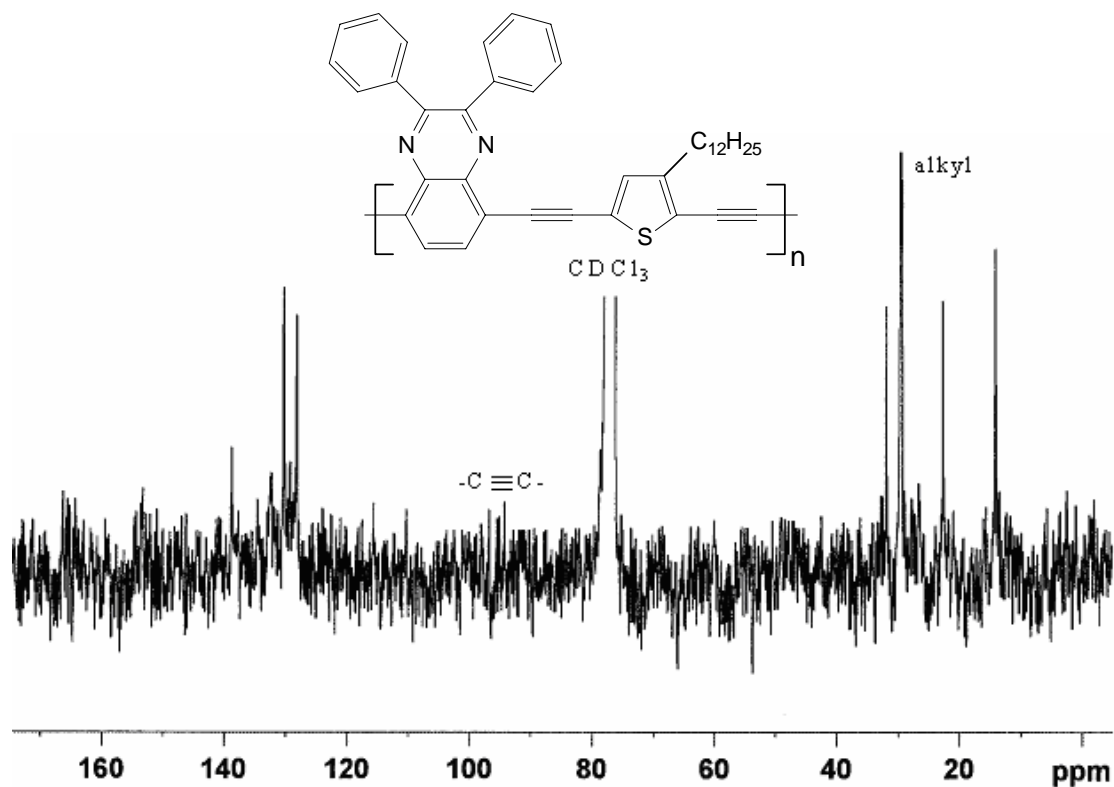


Figure 7.3. ^{13}C -NMR of P-3.

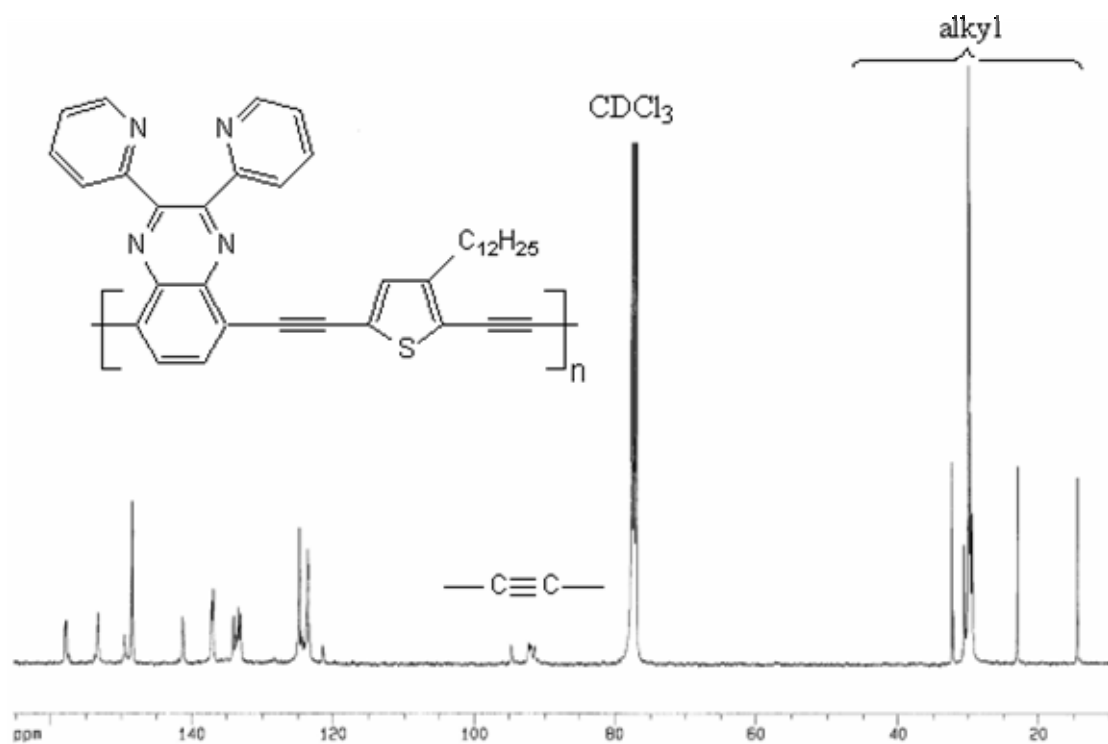
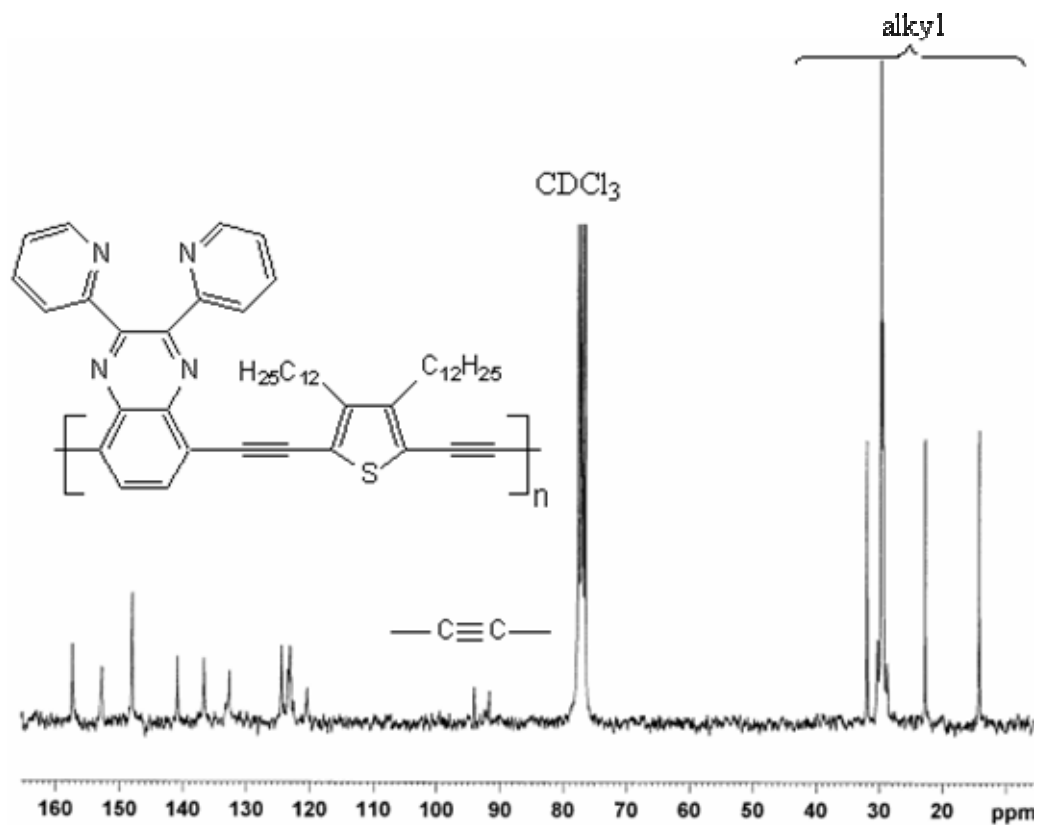
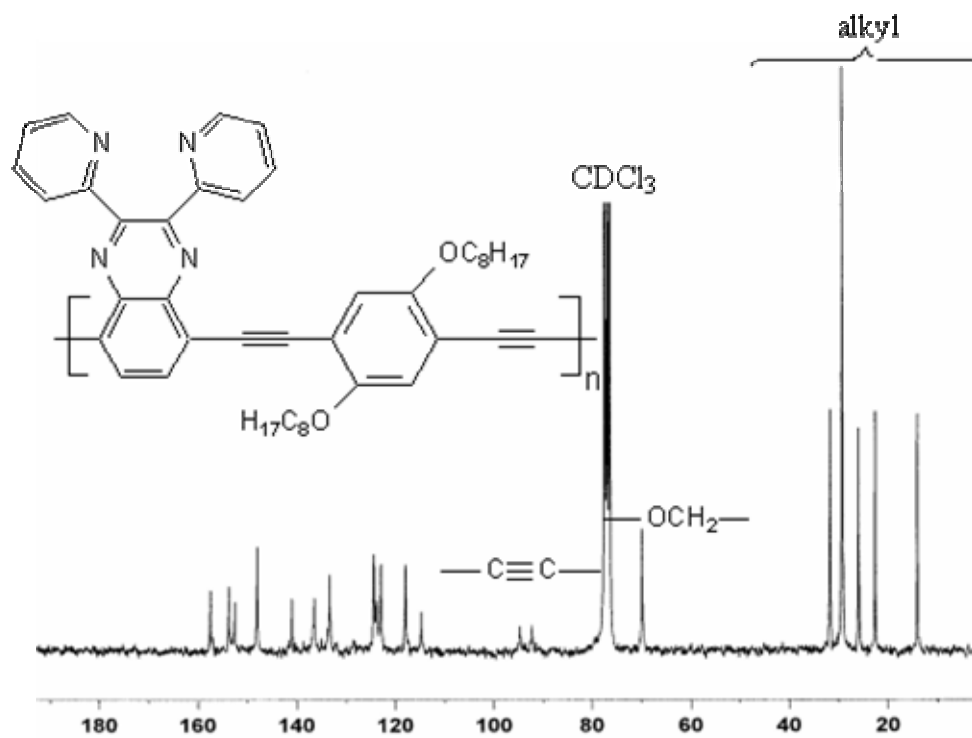


Figure 7.4. ^{13}C -NMR of P-5.

Figure 7.5. ^{13}C -NMR of P-6.Figure 7.6. ^{13}C -NMR of P-7.

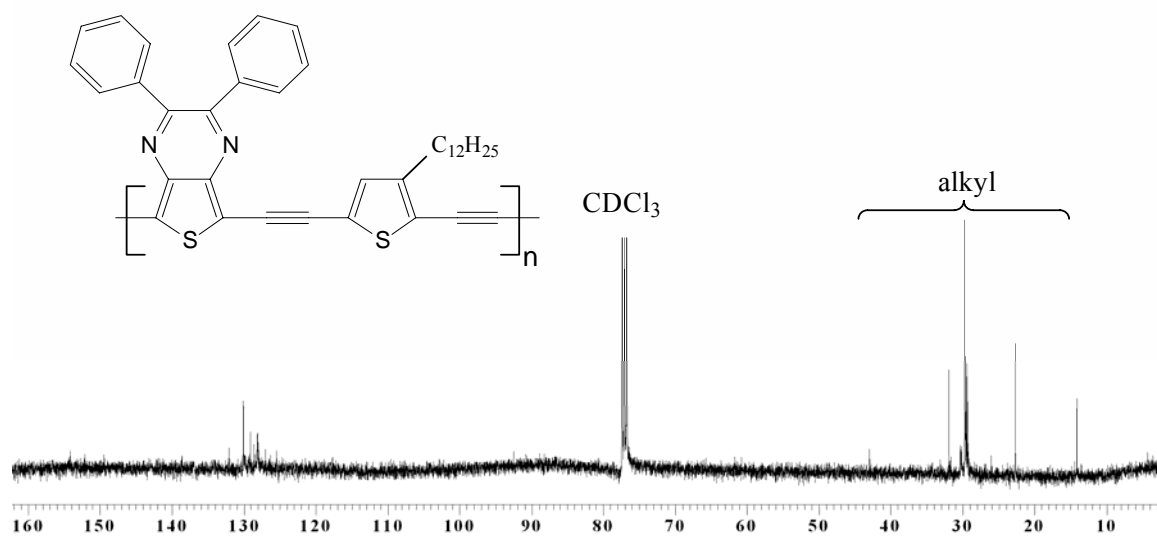


Figure 7.7. ^{13}C -NMR of P-8.

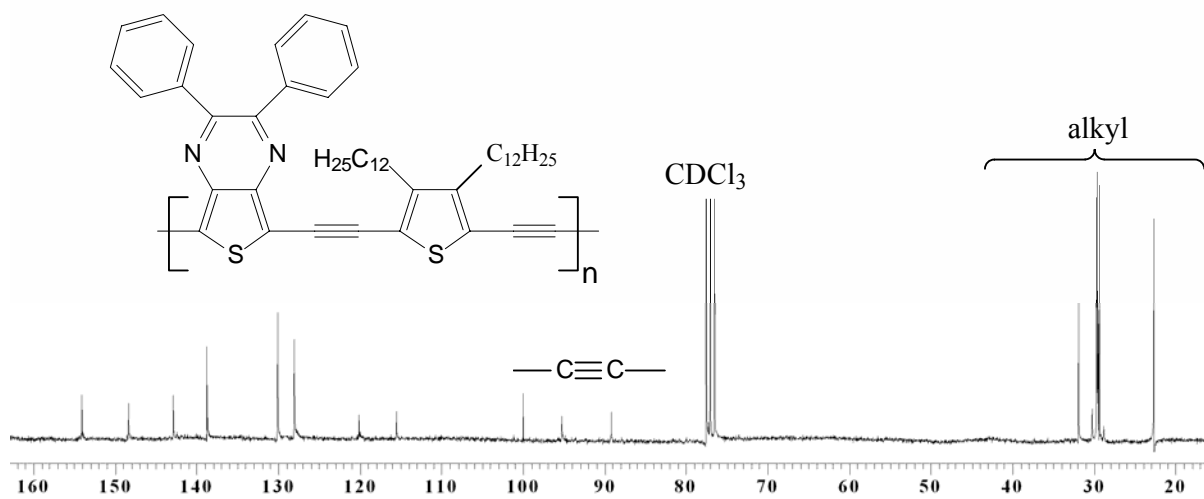


Figure 7.8. ^{13}C -NMR of P-9.

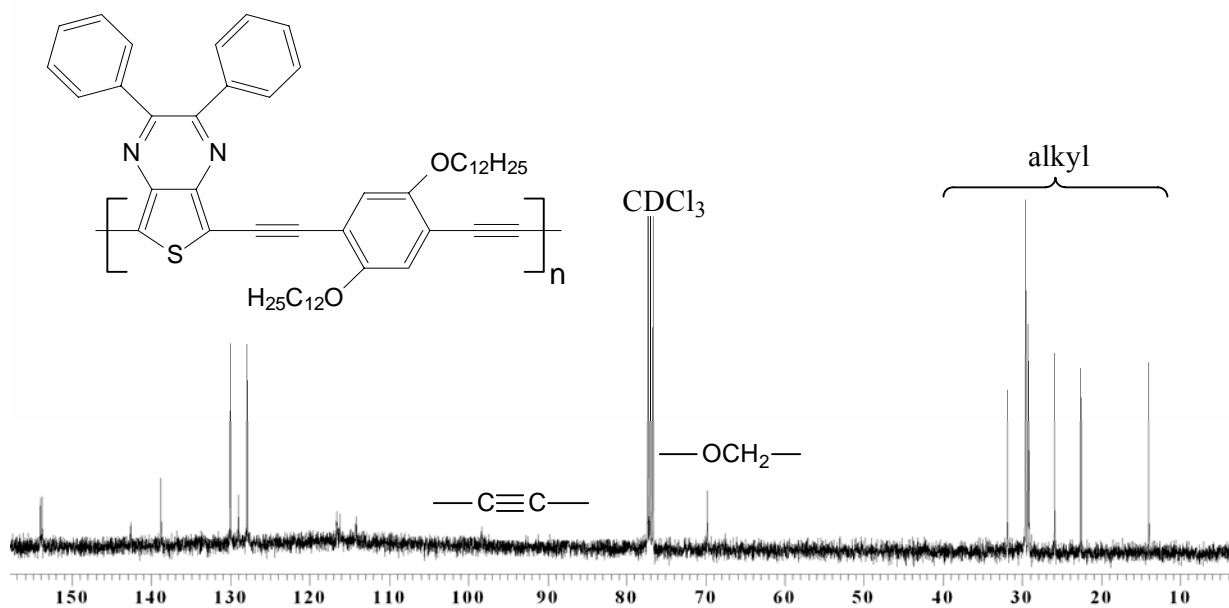


Figure 7.10. ^{13}C -NMR of P-10.

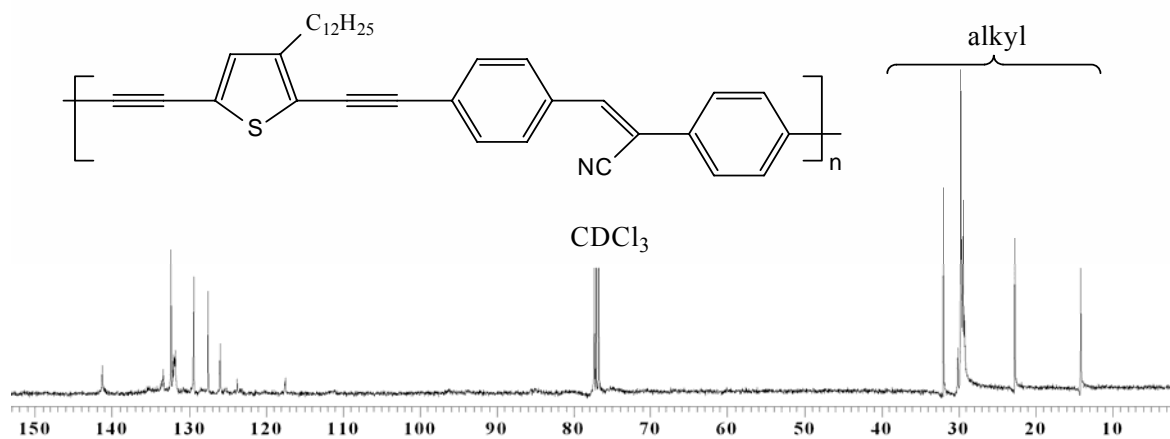


Figure 7.11. ^{13}C -NMR of P-11.

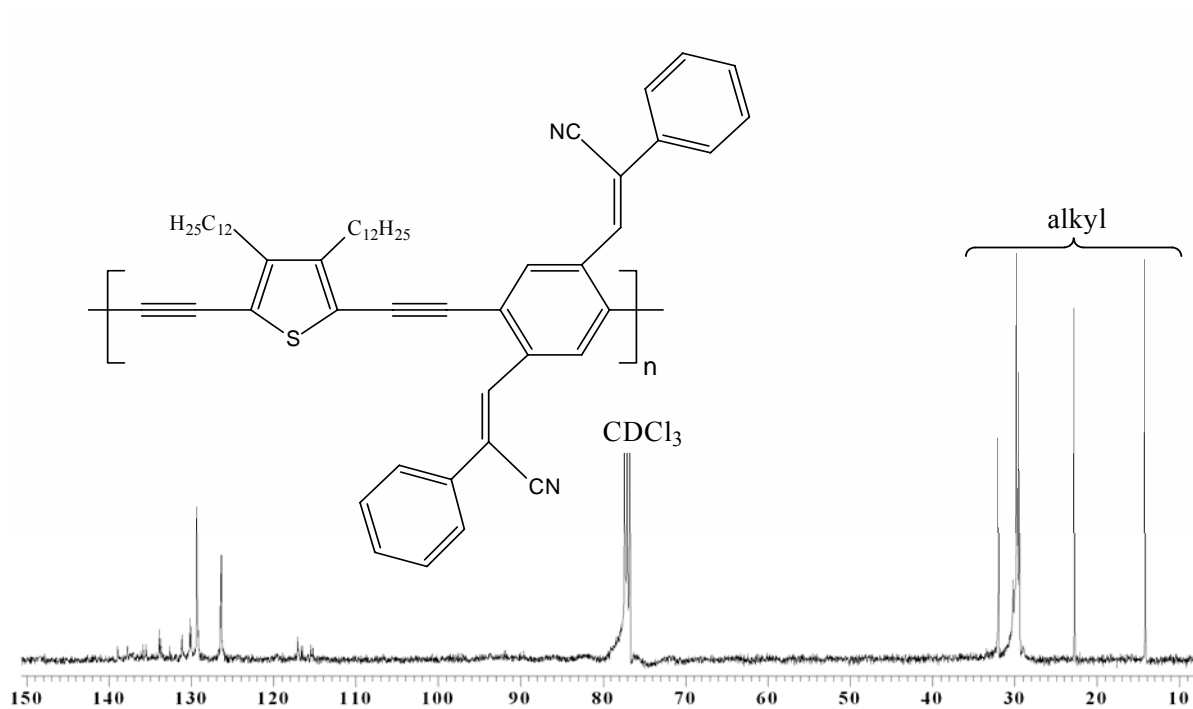


Figure 7.12. ^{13}C -NMR of P-13.

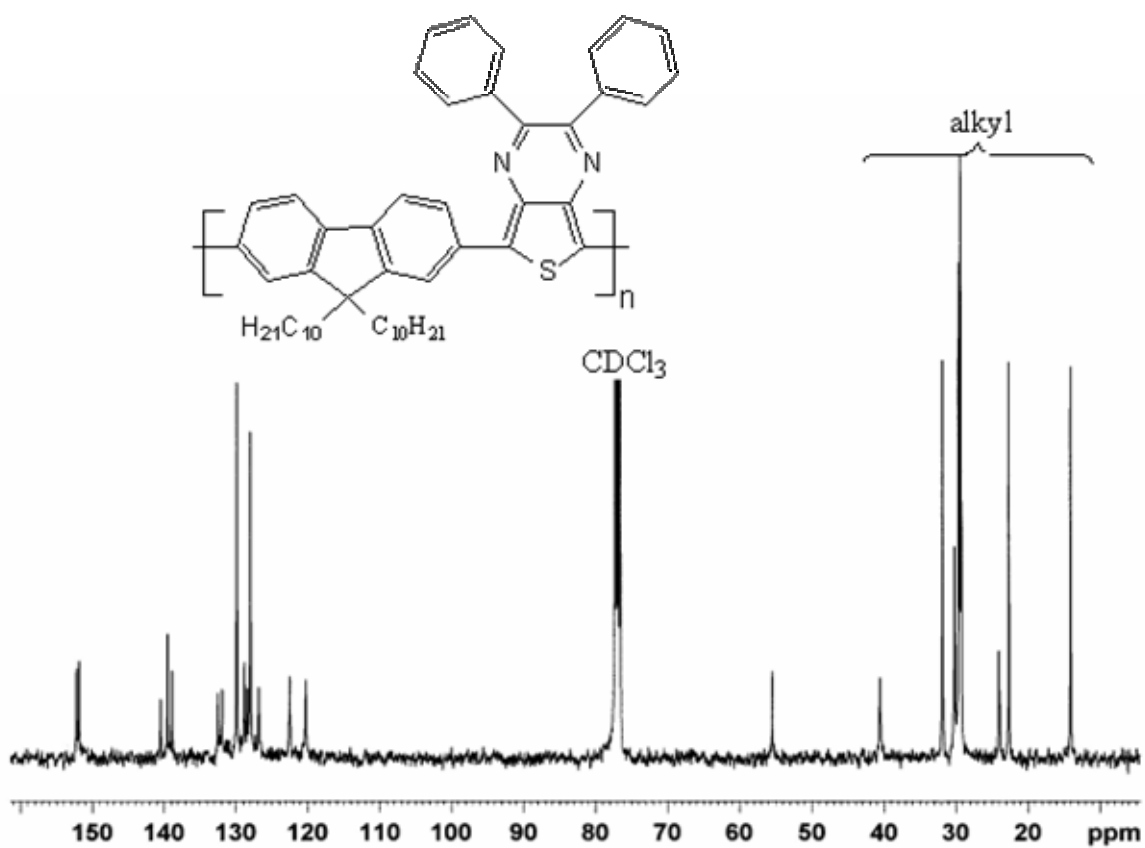
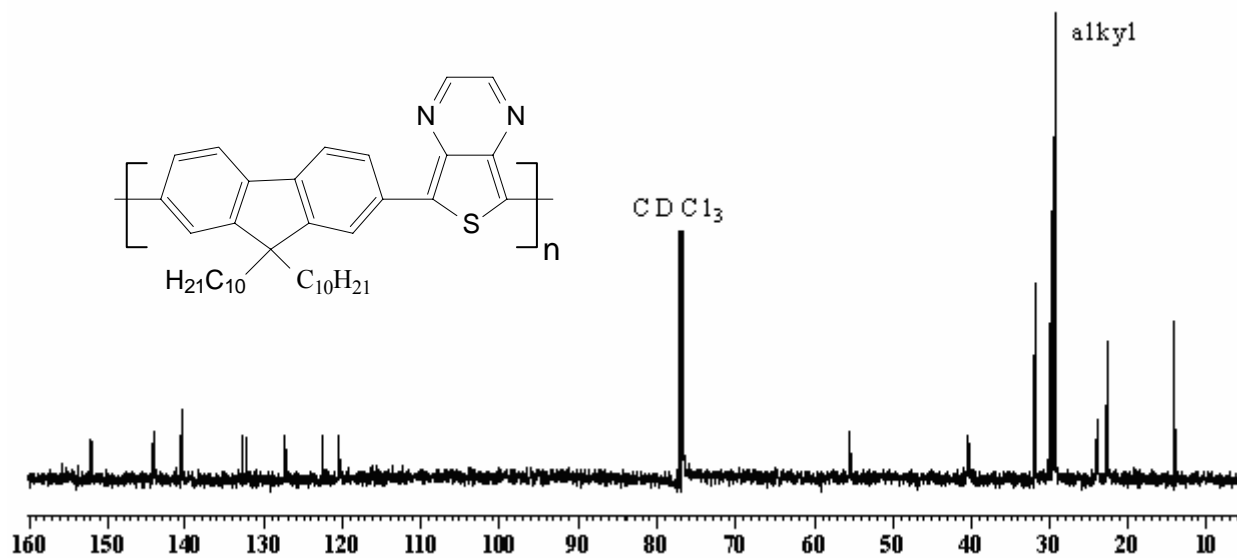
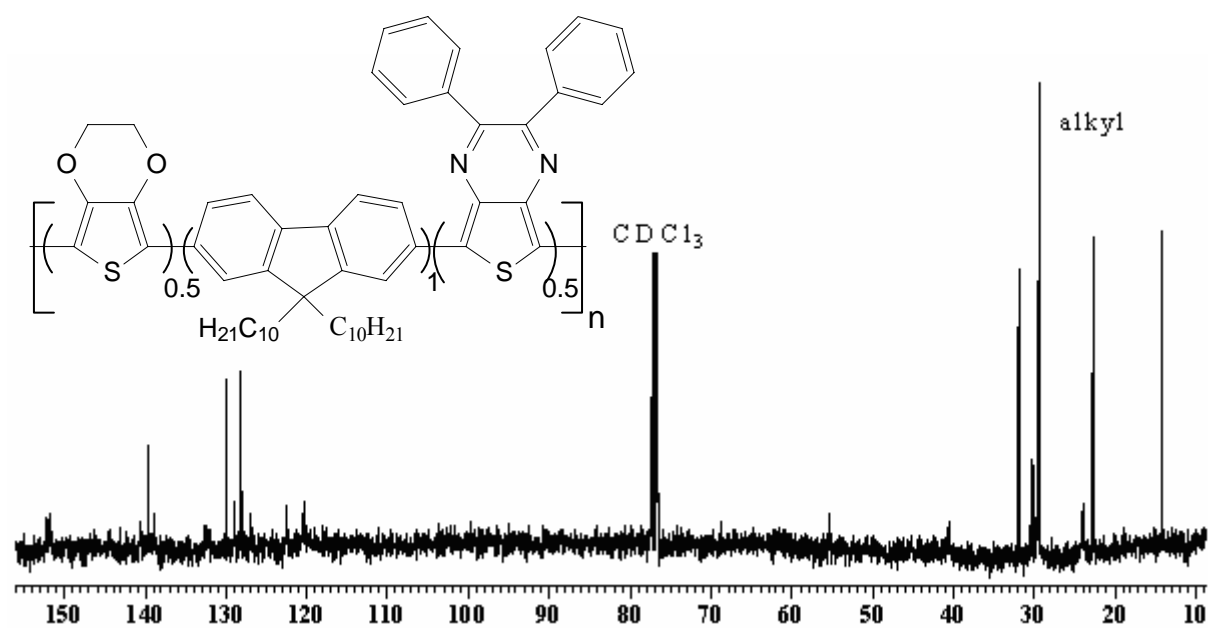


Figure 7.13. ^{13}C -NMR of P-14.

Figure 7.14. ^{13}C -NMR of P-15.Figure 7.15. ^{13}C -NMR of P-16.

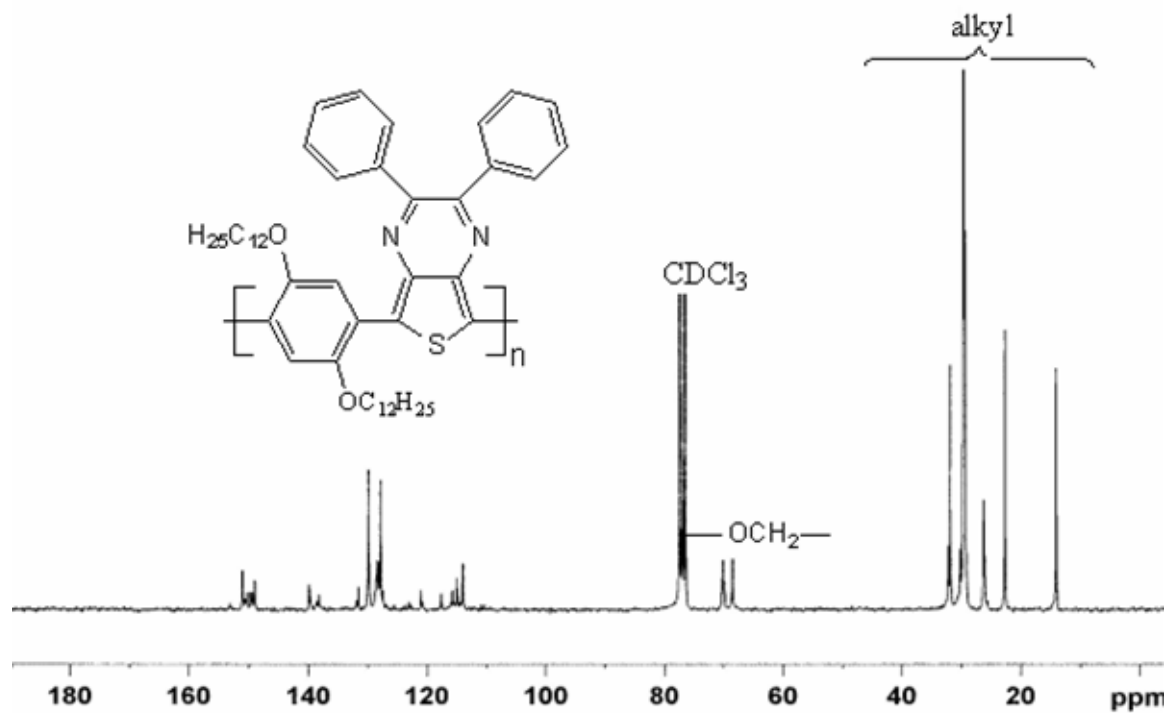


Figure 7.16. ^{13}C -NMR of P-17.

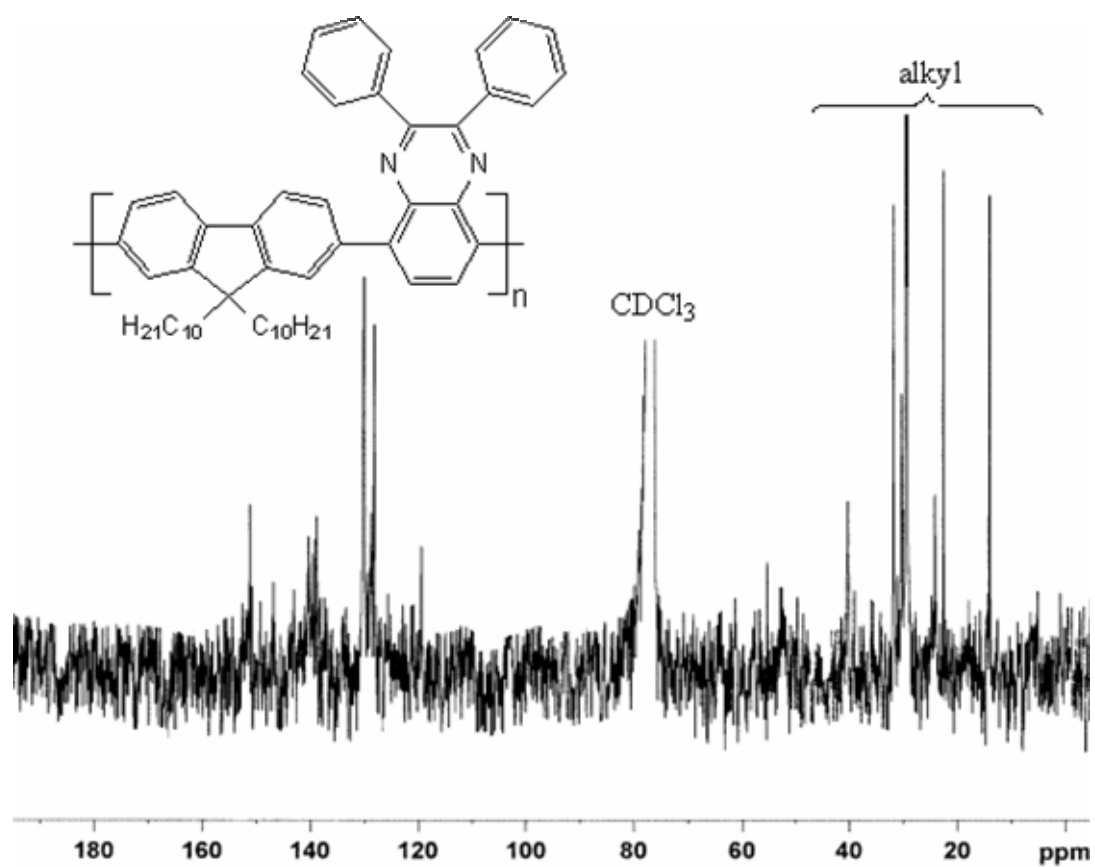


Figure 7.17. ^{13}C -NMR of P-18.

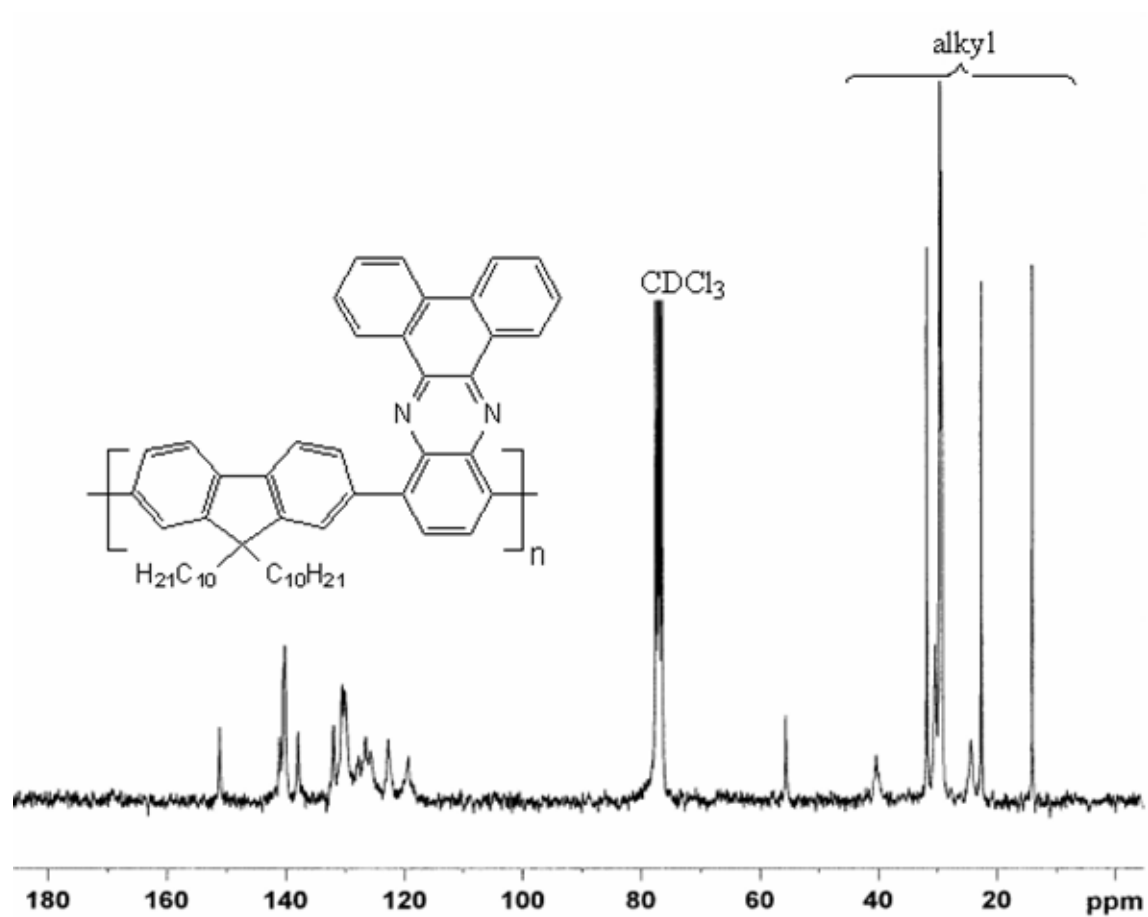
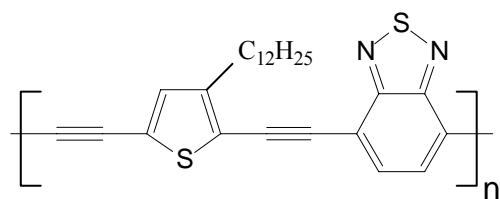
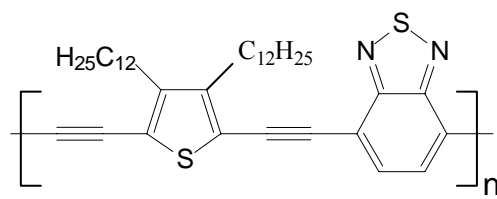


Figure 7.18. ^{13}C -NMR of P-19.

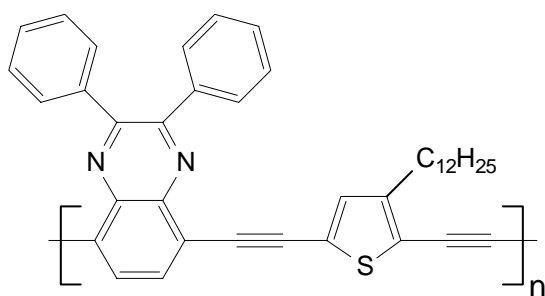
7.2 Molecular Formulae



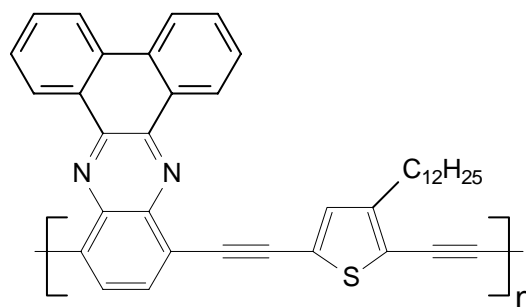
P-1 (PS-1)



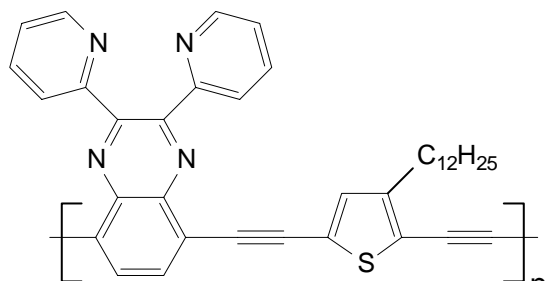
P-2 (PS-9)



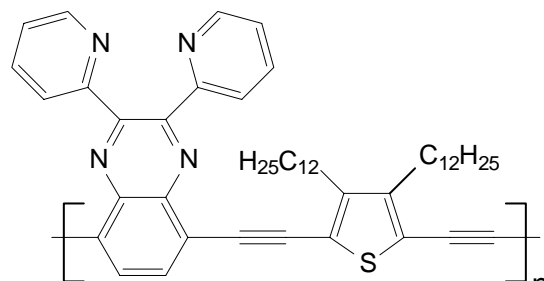
P-3 (PS-4)



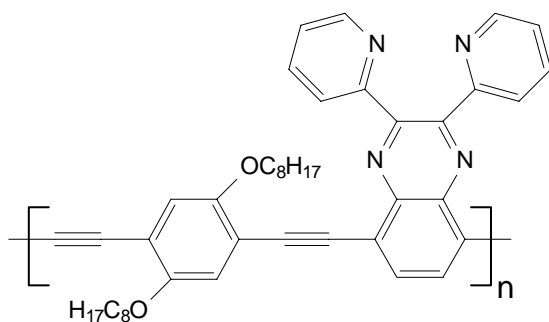
P-4 (PS-5)



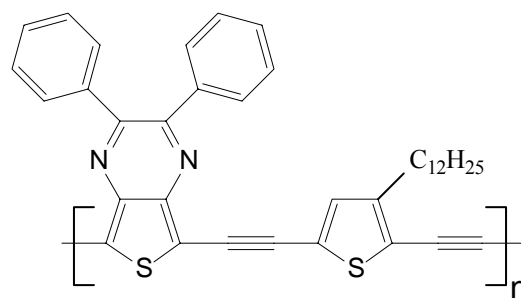
P-5 (PS-7)



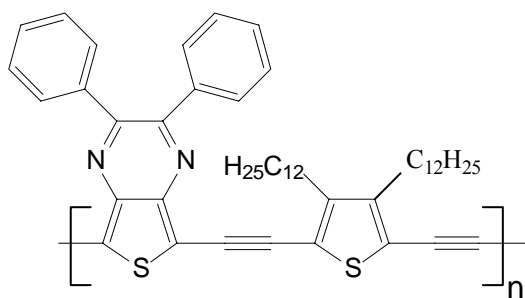
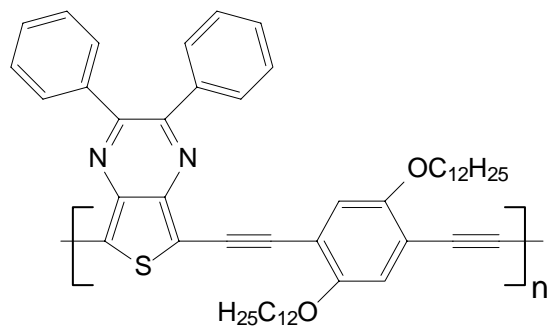
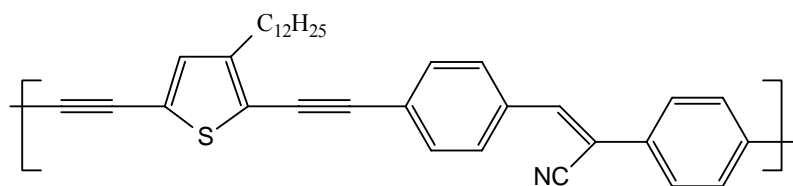
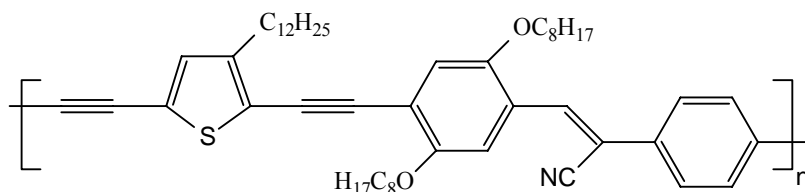
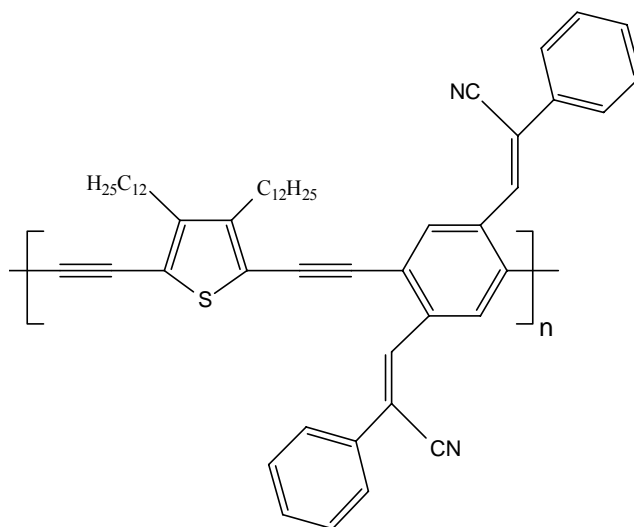
P-6 (PS-8)

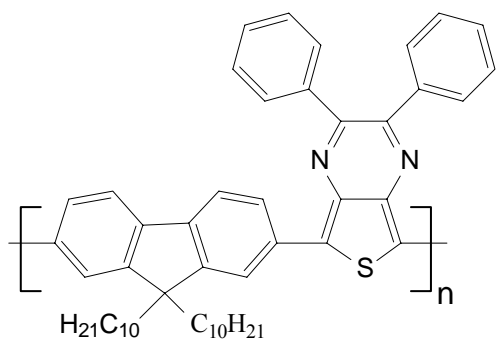
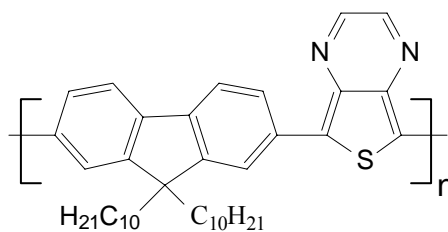
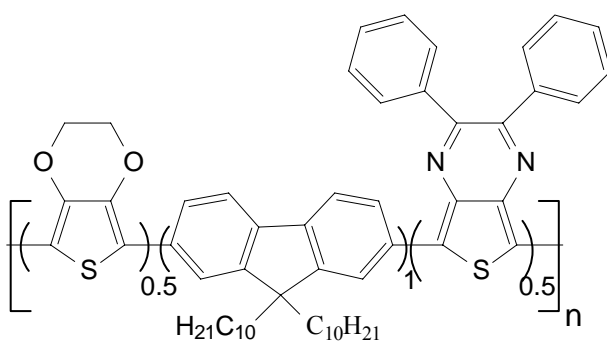
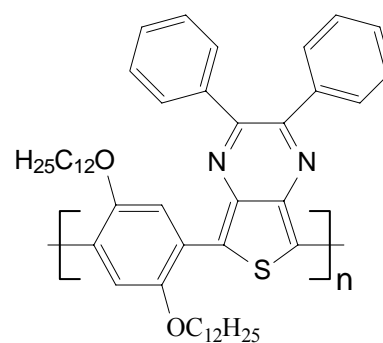
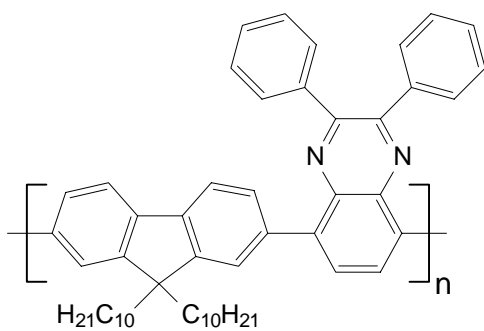
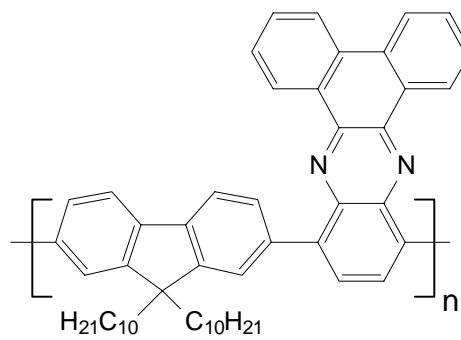


P-7 (PS-6)



P-8 (PS-14)

**P-9 (PS-15)****P-10 (PS-31)****P-11 (PS-61)****P-12 (PS-62)****P-13 (PS-21)**

**P-14 (PS-16)****P-15 (PS-17)****P-16 (PS-20)****P-17 (PS-22)****P-18 (PS-18)****P-19 (PS-19)**

7.3 Abbreviations

BuLi	Butyl lithium
CDCl_3	Deuterated chloroform
CHCl_3	Chloroform
CuI	Copper(I)-iodide
CV	Cyclic voltammetry
DMF	Dimethyl formamide
DMSO	Dimethyl sulfoxide
DSC	Differential scanning calorimetry
E_g	Band gap energy
$E_{g \text{ opt.}}$	Optical band gap energy
$E_{g \text{ ec}}$	Electrochemical band gap energy
E_{ox}	Oxidation potential
E_{red}	Reduction potential
eV	Electron volt
ε	Molar absorption coefficient
Φ_{fl}	Quantum luminescence yield
g	Gram
GPC	Gel permeation chromatography
H_2O	Water
HOMO	Highest occupied molecular orbital (valence band)
K	Kelvin
K_2CO_3	Potassium carbonate
LUMO	Lowest unoccupied molecular orbital (conduction band)
OLEDs	Organic light emitting diodes
LiPF_6	Lithium hexafluoro phosphate
λ_{max}	Wavelength at maximum absorption
$\lambda_{0.1\text{max}}$	Wavelength at longer wave length
$\lambda_{\text{max, em}}$	Wavelength at maximum emission
<i>m</i>	meta
mg	Milligram
MHz	Mega Hertz
mL	Milliliter

\bar{M}_n	Number-average molecular weight
\bar{M}_w	Weight-average molecular weight
M.P.	Melting point
n	Number of repeating units in polymer
Na ₂ CO ₃	Sodium Carbonate
NaOH	Sodium hydroxide
NMR	Nuclear magnetic resonance
<i>o</i>	ortho
<i>p</i>	para
PDI	Poly dispersity index
\bar{P}_n	Number-average degree of polymerization
PAE	Poly(aryleneethynylene) and poly(heteroaryleneethynylene)
PL	Photoluminescence
ppm	Part per million
PPP	Poly(<i>para</i> -phenylene) and Poly(heterophenylene)
PPV	Poly(<i>para</i> -phenylenevinylene)
RT	Room temperature
TGA	Thermogravimetric analysis
T _g	Glass transition temperature
THF	Tetrahydrofuran
UV/Vis	Ultraviolet/visible
VPO	Vapour pressure osmometry

Curriculum Vitae

Personal Data

Name	Raja Shahid Ashraf
Date of Birth	24-01-1976
Place of Birth	Gujrat (Punjab)
Marital Status	Married
Nationality	Pakistani
Languages	English, Urdu, Punjabi, Deutsch

Qualifications

1991	S.S.C. (Secondary School Certificate)
1991-1993	H.S.S.C. (Higher Secondary School Certificate)
1993-1996	B.Sc. Punjab University, Pakistan
1997-1999	M.Sc. in Chemistry, Punjab University, Pakistan
1999-2001	M.Phil in Organic Chemistry (Synthesis, Characterization and Metal Uptake Studies of Chelating Polymers Having Bidentate Pendent Groups) Quaid-i-Azam University, Pakistan
05/2002-2005	Doktorand/Wissenschaftlicher Mitarbeiter, FSU-Jena, Germany

Jena, 04-05-2004

.....
Raja Shahid Ashraf

List of Publications

- 1) Synthesis and properties of poly(heteroaryleneethynylene)s consisting of electron-accepting benzothiadiazole units and electron-donating alkyl thiophene units
R. S. Ashraf, E. Klemm, H. Hoppe
J Polym. Sci., A: Polym. Chem. in press.
- 2) New poly(aryleneethynylene)s consisting of electron-accepting quinoxaline units and electron-donating alkyl thiophene units. Synthesis and optical properties
R. S. Ashraf, E. Klemm
Macromol. Chem. Phys. in press.
- 3) Synthesis, characterization, photophysical and electrochemical properties of thiophene/cyanostilbene based copolymers
R. S. Ashraf, E. Klemm
Macromol. Chem. Phys. in press.

Poster Presentations

- 1) Novel Linear π -Conjugated Donor-Acceptor Copolymers: Synthesis and Optical Properties
R. S. Ashraf, D. A. M. Egbe, E. Klemm
3rd International and 13th National Chemistry Conference, Karachi, 2002.
- 2) New Soluble Alternating Donor-Acceptor Poly(heteroaryleneethynylene)s
R. S. Ashraf, D. A. M. Egbe, E. Klemm
Vortragstagung der GDCh, Fachgruppe Makromolekulare Chemie, Düsseldorf, 2004.
- 3) New Thiophene/ Quinoxaline CT Type Poly(aryleneethynylene)s. Synthesis and Optical Properties
R. S. Ashraf, E. Klemm
Polydays, Potsdam, 2004.

Acknowledgement

I offer my vehement sense of zealous gratitude to **Prof. Dr. Elisabeth Klemm**, for her constant encouragement, keen interest, endless patience, words of wisdom, thought provoking discussions and personal involvement through out my research work

I express my sense of gratitude to acknowledge *PD. Dr. Dietmer Stadermann, Dr. Daniel M. Egbe, Stephen Sell* with immense pleasure and want to express my feelings of indebtedness for valuable guidance, inspiring criticism, which they displayed for this research work.

I am much grateful to all coworkers of research group of the *Prof. Dr. Elisabeth Klemm* for their cooperation and moral support.

I am obliged to express my heart full thanks to *Frau G. Sentis* (UV/Vis measurements), *Dr. W. Günther* and *B. Friedrich* (NMR measurements), *E. Arnold* (GPC measurements), *H. Schönfeld* and *B. Lentvogt* (Elemental analysis), *J. Nowotny* (Photoluminescence and UV-Vis measurements), *Dr. E. Birkner* and *E. Kielmann* (fluorescence measurements), *Dr. S. Sensfuss* and *A. Kuse* (electrochemistry), *Dr. Flammersheim* and *P. Weiß* (DSC measurements), *H. Hoppe* (Photovoltaic studies) and our secretary *R. Klausnitzer* for their cooperation and help.

I ought to submit my thanks to my dear friends, who remember me in their prayers and hearts. I wish to acknowledge the support, co-operation and encouragement provided by *M. Nawaz, Mazhar Hussain, M. Ajaz, M. Ishtiaq and Zahid Shafiq*.

I extend my cordial thanks to my friends *Aftab, Waseem, and Gul Rashid* for their inspiration to elevate my moral courage.

I wish to acknowledge the encouragement and continuous support of my loving wife ***Munazza Shahid***.

I owe my heartfelt gratitude to my loving ***parents, parents in law & uncle Younas*** whose love, affection and prayers enabled me to achieve my aim in life. I wish to acknowledge the encouragement and moral support of my family members; especially my sweet brothers *Nadeem, Dr. Abrar, Mudasser, Israr, Sarmad, Shahzad, and Shahbaz*.

Selbständigkeitserklärung

Ich erkläre, dass ich die vorliegende Arbeit selbständig und nur unter Verwendung der angegebenen Hilfsmittel und Literatur angefertigt habe.

Jena, 04.05.2005

Raja Shahid Ashraf

Raja Shahid Ashraf